PHD

Membrane translocating peptides for the delivery of proteins

Mitchell, Stephen Anthony

Award date:
2003

Awarding institution:
University of Bath

MEMBRANE TRANSLOCATING PEPTIDES FOR THE DELIVERY OF PROTEINS

Submitted by Stephen Anthony Mitchell
for the degree of Doctor of Philosophy
of the University of Bath
2003

ProQuest LLC
789 East Eisenhower Parkway
P.O. Box 1346
Ann Arbor, MI 48106-1346

SUMMARY

Recently it was demonstrated that a number of proteins contain short peptide regions allowing the apparent free-movement of these proteins through cell membranes. In addition when fused as a chimera with other cargo proteins these peptides confer on them the ability to translocate into cells. These peptides have been termed protein transduction domains (PTDs), or membrane translocating peptides (MTPs).

The ability to deliver active gene products to cells rather than the genes themselves offers an attractive alternative to gene therapy approaches, bypassing the complications associated with the delivery of oligonucleotides to cells. However, with a number of PTDs identified, and the possibility of more being isolated in the future, it is necessary to undertake comparative quantification of the transduction potential of the sequences to determine those with the most favourable delivery attributes, allowing focused research on the lead candidates.

In this study three approaches to quantify protein transduction were explored using three different proteins as reporters; the green fluorescent protein (GFP), luciferase, and a pro-less variant of caspase-3, PLCasp3. Two peptide sequences, the HIV Tat PTD and the penetratin sequence from the *Drosophila* antennapedia protein, and one full length protein, the herpes simplex virus type 1 VP22 protein, previously reported to demonstrate protein transduction were used as test MTPs. A transfection protocol with *de novo* synthesis of MTP fusion protein was adopted for each approach, eliminating additional procedures associated with application of exogenously expressed recombinant proteins.

Confirmation of protein transduction was unsuccessful though three alternative methods for visualising protein transduction of MTP-GFP fusion proteins were employed. Vectors enabling production of MTP-luciferase fusion proteins were generated, it was not possible to develop a system by which separation of transfected, expressing cells from non-expressing cells could be accomplished. A system enabling potential quantification of protein transduction was developed for the PLCasp3 approach, but confirmation of transduction by this method was not

possible as a result of mutations in the DNA sequence arising during generation of the expression vectors.

DEDICATION

For David and Alicia Mitchell, my loving parents.

"A witty saying proves nothing."

- Francois Marie Arouet Voltaire (1694-1778)

ACKNOWLEDGEMENTS

My thanks are extended to Professor Colin W. Pouton for providing me with the opportunity to undertake this research in such a fascinating field. In his absence Drs. Anthony Smith and Barbara Reeves have supplied enthusiastic supervision and guidance, and their advice has been invaluable. Without financial assistance from the BBSRC none of this work would have been possible, and this is gratefully acknowledged.

I am very appreciative of members of the academic and support staff for their advice and assistance with various aspects of the project: Special thanks goes to Dr. Mick Arnott whose expertise in molecular biology matters provided me with the tools to do the job. He has also been a good friend and a patient listener. Dr. May Al-Nbaheen provided guidance in tissue culture, and Matt Gordon and Kevin Smith's assistance in the FACS analysis was much appreciated. Other members of labs 2.29, 2.14 and 2.34 were also always available to offer suggestions to many questions.

My family have offered continued support, something not easy when confronted with such an unfamiliar subject. Friends, new and old, have always willingly offered a means of escape and relaxation.

Finally, for the love and support given freely and without limit by Andrea Dowling, I am eternally indebted.

TABLE OF CONTENTS

TABLES

FIGURES

ABBREVIATIONS

ρNA	P-Nitroanilide
AIDS	Acquired immune deficiency syndrome
APC	Antigen presenting cell
APS	Ammonium persulphate
BBB	Blood brain barrier
BSA	Bovine serum albumin
CARD	Caspase recruitment domain
CFU	Colony forming units
CMV	Cytomegalovirus
Cp-DEVD-CHO	Cell-permeable-DEVD-CHO
CPP	Cell permeable/penetrating peptide/protein
CTL	Cytotoxic T-lymphocyte
Dox	Doxycycline
DD	Death domain
DED	Death effector domain
DIC	Differential-interfaced-contrast
DISC	Death-induced signalling complex
ECACC	European collection of animal cell cultures
ECL	Enhanced chemiluminescence
EGFP	Enhanced green fluorescent protein
FACS	Fluorescence-activated cell sorting
FITC	Fluorescein isothiocyanate
GFP	Green fluorescent protein
HIV	Human immunodeficiency virus
HPV	Human papillomavirus
HSV-1	Herpes simplex virus type 1
HTLV-III	Human T-cell Lymphotrophic virus type III
IF	Immunofluorescence
Luc	Luciferase
LTR	Long terminal repeat
MCS	Multiple cloning site
MHC	Major histocompatibility complex
MTP	Membrane translocating peptide/protein
PARP	Poly (ADP-ribose) polymerase
PLCasp3	Pro-less caspase-3
PTD	Protein transduction domain
SD	Standard deviation
SEM	Standard error of the means
SV40	Simian virus 40
Tc	Tetracycline
TGN	*Trans*-Golgi network
TK	Thymidine kinase

CHAPTER 1
INTRODUCTION

The development of methods by which genes can be delivered to mammalian cells has stimulated great interest in the potential to treat human diseases by gene-based therapies. Gene therapy can be described as the introduction of nucleic acids into cells for the purpose of altering the course of a medical condition or disease. The concept is based on the assumption that definitive treatment of genetic diseases should be possible by directing treatment to the site of the defect itself, the mutant gene, rather than to secondary effects of the mutant gene products. The research reported here focuses on the delivery of active gene products to cells, rather than the genes themselves, an approach that bypasses the requirement for delivery of oligonucleotides to cells. The vectors investigated for the protein delivery were peptide sequences with a reported ability to cross cell membranes and enter cells. To demonstrate why such a method may be preferable to treatment through gene therapy, a number of the underlying problems associated with the delivery of genetic material to cells are outlined below.

1.1 The Promise of Gene Therapy

Great promise was held for the use of gene therapy in the treatment of disease when trials were initiated in September 1990 (Blaese et al., 1995), but successful therapeutic rates and progress have been disappointingly slow due to a number of complications that currently limit the effectiveness of gene therapy approaches. In an attempt to overcome these complications alternative methods for the treatment of a number of diseases have been explored.

1.1.1 Viral Delivery of Oligonucleotides

There is an inherent obstacle that must be overcome in order for gene therapy approaches to succeed: evolution over many millennia has led to cells and organisms developing powerful mechanisms to protect themselves from the onslaught of environmental hazards, including the development of systems to avoid the accumulation of extraneous genetic material (Bestor and Tycko,

1996). However, advancement of these defence systems has necessitated co-evolution of entities whose survival is dependant on incorporation of their DNA into host genomes, resulting in generation of equally powerful counter-measures. Viruses have been particularly successful in overcoming these barriers, and, with the hope of capitalising on this, initial efforts at gene therapy were directed towards engineering viruses. There are four main types of problem associated with viral-based approaches: obtaining efficient delivery, transduction of DNA into quiescent or senescent cells, improving gene expression, and manufacturing the vector.

1.1.1.1 Efficient Delivery

When using retrovirus delivery vectors, there are a large number of cells from a broad range of cell types expressing cell surface viral receptors. This not only limits the target specificity of the system, but also limits the effectiveness of delivery. This is in large part due to the relatively low titre at which the retrovirus vectors can be generated, and the subsequent limit of particles delivered in a suitable dose volume. For example, at a titre of 10^7 colony-forming units (CFU) per millilitre (the maximum for amphotropic vectors such as murine leukaemia virus) a delivery volume of 100 ml will result in application of only 10^9 CFU. With around 5×10^{13} cells in the human body, even at a delivery efficiency of 100% only 1 in 50,000 cells will be targeted (Anderson, 1998).

There are approaches that can be adopted in an attempt to improve target cell specificity, increasing delivery efficiency. Altering the natural receptor-binding domain on the surface of the delivery particle to a domain that interacts with a target cell-specific receptor would increase association with that receptor. However, in instigating this change the whole structure of the envelope protein is altered, which can prevent fusion of the particles with cells, subsequent core entry into the cell, and delivery of the genetic cargo to the cells is unacceptably low as a result. An alternative approach is to direct the vector particles to a region surrounding target cells, increasing the concentration of retrovirus in the local environment of the cells. This can be achieved by inserting a ligand that recognises the extracellular matrix local to target cells (fibronectin or collagen

for example) into a part of the surface protein that does not interfere in the natural receptor-binding domain, leaving the viral cell-fusion mechanism unaffected.

1.1.1.2 Transduction of Non-Dividing Cells

Retroviruses are efficient at transduction into cells in culture. However, most cells *in vivo* are quiescent at any point in time, making the vector less useful for *in vivo* therapies, unless the cells in the target organ are stimulated to progress through the cell cycle. By using alternative viral vectors, such as lentiviruses (e.g. human immunodeficiency virus, HIV), non-dividing cells can be successfully infected. Safety concerns are raised, however, by the possibility that the vectors could undergo recombination with endogenous human viruses and produce a pathogenic virus strain. The likelihood of such an occurrence can be limited through the use of hybrid systems. It is possible to use just 22% of the HIV genome in a retroviral vector, with all genes responsible for pathogenicity removed (Kafri et al., 1997; Zufferey et al., 1997). Use of a non-HIV envelope reduces the chances of recombination further still.

1.1.1.3 Improving Gene Expression

If the problems associated with transducing target cells can be overcome the challenge of gene expression remains, and it is this that is probably the greatest shortcoming of current vectors (Miller and Whelan, 1997). The best approach to expressing a gene is to use the cell's own *cis*-regulatory DNA sequence to provide stable, long-term expression. However, identifying all of the components of a gene's regulatory system can be difficult, predominantly due to the size of the sequence the regulatory elements are spread over (about 100 Kb in the case of haemoglobin (β-globin gene)). Coupled with the fact that retrovirus vectors can contain only about 6-8 Kb of inserted sequence, alternative promoters have been used in place. These include the viral promoters from Simian virus 40 (SV40) and the cytomegalovirus (CMV). Unfortunately, one self-defence mechanism used by cells is to recognise foreign promoters and inactivate them through methylation or some other means (reviewed in Antequera et al., 1989, and Hendrich and Bird, 1998). Even where the gene remains active the immune system will recognise the therapeutic gene

product as foreign and eliminate the transgene product and the cells producing it. This is the case even where the product is a 'normal' protein, as the immune system will not have been exposed to it previously causing it to appear foreign.

The site of integration of the transgene into the target cells' genome, which will result in the sustained expression of the gene product, can also be problematic. The vector might insert itself into the genome at the site of a tumour suppressor gene, thereby increasing the propensity of the cell to become cancerous. Insertion of the transgene at different loci on the genome of cells within a target organ will have an effect on the level of expression within the transduced population, as the location of genes within the genome can affect their activity (Lercher et al., 2002).

Even when these obstacles have been overcome, regulation of the expression remains an issue. Many of the primary target genes for treatment through gene therapy are not expressed at the same level all of the time, but rather respond to physiological stimuli within the body (insulin, for example). It may not be necessary for the transduced cells to respond to such signals, but if this is the case, regulation must be provided by some other means, such as the administration of a drug to control the level of gene activity.

1.1.1.4 Manufacturing the Vector

It is necessary to use a biological system to produce the viral vectors. There are always quality control issues when using such systems for the obvious reason of natural variation. Such systems will also invariably give a low yield of product. However, there are other problems specifically associated with the production of viral vectors for use in gene therapy.

Retroviral vectors are produced in packaging cells that contain a packaging-defective viral genome, and because retroviruses have a high propensity for recombination, there is the possibility that a replication-competent retrovirus (RCR) could arise during the manufacturing process. This complication is compounded as every mammalian cell contains endogenous retroviruses. Incorporation of additional viral sequences into a RCR could replace those viral

elements removed in the generation of the vector, resulting in the formation of a pathogenic virus (Anderson et al., 1993b).

The organism of choice for manufacturing of vectors also needs to be considered. For example, mouse packaging cells produce retroviral vectors that are destroyed by human complement. Though this does make the vector particles 'safer', it does substantially reduce their half-life *in vivo*, and subsequently the delivery efficiency.

1.1.2 Oligonucleotide Delivery by Liposomes

Other, non-viral gene therapy approaches have been examined, in particular the use of cationic lipid-based delivery systems. These have a number of advantages over viral delivery systems: complexes are easy to prepare and there is no limit to the size of DNA molecule packaged. As there are no proteins involved there is less of an immune response evoked upon their administration. The genes delivered have low integration frequency and so cannot replicate or recombine, resulting in much less risk of generating an infectious form, or inducing tumourigenic mutations. A low integration frequency, however, means that sustained expression of the gene product is unlikely, and activity will decrease, probably as a result of degradation of the transgene. Another obstacle with such an approach is that, even though the complexes are easy to prepare, it is technically difficult to prepare the DNA/lipid complexes at concentrations where the injection volume into the animals is not too large, and large aggregates will not form.

1.2 Protein Therapy

Many of the obstacles discussed above result from specific aspects of the desired outcome, namely the sustained and regulated expression of the transgene. For a number of genetic disorders, including enzyme deficiencies or diseases such as cystic fibrosis and Duchenne's muscular dystrophy, such long-term and appropriately controlled expression is an absolute requirement. However, there are circumstances where such stringent criteria do not have to be met. A gene therapy approach for the treatment of cancer, for example, would result either in the direct induction of tumour cell death, or the induction or

enhancement of an immune-mediated response to the tumour. With the eradication of the tumour the requirement for the therapeutic gene product also ends. This short term requirement for the presence of a therapeutic gene product raises the possibility of achieving the same objective by the direct delivery of an active gene product itself, rather than the transgene; protein therapy. Using this approach, a number of the previously described complications associated with the administration of oligonucleotides to a patient can be circumvented.

1.2.1 Protein Delivery Methods

Proteins are generally unstable, have high molecular weights and are large in size, are hydrophilic and have low permeability. This makes delivery of polypeptides into the cytoplasmic and/or nuclear compartments of living cells without disrupting the plasma membrane and compromising a cell's integrity a significant obstacle. A number of approaches have been investigated whereby delivery of gene products to cells can be achieved. The successful introduction of these macromolecules into cells depends largely on the development of a delivery system that can overcome the limited chemical and physical stability associated with proteins, making them susceptible to proteolysis, chemical modification and denaturation (Cleland et al., 1993; Manning et al., 1989). Furthermore proteins usually have short half-lives in body fluids (Anderson and Sorenson, 1994).

Encapsulation of proteins within a protective barrier has been adopted to prevent premature degradation of the therapeutic molecule. Incorporation of cargo protein into polymer matrices, forming structures known as microspheres, is a popular approach for delivery where prolonged release of the therapeutic agent is required (recently reviewed in Sinha and Trehan, 2003). In addition to the delivery of oligonucleotides in gene therapy approaches, the use of small lipid vesicles, known as liposomes, is already widely used as a drug delivery system (Chonn and Cullis, 1995; Gregoriadis, 1995; Lasic, 1998). For protein delivery such a delivery vector is attractive as the encapsulated proteins are able to remain in their preferred aqueous environment within the vesicles while the liposomal membrane protects them against proteolysis and other destabilising factors. Liposomal preparations complexed with DNA vectors are regularly

used to transfect cells in culture, demonstrating their ability to convey cargo to the cytosol. This approach has been used by a number of groups to deliver proteins to both cultured cells and the cells *in vivo* (Chonn and Cullis, 1995; Lidgate et al., 1988; Ramjeesingh et al., 1998). Similarly, liposomes formed from cationic phospholipids have been used the deliver protein to cells *in vitro* (Debs et al., 1990; Sells et al., 1995) and *in vivo* (Guillaume et al., 2000). With these approaches, however, formation of the protein transfection complexes gives rise to a number of challenges. Interactions between the encapsulating 'coat' and the cargo protein will vary with the electrochemical nature of the cargo. The formation of each delivery complex will, therefore, have to be optimised for each cargo molecule. Similarly the fabrication process of the delivery systems may damage the proteins, due to their relatively fragile nature, reducing the biological activity within a sample.

Recent developments suggest that an alternative approach may address these problems - the use of "protein transduction". In this method full-length fusion proteins are generated that contain the transgene product and one of a number of peptide sequences from the membrane translocating peptide (MTP) family. These peptides have the unusual ability to enter cells freely, independent of receptors and transporters (Derossi et al., 1996; Derossi et al., 1994; Elliott and O'Hare, 1997; Mann and Frankel, 1991; Vives et al., 1997a). In this way the MTP is able to transport the therapeutic peptide across cell membranes and deliver it to the cytoplasm or nucleus where it is able to exhibit its biological effect (see Leifert and Whitton, 2003, for review). Where a gene therapy approach may be a more feasible option, due to long-term expression requirements, the importance of this technology is still evident. By generating a chimeric gene containing the protein of choice fused in frame to an MTP distribution of the gene product following expression in cells could be improved. This may go some way to overcoming problems associated with poor delivery efficiencies associated with DNA therapy approaches as discussed above.

1.2.2 Membrane Translocating Peptides and Protein Transduction

Over a decade ago, two research groups independently showed that the human immunodeficiency virus (HIV) Tat protein could enter cells when added to the culture media and retain its *trans*-activating ability (Frankel and Pabo, 1988), (Green and Loewenstein, 1988). Unlike growth factors or steroid hormones there appeared to be no receptor for this process, and there was no transient pore formed as occurs with some toxins. Since these initial observations a number of other proteins with this same unusual property of apparent energy-free cellular uptake have been identified (see Hawiger, 1999, and Lindgren et al., 2000, for reviews). The translocating abilities of the proteins HIV Tat, *Drosophila* antennapedia, and Herpes Simplex Virus type I (HSV-1) VP22 are the most widely studied of the cell permeable peptides and will be discussed in more depth presently.

The ability to freely enter cells is termed membrane translocation, and a protein capable of such an action is termed a cell permeable protein (CPP) or a membrane translocating peptide (MTP). Very little is known about the mechanism by which MTPs are able to target and to traverse lipid membranes. However, studies on proteins with such translocating properties have led authors to suggest that the mechanism of uptake does not appear to occur through classical receptor-, transporter-, endosome- or adsorptive-endocytosis-mediated processes (Derossi et al., 1996; Derossi et al., 1994; Elliott and O'Hare, 1997; Mann and Frankel, 1991; Vives et al., 1997a). There has, however, been controversy and disagreement in the field, and only recently is a consensus emerging. These issues are discussed in more detail below.

For antennapedia and HIV Tat short regions of the proteins, numbering only 11-16 amino acids in length, have been shown to be sufficient for membrane translocation; these sequences confer the translocation ability to the full length protein (Derossi et al., 1994; Schwarze et al., 1999; Vives et al., 1997a) (see table 1.1). The regions have been termed minimal protein transduction domains (PTDs), and these regions in the antennapedia protein and the Tat protein have been called penetratin and the Tat PTD, or TAT, respectively (Becker-Hapak et

al., 2001; Derossi et al., 1994; Schwarze et al., 1999). For VP22 the majority of the publications have used the full-length protein. Those that have used truncated peptide sequences derived from the full-length protein have focused on the C-terminus using peptides of varying lengths, which also exhibit the same translocatory attributes of VP22. These studies demonstrated that deletion of the 34 C–terminal amino-acids of VP22 is sufficient to abrogate the translocatory activity (Elliott and O'Hare, 1997). Therefore, by deduction, this domain can tentatively be termed a PTD, though no reports have been published to date using this short sequence alone (see table 1.1). Fusions of an MTP or PTD with other peptide or protein sequences can be achieved by chemical means, or by the preparation of a vector containing a cDNA sequence coding for the fusion protein. Work with such fusion proteins has demonstrated that VP22, the antennapedia homeodomain, and the Tat PTD, at least, are able to transport large cargoes (e.g. transport of the 116 kDa enzyme β-galactosidase) from an extracellular environment to the cytoplasm of cells, even targeting them to the nucleus, whilst the cargoes retained their biological activity ((Schwarze et al., 2000; Watson and Edwards, 1999) for reviews).

MTP	Amino Acid Sequence
HIV Tat PTD	YGRKKRRQRRR
Drome *	EGRRGKRDLLR
Penetratin	RQIKIWFQNRRMKWKK
VP22 †	DAATATRGRSAASRPTQ RPRAPARSASRPRRPVQ

Table 1.1. Amino acid sequences of the MTPs. The amino acid sequences of the MTPs used for the investigation. * Sequence for the test peptide, Drome. † The putative PTD of VP22 derived from results that analogues lacking the C-terminal 34 residues fail to translocate (Elliott and O'Hare, 1997).

Recently, intraperitoneal injection of Tat PTD peptide labelled with fluorescein into mice resulted in the delivery of significant amounts of fluorescein to all tissues examined by confocal microscopy, including the brain (Rousselle et al., 2000). This highlights the potential of PTDs to deliver small molecules,

previously with no bioavailability, to tissues *in vivo*. A potential application would be to deliver therapeutic chemicals, such as anticancer agents, through the blood-brain barrier (BBB) for the treatment of tumours in the brain, an area that drugs have a very limited access to, resulting in the failure of brain tumour chemotherapy. A report on the delivery of doxorubicin, an antineoplastic agent widely used in the treatment of several cancers, through the BBB by a peptide vector-mediated mechanism is very encouraging (Rousselle et al., 2000). In addition, work by Dowdy and his colleagues also showed that the intraperitoneal injection of a fusion protein of β-galactosidase (β-gal) with the Tat PTD in mice resulted in readily detectable β-gal enzymic activity in all tissues assayed, again including the brain (Schwarze et al., 1999). The delivery of an active enzyme into such an organism holds a tremendous amount of potential for protein therapy.

1.2.2.1 The HIV Tat Protein Transduction Domain

In addition to the traditional retroviral structural proteins gag, pol and env, human immunodeficiency virus type-1 (HIV-1), the cause of AIDS, encodes at least five novel proteins that appear to serve regulatory functions. One of these, the HIV-1 *trans*-activator gene, encodes Tat. The Tat protein *trans*-activates genes that are expressed from the HIV long terminal repeat (LTR) (Sodroski et al., 1985b) and Tat is essential for viral replication *in vitro* (Fisher et al., 1986). Tat is an 86 amino acid protein made from two exons of 72 and 14 amino acids, respectively. The N-terminal 72 amino acids, coded for by the first exon, are sufficient and necessary for full Tat activity (Mann and Frankel, 1991). This region contains a cysteine-rich region (with seven cysteines in 16 residues) (Arya et al., 1985; Sodroski et al., 1985a) that is important for metal-linked dimerisation *in vitro* (Frankel and Pabo, 1988), and a highly basic region (with 2 lysines and 6 arginines in 9 residues), which is involved in nuclear localisation (Dang and Lee, 1989). In 1988, independent studies using bacterially expressed (Frankel and Pabo, 1988) and chemically synthesised (Green and Loewenstein, 1988) Tat protein, respectively, showed that Tat, when added exogenously in culture, was taken up rapidly by cells. Through analysis of mutant Tat peptides

this protein transduction property was also shown to reside in the region encoded by the first exon, in amino acids 37-72 (Frankel and Pabo, 1988).

Since these initial observations much work has focused on the transduction property of Tat. In 1991, Mann and Frankel demonstrated that the domain encompassing amino acids 38-58 (the basic domain of Tat) retained the transduction capability, enabling both its nuclear and cytoplasmic accumulation (Mann and Frankel, 1991). A truncated version of the Tat protein, residues 35-62, was first found to be capable of transporting an antibody fragment into tumour cells in 1993 (Anderson et al., 1993a). A year later studies by Fawell and his colleagues demonstrated that a number of large molecules were taken up by cells *in vitro* when they were chemically cross-linked to either the amino acids encoded on the first exon, or by the residues 37-72 alone (Fawell et al., 1994). Using a β-galactosidase-Tat model they went on to show that uptake took place *in vivo* following intravenous injection of the chimeric protein in mice. Enzyme activity was found in most major tissues only 20 minutes after injection, though the protein was almost absent from the brain.

Work by Dowdy and his colleagues investigated Tat-mediated delivery by constructing fusion proteins between several polypeptides and proteins and a short region of Tat, residues 47-57 (Ezhevsky et al., 1997; Schwarze et al., 1999; Vocero-Akbani et al., 1999). This work culminated in success after undertaking similar *in vivo* experiments to Fawell *et al.* The group demonstrated the presence of β-galactosidase activity in several tissues 4 hours after intraperitoneal injection of the fusion protein into mice. In contrast with the earlier work, however, β-gal activity was also detected in the brain, though the blood-brain-barrier remained intact as demonstrated by Evans' blue exclusion test (Schwarze et al., 1999). This peptide has been determined as the minimal transduction domain of HIV Tat, and has been termed the Tat protein transduction domain (Tat PTD) (Schwarze et al., 1999), or TAT (Becker-Hapak et al., 2001) (see table 1).

Though there is much evidence for the uptake of Tat and its peptide derivatives, very little is known of the mechanism by which membrane translocation occurs. Physicochemical studies involving circular dichroism and energy minimisation on the Tat sequence including residues 38-60 indicated that this domain adopted a α-helical structure under certain conditions. The residues 38-45 within this region had a helix with amphipathic characteristics. The region encompassing the basic sequence 49-57 was unstructured under the same conditions (Loret et al., 1991). Biological data and physiochemical studies at this time were in keeping with a α-helix forming domain crucial in Tat uptake. A detailed study by Vivès and his colleagues in 1997 demonstrated that a shorter peptide still, encompassing only residues 48-60, which appears unstructured in solution, rapidly translocated through the plasma membrane and accumulated in the nucleus (Vives et al., 1997a). In undertaking this work it was also revealed that the region covering the Tat- (38-49) domain did not appear to be required for efficient and fast cell uptake, abrogating the role of an amphipathic helix in the translocation of Tat and its associated peptides.

Recent molecular modelling studies using protein structure and molecular surface predictive programs on the region of HIV Tat encompassing amino acids 47-57 revealed the structure to be that of a strong amphipathic helix (Ho et al., 2001). The structure of the Tat PTD, and its relative importance in membrane translocation, remains a matter for debate. However, a physicochemical property of this region that does appear to be of importance is the presence of the eight positive charges, six arginine and two lysine residues, within the short amino acids regions studied by either the Lebleu group, residues 48-60 (Vives et al., 1997a), or the Dowdy group, residues 47-57 (Schwarze et al., 1999). Studies have revealed a significant reduction in the membrane penetration ability when these positive residues are removed sequentially from either terminus (Vives et al., 1997b; Wender et al., 2000). Results from these studies indicate that at least seven positive charges are necessary for high efficiency delivery properties (Vives et al., 1997a), with a decrease in translocation ability of 50% and 75% following removal of one or two arginine residues, respectively (Wender et al., 2000).

It therefore appears that the Tat fragment encompassing the highly basic residues 49-57 alone may be responsible for the translocatory attributes exhibited by the peptides derived from Tat. Due to the transduction successes experienced by a number of groups *in vitro* and *in vivo* using the 11 amino acid sequence corresponding to the Tat PTD (Chen et al., 1999; Ezhevsky et al., 1997; Gius et al., 1999; Kim et al., 1997; Schwarze et al., 1999; Vocero-Akbani et al., 1999) it was this sequence that was selected to represent the Tat-derived peptides in this study. Since the start of this investigation a number of report citing transduction by the Tat PTD have been published (Eum et al., 2002; Gustafsson et al., 2002; Harada et al., 2002; Li et al., 2002; Nori et al., 2003; Ribeiro et al., 2003; Shibagaki and Udey, 2003; Tasciotti et al., 2003; Xia et al., 2001).

1.2.2.2 The Antennapedia Peptide, Penetratin

The antennapedia protein is a member of the *Drosophila* homeoprotein family. Homeoproteins belong to a class of *trans*-activating factors, first discovered in *Drosophila*, involved in several important biological processes occurring primarily, but not exclusively, during development (Gehring, 1987). The regulatory effect of homeotic proteins on genes depends on the proteins recognising and binding to consensus DNA sequences found in the promoter or enhancers of the genes through a highly conserved 60 amino acid C-terminal region (Biggin and Tjian, 1989). This region, the homeodomain, is structured in three α-helices with one β-turn between helices two and three (Qian et al., 1989).

In 1991, Joliot *et al.* reported that the 60 amino acid homeodomain of the antennapedia protein was able to enter nerve cells in culture when added to the culture media and to accumulate in the cells' nuclei. The internalised homeodomain remained capable of exerting biological effects on cultured neurons, resulting in morphological differentiation of the nerve cells. Studies at 37 °C and 4 °C showed this internalisation did not appear to involve classical receptor-mediated endocytosis (Joliot et al., 1991a), though there did appear to

be involvement of a polysialic acid on the neuronal surface (Joliot et al., 1991b). The influence on neuronal morphology, but not on cellular internalisation, was disrupted by generation of a mutant peptide with abolished DNA-binding properties (Bloch-Gallego et al., 1993). The mutation corresponded to a replacement of two residues with two proline residues (leucine 40 and threonine 41) within the turn between helices 2 and 3, which established that this region did not affect translocation of the homeodomain.

Subsequent work demonstrated that the homeodomain was capable of mediating the internalisation of foreign polypeptides, in the form of chimeras, and that it would convey such cargo to the nuclei of the cells (Perez et al., 1992). The region of the peptide responsible for its internalisation has been mapped to its third helix (residues 42 to 58) through studies using site directed mutagenesis (Le Roux et al., 1993). This finding has enabled work to establish that a 16 amino acid long peptide (see table 1) translocates at 37 °C and 4 °C across biological membranes, reaches the cytoplasm, and is eventually conveyed to the nucleus of cells in culture (Derossi et al., 1994). This peptide is known as penetratin.

Internalisation studies have been undertaken using a synthetic peptide with a primary sequence identical to penetratin but entirely composed of D-enantiomers, and with a second where the order of the residues had been reversed (Derossi et al., 1996). Both peptides were efficiently internalised by cells in culture demonstrating that this process does not require specific interactions with a chiral receptor (binding site or transporter). This finding was reinforced by the use of a *retro-inverso* analogue of the same sequence, which was internalised with a greater efficiency than the other forms. This increased efficiency was probably due to protection from degradation within the cultured neurons used for the investigation, as the native sequence contained two sites sensitive to neuronal endoproteases (Brugidou et al., 1995).

There have been a number of physicochemical studies undertaken on penetratin to evaluate the importance of physicochemical parameters on its cellular uptake, and to discern a possible mechanism for membrane translocation. The structure

of the penetratin region within the homeodomain of antennapedia had previously been shown to be that of an α-helix (Qian et al., 1989). However, studies of the penetratin sequence in isolation have shown that the nature of the medium in which the studies were performed could have a profound effect on the conformation adopted (Berlose et al., 1996; Drin et al., 2001; Lindberg and Graslund, 2001; Magzoub et al., 2002; Magzoub et al., 2001). It appears that the peptide adopts a mainly random coil structure when in an aqueous environment, with distinct secondary structures forming only when the peptide encounters a hydrophobic medium or synthetic membranes of phospholipids or SDS (Berlose et al., 1996; Magzoub et al., 2001). Though α-helical structures have been determined through spectroscopic data collected (Berlose et al., 1996; Drin et al., 2001; Lindberg and Graslund, 2001) it has been shown that penetratin analogues incapable of forming such structures, due to replacement of a number of residues with proline residues, are still capable of efficient translocation across cell membranes (Derossi et al., 1994). Studies where helical structures have been observed have utilised SDS micelles as a membrane mimetic, and as such any secondary structures should be extrapolated with caution. As membrane models phospholipids are far more realistic, and investigations using such negatively charged vesicles have shown penetratin to adopt predominantly β-sheet-like structures (Magzoub et al., 2002; Magzoub et al., 2001). Common to these and other studies is the finding that it is association with the membrane that is important for peptide uptake (Thoren et al., 2000). Though the helical amphipathicity may influence binding to some phospholipid bilayers it does not appear important for cellular uptake of penetratin (Drin et al., 2001). The uptake does, however, require a minimal hydrophobicity and net charge (Derossi et al., 1994; Drin et al., 2001), and it may be that affinity of the peptide for plasma membranes is the determining factor for cell internalisation.

Though all homeoproteins and homeodomains tested so far are internalised (Chatelin et al., 1996), penetratin was used during the course of these experiments due to the encouraging results of work previously undertaken on this short peptide's translocating and transduction capabilities (Chen et al., 1999; Derossi et al., 1996; Derossi et al., 1994). A mutated form of penetratin

described by Derossi *et al.* to no longer translocate (W6F, W14F) was also used as a control (Derossi et al., 1998).

1.2.2.3 Herpes Simplex Virus Type I VP22 Protein

VP22 is a 38 kDa, 301 residue protein encoded by the U_L49 gene of the herpes simplex virus type I (HSV-1) (Elliott and Meredith, 1992), which is expressed late in infection (Hall et al., 1982). It is a structural protein forming the major component of the nine or more gene products that make up the virus tegument; an amorphous region, located between the virion capsid and envelope (Pomeranz and Blaho, 1999). VP22 is subject to a large number of post-translational modifications including phosphorylation (Elliott et al., 1996) and nucleotidylation (Blaho et al., 1994). The localisation of VP22 in infected cells changes over the course of HSV-1 infection (Pomeranz and Blaho, 1999). It appears that phosphorylation of VP22 during infection cycle progression is responsible for translocation from a predominantly cytoplasmic distribution early in infection to predominantly nuclear late in infection (Pomeranz and Blaho, 1999).

VP22 is exported from cells in which it is synthesised, despite the absence of an export signal, by a Golgi-independent mechanism (Elliott and O'Hare, 1997) termed non-classical secretion (Kuchler, 1993). In 1997 Elliott and O'Hare demonstrated that, upon export, VP22 is able to re-enter surrounding cells with high efficiency, where it is targeted to the nucleus, despite lacking a nuclear localisation signal (although portions of the protein are highly basic), binds to chromatin and segregates to daughter cells (Elliott and O'Hare, 1997). Further investigation by this group suggested that this movement of VP22 between cells may involve actin microfilaments (Elliott and O'Hare, 1998).

A number of possible roles for VP22 have been proposed. Its ability to co-localise with microtubules (Elliott and O'Hare, 1998) and to bind to other tegument proteins and direct their localisation (Elliott et al., 1995) suggests that VP22 has the ability to redirect both cellular and viral proteins and may play a role in the modification of microtubule morphologies (Elliott and O'Hare, 1998). An additional study to determine the domain within VP22 responsible for

microtubule interaction has proposed a model for a bundling of microtubules that relies upon cross-linking of VP22 molecules across the space between two filaments (Martin et al., 2002). An alternative role suggested for VP22 relies on its ability to translocate between cells. By travelling from a newly infected cell to uninfected neighbouring cells VP22 may be able to alter cellular functions, thereby setting the cells up for subsequent infection (Elliott and O'Hare, 1997; Hawiger, 1999). Indeed, Sciortino *et al.* have shown that VP22 is capable of binding to mRNA from HSV-1 infected cells and that this bound RNA is delivered to neighbouring cells where it is subsequently translated (Sciortino et al., 2002). The delivery of a small number of mRNAs from infected cells to uninfected cells in the vicinity would allow the translation of proteins that favour viral replication and spread.

In addition to demonstrating the remarkable property of intercellular transport exhibited by VP22, Elliott and O'Hare also determined that VP22 was capable of transporting other proteins, in the form of fusion proteins, both after endogenous synthesis or exogenous application (Elliott and O'Hare, 1997). Numerous studies have since confirmed that VP22 is able to ferry large covalently linked heterologous protein sequences out of expressing cells and into various non-expressing cells. The tumour suppresser protein p53 was successfully spread throughout a population of cells when expressed as either a C- or N-terminal fusion with VP22 (Phelan et al., 1998). Furthermore, the p53 fusion proteins retained wild type p53 function and were able to induce widespread cytotoxicity in a p53-negative human osteocarcoma cell line. Similar demonstrations have been carried out with GFP (Aints et al., 1999; Brewis et al., 2000; Elliott and O'Hare, 1999a; Elliott and O'Hare, 1999b; Lai et al., 2000; Wybranietz et al., 1999), and HSV-1 thymidine kinase (Dilber et al., 1999; Liu et al., 2001).

In contrast to the HIV PTD and penetratin it is the full length *VP22* gene product that is favoured for protein transduction experiments. As a result the approach normally employed when working with VP22 fusion proteins is the indirect transduction of proteins into cells. This is achieved by first transfecting a population of cells with an expression vector in which the cDNA coding for a

protein is genetically fused to VP22. The transducable fusion protein is made by the cellular machinery and is transported from the primary transfected cells into the surrounding cells (for an overview of this approach see (Schwarze et al., 2000)).

There has been some effort towards discerning the region(s) of VP22 that is (are) responsible for the translocation function of the protein, with conflicting results reported. In the study by Elliott and O'Hare where intercellular trafficking of VP22 was initially demonstrated, a VP22 mutant lacking 34 residues from the C-terminus was shown to localise only in a filamentous pattern in transfected cells (Elliott and O'Hare, 1997). As no nuclear localisation pattern was observed, the factor used for determination of translocation of from transfected cells, this mutant was concluded to lack trafficking ability, see table 1. The importance of the C-terminus was confirmed in a later study using a C-terminal fragment of VP22 consisting of 143 residues (residues 159-301) (Kueltzo et al., 2000). The peptide was found to possess the full transport activity of native VP22, both the intrinsic transport ability and the ability to carry proteins of significant size. However, by constructing a series of deletion constructs of VP22 tagged by GFP Aints *et al.* mapped the region of VP22 necessary for intercellular transport to residues 81-195, with a peptide corresponding to the 106 C-terminal residues exhibiting no intercellular trafficking (Aints et al., 2001).

Due to the studies reporting successful protein transduction using fusions with full-length VP22 it was the full length HSV-1 VP22 gene that was used to generate the fusion proteins examined throughout the course of this study.

1.2.2.4 An Experimental 'MTP' – Drome

To test whether a system developed through the course of this study could be utilised to assess novel translocatory sequences a test sequence was generated and used alongside the known MTPs. The sequence was generated in the laboratory during the preparation of the MTP-GFP fusion proteins, and the sequence was retained for rest of the studies detailed here. The sequence was taken from the *Drosophila* regulator of chromosome condensation protein, Bj1.

The test peptide was derived from the same organism as the antennapedia protein, and thus penetratin. Bj1 is a chromatin-binding protein, and thus bears homology to one of the functions VP22. The sequence, as can be seen from table 1, also has a high proportion of basic residues, 5 out of the 11 coding bases, which appears to be a common feature of MTPs. With this combination of features from the known MTPs the sequence, termed Drome, appeared a potentially favourable test sequence to study for potential translocatory attributes.

1.3 Altering Biological Functions Through Protein Transduction

The MTPs discussed have been shown not only to deliver reporter molecules such as β-gal and EGFP to cells, but also to be capable of transporting biologically active molecules through the plasma membrane and into cells where they remain capable of imparting a pharmacological effect. It is this, rather than a proven ability to translocate into cells, that is of importance when the worth of such vectors for the treatment of disease, or the study of intracellular functions, is being investigated.

1.3.1 Pharmacological Studies Using Tat PTD as a Peptide Delivery Vector

Numerous reports have described the delivery of peptides to cells by fusion with the Tat PTD. Following delivery these molecules have retained functional activity and have elicited the desired pharmacological response within the recipient cells (Chellaiah et al., 2000; Dietz et al., 2002; Embury et al., 2001; Eum et al., 2002; Ezhevsky et al., 1997; Gius et al., 1999; Harada et al., 2002; Nagahara et al., 1998; Ribeiro et al., 2003; Shibagaki and Udey, 2003; Tasciotti et al., 2003; Vocero-Akbani et al., 1999; Xia et al., 2001). These reports have included both the delivery of exogenously applied fusion proteins as well as transport of protein expressed within one population of cells to a second non-expressing population. Some representative examples of these findings are examined below, highlighting the potential application of the Tat PTD as a protein delivery vector.

The introduction into cells of peptides able to interact with cellular machinery, thereby altering the cell's typical function, can provide a valuable method of discerning protein function. An example of this is in the study of cell cycle progression. In order to understand the timing and duration of cyclin D:Cdk4/6 complex formation involved in phosphorylating the retinoblastoma tumour suppressor pRb, and their requirement for G_1 cell cycle progression, a 20 amino-acid peptidyl mimetic corresponding to the cyclin-binding domain of the Cdk4/6 inhibitor $p16^{INK4a}$ was transduced into cells using an N-terminal TAT fusion (Ezhevsky et al., 1997; Gius et al., 1999). Cdk4/6 activity for a specific early G_1 phase cell cycle progression was identified, with the transduced mimetic arresting the cell cycle here by interrupting interaction with, and subsequent inhibition of, Cdk4/6 and $p16^{INK4a}$.

In 2001 Xia *et al.* demonstrated the mannose-6-phosphate independent uptake *in vitro* of the lysosomal enzyme β-glucuronidase using a recombinant viral vector with a Tat PTD C-terminal fusion. The group went on to show a significant increase in the enzyme distribution secreted from virally infected cells following intravenous or direct brain injection in mice (Xia et al., 2001). An approach using gene therapy with a vector engineered to express a Tat-modified recombinant lysosomal protein was effective in clearing storage pathology from β-glucuronidase-deficient mice.

In addition to rectifying pathological conditions the Tat PTD has also been successfully utilised in protection of 'normal' cells from various harmful insults. Islet cell transplantation during an immunosuppressive regimen (the Edmonton protocol) is a feasible means of attaining insulin independence in the treatment of diabetes (Shapiro et al., 2000). However, islet apoptosis triggered through isolation from a donor, and in subsequent *in vitro* culture, makes production of sufficient islets for this approach very difficult, and is a major limitation to such an approach. In 2001 Embury *et al.* demonstrated that tumour necrosis factor-α-induced apoptosis of a pancreatic β-cell line was prevented by the transduction of the anti-apoptotic protein $Bcl\text{-}X_L$ fused to Tat PTD and applied exogenously to cells *in vitro* (Embury et al., 2001). Ribeiro *et al.* showed protection of islets

could be equally afforded by the transduction of an active cytoprotective protein, heme oxygenase-1, rather than through inhibition of the apoptotic pathways (Ribeiro et al., 2003). Similarly, low-potassium-induced apoptosis of cerebellar granule cells was also inhibited by transduction of TAT-Bcl-X_L, demonstrating a possible neuroprotective therapy strategy (Dietz et al., 2002). The effectiveness of such an approach was later demonstrated *in vivo* through the reversion of hyperglycaemia in diabetic immunodeficient mice (Embury et al., 2001) and the protection of mouse retinal ganglion cells from retrograde neuronal apoptosis caused by optic nerve lesion (Dietz et al., 2002).

In contrast to such protective approaches, the Tat PTD has been used for the transport of molecules into cells with the aim of elimination of those cells through apoptosis. Thymidine kinase (TK) is a good candidate to control cellular proliferation in gene therapy, with obvious interest in the arrest of proliferation of tumour cells. Cells expressing TK convert the nucleoside analogues acyclovir and ganciclovir into their phosphorylated forms, which are in turn incorporated into replicating DNA where they block further chain elongation and consequently induce cell death (Miller and Miller, 1980). However, results using TK pro-drug therapy have shown only marginal clinical benefit, mainly due to the poor rate of delivery of the *HVS-TK* gene to tumours (Rainov, 2000; Shand et al., 1999). *In vitro* Tasciotti *et al.* showed that cells expressing TAT-TK would release the fusion protein into the cell culture medium, from where it was internalised by neighbouring, non-expressing cells. When treated with acyclovir this second population of cells then became susceptible to cell death (Tasciotti et al., 2003). The research shows that a possible method for the optimisation of TK suicide gene therapy approach may be to modify TK with the Tat PTD, or some other transduction domain, improving the bystander effect

Protein transduction has also been investigated as a means of killing HIV-infected cells through induction of apoptosis, using a fusion of a modified caspase-3 protein with the Tat PTD (Vocero-Akbani et al., 1999). The caspase-3 zymogen requires processing by upstream caspases at two recognition sites to remove a pro-domain and to cleave caspase-3 into a large and a small subunit,

allowing the formation of the active heterotetramer (Woo et al., 1998). Vocero-Akbani *et al* altered the recognition sites of caspase-3 from caspase recognition sites to sequences that would be specifically recognised by the HIV protease, identified through the sequencing of the AIDS virus, HTLV-III (Ratner et al., 1985). Transduction of the fusion protein was evident in about 100% of cells, irrelevant of their being HIV-infected or not. However, caspase-3 was only activated in infected cells containing the HIV protease, resulting in apoptosis. The zymogen remained inactive in the uninfected population. This strategy neatly circumvents the problems associated with the emergence of HIV strains resistant to the small inhibitory molecules currently employed as clinical treatments to prevent processing of HIV polyproteins by HIV protease, and thus maturation of infectious virions (Condra et al., 1995; Kohl et al., 1988). The work also suggests the possibility of substituting the proteolytic cleavage sites for those specific for other pathogens encoding specific proteases, such as malaria (Francis et al., 1997).

1.3.2 Pharmacological Studies Using Penetratin as a Peptide Delivery Vector

Though penetratin has also been extensively studied as a translocatory peptide there are fewer reports of full-length proteins in fusion with this PTD transducing cells and exhibiting a pharmacological activity (Han et al., 2000; Kato et al., 1998). This is a possible consequence of an apparent limitation of transportable cargo size exhibited by the peptide (Derossi et al., 1998). Penetratin has preferentially been utilised for the transport of short peptide sequences and has been involved in the study of regulation of cell proliferation (Ball et al., 1997; Bandara et al., 1997; Bonfanti et al., 1997; Chen et al., 1999; Cussac et al., 1999; Fahraeus et al., 1998; Fahraeus et al., 1996; Giorello et al., 1998; Hall et al., 1996; Herbert et al., 2000; Holinger et al., 1999; Kardinal et al., 2000; Kato et al., 1998; Kim et al., 1999; Lin et al., 2000; Mutoh et al., 1999; Riedel et al., 2000; Wang et al., 1999), cell migration (Fahraeus and Lane, 1999; Peck and Isacke, 1998), cellular immune responses (Schutze-Redelmeier et al., 1996), together with a number of other modulators of cellular processes (Hildt and Oess, 1999; Liu et al., 1999; May et al., 2000; Theodore et al., 1995; Troy et al., 1996). Some of these studies, which featured prospective therapeutic applications for penetratin, are discussed below.

The use of peptides, in place of whole proteins, in cytotoxic T lymphocyte (CTL) production is limited as exogenous antigens are generally internalised by receptor-mediated endocytosis and presented by the class II pathway to stimulate helper T cells. It is necessary for such peptides to reach the cytoplasmic compartment for processing, loading into class I molecules and subsequent presentation on the surface of antigen presenting cells (APCs) if induction of $CD8^+$ CTLs is to occur, in a manner analogous to presentation of endogenous antigens (Watts, 1997). Pietersz *et al.* demonstrated that the uptake of the 9-mer OVA-K^b CTL epitope into APCs was facilitated by penetratin linked to either the C- or N-terminus of the peptide. The synthetic peptides were also shown to protect vaccinated mice against growth of an ovalbumin expressing tumour cell line through the induction of CTLs (Pietersz et al., 2001). Using this system other epitopes may also be used for priming CTLs both *in vitro* and *in vivo*.

In order to prevent cells from undergoing inappropriate apoptosis there is in place a tightly-regulated, intricate control system with levels of inhibitory and counter inhibitory molecules (for an introduction to this complexity see Salvesen and Duckett's review of the 'inhibitor of apoptosis' gene family (Salvesen and Duckett, 2002)). The delivery of short (4-8 amino acids) N-terminal peptides of the pro-apoptotic protein Smac/DIABLO fused to penetratin to a number of immortalised cell lines was shown to enhance the induction of apoptosis and long term anti-proliferative effects of a diverse range of antineoplastic agents (Arnt et al., 2002). Displacement of caspase-3 from cytoplasmic aggregates with its inhibitors by the peptide was responsible for this, and so demonstrates that modulation of such inhibitors by this approach can positively adjust the efficacy of antineoplastic agents. Such modulation may limit patient exposure to chemotherapeutic agents, and therefore reduce associated side effects.

Penetratin has also been used to transport a $p16^{INK4a}$ peptide to investigate the effect on cell proliferation (Hosotani et al., 2002). This study, in contrast to those using the Tat PTD (Ezhevsky et al., 1997; Gius et al., 1999), examined the

influence of the peptide on murine tumour models *in vivo*. Daily intraperitoneal injections of penetratin conjugated with the 21-mer peptide were shown to significantly inhibit tumour growth in mice, and to increase the survival of treated mice compared to controls. These results are of obvious interest for therapeutic approaches to treating the large numbers of cancers where $p16^{INK4a}$ is inactivated (Yang et al., 1995).

1.3.3 Pharmacological Studies Using VP22 as a Peptide Delivery

Unlike TAT and penetratin, the transduction attributes of VP22 are usually employed using fusions with the full-length protein. A number of studies have been undertaken to explore the potential of VP22 to deliver both full-length proteins capable of eliciting a therapeutic effect within recipient cells (Derer et al., 2001; Dilber et al., 1999; Liu et al., 2001; Phelan et al., 1998) and also with regard to enhancing immune responses through the priming of cells (Cheng et al., 2001b; Hung et al., 2001; Michel et al., 2002).

As with $p16^{INK4a}$, the product of the tumour suppressor gene *p53* is mutated in a wide range of human malignancies (Levine, 1997). Failure to synthesise p53, or more commonly, synthesis of a mutated form of the protein results in uncontrolled proliferation and tumour formation. In 1998, Phelan *et al* demonstrated the p53-VP22 chimeric protein was able to spread from transfected COS-1 cells expressing the fusion protein to untransfected *p53*-negative human osteosarcoma cells (Phelan et al., 1998). The work showed apoptosis induction in recipient cells, indicating recovery of p53 regulation of cell cycle arrest, and subsequent controlled cell death.

As with the Tat PTD, the potential of VP22 to transport thymidine kinase has been explored (Dilber et al., 1999; Liu et al., 2001). In co-cultured monolayers, cell death in response to ganciclovir treatment was observed in neuroblastoma cells when the sole source of TK was transfected COS cells (Dilber et al., 1999). As the neuroblastoma cells were gap junction-negative this effect was proof of direct transport of the enzyme to these cells rather than a bystander effect elicited by spread of the activated pro-drug generated in the expressing cells. Through a characterisation of the increase of cytotoxicity of this TK/GCV

suicide strategy, Liu *et al* showed lower concentrations of GCV were necessary when the fusion protein was employed in preference to TK alone (Liu et al., 2001). This may alleviate the toxic side effects associated with high concentrations of GCV necessary *in vivo* (Engelmann et al., 1999; LeMay et al., 1998).

Because of their association with most cervical cancers, human papillomaviruses (HPVs), and in particular HPV-16, present an attractive target for developing a means of treatment and prevention of HPV-associated cancers (Bosch et al., 1995). A prime candidate in the development of an immunotherapy strategy for cervical cancer is the use of the HPV 16 E7 protein as a tumour antigen. HPV 16 E7 is expressed in most HPV-containing cervical cancers, and studies have shown E7 to be required for growth of tumour cells *in vitro* (Doeberitz et al., 1988; Schwarz et al., 1985). Expression of a fusion protein of VP22 with HPV 16 E7 from a Sindis virus RNA replicon vector resulted in enhancement of E7-specific $CD8^+$ T cell activities in vaccinated mice (Cheng et al., 2001b). In a DNA vaccination model, VP22 fused to E7 resulted in a strong E7-specific $CD8^+$ T cell response, reduction in pulmonary metastases, and $CD8^+$ T cell-dependant, and natural killer cell-dependant tumour-free survival in immunised mice (Hung et al., 2001). Other studies have seen similar effects using VP22-E7 fusion constructs (Michel et al., 2002). These investigations indicate that the potency of a DNA/RNA vaccine may be dramatically improved through intercellular spreading and enhanced MHC class I presentation of antigens that otherwise induce a rather inefficient CTL response.

1.4 Are MTPs Delivering?

It is commonly accepted that the internalisation of MTPs does not involve receptor-mediated endocytosis or specific protein transporters. The only factor common to translocation of MTPs appears to be an absolute dependence on basic amino acids within the transport sequences (Wender et al., 2000). There is rapid uptake to the cytoplasm and the nucleus, taking place in less than 15 minutes, which occurs in an ATP- and temperature-independent manner (Vives et al., 1997a; Derossi et al., 1996). This transfer through lipid membranes has

been attributed to a direct penetration-driven model (Vives et al., 1997a; Derossi et al., 1996). Energy may be provided from the refolding of partially denatured cargo proteins following transport to the cytoplasm, as such cargos are transported with a higher efficiency (Nagahara et al., 1998). For delivery of small molecules by hydrophobic peptide carriers, such as penetratin, an inverted micelle system has also been proposed, with the formation of unilamellar phospholipid bubbles induced by membrane destabilisation by tryptophan residues (Derossi et al., 1998).

From the volume of literature detailing novel uses for MTPs, there appears to be incontrovertible evidence from a large number of functional studies to show that fusions of HIV Tat, antennapedia and VP22 (and their relative PTDs) can have biological consequences. While many of the observed outcomes reported are consistent with translocatory activity, these promising observations have been questioned by some recent studies that have addressed the uptake mechanism (Koppelhus et al., 2002; Leifert et al., 2002; Lundberg et al., 2003; Richard et al., 2003; Sandgren et al., 2002). The data collected from these studies indicate that the effects may instead be explained by well-characterised biophysical interactions and recognised cellular transport pathways.

It has been difficult to visualise protein transduction between living cells (Brewis et al., 2000; Elliott and O'Hare, 1999a; Fang et al., 1998) and many reports of translocation are based on microscopic analysis of fixed cells. However, it has been observed that the use of some organic fixation agents introduces a profound artefact into subsequent analysis. Translocation studies with transfected cells expressing VP22-GFP fusion proteins showed a large difference in the number of GFP positive cells before and after permeabilisation with methanol (Aints et al., 1999; Brewis et al., 2000). Application of exogenously expressed VP22-GFP to cells has resulted in strong fluorescence from protein associated with the membrane of living cells, with no apparent nuclear fluorescence. However, directly after methanol fixation and rehydration of cells in PBS, the cells exhibited nuclear GFP fluorescence (Lundberg and Johansson, 2001). VP22 has also been shown to readily associate with the nuclei of cells following application of bacterially expressed VP22-GFP fusion

proteins to methanol-fixed cells (Lundberg and Johansson, 2001; Lundberg and Johansson, 2002). Quantification of the translocatory ability of Tat PTD-GFP fusion protein in live cells also showed no intercellular transfer. GFP fluorescence was, however, observed in cells subjected to methanol fixation where no fluorescence was observed in the cells prior to fixation (Leifert et al., 2002). Under even the mild fixation conditions of paraformaldehyde treatment artifactual uptake of TAT and penetratin has been observed (Richard et al., 2003). Rather than acting to actively transport cargoes across cell membranes it has now been hypothesised that the electrostatic interaction of the short, highly basic motifs of MTPs with the cell surface allows the labelled proteins to remain attached to cells during washing, and that this protein may constitute a 'reservoir' that is released when the membrane is disrupted during fixation (Lundberg and Johansson, 2001). Recently, rapid association of the Tat PTD with cell membrane components, rather than its uptake, was demonstrated by FACS analysis, where a decreased number of live cells exhibiting GFP fluorescence are observed following trypsin treatment (Richard et al., 2003).

Such dependence of association of MTPs with components of cell membranes for their subsequent uptake has been observed. The original studies on HIV Tat implicated heparan sulphates (HS) to be low-affinity binding sites for HIV Tat (Frankel and Pabo, 1988). Cells genetically defective in the biosynthesis of fully sulfated HS have been shown to be selectively impaired in the internalization of recombinant Tat fused to GFP, as evaluated by both flow cytometry and functional assays (Tyagi et al., 2001). Polysialic acid appeared to act in a similar way for the antennapedia homeodomain (Bloch-Gallego et al., 1993). It is worth noting that cations that bind to cell-surface heparans may be internalised by endocytosis (Fuki et al., 2000).

The redistribution artefact observed following fixation with organic solvents could result from subsequent electrostatic interactions between the same basic motifs and oligonucleotide molecules within the cell, which are particularly concentrated in the nucleus. However, recent investigations of the Tat PTD, using both live (Richard et al., 2003) and paraformaldehyde fixed cells (Koppelhus et al., 2002; Sandgren et al., 2002), have shown not only intense

membrane association, but also intercellular localisation almost exclusively within endosomal structures. The involvement of endocytosis in uptake of exogenous MTPs is also appealing as early experiments showed enhanced translocation of HIV Tat when cells were also treated with lysomotropic agents (Frankel and Pabo, 1988). Taken together these observations suggest that rapid electrostatic interaction with cell membranes, causing enrichment of MTPs at the cell surface, followed by uptake through the well-characterised process of endocytosis, may be a more plausible mechanism for their uptake than an unconventional, energy-independent, non-endocytotic process.

However, despite the compelling studies demonstrating the uptake of fusion proteins by these peptides, quantitative analysis shows that this uptake may not be as efficient as first stated. For example, Falnes *et al.* undertook studies using low-dose VP22 or Tat PTD fused to diphtheria toxin A (dtA) (Falnes et al., 2001). In the context of a holotoxin with diphtheria toxin B (dtB), dtA is able to efficiently translocate to the cytosol where the presence of a single dtA molecule is sufficient to kill a cell (Falnes et al., 2000). Though considerable cell-associated MTP-conjugated dtA was detected, substantially more so than the wild-type toxin itself, no cytotoxicity was detected. With the protein concentrations used these results indicated that these carrier proteins were at least 4 orders of magnitude less efficient than dtB in translocating dtA to the cytosol (Falnes et al., 2001). Though success was reported using a similar approach with penetratin as the delivery vector, any cytotoxicity was only detected using fusion protein concentrations 1,000 fold above wild-type toxin levels, and at these concentrations only a slightly higher toxicity was detected than application of dtA alone (Keller et al., 2001). The concentration of MTP fusion protein applied to cells in culture before the any biological effect is observed is relatively high, at a concentration of around 0.1 μM (Bennett et al., 2002; Nagahara et al., 1998). This is in contrast with the low ligand concentrations needed to trigger responses in other biological pathways such as receptor-mediated internalisation (10^{-10} to 10^{-11} M) (Arora and Leppla, 1994; Arora et al., 1994; Falnes et al., 2000).

A single pharmacokinetics study has been carried out to assess delivery efficacy of MTPs. This study, undertaken by Lee and Pardridge, explored a number of parameters associated with the delivery of TAT and TAT-protein conjugates to tissues *in vivo* (Lee and Pardridge, 2001). The work showed that there was near instantaneous clearance from the plasma by all tissues of femoral vein injected rats by unconjugated TAT-biotin. TAT-biotin/streptavidin conjugate clearance was reduced about 20-fold relative to that of the unconjugated TAT peptide, but this was about 20-fold higher than the clearance of unconjugated streptavidin. However, pharmacological effects *in vivo* are measured not by the organ clearance parameter, but by the organ uptake (percent injected dose (%ID) per gram of tissue), which is a function of both membrane permeability, and of the area under plasma concentration curve (AUC). The AUC is a measure of the amount of drug available for delivery, within the plasma, over a specified time following an injected dose. A point of interest of this study was that the marked increase in the rate of removal of the conjugated protein was reflected by a reduced plasma AUC. These have offsetting effects on the organ %ID/g, and as a result the organ %ID/g of streptavidin is not increased in proportion to the increase in the membrane permeation caused by its conjugation to the Tat PTD, as may be expected.

However, it is clear from the large number of studies showing biological activity attributable to cargo proteins transported to the inside of target cells, by MTPs, that some form of transfer is occurring. Rather than belonging to a novel family of translocatory proteins, HIV Tat, antennapedia, and VP22, and their PTDs may instead be additional members to a family of molecules that have been known for many years to enhance the delivery of many different molecules, members of which include polyethyleneimine, poly-L-lysine, and various lipids – cationic reagents.

The ability of polylysine to improve the uptake of associated protein was demonstrated 25 years ago (Shen and Ryser, 1978), and this process has been shown to rely on non-receptor-mediated (i.e., nonsaturable) adsorptive endocytosis (Ryser et al., 1982). It may be that in generating fusion proteins with membrane translocatory proteins or peptides that cationic activity mediated

by the PTD is tightly co-localised with the molecule of interest, in a similar manner to the generation of complexes during transfection procedures (Leifert and Whitton, 2003). Indeed, by simply mixing plasmid DNA with the Tat PTD transfer of DNA into cells can be enhanced, albeit less effectively than cationic lipids (Futaki et al., 2001).

The current data and understanding of these proteins suggest that the term "protein transduction domain" should be reconsidered (Falnes et al., 2001; Green et al., 2003; Leifert et al., 2002; Richard et al., 2003). Perhaps a term that would more accurately reflect the mode of action upon which the biological effects rely would be the term "integral cationic region" (Leifert and Whitton, 2003).

1.5 Aims

Internalisation of exogenous macromolecules, in particular proteins, by live cells provides a powerful approach for studying cellular functions. More significantly, transfer of proteins from the extracellular milieu to the cytoplasm and nucleus could also contribute to the development of new therapeutic approaches. A number of proteins, and peptides derived from them have shown the unexpected properties of membrane translocation and protein transduction, allowing such a transfer to take place. Such peptides are known as membrane translocating proteins/peptides (MTPs). This study focused on an investigation of the most widely studied MTPs; the HIV Tat protein, the *Drosophila* antennapedia protein and the Herpes Simplex Virus type 1 (HSV-1) VP22 protein, and the peptides derived from them (the Tat protein transduction domain (PTD) and penetratin for Tat and antennapedia, respectively).

Though the potential of these peptide sequences to deliver cargo polypeptides has been extensively studied following the initial observations of the transduction potential of MTPs, 1994 for Tat (Fawell et al., 1994), 1992 for the antennapedia homeodomain (Perez et al., 1992), and 1997 for VP22 (Elliott and O'Hare, 1997), little work has been carried out to quantify the degree to which this protein transduction occurs (Ye et al., 2002). More importantly, for the potential of these sequences in therapeutic applications to be realised, direct comparisons of transduction efficiency is desirable, to enable the selection of favourable candidates for further, focused investigation. The aim of this study was to develop a system whereby the protein transduction efficiencies of the Tat PTD, penetratin and VP22 could be compared quantitatively.

Throughout the course of this study a reporter has been sought which would satisfy the following criterion: the reporter must be a protein capable of providing a detectable signal. The focus of this research was to develop a protocol by which comparative quantification of the transport efficiency of MTPs could be undertaken in order to find suitable candidates for use in protein therapy approaches. It is possible to use small molecules, or peptides as reporter molecules, but such a reporter would tell nothing of the ability of the vectors to

a transport a target protein, and for that protein to still be capable of eliciting its desired effect within the target cells.

Three different proteins were investigated to explore their suitability as reporters for quantification of protein transduction in a *de novo* synthesis system. Expression vectors were designed to encode specific reporter proteins in-frame with each MTP, enabling expression of MTP-reporter fusion proteins in transfected mammalian cells. The ease with which transduction of the reporter protein could be detected from transfected to non-transfected cells was then investigated.

The three reporters were the green fluorescent protein (GFP), luciferase, and an analogue of caspase-3 lacking the pro-domain found in the wild-type protein, pro-less caspase-3 (PLCasp3). The reporter proteins GFP and luciferase were utilised with the aim of capitalising on the information available for undertaking assays with these well-characterised reporters. It was hoped that at least one of the two systems would enable rapid development of a protocol to assess the protein transduction capabilities of the tested MTPs. There has been little work undertaken with the third protein (Meergans et al., 2000; Pop et al., 2001), and these have focused on examining the properties of the caspase-3 analogue itself. By using such an enzyme the aim was to examine the potential of harnessing an endogenous signaling pathway to monitor protein transduction. Such an approach has the potential to allow development of a system with sensitivity analogous to the harnessed pathway.

CHAPTER 2
MATERIALS AND METHODS

2.1 Large-Scale DNA Preparation

A number of different vectors were used during the course of these studies. The method that follows was used to produce milligram quantities of each of the plasmids used throughout the course of this work for transfection experiments and cloning procedures. Presented here are the steps required to propagate, isolate, purify and quantify any of the plasmids.

2.1.1 Plasmid Propagation

Escherichia coli strain JM109 was used for the propagation of all of the plasmids. Competent *E. coli* JM109 cells were prepared as described (appendix B) and transformed with the appropriate plasmid using the heat shock technique (appendix B). A single colony of *E. coli* JM109 containing the appropriate plasmid was isolated from a LB agar plate supplemented with ampicillin (125 µg/ml) and inoculated into 250 ml of LB broth containing the same antibiotic. This culture was grown overnight at 37 °C on a shaking incubator at 300 rpm.

2.1.2 Plasmid Isolation and Purification

The plasmid was isolated and the cell lysate purified using a modified version of the alkaline lysis method described by Sambrook *et al.* (Sambrook et al., 1989). Cells were pelleted by centrifugation at 5000 rpm for 15 minutes in a Beckmann floor centrifuge. The cell pellet was resuspended in 5 ml ice-cold alkaline lysis solution I (20 % glucose, 1 M Tris-HCl pH 8.0, 0.5 M EDTA pH 8.0). The suspension was transferred to a 50 ml centrifuge tube (Greiner Labortechnik Ltd, Germany) and placed on ice. Ten millilitres alkaline lysis solution II (0.2 M NaOH, 1 % SDS) was added and the suspension mixed by inverting the tube 3 or 4 times. The suspension was incubated on ice for 10 to 15 minutes. Seven and a half millilitres alkaline lysis solution III (3 M potassium acetate, 11.5 % v/v glacial acetic acid) was added, the solution mixed by vortexing, and incubated on ice for 15 minutes. Cell debris was removed by centrifugation at 7500 rpm for 15 minutes and the supernatant decanted into a sterile 50 ml

centrifuge tube. One hundred microlitres RNAseA solution (10 mg/ml) was added to the supernatant prior to incubation in a water bath at 37 °C for 30 to 60 minutes. Ten millilitres of phenol:chloroform:isopropanol (25:24:1) solution was added and the phases mixed by vortexing. The resulting emulsion was centrifuged as before. The clear- (upper-) phase was transferred to a clean 50 ml centrifuge tube. Twenty-three microlitres 100 % ethanol was added and the solution mixed by vortexing. The solution was centrifuged as before following incubation at room temperature for 1 to 2 minutes. The supernatant was decanted and the pellet washed briefly in 5 ml 70 % ethanol. The tube was inverted over paper towels and the pellet left to dry. The pellet was resuspended in 555 µl water and transferred to a 1.5 ml microcentrifuge tube (Tyco Healthcare Group, MA, USA). One hundred and six microlitres 5 M NaCl (in water) and 172 µl 50 % PEG_{6000} (in water) were added and the solution was vortexed. The solution was then incubated on ice for 30 minutes. The plasmid was pelleted by centrifugation at 13,000 rpm for 15 minutes in a MicroCentaur centrifuge (MSE, UK) and the supernatant was removed with a pipette. The DNA pellet was washed with 1 ml 70 % ethanol, which was removed immediately, and the pellet air dried for 15 minutes. The isolated DNA was dissolved in 300 µl TE buffer (10 mM Tris-Hcl pH 8.0, 1 mM EDTA pH 8.0) and stored at –20 °C.

2.1.3 Sample Purity and Quantification

For quantification of plasmid DNA, a 5 µl sample was diluted to 1 ml with water and the absorbance of the solution measured at 260 nm (A_{260}) and 280 nm (A_{280}) on a GeneQuan II spectrophotometer. Five microlitres TE buffer diluted to 1 ml in water was used as a standard reference. The display gave the calculated concentration of the original solution. The purity of the sample was calculated as follows:

$$\text{Ratio} = \frac{A_{260}}{A_{280}}$$

Ratios between 1.75 and 1.90 were consistently obtained.

2.2 Cell Culture

2.2.1 Solutions

2.2.1.1 Water

Fresh Milli-Q water was used for the preparation of all culture media and solutions and was obtained from a Milli-Q PF Plus system with ultrafiltration cartridge (Millipore UK Ltd).

2.2.1.2 Phosphate Buffered Saline

Phosphate buffered saline solution (PBS) tablets without magnesium or calcium ions were obtained from Oxoid Ltd, UK. One tablet was dissolved in 100 ml of Milli-Q water with a final pH of 7.3. Solutions were sterilised by autoclaving at 121 °C for 15 minutes.

2.2.1.3 HEPES Buffered Saline

HEPES acid, 0.554 g, was dissolved in 100 ml water and the pH titrated to 7.05 with 5 M NaOH. The solution was filter sterilised (0.2 μm acrodisc) and 10 ml aliquots were stored at –20 °C until required.

2.2.1.4 Trypan Blue

Trypan blue, used for assessing cell viability, was obtained from BDH Laboratory Reagents Ltd and was prepared as a 0.1 % (w/v) solution in PBS.

2.2.1.5 Trypsin

Trypsin was obtained at 10x concentrate (2.5 % [v/v]) and was prepared as a 0.25 % (v/v) solution in PBS and filter sterilised (0.2 μm acrodisc).

2.2.1.6 Polyethyleneimine

Polyethyleneimine (PEI), Mr = 25 kDa, was obtained from Sigma-Aldrich. A stock solution of 20 mM PEI in Milli-Q water was prepared, neutralised with 0.1 M HCl and filtered (0.2 μm acrodisc). The PEI solution was stored at 4 °C.

2.2.1.7 Formaldehyde Solution

Paraformaldehyde obtained from Sigma-Aldrich was dissolved in PBS at 70 °C to prepare a 4 % (w/v) solution. The solution was allowed to cool to room temperature, adjusted to a final pH of 7.4, and stored at 4 °C. A fresh solution was prepared monthly.

2.2.2 Caspase-3 Inhibitors

The caspase-3 inhibitor N-Acetyl-Asp-Glu-Val-Asp-al (AC-DEVD-CHO) was obtained from Sigma-Aldrich. A 10 mM stock solution was prepared in DMSO and stored at –20 °C until required. Further dilutions were performed in OptiMEM and used immediately.

The cell permeable caspase-3 inhibitor Ac-Ala-Ala-Val-Ala-Leu-Leu-Pro-Ala-Val-Leu-Leu-Ala-Leu-Leu-Ala-Pro-Asp-Glu-Val-Asp-CHO (cp-DEVD-CHO) was obtained from BD Biosciences (Abingdon, UK). A 1 mM stock solution was prepared in DMSO and stored at –20 °C. Further dilutions were performed in OptiMEM and used immediately.

2.2.3 Culture Media and Additives

All solutions used for the preparation of culture media for mammalian cells were obtained from Gibco-BRL, Paisley, unless otherwise stated. Dulbecco's Modified Eagle's Medium (DMEM) and OptiMEM were obtained at 1x concentrates and were supplied with sodium bicarbonate, GLUTAMAX I (L-Alanyl-L-Glutamine, a stable glutamine dipeptide used in place of L-Glutamine), and contained phenol red as an indicator. OptiMEM was supplied supplemented with trace elements and growth factors. Modified Eagle's Medium non-essential amino acids solution (MEM-NEAA) and penicillin (10,000 IU/ml)/streptomycin (10,000 µg/ml) were obtained as 100x concentrates. Heat inactivated foetal bovine serum (FBS) were used in growth media.

Growth media were prepared aseptically according to the formulae shown below in table 2.1, stored at 4 °C, and used within 4 weeks of preparation.

Reagent	DMEM (10 % [v/v] FBS) Volume (ml)
DMEM 1x	440
FBS	50
Pen-Strep 100x	10
MEM-NEAA 100x	5

Table 2.1. Formulae for the preparation of cell culture media

2.2.4 Additional Antibiotics

Tetracycline (Tc) and doxycycline (dox) were obtained from Sigma-Aldrich. A 1 mg/ml stock solution of Tet was prepared in ethanol and stored in the dark at –20 °C. A 1 mg/ml stock solution of dox was prepared in sterile Milli-Q water and stored in the dark at –20 °C. G418 was obtained from Sigma-Aldrich as a 50 mg/ml solution and was stored in the dark at 4 °C.

Staurosporine was obtained from Sigma-Aldrich. A 1 mM stock solution was prepared in DMSO.

2.2.5 Equipment

2.2.5.1 Laboratory Equipment

All aseptic techniques were carried out in a laminar flow cabinet (MDH, UK) designed for vertical re-circulation of air. Cells were cultured in an LEEC PF2 anhydric incubator. Growing cells were viewed daily under an inverted light microscope. For determination of cell concentration in suspension, appropriately diluted samples were counted on a standard double grid haemocytometer (Neubauer 0.1 mm Dept, Weber, UK).

2.2.5.2 Disposable Items

Sterile 25 cm^2, 75 cm^2 and 175 cm^2 filter top tissue flasks; 96-, 12-, and 6-well plates, 60 mm diameter culture dishes and sterile cell scrapers were obtained

from Helena Biosciences, UK. Ninety millimetre diameter culture dishes were obtained from Fisher Scientific, UK. Cryopreservation ampoules used for storing frozen cells in liquid nitrogen were obtained from Corning, UK.

2.2.6 Culture Methods

2.2.6.1 Cell Lines

All cell lines were maintained at 37 °C in a humidified atmosphere consisting of 95 % air/5 % CO_2 (v/v). Cells were visualised on a daily basis to assess growth and to check for evidence of microbial contamination.

The COS-7 cells, an SV40 transformed African green monkey kidney cell line, were obtained from the European Collection of Animal Cell Cultures (ECACC, Porton Down, Salisbury, UK). The rat embryo derived Rat-1 cell line and the transformed human cervical epithelioid carcinoma derived HeLa Tet-Off cell line (Clontech) were already present in the laboratory. All cells were grown in DMEM containing 10 % (v/v) FBS. The media was supplemented with 200 µg/ml G418 for maintenance of HeLa Tet-Off cells. For routine culture, cells were subcultured 1 in 8 twice weekly (or 1 in 20 weekly) and the media changed every 48 hours.

2.2.6.2 Subculturing

Cell lines were grown as adherent monolayer cultures and subcultured at 80-100 % confluence. For subculture, 75 cm^2 flasks were rinsed twice with 3 ml aliquots of PBS and then incubated with 2 ml 0.25 % trypsin for approximately 6 minutes. Detached cells were diluted to 15 ml with complete culture medium and transferred to a 50 ml centrifuge tube. The suspension was centrifuged at 1000 rpm for 8 minutes, and the supernatant discarded. The cells were resuspended in 1 ml complete culture medium. Three or 4 ml additional media were added and 200 µl or 500 µl of this suspension transferred into a sterile 75 cm^2 flask containing 10 ml fresh culture medium (for 1 in 20 or 1 in 8 subcultures, respectively) for subsequent culture.

2.2.6.3 Determination of Cell Concentration

Following the detachment of cells from a flask and pelleting of the cells, the cells were resuspended in 1 ml medium and the cell suspension was briefly pipetted to break up clumps of cells. Ten microlitres of suspension was added to 40 µl of PBS and 50 µl of 0.1 % (w/v) Trypan blue solution. Six microlitres of this sample was loaded on to a grid haemocytometer under an overlaying coverslip. Viable cells were detected by a bright 'halo' light around their cell membranes whereas dead cells were permeabilised and stained blue. The viable cell numbers in the four squares surrounding the central square were counted using an inverted light microscope. The viable cell concentration in the original suspension was calculated using the following equation:

$$\text{Cells per ml} = \frac{\text{Total cell count in 4 chamber x } 10\text{x}10^4}{4}$$

2.2.6.4 Cell Storage and Recovery

Cells were prepared for storage by the detachment of a near confluent monolayer from a 75 cm^2 flask according to the standard protocol (see 2.2.4.1) followed by centrifugation at 1000 rpm for 8 minutes. The supernatant was then discarded and the cells resuspended in 10 ml filter sterilised (0.2 µm acrodisc) culture medium supplemented with 10 % (v/v) dimethyl sulphoxide (spectrophotometric grade, Aldrich, UK) as a cryopreservative. Cell suspensions were then dispensed in 1 ml aliquots into cryopreservation ampoules, placed in an insulated freezer box and transferred to a –80 °C freezer (Lab Impex research, UK) to cool to –80 °C overnight. The cells were then transferred to a Linde liquid nitrogen freezer where they were stored at approximately –148 °C.

For cell recovery from frozen stocks, the contents of an ampoule was thawed in a 37 °C water bath for five minutes and transferred to a 15 ml centrifuge tube (Helena Biosciences, UK). Ten millilitres of fresh medium was added to the thawed cells drop wise, with mixing by inversion after addition of every ~2-3 ml medium. Cells were centrifuged for 8 minutes at 1000 rpm and the supernatant was discarded. The cells were then resuspended in 1 ml fresh medium and

transferred to a 75 cm^2 flask containing 10 ml fresh medium and subsequently incubated under standard conditions. Cells were cultured for at least two passages in order to establish them before any experiments were carried out.

Where cells were purchased from the ECACC they were supplied in the form of frozen ampoules. These were stored in a liquid nitrogen freezer until required. The cells were recovered according to the supplied protocol. This followed the standard protocol, but the resuspended cells were transferred to a 25 cm^2 flask containing 5 ml fresh medium and then incubated under standard conditions. Again, cells were cultured for at least two passages in order to establish them before any experiments were carried out or stocks were prepared for storage.

2.2.7 Transfection of Mammalian Cells

Mammalian cell transfection was undertaken by use of either polyethyleneimine or GeneJuice as a carrier. Protocols for each are outlined below.

2.2.7.1 Preparation of Polyethyleneimine Transfection Complexes

Polyethyleneimine (PEI), Mr = 25 kDa, was obtained from Sigma-Aldrich. A stock solution of 20 mM PEI in Milli-Q water was prepared, neutralised with 0.1 M HCl and filtered (0.2 µm acrodisc). The PEI solution was stored at 4 °C.

A total of 2 µg plasmid DNA was diluted to 50 µl with HBS in a sterile 0.5 ml microcentrifuge tube (Tyco Healthcare Group, MA, USA). Separately, 3 µl of PEI solution (20 mM) was diluted to 50 µl in HBS. Complexes were prepared by adding the 50 µl of PEI solution to the 50 µl of DNA. Gentle mixing of the two solutions was achieved by pipetting the solution up and down 5 times with a 200 µl Gilson pipette. The complex solution was formulated at a total DNA concentration of 20 µg/ml.

2.2.7.2 Transfection of COS-7 Cells with PEI Transfection Complexes

Transfection using PEI required exponentially growing cultures. Cos-7 cells were seeded at a density such that at the time of transfection monolayers were 40 - 50 % confluent. For both of the cell types studied this density was

determined to be 1 x 10^5 cells per 35 mm well on a 6 well plate. Where larger transfections were required the number of cells seeded onto the culture surface was increased in line with the increase in growth area. One hour prior to transfection growth medium was aspirated from monolayers of rapidly dividing cells and replaced with 1.9 ml OptiMEM, a serum-free medium specifically designed for transfection experiments. One hundred microlitres of transfection complex containing a total of 2 µg of DNA was added to each well. Transfection was carried out for 4 hours at 37 °C after which time the transfection media was replaced with fresh complete media, and cells cultured further, as required, before harvesting for analysis.

2.2.7.3 Transfection of Cells with GeneJuice

The transfection reagent GeneJuice was obtained from Novagen (Merck Biosciences Ltd, Nottingham, UK), stored at 4 °C and used within 6 months of delivery.

Routinely, cells seeded in 6-well plates were transfected. Cos-7 cells were seeded at a density of 1x10^5 cells per well and HeLa Tet-Off cells at a density of 4x10^5 cells per well 24 hours prior to transfection.

Three microlitres of GeneJuice was added to 97 µl OptiMEM. The solution was mixed by gentle vortexing and incubated at room temperature for 5 minutes. A total of 1 µl of DNA was added to the solution, mixed as before, and incubated for a further 15 minutes at room temperature. The DNA-containing solution was then added to the cells and dispersed evenly by gently shaking the growth receptacle. Cells were grown as normal until cells were harvested for analysis, normally 24-48 hours post-transfection.

2.2.8 Susceptibility of COS-7 Cells to G418

The sensitivity of the COS-7 cells to G418 was examined to determine the minimum concentration of the antibiotic necessary for almost 100 % mortality over a two week period. Thirty-five millimetre wells were seeded with 5x10^4 cells and grown as normal. Twenty-four hours after seeding, various

concentrations of G418 were applied to each well, and cells again grown as normal. At 48 hours intervals following the application of G418 cells from one well at each dose concentration were harvested by trypsinisation (incubation with 200 µl, 0.25 % trypsin for 8 minutes at 37 °C) and pelleted by centrifugation at 1000 rpm for 8 minutes. The medium was discarded and cells resuspended in 100 µl fresh medium. The number of viable cells in each sample was determined by performing cell count on a haemocytometer as outlined above (see 2.2.4.2). Remaining samples had their media changed for fresh media supplemented with G418 every 48 hours. Cell counts were performed for a total of 15 days from seeding of the wells. The amount of G418 required for 100 % mortality of Cos-7 cells over this time period was determined to be 750 µg/ml.

2.2.9 Generation of a Stable COS-7 Cell Line Expressing EGFP

Thirty-five millimetre wells were seeded with $5x10^4$ COS-7 cells and grown for 24 hours. Each well was transfected with 2 µg pEGFP-N1 using PEI as a transfection reagent. Twenty-four hours post-transfection, growth media was supplemented with 750 µg/ml G418, and cells grown as normal. Media was changed for fresh media supplemented with G418 every 72 hours. Eighteen days after transfection individual plaques of surviving cells were harvested. Media was aspirated from the wells and cells washed in PBS. Plaques were detached by application of 15 µl, 0.25 % trypsin to the individual plaques and incubation for 3 minutes at room temperature. Cells were gentle agitated from the growth surface with a pipette tip and transferred to the individual wells on a 96-well microtitre plate. Two hundred microlitres of fresh media supplemented with G418 was added per well. After 24 hours incubation, media was removed and cells detached from the growth surface by trypsinisation and harvested by the addition of 200 µl fresh media with G418. Cells were transferred to a new well to ensure even growth over well surface. In addition, 30 µl of the cell suspensions were transferred to the wells on a multi-well slide (Fisher Scientific, UK) contained within 70 mm dishes. The slides were incubated as normal and after a 24 hour period to allow adherence of the cells to the slide's surface, slides were covered with fresh medium. After a further 48 hours the

slides were washed with PBS and the presence of fluorescence within the samples confirmed under a fluorescence microscope. Colonies in the 96-well plate corresponding to those exhibiting the most consistent and brightest EGFP expression were successively grown up to give stable populations. Cell lines were harvested and stored as outlined previously.

2.2.10 Regulation of expression in HeLa Tet-Off cells

The antibiotic (tetracycline or doxycycline) was added directly at the start of transfection using concentrations as described.

2.2.11 Induction of Apoptosis

For routine induction of apoptosis cells were exposed to 1 μM staurosporine for 3 hours.

2.3 Methods for Quantifying Protein Expression

2.3.1 Detergent Lysis Method 1

After an appropriate period of incubation post-transfection, the cell monolayer was washed twice in 2 ml of PBS. The washed monolayers were treated with 250 μl of Promega lysis buffer (1x: 25 mM Tris-phosphate, pH 7.8; 2 mM DTT; 1,2-diaminocyclohexane-N,N,N',N'-tetraacetic acid; 10 % glycerol, 1 % Triton X-100 and BSA 1 mg/ml) and incubated at room temperature for 15 minutes. The cell extracts were collected and transferred to sterile micro-centrifuge tubes and vortexed for 15 seconds. Cell debris was pelleted by centrifugation at 13,000 rpm for 15 seconds in a MicroCentaur. The supernatant was transferred to a clean microcentrifuge tube and stored on ice for immediate use. For prolonged storage before assaying of the lysate, samples were snap frozen in a dry-ice/ethanol bath and stored at –80 °C.

2.3.2 Detergent Lysis Method 2

At the desired time following transfection/induction of apoptosis, media was removed from cells and transferred to a 15 ml Falcon tube. Cells were washed twice with 1 ml PBS, with washes removed and added to the saved medium.

Attached cells were incubated in 200 µl 0.25 % trypsin for 8 minutes at 37 °C. Cells were harvested by the addition of 1 ml PBS and transferred to the Falcon tube. Cells were pelleted from suspension by centrifugation at 1,000 rpm for 8 minutes, and the supernatant discarded. Cells were resuspended in 1 ml PBS and transferred to a 1.5 ml microcentrifuge tube. Cells were pelleted by centrifugation at 13,000 rpm for 30 seconds in a MicroCentaur. The supernatant was discarded and cells resuspended in the 120 µl NET buffer (150 mM NaCl, 1 mM EDTA, 50 mM Tris-HCl, 0.1% Igepal CA630, pH 7.6) and incubated on ice for 15 minutes. Cell debris was pelleted by centrifugation at 13,000 rpm for 10 minutes. The supernatant was transferred to a clean microcentrifuge tube and stored on ice for immediate use. For prolonged storage before assaying of the lysate, samples were snap frozen in a dry-ice/ethanol bath and stored at –80 °C.

2.3.3 Luciferase Activity Assay

Luciferase levels within cells were quantified using the Promega luciferase assay system (Promega, UK) according to the manufacturer's instructions. As little as 10^{-20} moles (0.001 pg) of firefly luciferase can be measured using this kit. The detergent lysis protocol detailed above (see 2.3.1) was followed. After centrifugation of the cell lysate, 20 µl of room temperature cell extract (supernatant) were mixed with 100 µl of luciferase assay reagent again at room temperature. The disposable test tube containing the reaction was vortexed briefly and immediately placed in a TD-20/20 luminometer (Turner Designs, UK). The instrument settings were as follows: sensitivity 25.1, delay, 5 seconds and the integration 10 seconds. The relative activity of the samples was found by correcting for the protein content of the samples, determined by Bradford assay (see below).

2.3.4 Caspase-3 Activity Assay

Caspase-3 activity within cells was quantified using a colorimetric assay as outlined in the Oncogene Research Products apoptosis catalogue and technical guide, with alterations as noted.

To determine caspase-3 activity within the samples 105 µl of cell lysate from NET buffer lysis (see 2.3.2) was transferred to a 500 µl microcentrifuge tube. Two hundred and ten microlitres of assay buffer (50 mM Hepes, pH 7.4; 100 mM NaCl; 0.1% w/v CHAPS; 10 mM DTT; 100 µM EDTA; 10% glycerol) and 35 µl of substrate Ac-DEVD-ρNA (100 mM N-acetyl-Asp-Glu-Val-Asp ρ-nitroanilide, CN Biosciences, UK) was added to the cell lysate. The reaction mixture was mixed by briefly vortexing. One hundred microlitre aliquots were loaded on a 96 well microtitre plate (Fermentas, UK), which had equilibrated to 37 °C, in triplicate. The absorbance at 405 nm was read at 5 minutes intervals for 120 minutes in a Thermomax kinetic microtitre plate reader (Molecular Devices, UK) using SoftMax 2.3 software (Molecular Devices Corp., Menlo Park, California, USA). One hundred microlitres of 10 mM substrate was used as a blank.

The linear portion of the absorbance at 405 nm versus time plot for each sample was used to calculate the V_{max} using the SoftMax software. The V_{max} of the replicate samples were averaged, and the value of the slope for the blank sample was subtracted from these values. The relative activity of the samples was found by correcting for the protein content of the samples, determined by Bradford assay (see below).

2.3.4 Protein Assay

The luciferase and caspase-3 activity in each sample was expressed per microgram of protein by dividing the activity level per sample by the amount of soluble protein (µg) in the sample. The protein content in cell extracts was measured using the Sigma Bradford assay according to manufacturer's instructions. Measurements on 10 µl aliquots of room temperature cell extract (supernatant) from each sample were taken, and calibration curves were constructed using bovine serum albumin as a standard (see appendix A). Spectrophotometric measurements were made at 595 nm. Where the protein concentration of a sample was above the upper limit of the calibration curve the sample was diluted so the protein content of 10 µl of the diluted sample would be measurable within the limits of the calibration curve.

2.4 Fluorescence Microscopy

2.4.1 Sample Preparation for Visualisation of Green Fluorescent Protein

Coverslips (22 x 22 mm) were cleaned and sterilised by heating at 180 °C overnight. A single sterile coverslip was placed into each well of a 6 well plate and the wells filled with 2 ml DMEM. NIH 3T3 or COS-7 cells were plated onto the coverslips at a density of $1x10^5$ cells per well and allowed to adhere and grow overnight. After incubation for 16 to 24 hours the old medium was removed and replaced with 1.9 ml OptiMEM. The cells were then ready for the addition of the 100 µl of DNA complex (see 2.2.5.3). Following addition of the complexes the cells were incubated for an allotted time period. At the end of this incubation period the cells were fixed. The transfecting medium was aspirated from the cells, and the monolayer washed three times with PBS and then fixed in 4 % paraformaldehyde at room temperature for 20 minutes. The coverslips were washed twice in PBS and permeabilised in 100 % methanol at – 20 °C for 5 minutes. If no immunostaining of the cells was to be undertaken the coverslips were mounted by inverting them onto a drop of Vectashield (Vector Laboratories Inc, CA, USA) on a microscope slide. Vectashield contains an anti-oxidant that helps to prevent bleaching of the fluorescence. Excess Vectashield was removed from around the upturned coverslip and the edges of the coverslip sealed using clear nail polish. The slides were left to dry overnight, in the dark, before being cleaned. Mounted samples were stored at 4 °C.

2.4.2 Co-Culture of COS-7 Cells with Rat-1 cells

Twenty four hours post-transfection with GeneJuice, transfected COS-7 cells, and untransfected Rat-1 cells were detached from 35 mm wells by incubation with 200 µl, 0.25 % trypsin. Cells were harvested by addition of 2 ml media and cell populations were combined in a single 15 ml Falcon tube. Cells were pelleted by centrifugation at 1000 rpm for 8 minutes at room temperature. The media was discarded and cells resuspended in 1 ml fresh medium. Five hundred microlitres of the suspension was used to seed a 35 mm well containing a sterile 22 mm coverslip. Cells were grown for a further 24 hours before fixing and

staining. Cells were fixed by PFA and methanol treatment as described above (see 2.4.1).

2.4.3 Immunofluorescence

Where antibodies directed against green fluorescent protein or the rat-specific TGN38 protein were used additional steps were required, subsequent to permeabilisation with methanol and prior to the mounting of the coverslips on microscope slides. The cells were washed once with PBS and then blocked with PBS supplemented with 0.2 % BSA at room temperature for 5 minutes.

For immunofluorescent staining directed against GFP the coverslip was next inverted onto 70 µl of anti-GFP antibody (Santa Cruz Biotechnology, USA), 20 µg/ml in 0.2 % BSA, and incubated at room temperature for an hour. The coverslip was then returned to the 35 mm well and washed twice for 5 minutes in 0.2 % BSA. The cells were then washed twice for 5 minutes with PBS and the coverslip inverted onto 70 µl of the rhodamine-conjugated, anti-rabbit IgG secondary antibody (Molecular Probes, Leiden, Holland), 20 µg/ml in 0.2 % BSA. Incubation with the 2^{o} antibody was carried out for 2 hours in the dark to prevent photobleaching of the fluorophore, as were all subsequent stages of staining and mounting. The coverslip was again returned to the 35 mm well and washed as before. Cells were mounted, as above (see 2.4.1), and images obtained as described below (see 2.4.3).

For species-specific immunostaining, the coverslip was next inverted onto 70 µl rabbit polyclonal antiserum to a member of the *trans*-Golgi network (TGN), TGN38 (a gift from G. Banting, University of Bristol, UK) diluted 1:200 in blocking buffer, and incubated at room temperature for 90 minutes. The coverslip was washed twice in blocking buffer for 5 minutes, and twice in PBS alone. The coverslip was next inverted onto 70 µl, x µg/ml Alexa Fluor 564-conjugated goat anti-rabbit IgG secondary antibody (Molecular Probes, Leiden, Holland) diluted 1:300 in blocking buffer. Incubation was carried out for 2 hours in the dark to prevent photobleaching, as were all subsequent stages of

staining and mounting. The coverslip was washed as before and cells were mounted as detailed previously, and images obtained as described below.

2.4.4 Confocal Imaging

Differential-interfaced-contrast (DIC) and fluorescence images of the samples were obtained using a Zeiss LSM-510 confocal laser-scanning microscope (Zeiss LSM-510 system with inverted Axiovert microscope) equipped with a krypton-argon laser. Green fluorescent protein was imaged with excitation at 488 nm and emission from 515 to 540 nm, Alexa Fluor 564 was imaged with excitation at 568 nm and emission at 590 nm.

2.5 Fluorescence Activated Cell Sorting (FACS) Analysis

Monolayers of cells transiently washed twice with 1 ml PBS and cells detached by incubation with 200 µl, 0.25 % trypsin for 8 minutes, 37 °C. Cells were harvested by the addition of 2 ml media, and transferred to a 15 ml Falcon tube, on ice. Cells were pelleted by centrifugation at 1,200 rpm, 4 °C. Media was discarded and cells washed twice by resuspending in 1 ml cold PBS and pelleting cells by centrifugation for 30 seconds at 13,000 rpm in a MicroCentaur. Cells were finally resuspended in 1 ml cold PBS and stored on ice until processed.

Fluorescent analysis of cell populations for EGFP fluorescence, and cell sorting was performed using a Becton Dickinson FACSVantage instrument at excitation and emission wavelengths of 488 nm and 530 nm (±15 nm) using an argon laser, and a single band pass FL1-H filter. A minimum of 10^4 cellular events was analysed.

To collect EGFP-expressing cells from a mixed sample of EGFP-expressing and non-expressing cells, a non-fluorescent population of cells was analysed. A high-fluorescence capture gate was set so that less than 0.5 % of the non-population fell within the gated region. To sort cells, a minimum of $5x10^5$ events was analysed using a gated region, as determined above. Cells collected

from this high-fluorescence bracket were pelleted and resuspended in a suitable volume, routinely 200 µl, cold PBS before the sample was re-analysed.

2.5 SDS-PAGE and Western Blots

2.6.1 Sample Preparation

Following extraction of the cytosolic fraction from cells by detergent lysis, protein content was determined by Bradford assay. Samples were diluted to 0.4 mg/ml in 1x SDS sample buffer (10 % w/v SDS; 50 % v/v glycerol; 0.2 M Tris, pH 6.8; 5 % v/v 2-β-mercaptoethanol; two grains bromophenol blue), and boiled for 3 minutes. Samples were stored on ice (short term), or at –80 °C.

2.6.2 SDS-PAGE

Polymerisation of a 10 % running gel (10% v/v acrylamide (Sigma Aldrich, UK); 0.375 M Tris, pH 8.8; 0.15 % w/v SDS) was induced by the addition of 50 µl, 10 % w/v ammonium persulphate (APS) and 20 µl TEMED, with thorough mixing. The running gel was poured into the assembled apparatus (BioRad, UK) to about 5 mm below the level the bottom of the wells would descend to when the comb was inserted. A layer of water-saturated n-butanol (Sigma, UK) was pipetted on top of the gel and the gel allowed to set. The butanol was removed, and stacking gel (4 % v/v acrylamide; 0.125 M Tris, pH 6.8; 0.15 % w/v SD) poured. Polymerisation induced by the addition of 50 µl, 10 % w/v APS and 20 µl TEMED). A comb was carefully inserted ensuring no air was trapped within the wells. Once the gel had set the apparatus was transferred to a gel tank (BioRad, UK) containing 1X running buffer (0.3 % w/v Tris-HCl; 0.2 M glycine; 0.1 % w/v SDS). Eight micrograms of prepared sample was loaded per well together with a positive control, and molecular weight markers. Samples were run at 50 V for 25 minutes, until they had reached the bottom of the stacking gel, and then at 180 V for a further hour.

Gels were stained in coomassie blue stain (Sigma Aldrich, UK) for 3 hours and incubated overnight on a rocker in de-stain buffer (10 % v/v acetic acid; 50 % v/v methanol). Stained gels were rinsed in water and dried between two sheets of gel drying membrane (Promega, UK) in a gel-drying frame (Promega, UK).

2.6.3 Western Blots

Following separation of sample proteins by SDS-PAGE the gel was removed and equilibrated in 1X trans-blot buffer (0.3 % w/v Tris-HCl; 0.2 M glycine; 20 % v/v methanol) for 15 minutes. All trans-blot equipment (BioRad) was also equilibrated in 1x trans-blot buffer for 15 minutes prior to apparatus assembly. Following assembly the cassette was inserted into a gel tank containing1X trans-blot buffer, and protein transferred to the membrane by the application of 100 V across the gel and membrane for 60 minutes. Protein transfer was confirmed by staining the membrane in Ponceau S solution (Sigma Aldrich, UK). The stain was removed by briefly rinsing in water.

The membrane was incubated in blocking buffer (5 % Marvel skimmed milk powder in PBS) overnight. The membrane was sealed into small plastic envelopes containing primary antibody (2 ml, 1:1000 dilution of 1 mg/ml goat anti-luciferase antibody (Promega, UK) in blocking buffer, previously subtracted against COS-7 cells (see below)), and incubated overnight on a rocker, at room temperature. The membrane was then removed from the envelope and washed three times in PBS supplemented with 0.1% v/v Tween-20, and a further three times in PBS alone. The secondary antibody (25ml, 1:10,000 dilution rabbit anti-goat IgG horseradish peroxidase-conjugated antibody (Sigma Aldrich, UK) in blocking buffer) was applied, and the membrane incubated on a rocker for 45 minutes, at room temperature. The membrane was washed as before. ECL reagent (Amersham Pharmacia and Biotech, UK) was prepared by adding 0.5 ml Solution A to 0.5 ml Solution B according to the manufacturers instructions, and incubating for 1 minute. One millilitre prepared ECL reagent was applied to the membrane for one minute, the excess removed, and the membrane wrapped in Saran wrap. Hyperfilm film (Amersham Pharmacia and Biotech, UK) was exposed to the membrane in a light-proof cassette for one hour, and developed.

2.6.4 Antibody Subtraction

Following transfer of proteins from lysed COS-7 cells onto nitrocellulose membrane, the membrane was incubated in blocking buffer overnight. The

membrane was next sealed in a small plastic envelope containing primary antibody (2 ml, 1:1000 dilution of goat anti-luciferase antibody in blocking buffer). The membrane was incubated on a rocker overnight, at room temperature. The antibody solution was carefully removed from the membrane and transferred to a cryotube (Helena Bioscience, UK). Subtracted antibody was stored at –20 °C.

CHAPTER 3
GREEN FLUORESCENT PROTEIN AS A REPORTER FOR PROTEIN TRANSDUCTION

3.1 Introduction

There are a number of reporters that are universally used to confirm the presence of a protein in a sample (by use of fusion proteins for example), or to determine effect changes to a promoter/enhancer region have on gene expression. Where the of study protein transduction is concerned the most common reporter by far is the green fluorescent protein (GFP). This is usually a tool for showing that the process of transduction has occurred, and to visualise the subcellular localisation of the transported protein within the target cell. A similar approach has been to use the enzyme β-galactosidase (β-gal). This can be visualised in a manner similar to that of GFP, but has an advantage in that, as an enzyme, any signal is amplified providing there is sufficient substrate available. However, endogenous, ubiquitously expressed proteins within cells and tissues can also act on the β-gal substrate, giving rise to background noise and potential false-positive results.

The green fluorescent protein (GFP) is coded for by the *gfp* gene from the jellyfish *Aequorea victoria*. Purified GFP, a protein of 238 amino acids, absorbs blue light (maximally at 395 nm) and emits green light (peak emission at 509 nm). This fluorescence is very stable, has no requirement for exogenous substrates or cofactors, and is not destructive to tissues (Chalfie et al., 1994). GFP can be visualised at a high resolution using laser-scanning confocal microscopy, which allows the precise localisation of the fluorescence. Various mutated forms of GFP have been engineered to enhance the wild-type's emission signal, alter the absorption wavelength or the emission spectrum to change the colour of the fluorescent signal, or to improve upon the stability of the protein for use in model systems. A comprehensive review by Roger Tsien (Tsien, 1998) discusses GFP and its isoforms. For the work undertaken here, the class 2 GFP mutant F64L, S65T, enhanced GFP (EGFP), was used. This has an

altered emission spectrum, allowing visualisation with a fluorescence microscope using the readily available FITC filter set, and has a fluorescence signal with a magnitude over twenty times that of wild-type GFP.

GFP has been used for a number of protein transduction studies of both TAT and VP22 (Aints et al., 2001; Brewis et al., 2000; Del Gaizo and Payne, 2003; Elliott and O'Hare, 1999a; Elliott and O'Hare, 1999b; Fang et al., 1998; Harms et al., 2000; Koshizuka et al., 2001; Lai et al., 2000; Liu et al., 2001; Lundberg et al., 2003; Wybranietz et al., 1999), but there has been only one account of trafficking of GFP in fusion with penetratin (Han et al., 2000).

Three approaches were examined to explore protein transduction of MTP-EGFP fusion proteins. The first approach used indirect immunofluorescence (IF) analysis to detect the fusion proteins. The primary antibody was an anti-GFP antibody, and the secondary antibody was rhodamine-conjugated. It was hoped that an indirect approach would allow visualisation of the fusion proteins in situations where diffusion of the proteins following transduction reduced the fluorescence of EGFP to levels below those detectable by confocal microscopy. The indirect approach would also enable detection of protein that had been denatured, possibly as a result of the transduction process. The second approach was to utilise IF to differentiate transfected cells expressing the fusion proteins from recipient cells that were not transfected. In doing this co-localisation of direct EGFP fluorescence and IF would indicate the presence of fusion protein in a cell that was not expressing it. The final approach was to examine live cells by FACS. This would avoid any possible artefacts introduced during fixation, and allow analysis of large samples of cells for variation in the number EGFP-positive cells, and the distribution of fluorescence within the samples.

3.2 Results

3.2.1 Control Transfections with EGFP-N1 Alone

To observe protein translocation of the MTP-EGFP fusion proteins from transfected cells to untransfected cells, a level of transfection was required that would result in isolated transfected cells on a background 'carpet' of untransfected cells. By varying the amount of pEGFP-N1 expression vector used for a transfection, a suitable amount could be determined for future experiments. However, for successful polyethyleneimine (PEI)-mediated transfection it is important for the nitrate to phosphate charge ratio of PEI to DNA to remain constant at around 9. This requires 2 μg of DNA for 3 μl of PEI (20 mM). To ensure the amount of DNA in each transfection remained constant at 2 μg, where less than 2 μg of pEGFP-N1 was used, the amount of DNA in each transfection was made up to a total of 2 μg with the non-specific DNA. The DNA of choice was the expression vector pcDNA3.1(+). To ensure that transfection with this DNA would not affect fluorescence images, transfections of COS-7 cells were carried out using 2 μg pcDNA3.1(+) alone. Cells were fixed 48 h post-transfection by sequential treatment with paraformaldehyde (PFA) and methanol, and mounted cells were examined using laser-scanning confocal microscopy. Figure 3.1. shows transfected cells imaged at 10x and 40x magnifications. No cells exhibited any fluorescence. The fluorescence observed at the higher magnification is autofluorescence. The detector gains were raised until autofluorescence was visualised to demonstrate that not even low levels of GFP fluorescence were present.

COS-7 cells were then transfected with varying amount of pEGFP-N1 by PEI-mediated transfection. Cells were fixed 48 hours post-transfection, as before, and examined using by laser-scanning confocal microscopy. Figure 3.2 shows cells treated with decreasing amounts of pEGFP-N1 at x10 magnification. For studies using 2000 ng to 200 ng of pEGFP-N1 the amount of EGFP expression

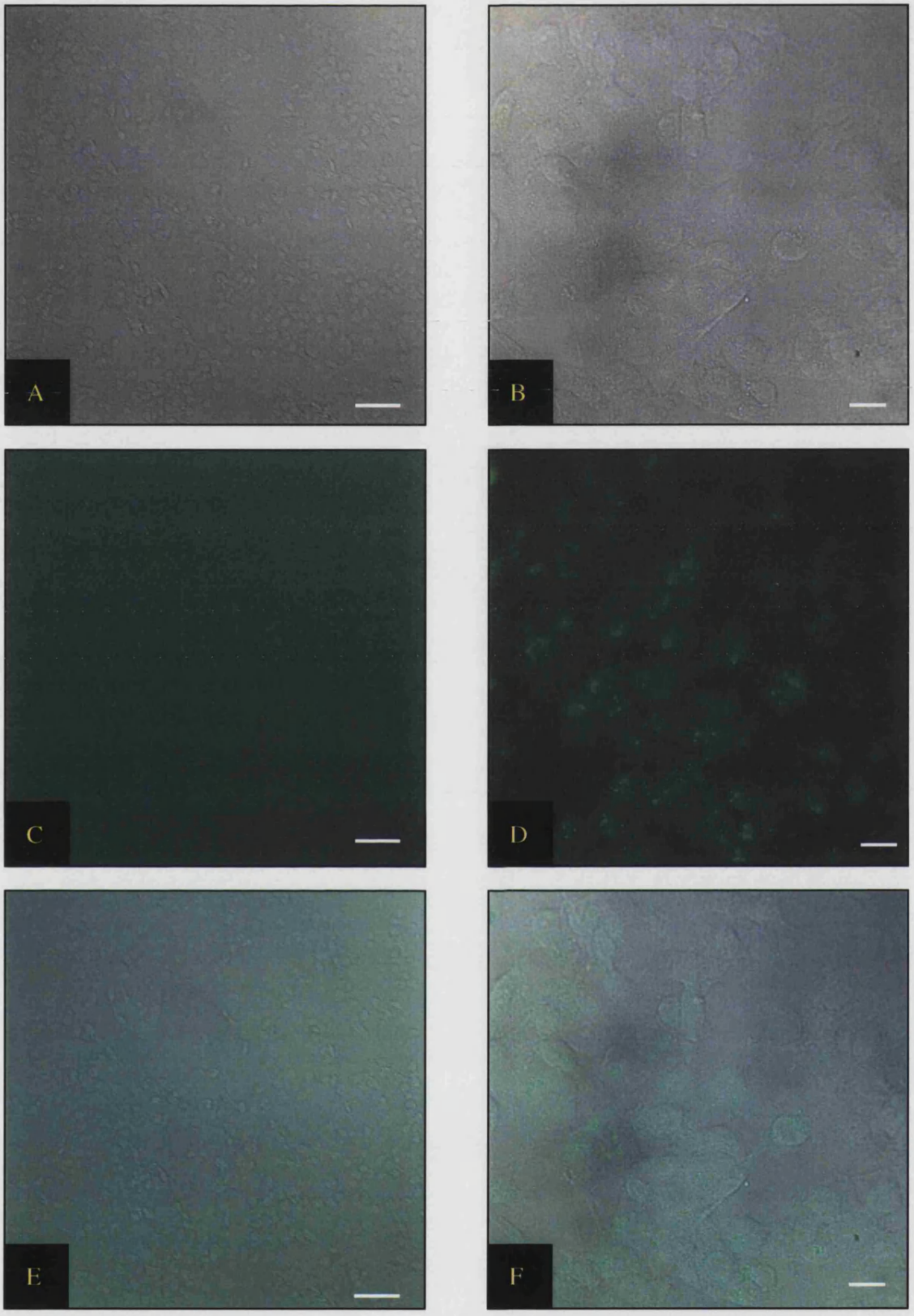

Figure 3.1. Transfections with pcDNA3.1(+). COS-7 cells were transfected with 2000 ng of the vector pcDNA3.1(+) as a control. Images A and B are confocal DIC images. Images C and D are confocal images, excitation 488 nm, FITC filter. Images E and F are overlays of panels A and C, and B and D, respectively. Images A, C and E are at 10x magnification (bars indicate 100μm) and images B, D and F are at 40x magnification (bars indicate 20 μm).

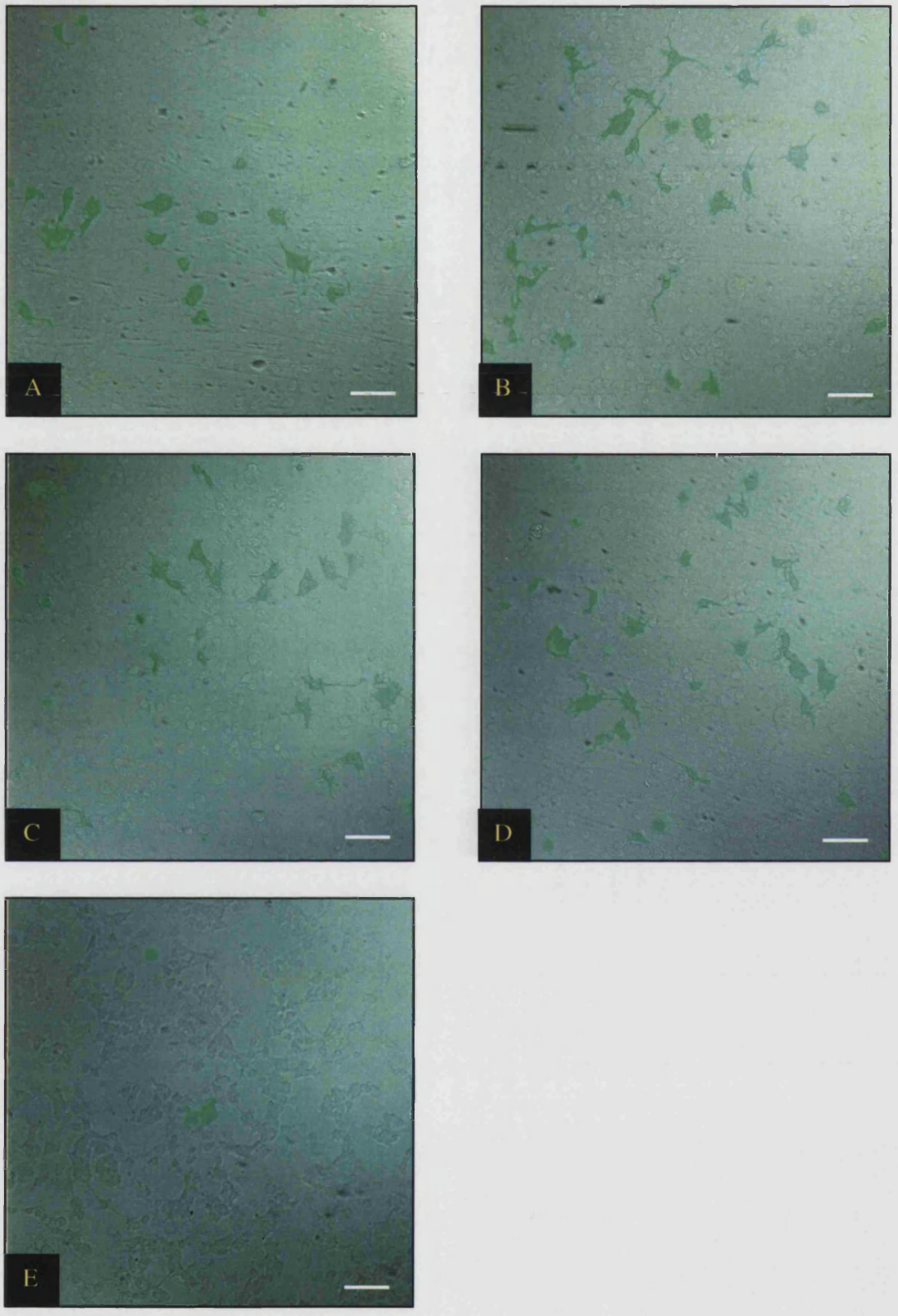

Figure 3.2. COS-7 cells transfected with pEGFP-N1. Images are confocal images, excitation at 488 nm, FITC filter, overlaid onto DIC images of the same cells. Transfections were carried out using 200 ng, 100 ng, 50 ng, 10 ng and 5 ng pEGFP-N1 per 35 mm well (A to E, respectively). Bars indicate 100 μm.

vector used in the transfections appeared to have little affect on the number of fluorescent cells observed in any one visible frame. Images for transfections using more than 200 ng pEGFP-N1 are not shown. An appreciable difference was only observed when just 5 ng pEGFP-N1 is used in the transfections. The images were captured using setting identical to those for the pcDNA3.1(+) transfection experiments, which results in very intense fluorescence preventing visualisation of any detail in the transfected cells. The experiment was carried out on a minimum of three separate occasions to confirm observations, and the images are representative examples from a single set of transfections.

3.2.2 An Immunofluorescence Analysis Approach

Transduction of EGFP from expressing cells by the MTPs could result in diffusion of the fusion protein throughout the cultured cells. This could result in the recipient cells possessing insufficiently concentrated EGFP to allow detection of the fusion protein by direct fluorescence analysis. Similarly, it is possible that during the process of translocation the fusion proteins could be subjected to some degree of denaturation, resulting in loss of fluorescence. An indirect IF approach was adopted that would allow the detection of the EGFP fusion proteins. A primary rabbit anti-GFP antibody would bind to each of the EGFP fusion proteins. A rhodamine-conjugated mouse anti-rabbit IgG antibody would then allow visualisation of the proteins at a different excitation wavelength from direct visualisation of EGFP. It was hoped that the sensitivity of this approach would be greater than direct EGFP analysis, allowing detection of lower levels of the fusion proteins that may result following translocation from expressing cells. The primary antibody is also able to bind to denatured protein. Figure 3.3 shows the direct and indirect imaging of pEGFP-N1 transfected COS-7 cells viewed at 40x magnification. Indirect IF was only detected in cells expressing EGFP, demonstrating the specificity of the IF approach with no non-specific binding of the anti-GFP antibody to endogenous epitopes.

3.2.3 Immunofluorescence Analysis of Transfer of MTP-EGFP Fusion Proteins in Transfected Cells

Fusions at either terminus of EGFP retain the fluorescent properties of the native protein, allowing localisation studies of the fusion protein. Vectors encoding N-

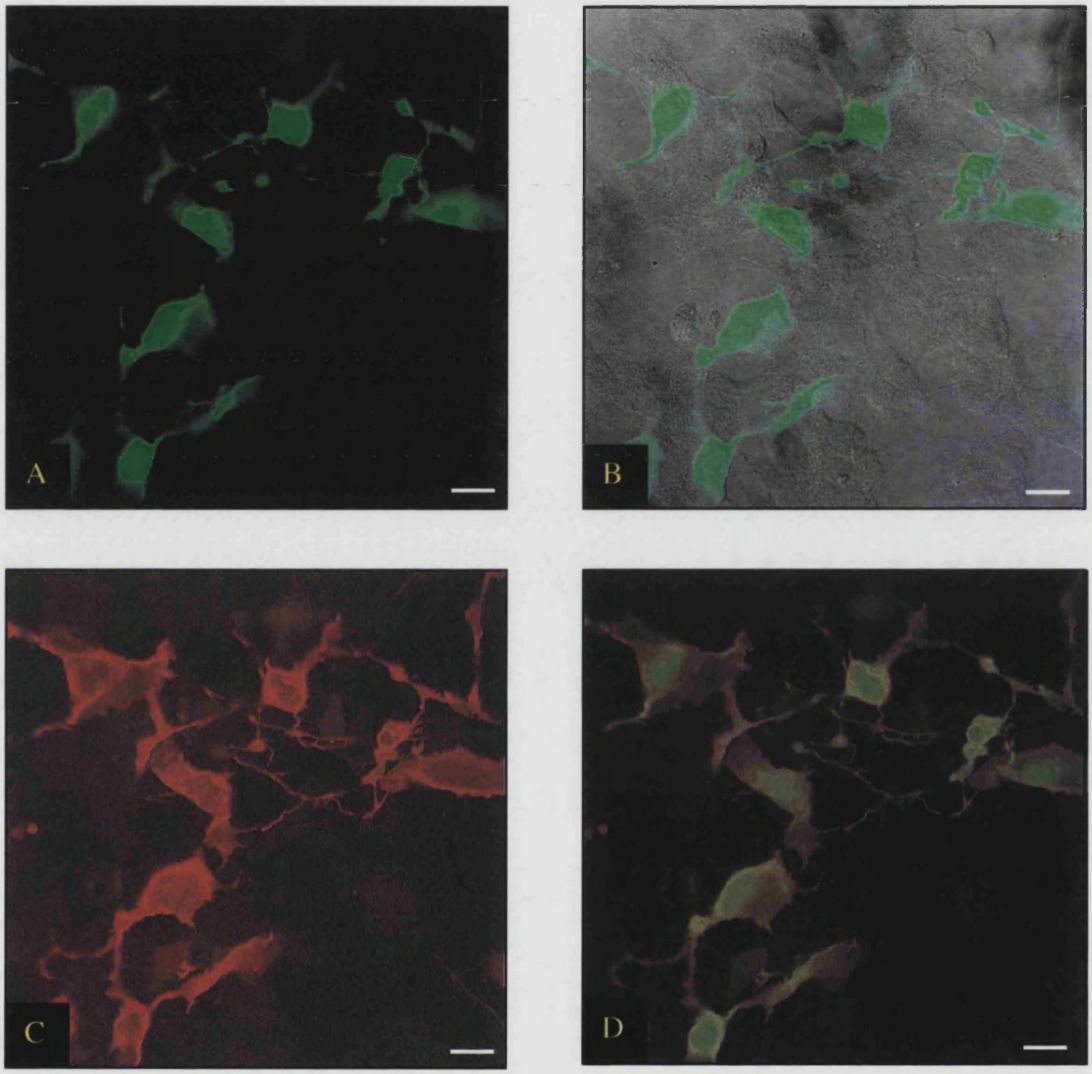

Figure 3.3. Immunofluorescence analysis of COS-7 cells transfected with pEGFP-N1. (A) Direct visualisation of GFP by excitation at 488 nm, FITC filter. (B) Overlay of panel A on DIC image of the same cells. (C) GFP detected by immunocytochemistry using rabbit anti-GFP IgG followed by mouse anti-rabbit IgG-TRITC, excitation 568 nm, TRITC/rhodamine filter. (D) Merge of Panels A and C. Bars indicate 20 μm.

terminus fusions of TAT, Drome, wild-type penetratin (WTPen) and mutant penetratin (mPen) with EGFP were gifts from Dr Arnott. The vector encoding VP22 in fusion with EGFP was a C-terminus fusion, and was a gift from Dr O'Hare. Cells were transfected with vectors coding for MTP-EGFP fusion proteins and expressed protein visualised for direct EGFP fluorescence and indirect IF by confocal microscopy. Any difference in the localisation of direct and indirect fluorescence in transfected samples would be examined as evidence of protein transduction, for the reason discussed above. All experiments were carried out on a minimum of three separate occasions and images are representative of the samples examined.

3.2.3.1 Transfection with pTAT-EGFP

Figure 3.4 shows COS-7 cells transfected with 200 ng pTAT-EGFP. The overlay of green fluorescence on the DIC image (Fig. 3.4 B) makes it apparent that the number of transfected cells is lower here than when cells were transfected with the other EGFP expression vectors (see figures 3.3, 3.5, 3.6, 3.7 and 3.8), with only two transfected cells captured in the frame. Transfected cells stained positive using both the anti-GFP antibody and the indirect IF protocol and direct EGFP fluorescence.

3.2.3.2 Transfection with pDrome-EGFP

Figure 3.5 shows COS-7 cells transfected with 200 ng pDrome-EGFP. Observation of direct GFP fluorescence shows a majority of the cells within the captured frame to contain EGFP. The fusion protein is localised in a diffuse pattern throughout the cells, though some regions exhibit brighter direct fluorescence than other regions. The differences are less apparent when indirect IF is examined, though this approach does generate a staining pattern that is generally brighter around the cells' peripheries. By merging the direct fluorescence and indirect IF images, panel D, the fluorescence patterns are shown to have considerable similarity when GFP is detected by either the direct or indirect methods.

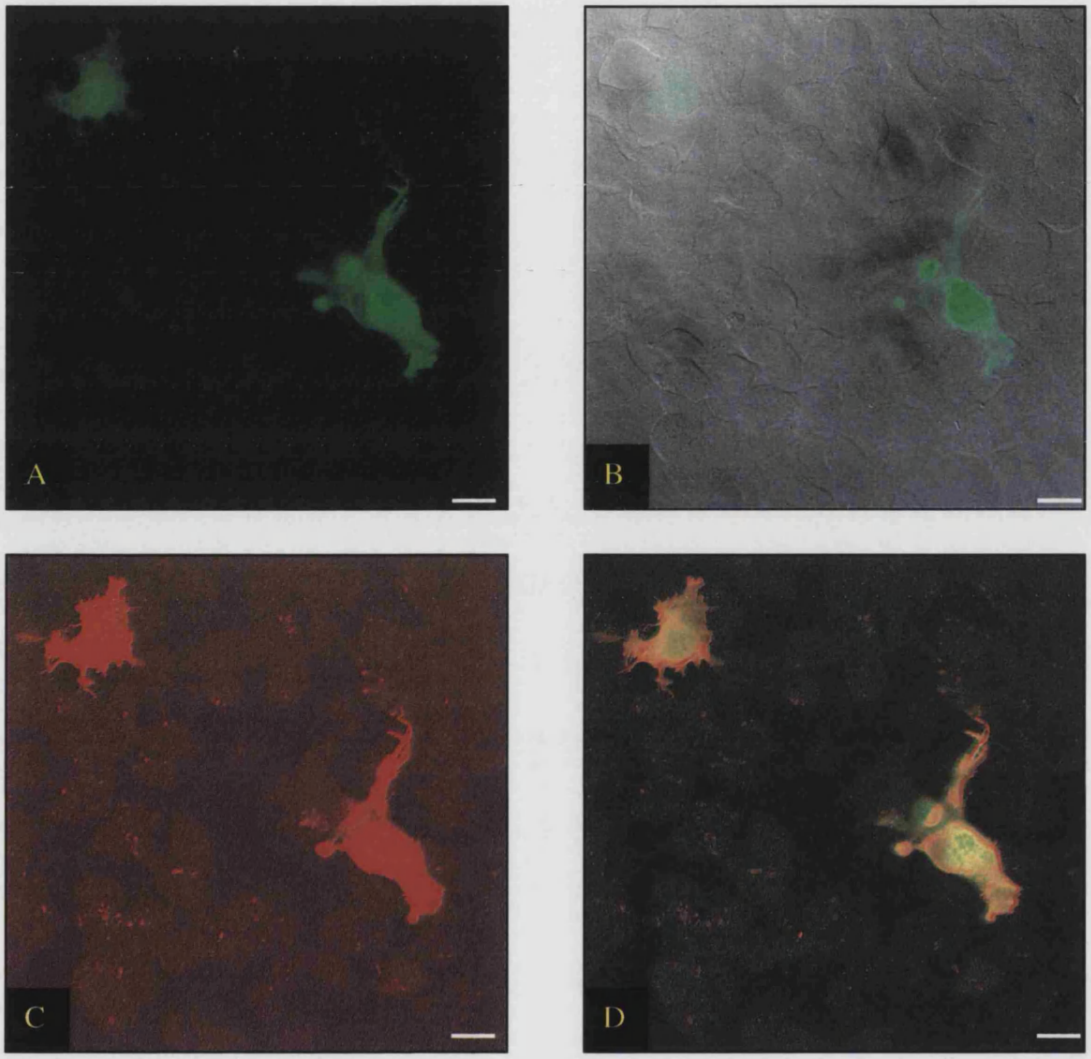

Figure 3.4. Immunofluorescence analysis of COS-7 cells transfected with pTAT-EGFP. (A) Direct visualisation of GFP by excitation at 488 nm, FITC filter. (B) Overlay of panel A on the DIC image of the same cells. (C) GFP detected by immunocytochemistry using rabbit anti-GFP IgG followed by mouse anti-rabbit IgG-TRITC, excitation 568 nm, TRITC/rhodamine filter. (D) Merge of panels A and C. Bars indicate 20 μm.

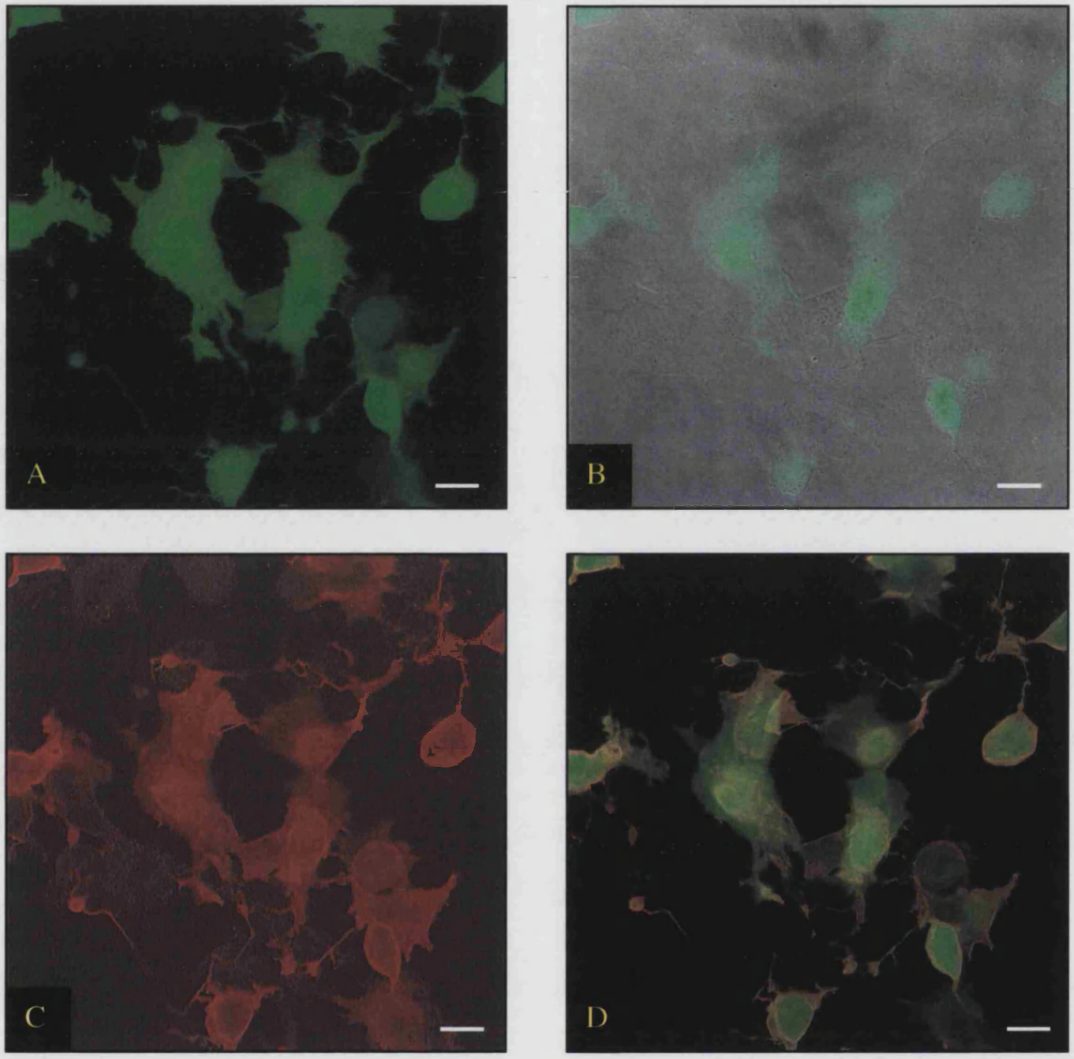

Figure 3.5. Immunofluorescence analysis of COS-7 cells transfected with pDrome-EGFP. (A) Direct visualisation of GFP by excitation at 488 nm, FITC filter. (B) Overlay of panel A on the DIC image of the same cells. (C) GFP detected by immunocytochemistry using rabbit anti-GFP IgG followed by mouse anti-rabbit IgG-TRITC, excitation 568 nm, TRITC/rhodamine filter. (D) Merge of panels A and C. Bars indicate 20 μm.

3.2.3.3 Transfection with pPen-EGFP and pmPen-EGFP

Figures 3.6 and 3.7 show 40x images of COS-7 cells transfected with 200 ng pPen-EGFP and pmPen-EGFP, respectively. Detection by both the direct and indirect approach (A and C, respectively, in both figures) results in observation of a similar distribution of fluorescence for both fusion proteins. This similarity is emphasized where the images have been merged (D). All cells positively stained for Pen-EGFP and mPen-EGFP by indirect IF also exhibit intrinsic GFP fluorescence. However, the intracellular distribution of WTPen-EGFP differs when its presence is detected by intrinsic GFP fluorescence compared to indirect IF. Figure 3.6 D, a merge of the direct fluorescence and indirect IF, shows the fusion protein to be detected predominantly in the cytoplasm of the cells when IF is examined compared to brighter nuclear staining detected by direct GFP fluorescence alone. The same is not observed for mPen-EGFP (Fig 3.7 D). Here the two fluorescent patterns are virtually identical.

3.2.3.4 Transfection with pGE155 (pEGFP-VP22)

The construct pGE155 was a gift from the O'Hare group. This plasmid encoded a C-terminal fusion of VP22 to EGFP rather than a N-terminal fusion as is the case for the other EGFP constructs. This vector was generated by insertion of VP22 into the pEGFP-C1 vector (Clontech), and thus for descriptive simplicity and consistency the construct will be referred to as pEGFP-VP22.

Figure 3.8 shows COS-7 cells transfected with 200 ng pEGFP-VP22. The intensity of the indirect IF is very low in comparison to that of the intrinsic GFP fluorescence. This may be a result of photobleaching from prolonged exposure during imaging, or potentially obstruction of the GFP epitope by the full-length VP22 protein. GFP fluorescence is observed diffuse throughout the cells, though the nuclei exhibit more intense staining than the cytoplasmic regions. A very intense region of localised GFP fluorescence was observed in most cells. This is thought to be aggregated protein situated at the nuclear periphery. A merge of the two images (Fig. 3.8 D) shows cells stained positive by both approaches.

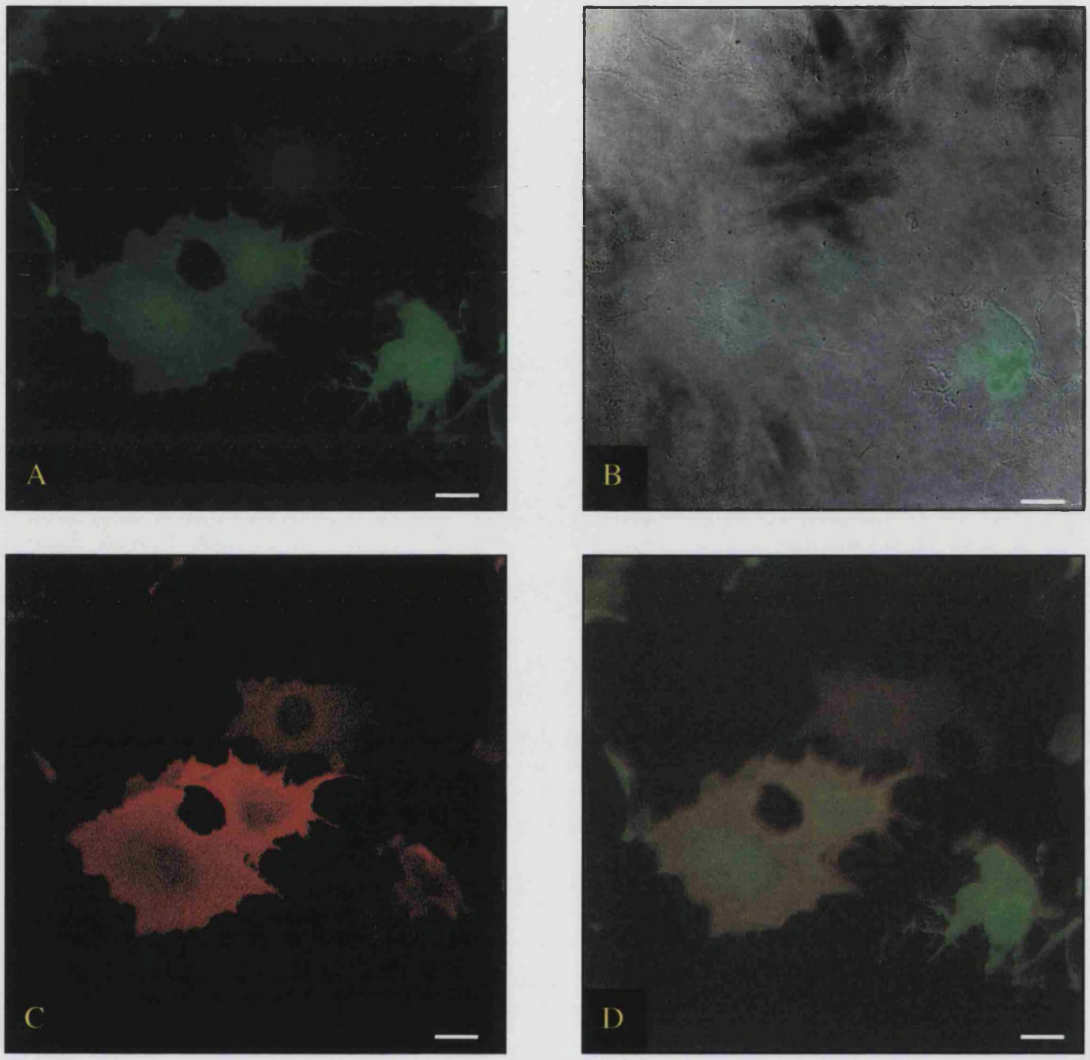

Figure 3.6. Immunofluorescence analysis of COS-7 cells transfected with pWTPen-EGFP. (A) Direct visualisation of GFP by excitation at 488 nm, FITC filter. (B) Overlay of panel A on the DIC image of the same cells. (C) GFP detected by immunocytochemistry using rabbit anti-GFP IgG followed by mouse anti-rabbit IgG-TRITC, excitation 568 nm, TRITC/rhodamine filter. (D) Merge of panels A and C. Bars indicate 20 μm.

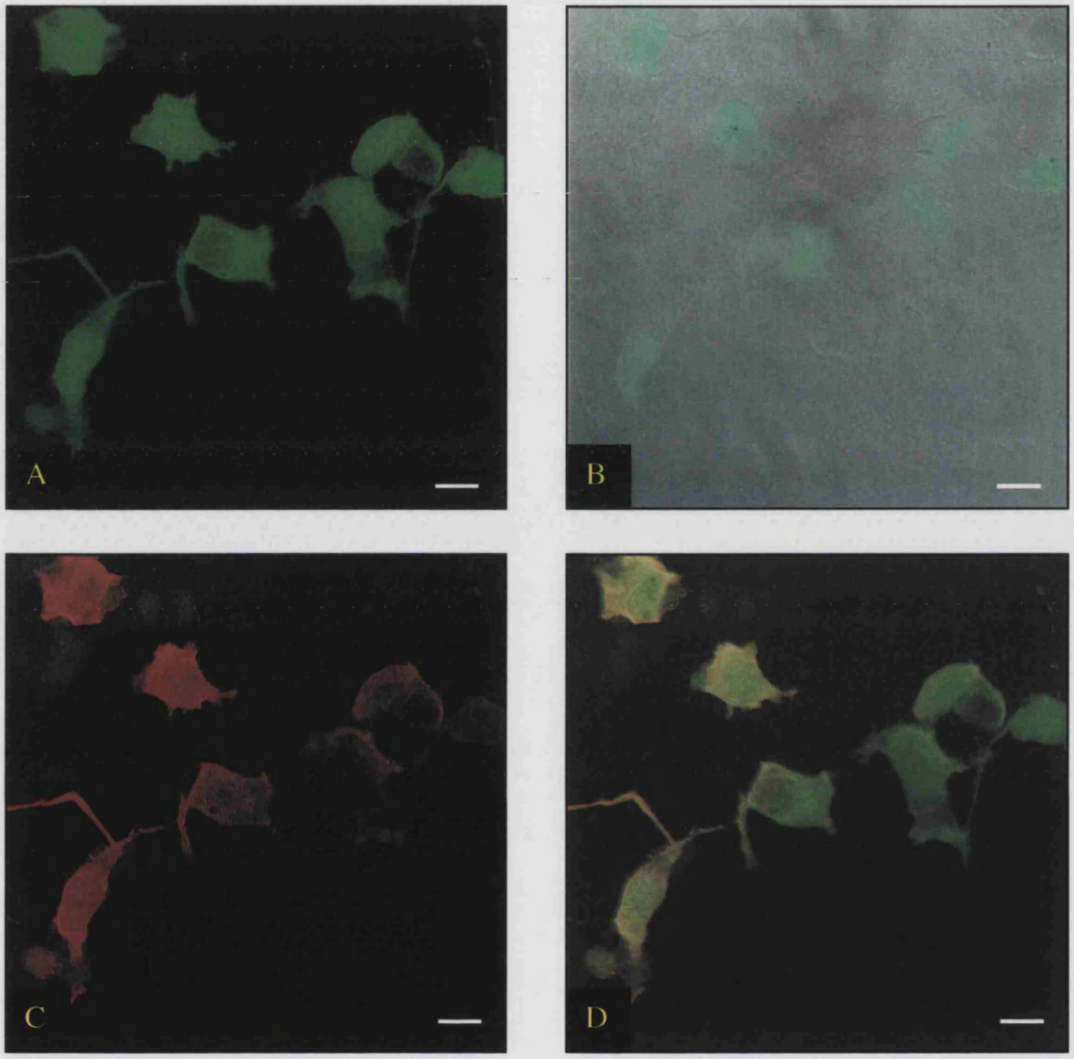

Figure 3.7. Immunofluorescence analysis of COS-7 cells transfected with pmPen-EGFP. (A) Direct visualisation of GFP by excitation at 488 nm, FITC filter. (B) Overlay of panel A on the DIC image of the same cells. (C) GFP detected by immunocytochemistry using rabbit anti-GFP IgG followed by mouse anti-rabbit IgG-TRITC, excitation 568 nm, TRITC/rhodamine filter. (D) Merge of panels A and C. Bars indicate 20 μm.

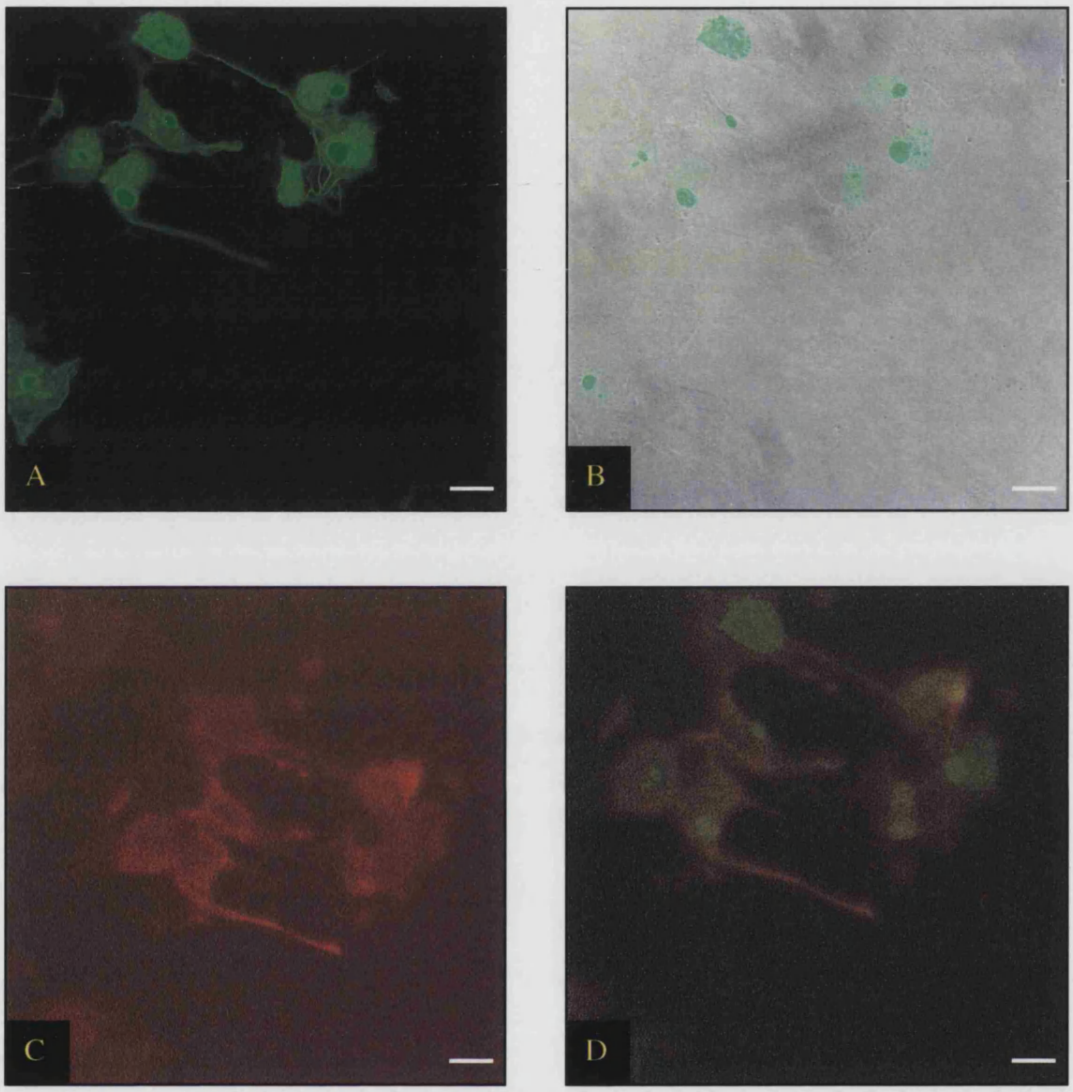

Figure 3.8. Immunofluorescence analysis of COS-7 cells transfected with pEGFP-VP22. (A) Direct visualisation of GFP by excitation at 488 nm, FITC filter. (B) Overlay of panel A on the DIC image of the same cells. (C) GFP detected by immunocytochemistry using rabbit anti-GFP IgG followed by mouse anti-rabbit IgG-TRITC, excitation 568 nm, TRITC/rhodamine filter. (D) Merge of panels A and C. Bars indicate 20 μm.

3.2.4 Determination of MTP-EGFP Transfer in Co-Cultured Cells

The indirect IF approach described above had demonstrated the presence of the fusion proteins in only those cells exhibiting direct EGFP fluorescence. The protocol did not, however, allow for separation of cells expressing the fusion proteins from recipient, untransfected cells. Being able to distinguish one group of cells from the other would enable detection of direct EGFP fluorescence in cells that were not expressing the protein, confirming that protein transduction had taken place. An approach was therefore adopted whereby transfected cells were co-cultured with untransfected cells from a different species. Through the use of indirect IF using a species-specific primary antibody and a red fluorescent secondary antibody expressing cells could be distinguished from non-expressing cell, and thus allow validation of protein transduction.

The protocol undertaken was as follows. COS-7 cells were transfected with the fusion constructs. To ensure that the transfection occurred with high efficiency GeneJuice was used as the transfection vector and 1 μg of vector used for each transfection. Cells were grown for 24 h following transfection, when they were harvested and used to set up co-cultures with untransfected Rat-1 cells. Twenty-four hours after plating of co-cultures cells were processed ready for examination by confocal microscopy. Subsequent to fixation cells were subjected to immunofluorescence using rabbit polyclonal antiserum to a member of the *trans*-Golgi network (TGN), TNG38. The antiserum was species-specific and only the TGN of the Rat-1 cells would be stained. Alexa Fluor 564-conjugated goat anti-rabbit IgG secondary antibody was used to enable visualisation of the stained Rat-1 cells by confocal microscopy.

A control co-culture was set up using pEGFP-N1 transfected COS-7 cells and untransfected Rat-1 cells to ensure that there was no cross-reactivity between the antiserum and the COS-7 cells that would prevent differentiation of the two cell lines. Direct visualisation of EGFP-expressing COS-7 cells showed the presence of pEGFP-N1 transfected COS cells, with diffuse staining throughout the cells (Fig. 3.9 A). Rat-specific TGN38 IF analysis showed many Rat-1 cells in the same frame, identifiable by their stained Golgi (Fig. 3.9 B). As expected this staining was predominantly in a crescent pattern around what would be the

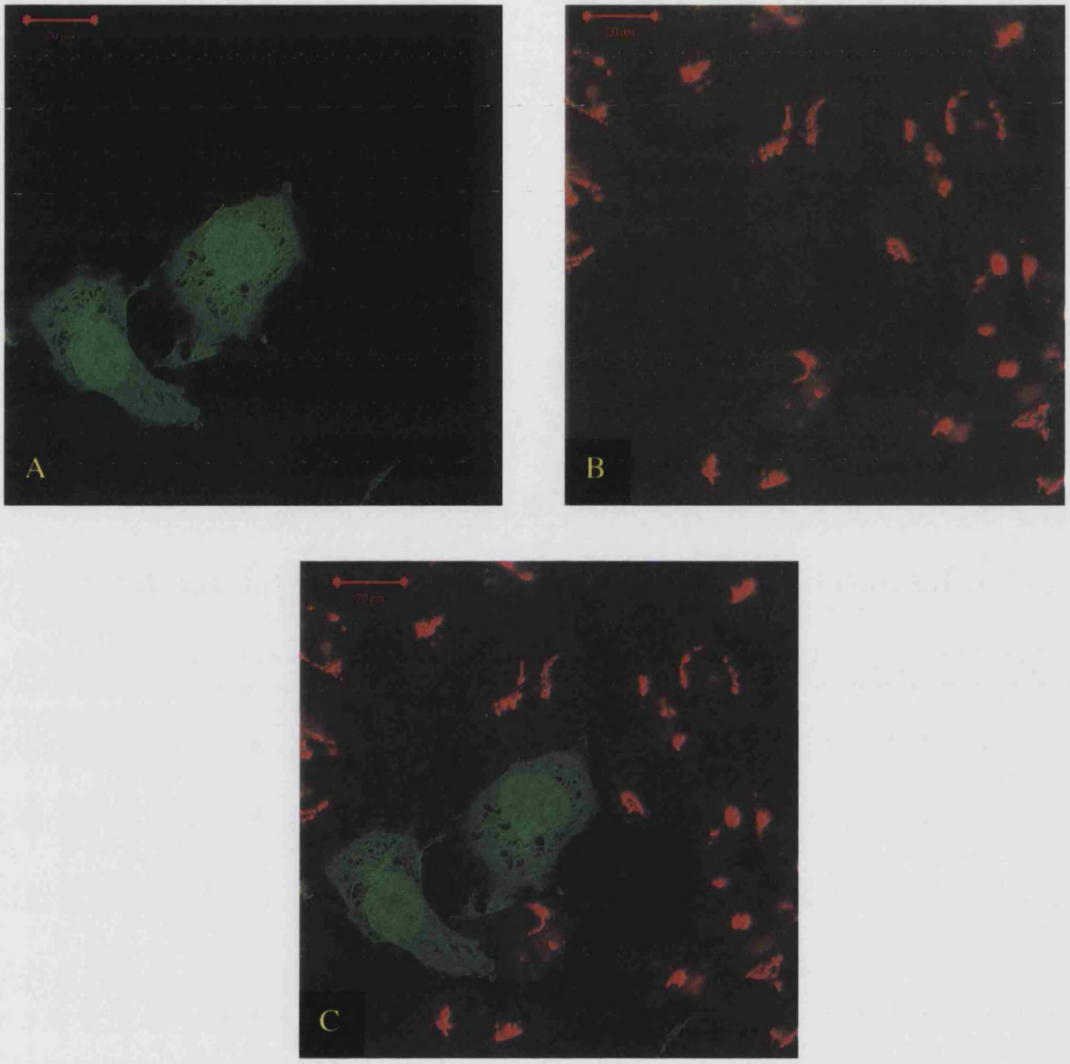

Figure 3.9. Confocal images of COS-7 cells transfected pEGFP-N1co-cultured with non-transfected Rat-1 cells. (A) Direct visualization of GFP by excitation at 488 nm, FITC narrow band emission filter. (B) Immunostaining against rat-specific TGN46, excitation 568 nm, TRITC/rhodamine filter, indicating Rat-1 cells. (C) Merge of images A and B. Bars indicate 20 μm.

nucleus of the Rat cells. An overlay of the two images showed that there was no cross-reactivity of the antiserum to COS-7 cells, and that it was only the COS-7 that exhibited GFP-associated fluorescence (Fig. 3.9 C).

Following confirmation that the two cells lines could be differentiated by this IF approach, the vectors for the MTP-EGFP fusion proteins were used to transfect the COS-7 cells, and these cells then used to seed co-cultures with the Rat-1 cells. The presence of GFP fluorescence in TGN38-positive cells would offer an indication as to spread of the fusion protein from the expressing COS cells to non-expressing Rat cells. All experiments were carried out on at least three separate occasions and images are representative of each.

3.2.4.1 Transfection with pTAT-EGFP

Direct visualisation of GFP fluorescence (Fig. 10 A) showed the presence of pTAT-EGFP transfected COS-7 cells exhibiting a diffuse pattern of staining throughout the cells. However, on occasion small, round arrangements of punctate staining was also observed. Two such regions are indicated by arrows in figure 10 A. A merge of cells exhibiting GFP fluorescence with non-EGFP expressing Rat-1 cells in the same frame shows no co-localisation of the antiserum with cells displaying diffuse GFP fluorescence (Fig. 3.10 C). However, for at least one of the regions of round, punctate GFP fluorescence staining of Golgi networks is observed in close proximity (circled in Fig. 3.10 C). No other areas where both GFP and indirect Golgi IF co-localised were discerned.

3.2.4.2 Transfection with pDrome-EGFP

Direct visualisation of GFP fluorescence showed the presence of pDrome-EGFP transfected COS-7 cells, which exhibited a diffuse pattern of staining similar to that of pEGFP-N1 transfected cell. As with the co-culture studies using

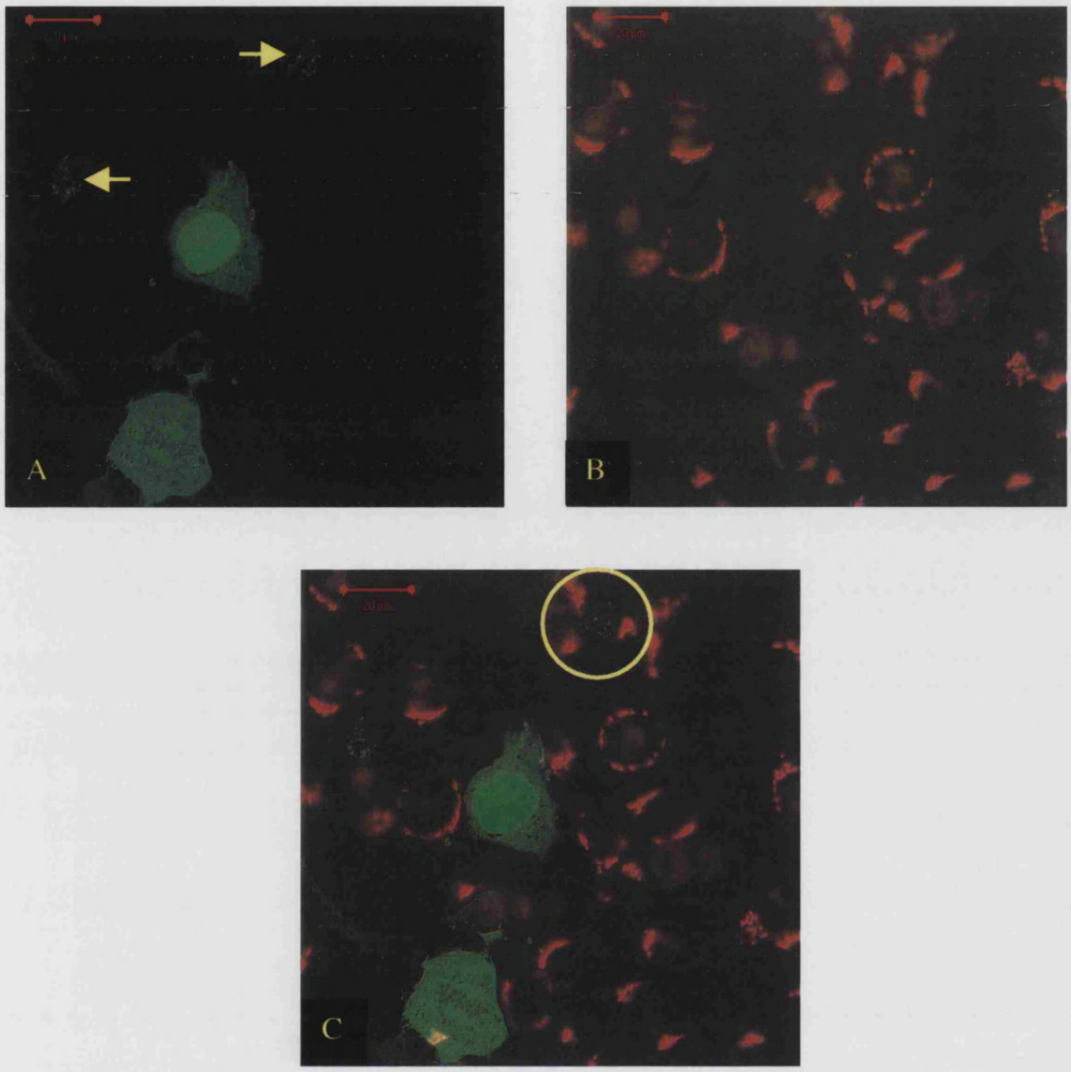

Figure 3.10. Confocal images of COS-7 cells transfected with pTAT-EGFP co-cultured with non-transfected Rat-1 cells. (A) Direct visualization of GFP by excitation at 488 nm, FITC narrow band emission filter. (B) Immunostaining against rat-specific TGN46, excitation 568 nm, TRITC/rhodamine filter, indicating Rat-1 cells. (C) Merge of images A and B. Bars indicate 20 μm.

pTAT-EGFP transfected COS-7 cells, however, other staining patterns were observed on occasion. Two such patterns are visible within the captured frame and are marked with arrows (Fig. 3.11 A). One, on the right hand side of the image is an area of fluorescence similar to the small, round, punctate regions of GFP fluorescence observed in the pTAT-EGFP studies (Fig. 3.10 A and C). The other region of GFP fluorescence, at the top left of the image, takes the form of a pearls-on-a-string structure. The areas of interest are boxed in figure 11 C, and shown at a higher magnification. The merged image, revealing IF of the non-EGFP expressing Rat-1 cells, shows a tight association between these two small regions of GFP fluorescence and the stained Golgi networks of the Rat-1 cells (Fig. 3.11 C). Such an association is not observed with the cell exhibiting the diffuse GFP-fluorescence at the bottom of the image, marking this as a transfected COS-7 cell.

3.2.4.3 Transfection with pWTPen-EGFP and pmPen-EGFP

The pWTPen-EGFP transfected cells observed in the co-cultures through direct visualisation of GFP fluorescence exhibited fluorescence distributed diffusely throughout the cells' entireties (Fig. 3.12 A). EGFP fluorescence was only evident in the large COS-7 cells. These cells have a tendency to expand over the growth surface, and are able to spread over neighbouring cells. This is evident in the merged image (Fig. 3.12 C) where an arrow indicates an area inhabited by both a COS-7 cell and a Rat-1 cell. This can give the appearance of co-localisation of EGFP with the Golgi IF, but confocal analysis revealed this to be a COS-7 cell overlaid on a Rat-1 cell.

The pmPen-EGFP transfected cells exhibit the same diffuse staining as cells expressing the wild-type penetratin-EGFP fusion protein, though the fluorescence is less intense (Fig. 3.13 A). An merged image of the co-cultured cells shows no direct EGFP fluorescence co-localised with the indirect IF, demonstrating that, as expected, translocation has not taken place (Fig. 3.13 C).

3.2.4.4 Transfection with pEGFP-VP22

The predominant distribution of fusion protein within the cells exhibiting GFP fluorescence in co-cultures involving pEGFP-VP22 transfected cells was that of

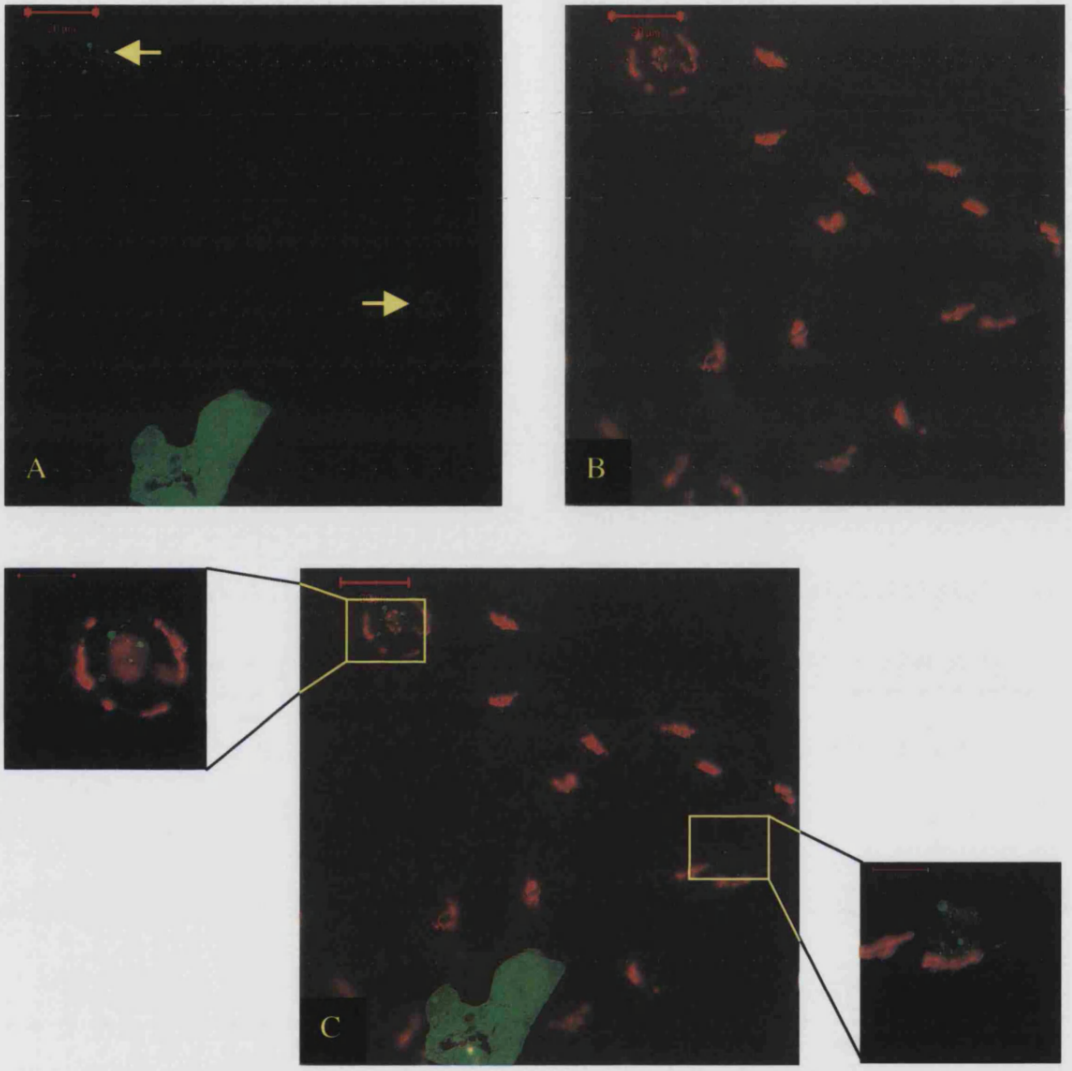

Figure 3.11. Confocal images of COS-7 cells transfected with pEGFP-Drome co-cultured with non-transfected Rat-1 cells. (A) Direct visualization of GFP by excitation at 488 nm, FITC narrow band emission filter. (B) Immunostaining against rat-specific TGN46, excitation 568 nm, TRITC/rhodamine filter, indicating Rat-1 cells. (C) Merge of images A and B, with boxed areas shown at a higher magnification. Bars indicate 20 μm or 10 μm for the higher magnification images.

largely nuclear staining, though fainter cytoplasmic fluorescence was apparent, with a small, intensely fluorescent region located just outside the nucleus (arrow in Fig. 3.14 A), which is probably aggregated protein. However, other fluorescence patterns were observed and these are represented, and numbered, in figure 3.14 A: Cytoplasmic (1), nuclear (2), and 'other' (3). The cytoplasmic fusion protein appears largely associated with filamentous structures, which are probably actin microfilaments. The 'other' fluorescence patterns observed varied, but appeared to involve association with chromatin, and segregating chromosomes during the formation of daughter cells are clearly visible in figure 3.14 A.

Though the fusion protein was showing functional similarity to the native VP22 protein, namely association with actin filaments and microtubules, and chromatin binding, there was no evidence that membrane translocation had taken place. An overlay image allowing visualisation of both GFP fluorescence and immunostaining of Rat-1 cells shows that though in close proximity there is no transfer of EGFP-VP22 fusion protein from the transfected COS-7 cells to the untransfected Rat-1 cells (Fig. 3.14 C).

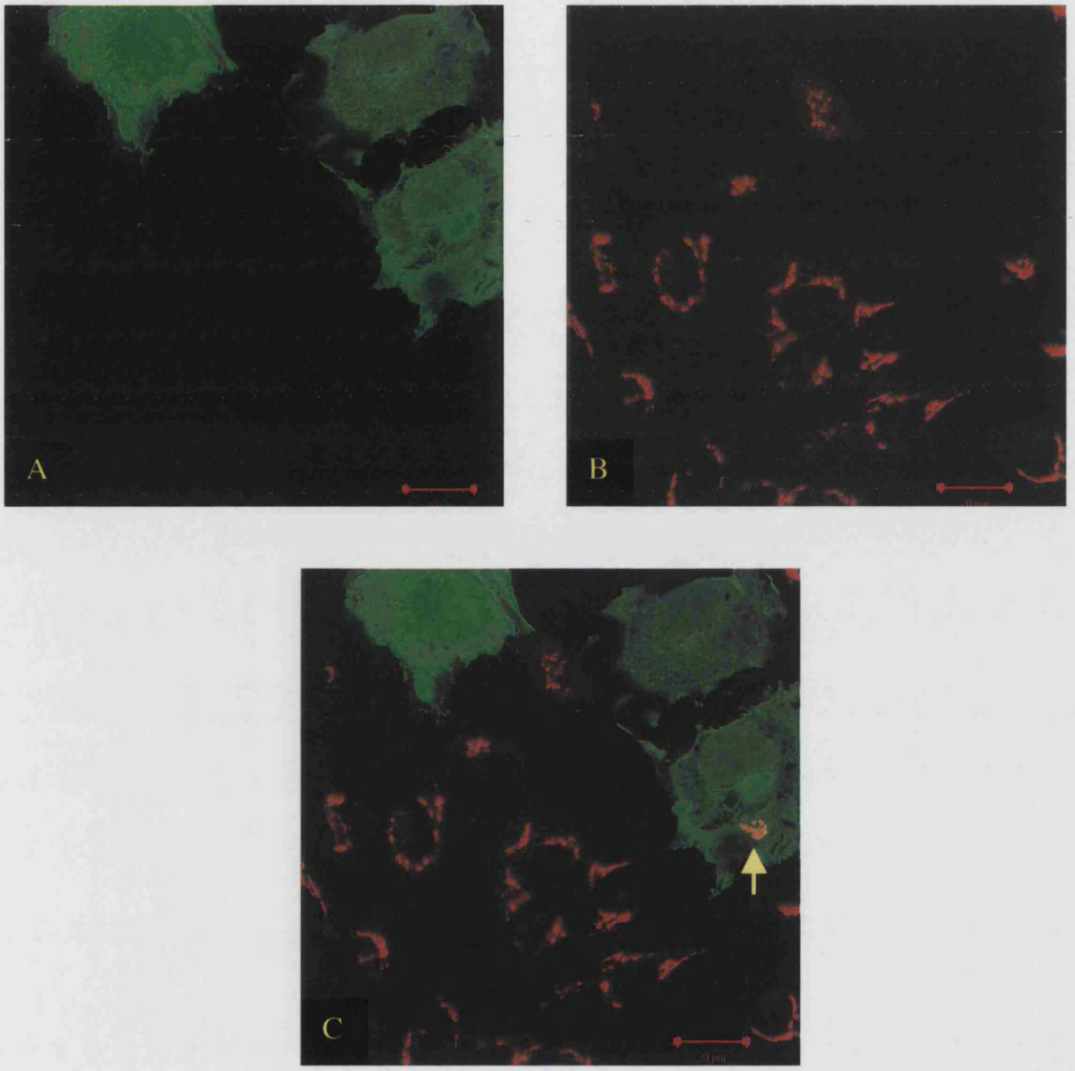

Figure 3.12. Confocal images of COS-7 cells transfected with pWTPen-EGFP co-cultured with non-transfected Rat-1 cells. (A) Direct visualization of GFP by excitation at 488 nm, FITC narrow band emission filter. (B) Immunostaining against rat-specific TGN46, excitation 568 nm, TRITC/rhodamine filter, indicating Rat-1 cells. (C) Merge of images A and B. Bars indicate 20 μm.

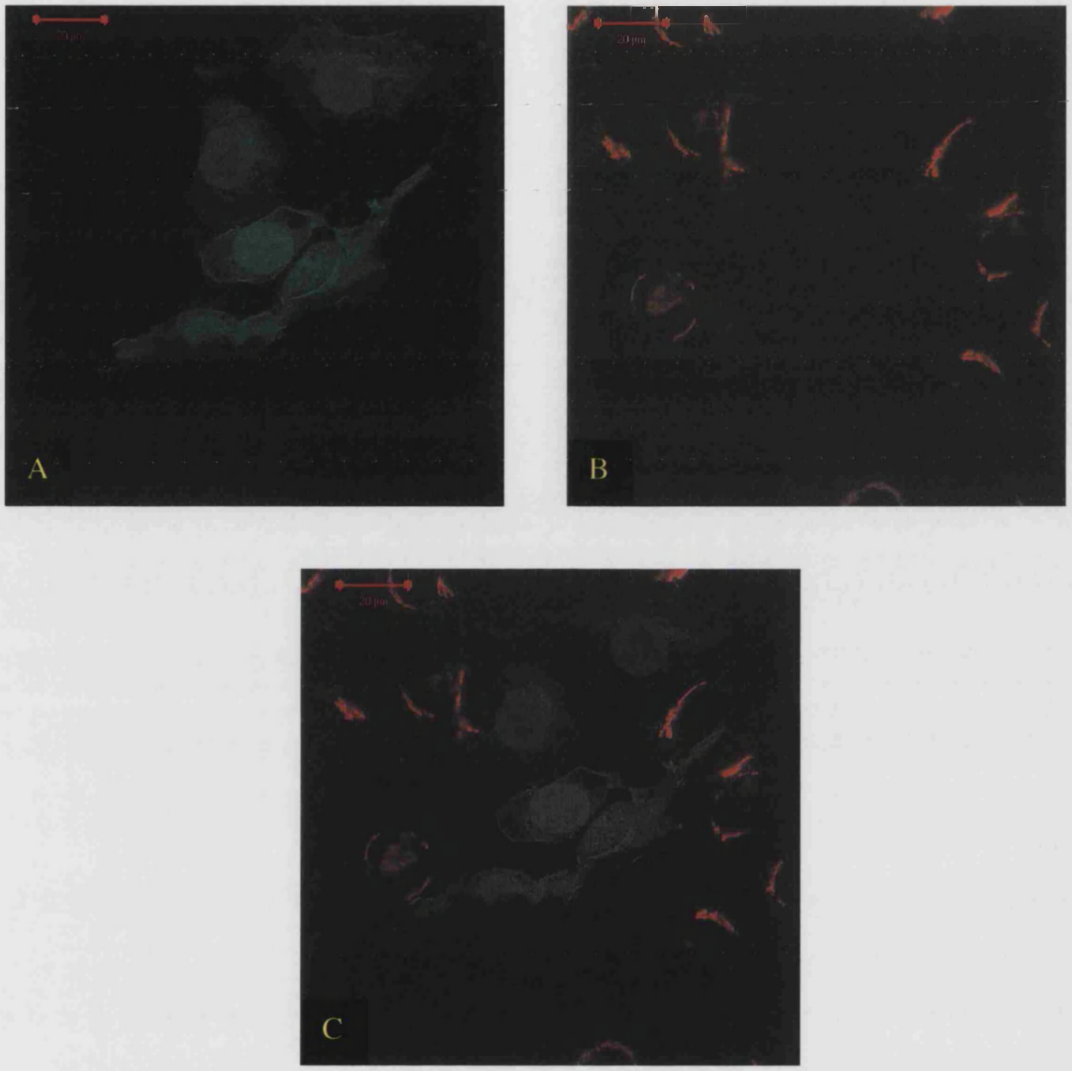

Figure 3.13. Confocal images of COS-7 cells transfected with pmPen-EGFP co-cultured with non-transfected Rat-1 cells. (A) Direct visualization of GFP by excitation at 488 nm, FITC narrow band emission filter. (B) Immunostaining against rat-specific TGN46, excitation 568nm, TRITC/rhodamine filter, indicating Rat-1 cells. (C) Merge of images A and B.

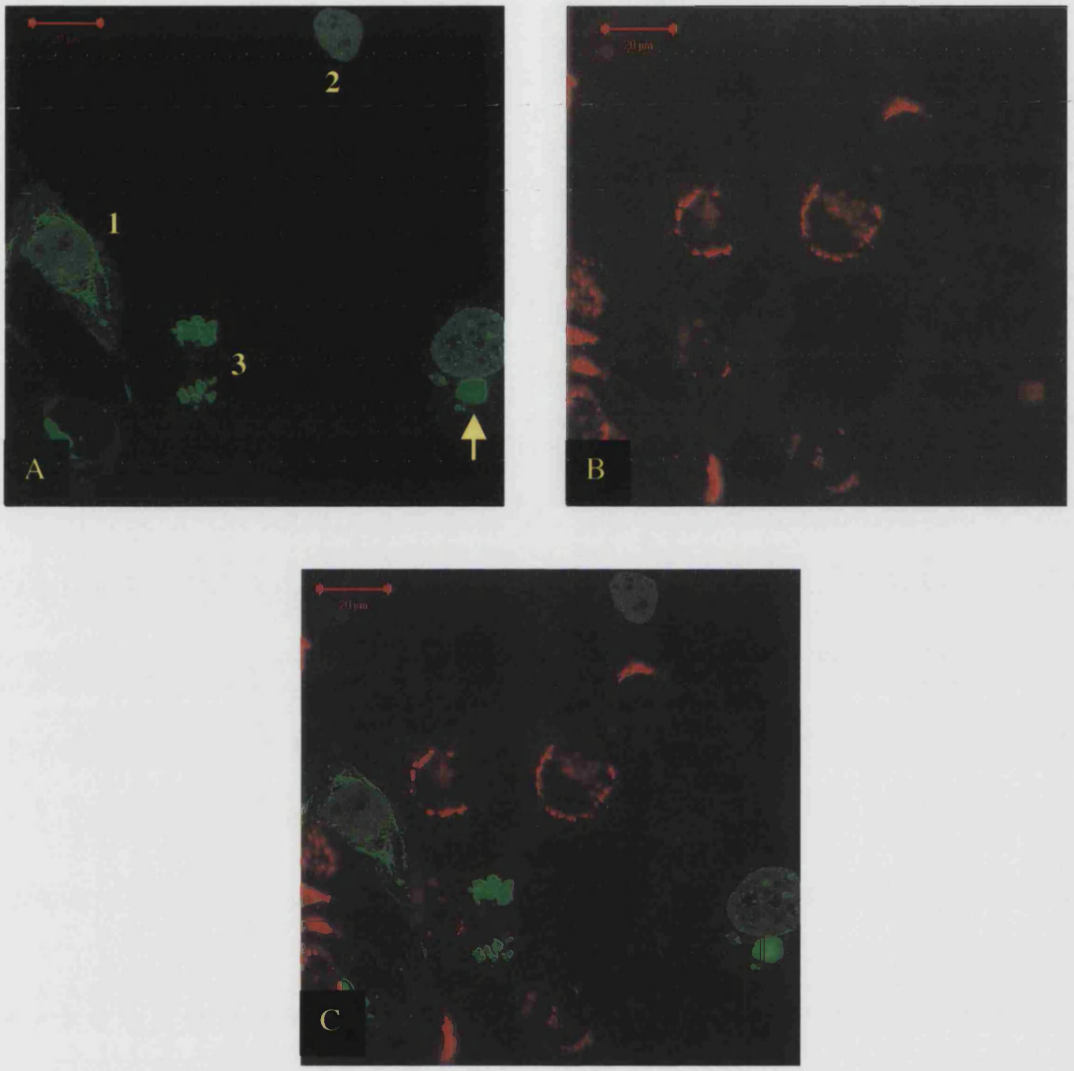

Figure 3.14. Confocal images of COS-7 cells transfected with pEGFP-VP22 co-cultured with non-transfected Rat-1 cells. (A) Direct visualization of GFP by excitation at 488 nm, FITC narrow band emission filter. (B) Immunostaining against rat-specific TGN46, excitation 568 nm, TRITC/rhodamine filter, indicating Rat-1 cells. (C) Merge of images A and B. Bars indicate 20 μm.

3.2.5 Quantification of Membrane Translocation of EGFP-MTP Fusion Proteins by Fluorescence-Activated Cell Sorting Analysis

Fluorescence-activated cell sorting (FACS) analysis allows objective and accurate quantification of the number of live cells exhibiting EGFP fluorescence, and the intensity of this fluorescence within each cell, in a way that is not possible through the confocal microscopy approaches. The number of MTP-EGFP-positive cells in a sample would be greater than the number in a sample of cells expressing EGFP alone if protein transduction had taken place. However, subtle differences in the distribution of the fluorescence throughout the MTP-EGFP expressing samples may occur in addition to, or in place of, an overall increase in the number of EGFP-positive cells. Protein may be transduced from cells exhibiting very intense EGFP fluorescence, indicative of cells expressing high levels of the fusion protein, to cells with a lower level. In such a scenario there may be no overall increase in the number of EGFP-positive cells, but rather a shift in the fluorescence distribution of the sample, with fewer cells exhibiting high and low fluorescence intensities and more cells with exhibiting moderate fluorescence intensities. To account for this, the percentage of cells occupying a number of fluorescence intensity strata would be monitored, and changes in the distribution between samples examined

COS-7 cells were transfected with 50 ng of EGFP expression vector 48 hour before processing for FACS analysis. The small amount of DNA used ensured that only a proportion of the cells would be successfully transfected, allowing a proportion to remain available as 'acceptor' cells for the transduced fusion protein. Cells were co-transfected with 1 μg pcDNA-luc, a luciferase expression vector that would allow consistent transfection efficiencies across the samples to be confirmed. Transfected cells were detached from the growth surface by trypsinisation, which had the additional benefit of removing any fusion protein that may be associated with the extracellular surface of the cells, rather than inside the cell. An aliquot of each sample was lysed and analysed for luciferase activity.

Representative histograms of the transfected samples are shown in Figure 3.15 B-G, with data from 10,000 events. Because cells exhibit autofluorescence a

sample of pcDNA-luc transfected cells was used for calibration so ≥ 98% of this sample occupied the first log cycle (1-10 AU) of the fluorescence intensity scale (arbitrary units covering 4 log cycles describing the fluorescence intensity exhibited by the cells). Three regions encompassing cells exhibiting different fluorescent intensities above this background level were established (10-100 AU, 10-1,000 AU, and 10-10,000 AU), as shown on the histograms. Assessment of the number of cells within each region would allow determination of how any MTP-driven translocation of EGFP affected the fluorescence distribution throughout a population of cells. Figure 3.15 A shows the mean percent of cells, from three experiments, within each of the regions of fluorescence intensity, and error bars indicate standard deviations.

For each sample the percentage of EGFP-positive cells was very similar in each of the three strata of fluorescence intensity examined (10-100 AU, 100-1,000 AU, and 1,000-10,000 AU) demonstrating a large variance in the fluorescence intensity of the cells. The result is a trend for a linear increase in the cumulative percent of events from 10-10,000 AU for each of the samples, with about 40-50% of cells from each transfected sample exhibiting fluorescence intensities above auto-fluorescence background (i.e. ≥ 10 AU). Expression of EGFP as a fusion with the MTPs neither increased the number of fluorescent cells observed in the transfected populations, nor greatly altered the distribution of fluorescence intensities in the populations. Luciferase activities determined for the samples demonstrated that transfection had taken place with comparative efficiency in all samples.

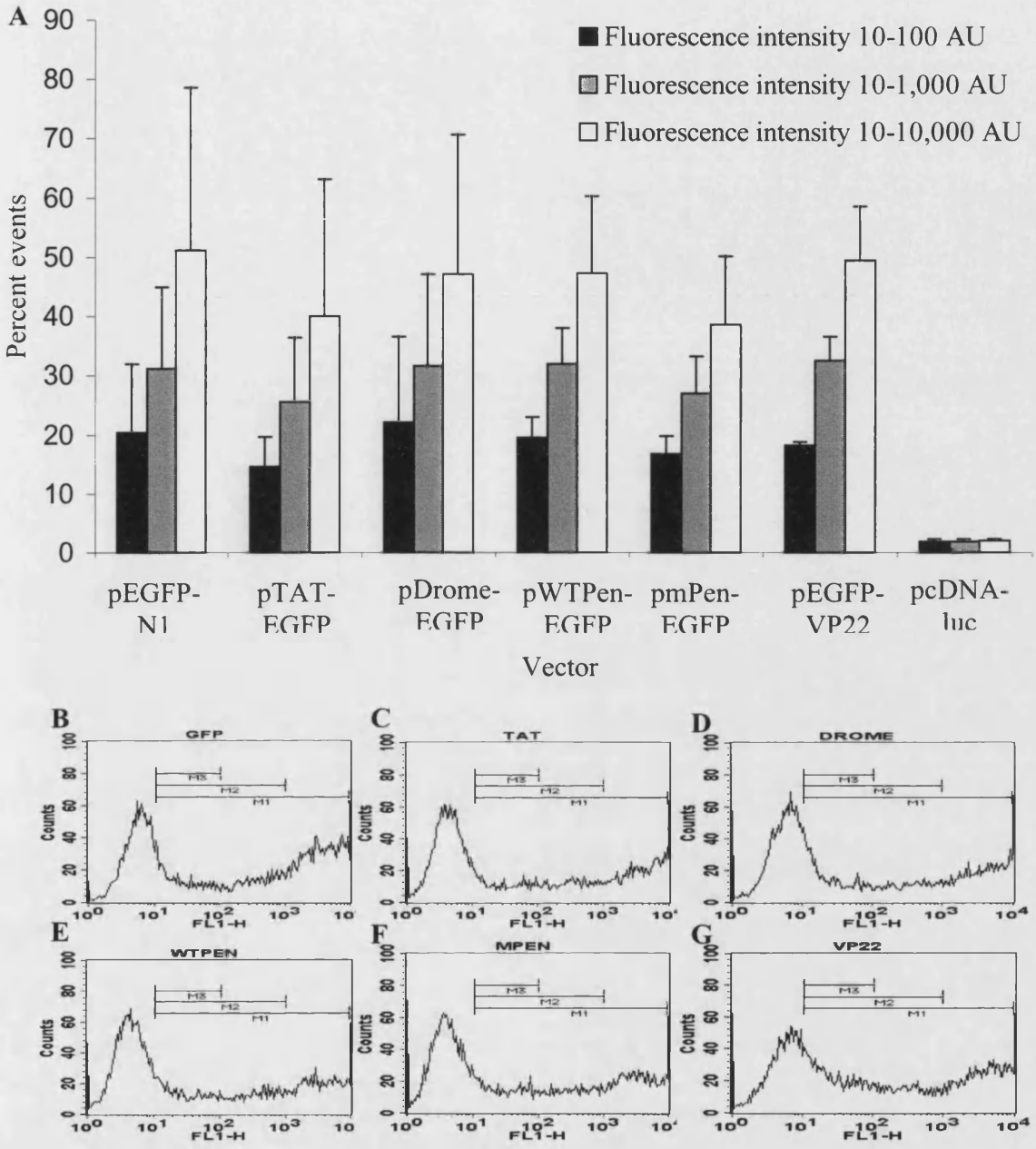

Figure 3.15. FACS analysis to quantify protein transduction of EGFP-MTPs in live cells. (A) COS-7 cells were transfected with pcDNA-luc alone, as a control, or co-transfected with each of the EGFP expression vectors as indicated. Forty-eight hours post-transfection cells were washed, trypsinised and immediately processed for direct FACS analysis. The number of GFP-positive cells was determined by FL1-H fluorescence, and the percent events in 3 regions of fluorescence intensity (M1 = 10-10,000 AU; M2 = 10-1,000 AU; M3 = 10-100 AU) determined. Data represent mean ± S.D. (n = 3). (B-G) Representative histograms of each of the samples trans-

fected with pEGFP-N1 (B), pTAT-EGFP (C), pDrome-EGFP (D), pWTPen-EGFP (E), pmPen-EGFP (F), and pEGFP-VP22 (G), with the bars indicating the 3 fluorescence intensity regions studied (M1-M3).

3.3 Discussion

The green fluorescent protein was used as a reporter due to the success of a number of groups in observing protein transduction carried out by MTPs using this protein (Aints et al., 1999; Brewis et al., 2000; Elliott and O'Hare, 1999a; Han et al., 2000; Harms et al., 2000; Kafri et al., 1997; Lai et al., 2000; Wybranietz et al., 1999). The aim of the study was two fold: To confirm reports that the Tat PTD, penetratin and VP22 could direct the transport of proteins between cells, and to examine whether it would be possible to quantify the efficiency of this process using GFP fusion proteins. As a method of transduction quantification was sought that could be used to compare the relative efficiencies of these and potentially novel MTPs, it was necessary to develop a system that could readily accept new sequences for assessment. For this reason an approach was adopted whereby transport would be monitored from cells expressing the fusion proteins rather than one involving application of protein expressed from an exogenous source. In doing this steps involving the purification of expressed proteins were removed, creating a less time consuming, more cost effective, more accessible system.

3.3.1 Anti-GFP Immunofluorescence Studies of Protein Transduction

Observations of transfected cells were initially undertaken through an immunofluorescence (IF) approach using an antibody to the reporter itself, EGFP. The protocol adopted, using a rhodamine-conjugated secondary antibody for IF, allowed both direct and indirect visualisation of GFP. Observations of direct fluorescence alone were substantiated using an indirect IF approach because of a report by Elliott and O'Hare stating that the sensitivity of detecting VP22 spread was significantly increased using an IF approach (Elliott and O'Hare, 1999a). In addition a recent study had addressed an observation that the nature of fixation conditions could influence interpretation of translocation results (Brewis et al., 2000). It was suggested that spread of GFP-VP22 could be detected by IF after paraformaldehyde (PFA) fixation and detergent permeabilisation, though at lower levels than that observed using organic solvents. However, the report also demonstrated that a small but discernable displacement of VP22 from methanol-fixed cells increased the detection of spread observed. As a result, cells examined here were fixed with

PFA prior to methanol-mediated permeabilisation of cell membranes to cross-link cellular proteins. This prevented the expressed proteins from being eluted from the cells during the washing steps associated with IF.

Observation of monolayers of cells transfected with the MTP-EGFP expression constructs by IF showed localisation of the anti-GFP antibody to only those sites that also exhibited intrinsic GFP fluorescence. It was hypothesised that there were at least two possible outcomes as a result of translocation of the fusion proteins from expressing cells to adjacent non-expressing cells. The first was that diffusion of GFP as spread occurred from a central expressing cell would cause local concentration of GFP to fall below the detectable levels. Other groups have reported such a phenomenon, with transduction from transfected cells visualised as individual brighter cells surrounded by cells showing less intense signal (Elliott and O'Hare, 1997; Hung et al., 2001; Wybranietz et al., 1999). In IF experiments with an anti-VP22 antibody it was noticed that the intensity of transduced cells' nuclei decreased as their distance from an expressing cell increased, as would be consistent with the cell-to-cell transfer of VP22 containing fusion proteins (Liu et al., 2001). A similar phenomenon would be observed as the EGFP protein was diluted as a result of cell division.

The second outcome was that the fusion proteins might become denatured as part of the translocation process, resulting in loss of detectable intrinsic fluorescence in transduced cells. Such an occurrence may be expected as enhanced delivery has been observed following denaturation of TAT fusion proteins prior to administration (Becker-Hapak et al., 2001; Nagahara et al., 1998; Vocero-Akbani et al., 2000). By using IF with an anti-GFP antibody it would be possible to detect partially denatured fusion protein if this were to occur. Whether denaturation would transpire following synthesis of a fusion protein *in vivo*, as with the system employed during this investigation, does not seem likely, especially in light of work undertaken by Kahn *et al.* demonstrating that GFP can be expressed with reasonable efficiency in a cell-free *in vitro* translation system (Kahn et al., 1997). So, if denaturation were to take place as a result of protein transduction it is likely that autonomous refolding would follow.

For the MTPs examined there was no obvious evidence that protein transduction had taken place. The staining observed for direct GFP fluorescence and IF was virtually identical in each case, with only slight variance in fluorescence intensities between detection methods. For the short MTP fusion proteins (i.e. fusions with TAT, Drome, penetratin and mutated penetratin) staining was detected in a pattern very similar to that exhibited by the pEGFP-N1 transfected cells. Diffuse fluorescence was detected throughout the cells, in both cytoplasmic and nuclear regions. The nuclear intensity was perceived to be higher in some of the cells examined for these samples, and this may be a result of the propensity for the basic MTP domains to adhere to negatively charged structures within the cells (Lundberg et al., 2003).

The staining observed for EGFP-VP22 was very different from that of the short MTPs. Again fluorescence was detected throughout the cells, but there were small, round regions exhibiting very intense fluorescence. This was only observable by direct GFP fluorescence as IF appeared to have suffered photobleaching. Association of VP22 with microtubules has been previously documented (Elliott and O'Hare, 1998; Harms et al., 2000; Martin et al., 2002), and the intense fluorescent regions observed could be the microtubule organising centre, or centrosome, situated on the periphery of the nucleus. Alternatively these regions of fluorescence may correspond to aggregates of the fusion protein within the cells, as protein aggregates are often located to the periphery of the nucleus. Groups have reported that VP22 translocation can be recognised by a difference in the subcellular localisation of the protein between expressing and transduced cells, with expressing cells exhibiting largely cytoplasmic localisation and recipient cells demonstrating predominantly nuclear fluorescence (Aints et al., 2001; Brewis et al., 2000; Elliott and O'Hare, 1997; Liu et al., 2001). No distinguishable differences were observed in the fusion protein localisation in cells demonstrating GFP fluorescence.

3.3.2 Co-Culture Studies of Protein Transduction

As no transduction had been observed by direct or indirect visualisation of the fusion proteins, an alternative approach was undertaken. Separation of

transfected 'donor' cells expressing the fusion protein and non-expressing recipient cells was undertaken through species-specific IF staining. Transduction does not appear to be a cell-type specific process with studies performed on a broad range cell types from different species. Indeed in one study alone VP22-mediated transduction of GFP was observed in 15 different cell lines (Wybranietz et al., 1999). Though impaired uptake has been observed for the native Tat protein and the antennapedia homeodomain in cell lines with defective cell-surface proteoglycan biosynthesis machinery (Bloch-Gallego et al., 1993; Tyagi et al., 2001), no such requirement has been observed for VP22 or the short MTPs derived from these peptides.

Control co-cultures using pEGFP-N1 transfected COS-7 cells and untransfected Rat-1 cells showed that the two cell lines could be differentiated by IF with antiserum specific to rat *trans*-Golgi network, with no cross reactivity to the Golgi network of the COS cells. As expected, when co-cultures were set up using the EGFP fusion vectors the transfected cells exhibited the same GFP fluorescence as cells observed during the anti-GFP IF studies. However, for the TAT-EGFP and Drome-EGFP fusion proteins there was some evidence that protein translocation may be taking place. Transfected cells in these samples were clearly perceived as large cells exhibiting diffuse GFP fluorescence throughout the cell. Also distinguishable were isolated regions of fluorescence, which appear to be in the locale of nuclei. In addition, these regions were in close proximity to, and in some cases surrounded by, IF staining of Rat-1 cell Golgi. A curious observation was that there were no transfected cells in the immediate vicinity of these regions, yet there were clearly Rat cells harbouring no GFP fusion protein closer to expressing COS cells.

Though early studies exploring the effect that fixation conditions had on observable VP22 translocation concluded that permeabilisation with methanol could not account for the observed spread of VP22 through a monolayer (Brewis et al., 2000), these observations have since been questioned. Lundberg and Johansson applied VP22 directly to cells already fixed by treatment with methanol and found that the protein could be detected in the nuclei of the cells, even after extensive washing, following only a 2 minute incubation (Lundberg

and Johansson, 2001). In addition, exogenous application of VP22-GFP to live cells resulted in detection of the fusion protein associated with the cell membrane only. However, directly after methanol fixation and rehydration in PBS, the cells exhibited nuclear GFP fluorescence (Lundberg and Johansson, 2001). Further studies by the group have supported these findings (Lundberg and Johansson, 2002; Lundberg et al., 2003). A study using only mild PFA fixation condition in place of methanol permeabilisation reported artifactual redistribution of TAT into the nucleus of cells following exogenous application, giving rise to altered images as compared with the experiments performed on unfixed cells (Richard et al., 2003), and photomicrographs of identical fields of cells demonstrated the apparent spread of TAT-EGFP from transfected to cells to neighbouring cells following fixation with methanol (Leifert et al., 2002). The neighbouring cells had exhibited no fluorescence prior to fixation.

The distribution of the TAT-EGFP and Drome-EGFP fusion proteins in small, isolated regions can be explained by three possible events. The first is that the fluorescence is coming from COS-7 cells expressing low levels of the fusion protein, which is predominantly localised within the nucleus. The second is that the fixation conditions used have resulted in artefactual redistribution of the fusion proteins from expressing cells. The third possible occurrence is that protein transduction of the fusion proteins has taken place, resulting in detection of GFP-fluorescence in Rat-1 cells. It is unlikely that the GFP fluorescence detected is attributable to expressing cells as such distribution had not been observed in other transfection experiments. The size of the regions, if they were nuclei, was also appreciably smaller than the nuclei of the obviously transfected COS-7 cells. Problems are also posed when accounting for fluorescence arising from the other two events. It would be expected that redistribution of the fusion protein by either translocation, or by a fixation-induced artefact, would be marked by spread to cells immediately adjacent to the expressing cells, yet IF staining demonstrates the presence of Rat-1 cells occupying the area between the expressing cells and the isolated regions of fluorescence.

It is possible that redistribution has occurred, and that the cells exhibiting the GFP fluorescence have greater propensity for the fusion proteins than the other

cells. For the artefactual spread of the fusion protein, increased accessibility of the intracellular environment to the extracellular milieu would increase the possibility that basic MTPs eluted from expressing cells could interact with negatively charged cellular components. It is possible that only some cells have had complete permeabilisation of their nuclear membranes, allowing fusion proteins eluted from the cytoplasm of the expressing cells access to the highly negatively charged oligonucleotide molecules, with which they associate through electrostatic interactions. These cells would therefore exhibit nuclear localisation of the GFP fusion proteins. If protein transduction has taken place, then uptake in these cells must have occurred to a greater extent than in the intervening cells. A possibility is that the cells are exhibiting an altered expression profile, and are synthesising some component of the extracellular matrix, or cell surface which increases the local concentration of the fusion proteins following their escape from the COS cells. Such a concentration increase would preferentially favour transduction to these cells whilst decreasing the protein available to other cells.

An interesting observation, captured in figure 3.14 A, was the variety of GFP localisation found within pEGFP-VP22 transfected cells. Cells showing distinct cytoplasmic and nuclear staining were frequently observed, and the presence of these two localisations has been used as a demonstration of protein transduction from expressing cells (cytoplasmic localisation) to recipient cells (nuclear localisation) (Aints et al., 2001; Brewis et al., 2000; Elliott and O'Hare, 1997; Liu et al., 2001). Also evident was strong association with chromatin in cells undergoing mitosis, which has again been observed previously (Elliott and O'Hare, 1997; Harms et al., 2000; Martin et al., 2002). Many cells exhibiting cytoplasmic staining for GFP also exhibited a localisation of the EGFP-VP22 to a region outside of the nucleus as demonstrated by figures 3.8 and 3.14. This is thought to be aggregated protein. An alternative explanation to transduction being accountable for the different cytoplasmic and nuclear staining would be that protein in expressing cells could be predominantly cytoplasmic until specific cellular cues prompted association with chromatin. If this were to occur when the nuclear envelope began to disassemble the protein would not be required to cross this barrier in order to gain access to and bind DNA.

Following separation of daughter cells, this protein would then be trapped within the nucleus as the nuclear envelope reformed.

3.3.3 FACS Studies

As the microscopy approaches had only detected limited, if any, transduction FACS was employed to allow an objective and accurate quantitation of transduction. Several groups have previously used flow cytometry analysis of living cells to determine the uptake of MTPs (Ho et al., 2001; Nagahara et al., 1998; Schwarze et al., 1999; Vives et al., 1997a; Vocero-Akbani et al., 1999; Wybranietz et al., 1999). Analysis was undertaken on live cells, so artefactual redistribution through fixation would be ruled out. In addition, a large sample of cells could be analysed, with the level of GFP fluorescence detected in each cell examined in a manner not possible by the confocal methodology.

Three ranges of fluorescence intensity were examined for each sample, from cells exhibiting low fluorescence (above background) to highly fluorescent cells. This covered a range of fluorescent intensity over three orders of magnitude. Though transduction could result in an overall shift in the number of cells exhibiting high levels of fluorescence, it was hoped that by examining the different ranges subtle events would be detected. Such an event would include transduction from highly fluorescent cells to cells expressing only low levels of protein. This would not affect the total number of GFP positive cells but would shift cells from both the low and high fluorescent ranges into the mid-fluorescent range.

None of the populations of cells expressing MTP-EGFP fusion proteins exhibited a higher percentage of cells exhibiting GFP fluorescence than the pEGFP-N1 control sample. In addition, the cells detected in each of the three fluorescence intensity regions increased in a very similar manner for all of the samples, indicating an almost identical distribution of fluorescence intensities for the GFP-positive cells in each sample. Such a distribution is similar to that FACS analysis of cells expressing TAT-EGFP or EGFP where observations were taken of the percentage of cells occupying 9 strata of fluorescence intensity (Leifert et al., 2002). Investigators have reported that an apparent translocation

of exogenously applied MTPs is detected in live cells by FACS analysis, but that treatment of cells with trypsin (Richard et al., 2003) or heparin (Lundberg et al., 2003) indicates that this protein is actually cell surface associated and not internalised. The cells examined in this study were subjected to a minimum of 8 minutes treatment with trypsin, removing any protein that may have left expressing cells and merely become associated with the cell membranes of other cells.

Summary

Exploration of protein transduction mediated by the MTPs by direct and indirect visualisation of GFP, differentiation of transfected from non-transfected cells in co-culture, and by FACS analysis failed to confirm whether the transduction phenomenon had taken place. Different localisation characteristics exhibited by cells expressing EGFP-VP22 are as a result of attributes exhibited by the native VP22 protein. Identification of some GFP-positive cells in pTAT-EGFP and pDrome-EGFP transfected cell co-cultures that were probably not transfected was most likely an artefact introduced during fixation.

CHAPTER 4
LUCIFERASE AS A REPORTER FOR PROTEIN TRANSDUCTION

4.1 Introduction

The three approaches to detect translocation of MTP-EGFP fusion proteins yielded no definitive evidence that transduction had taken place. If the phenomenon were occurring in the cells it would be only to a very limited degree. To discern whether any transduction was being carried out by the MTPs a more sensitive method was required, enabling even low levels of translocated protein to be detected. The reporter chosen was luciferase, due to the ease with which the enzyme's activity is assayed, and the sensitivity of the system.

The *luc* gene from the North American firefly *Photinus pyralis* encodes luciferase (LUC) which catalyses the ATP-dependent oxidative decarboxylation of beetle luciferin in a bioluminescence reaction, leading to light emission which can be quantified in a luminometer. The reaction is shown below:

$$\text{luciferase} + \text{luciferin} + \text{ATP} \xrightarrow{Mg^{2+}} \text{luciferase} \bullet \text{luciferyl-AMP} + PP_i$$

$$\text{luciferase} \bullet \text{luciferyl-AMP} + \text{oxygen} \longrightarrow \text{luciferase} + \text{oxyluciferin} + \text{AMP} + CO_2 + h\nu$$

The luciferase cDNA sequence was originally isolated through screening of a *P. pyralis* lantern cDNA library, and cloned for expression in mammalian cells in 1987 (Dewet et al., 1987). It has since become a very popular reporter gene, especially in the studies of promoters or regulation of gene expression. The already sensitive catalytic reaction has subsequently been improved with advances in detection technology allowing detection of as little as 10^{-20} moles of luciferase under optimal conditions (Wood, 1991). This is over 100 fold more sensitive than the popular chloramphenicol acetyltransferase reaction. It is possible to study the luciferase activity in individual cells using single photon imaging systems, but this equipment is not yet widely available.

Luciferase activity can be detected in live or lysed cell samples, but the activity measured reflects the luciferase levels present for the whole sample, not the individual cells. It would therefore be necessary to develop a system in which transfected cells expressing the luciferase-MTP fusion proteins could be distinguished and separated from non-expressing recipient cells. This would allow the activity within the recipient cells to be measured and the level of transduction therefore quantified.

4.2 Results

4.2.1 Construction of the Luciferase Expression Vector pSAM1

4.2.1.1. Cloning Strategy

A vector was required that would express luciferase in mammalian cells under the control of a strong promoter. The ideal vector would contain a multiple cloning site (MCS) at the N-terminus of the luciferase gene that would allow the in-frame insertion of each MTP-encoding sequence into the vector to produce MTP-luciferase fusions. There were no commercially available vectors for generation and expression of luciferase fusion proteins in a eukaryotic system. As a result, the gene encoding luciferase had to be excised from a prokaryotic vector and inserted into a eukaryotic expression vector with a MCS. Following insertion of luciferase into the eukaryotic vector, sufficient restriction sites would have to be retained in the MCS to allow the subsequent insertion of the MTP-encoding sequences at the N-terminus of luciferase.

The vector pGEM-*luc* was selected as the source of the firefly luciferase gene. The vector has a number of unique restriction sites at both ends of the gene, allowing its excision. The vector pcDNA3.1(+) was selected as the eukaryotic expression vector into which the luciferase gene would be inserted. It has a cytomegalovirus (CMV) enhancer-promoter for high level expression, and a MCS containing complementary restriction sites to those in pGEM-*luc*.

4.2.1.2. Construction of pSAM1 (pcDNA3.1(+)-luc)

The luciferase gene was removed from the pGEM-*luc* vector on sequential digestions with the *Bam* H1 and *Xho* 1 restriction enzymes. The luciferase gene was isolated by gel purification. The pcDNA3.1(+) vector was subjected to the same series of digests and purification procedures. A standard ligation reaction was then carried out to insert the luciferase gene into the linearised pcDNA3.1(+) vector, thus producing pcDNA3.1(+)-*luc* vector that will be referred to as pSAM1. The orientation of the *luc* gene in pcDNA3.1(+) was known to be correct as a result of the non-identical sticky ends generated

following restriction digestion of the two vectors. The presence of the luciferase gene within pcDNA3.1(+) was confirmed by restriction analysis, see figure 4.1.

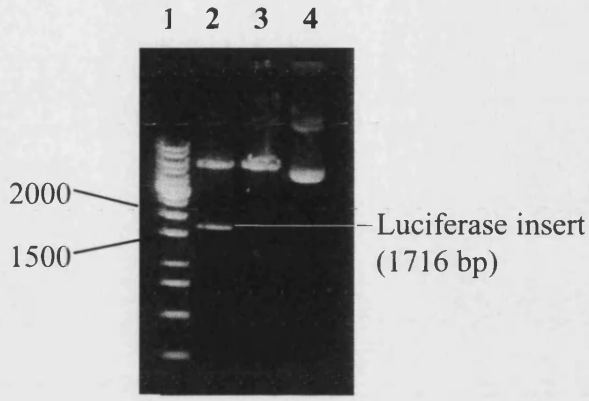

Figure 4.1. ***Bam* HI/*Xho* I digest of pSAM1.** Lane 1: Molecular weight markers, lane 2: digested pSAM, lane 3: pcDNA3.1(+) subjected to the same digests, and lane 4: uncut pcDNA3.1(+) plasmid DNA.

4.2.1.3 Activity Study of the pSAM1 Expression Product

Having successfully inserted the *luc* gene into the pcDNA3.1(+) vector it was necessary to determine if cells transfected with the construct would express an active gene product. COS-7 cells were transiently transfected with different amounts of pSAM1 using PEI as a transfection agent. A total of 2 µg of DNA was used in each transfection, and where less than 2 µg of pSAM1 was used non-specific pcDNA3.1(+) DNA was added to make up the short-fall.

Luciferase activity was detected in the cytosolic extracts of cells 48 h post-transfection using as little as 125 ng pSAM1 (Fig. 4,2). Up to 2 µg pSAM1 the luciferase activity exhibited by the cells increased in a linear manner as the amount of DNA used for the transfections was increased.

As the gene product of pSAM1 was active the vector could act as a 'parent' vector for subcloning of MTPs, enabling generation of MTP-luciferase fusion products.

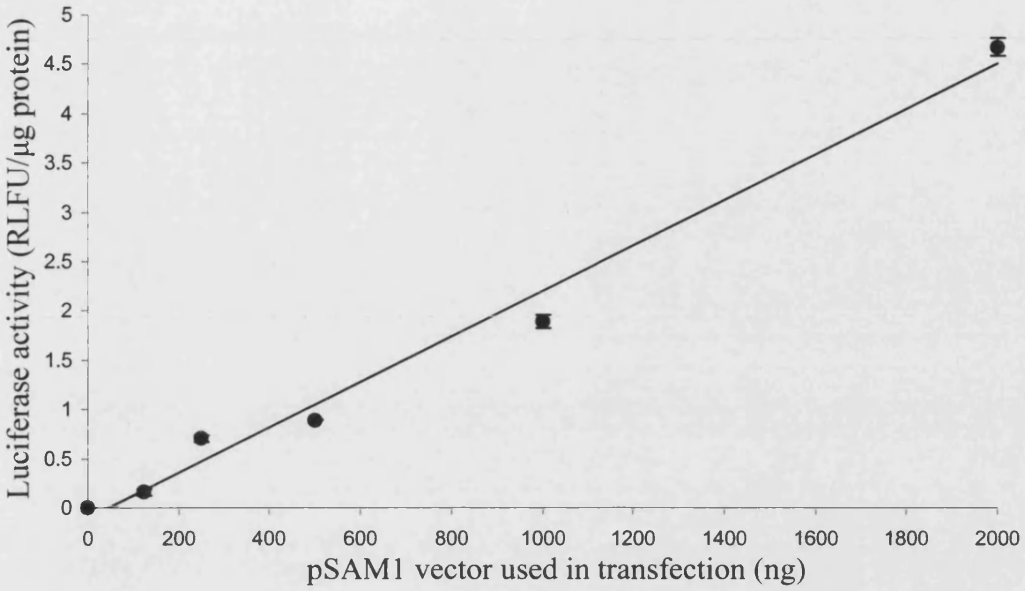

Figure 4.2. Activity of COS-7 cells transfected with pSAM1. COS-7 cells were transfected with the amount of pSAM1 DNA indicated and the luciferase activity in the cytosolic extract of cells measured 48 h post-transfection. Triplicate readings were taken and data represent the average of 3 experiments ± S.E.M.

4.2.2 Construction of MTP-Luciferase Expression Constructs

As luciferase was to act as a reporter to quantify the protein transduction efficiency of each of the translocating sequences it was necessary to generate expression vectors that would allow the production of luciferase as a fusion protein with each of the MTPs. The vector pSAM1 was to act as the 'parent' vector, and subcloning was undertaken to generate constructs coding for the MTP sequences in N-terminal fusions with luciferase.

4.2.2.1 Oligonucleotide Design

For the cloning of the peptides Tat PTD, wild-type penetratin, mutant penetratin and Drome oligonucleotide sequences were designed for the sense and antisense strands of each coding region. The sequences would be ordered (Sigma, Genosys, UK), and the complementary sense and antisense sequences phosphorylated and annealed to generate double-stranded DNA sequences coding for each short MTP. For successful generation of MTP-luciferase fusion

protein it was necessary to include additional bases at the ends of the pairs of oligonucleotides to ensure the incorporation of:

a) a 5' *Hind* III restriction site

b) a start codon preceding the peptide sequence

c) a 3' *Bam* HI restriction site

d) additional bases between the peptide coding sequence and the *Bam* HI restriction site so that on ligation into pSAM1 the luciferase gene was in the same reading frame as the start codon and coding sequence of the peptide.

The sense and anti-sense pairs of oligonucleotides designed for each of the short MTP sequences are shown in table 3, including the bases needed to satisfy the criteria above.

For the cloning of a vector containing the coding sequence for the VP22-luciferase fusion protein, a PCR product was required. Oligonucleotide primers were designed to amplify VP22 from the vector pGE155 (the plasmid coding for a EGFP-VP22 fusion protein referred to as pEGFP-VP22 in chapter 3). Additional 5' bases were included to allow insertion into pSAM1. The sense primer contained a *Hind* III restriction site and a start codon. The antisense primer contained bases to ensure VP22 and luciferase would be in the same reading frame when VP22 was inserted into pSAM1, and a *Bam* HI restriction site. The oligonucleotide primers are shown in table 4.1.

4.2.2.2 Construction of pSAM1-MTP Expression Vectors

The pSAM1 vector was subjected to sequential digests with the *Bam* H1 and *Hind* III restriction enzymes, and the linearised vector isolated by gel purification. For the insertion of the TAT and Drome coding sequences the annealed and phosphorylated oligonucleotides were used in a standard ligation reaction with linearised pSAM1 vector, thus producing pSAM1-Tat and pSAM1-Drome respectively. Transformed *E. coli* were screened for the presence of each construct by restriction analysis of their DNA. By using the *Bam* H1/*Hind* III double digest successful insertion of an MTP into pSAM1 would result in the destruction of a *Kpn* 1 site. The correct inserted sequence was then confirmed by sequence analysis using the pSAM1 sequencing primer (Appendix B12). The sequence traces can be seen in figure 4.3 A and B.

Peptide (**peptide sequence**)	Sense oligonucleotide	Antisense oligonucleotide
HIV-Tat **MYGRKKRRQRRR**	5'AgCTTATGTATggCAgg AagAAgCggAgACagCgAC gAAgAgg 3'	5'gATCCCTCTTCgTCgCTg TCTCCgCTTCTTCCTgCCA TACATA 3'
Wild-type Penetratin **MRQIKIWFQNRRMKWKK**	5'AgCTTATgCgCCAgAT AAAgATTTggTTCCAGA ATCggCgCATgAAgTggA AgAAggg 3'	5'gATCCCCTTCTTCCACTT CATgCgCCgATTCTggAAC CAAATCTTTATCTggCgCA TA 3'
Mutant Penetratin **MRQIKIFFQNRRMKFKK**	5'AgCTTATgCgCCAgAT AAAgATTTTCTTCCAgA ATCggCgCATgAAgTTCA AgAAggg 3'	5'gATCCCCTTCTTgAACTT CATgCgCCgATTCTggAAgA AAATCTTTATCTggCgCAT A 3'
Drome **MEGRRGKRDLLR**	5'AgCTTATggAAggTCgT CgTggTAAACgTgACCTg CTgCgTgg 3'	5'gATCCCACgCAgCAggTC ACgTTTACCACgACgACCT TCCATA 3'
VP22	5'ATTATAAgCTTATgAC CTCTCgCCgCTCCgTgAA gTCgggTCCgC 3'	5'TATggATCCgCTCgACggg CgTCTggggCgAgAAgCggAg 3'

Table 4.1. Sense and antisense oligonucleotides designed to produce MTP-coding sequences for insertion into pSAM1. The peptide sequences the oligonucleotides code for are shown in bold. The oligonucleotides given for VP22 are primers for the PCR amplification of VP22. For the mutated form of penetratin mutated codons and residues are underlined.

Due to failed attempts to generate the vectors pSAM1-WTPen and pSAM1-mPen, insertion of the sequences coding for wild-type penetratin and mutant penetratin required additional steps to purify the respective annealed and phosphorylated oligonucleotides. These steps were undertaken following vertical polyacrylamide gel electrophoresis to ensure successful phosphorylation and annealing of the primers had been achieved. Following successful isolation of the coding sequences, insertion into pSAM1 was carried out in an identical manner to the insertion of the TAT and Drome sequences, and screening undertaken. The sequence traces confirming the presence of penetratin and mutant penetratin in pSAM1 can be seen in figure 4.3 C and D, respectively.

The VP22 coding sequence was amplified from the vector pGE155 by PCR, using primers from table 4.1. The following PCR reaction was set up, and the following conditions were used:

Reagent	Volume (µl)
Reaction mix	25.0
MgCl	1.5
Template* (PGE155)	1.0
Sense primer**	1.0
Anti-sense primer**	1.0
H_2O	21.5

* 100 ng ** 10 pmol

Temperature (°C)	Time (s)	
95	120	30 cycles
94	45	
55	90	
72	60	
72	600	
4	hold	

Following amplification, the VP22 fragment was gel purified, double digested with *Bam* H1 and *Hind* III, and the DNA ready for insertion into pSAM1 gel purified again. Following successful isolation of the coding sequences, insertion into pSAM1 was carried out in an identical manner to the insertion of the other MTP sequences. Screening was undertaken by *Bam*H1/*Hind* III digestion of pSAM1-VP22. Sequencing of the vector was undertaken using the pSAM1 sequencing primers (Appendix B12) to check for mutations in the PCR product, and the sequence data is shown in figure 4.4 A and B. The data showed that an in-frame fusion of VP22 and luciferase had been generated, but a single point mutation was identified that resulted in a threonine to serine change-of-base mutation in residue 135. However, as transduction studies have been successfully undertaken using only a C-terminal fragment of VP22 (bases 159-301 (Kueltzo et al., 2000)) it appears that this base is not involved in the processes of VP22 translocation or protein transduction. For this reason no further attempt was made to generate a construct without mutation, and the vector described above was used for subsequent studies.

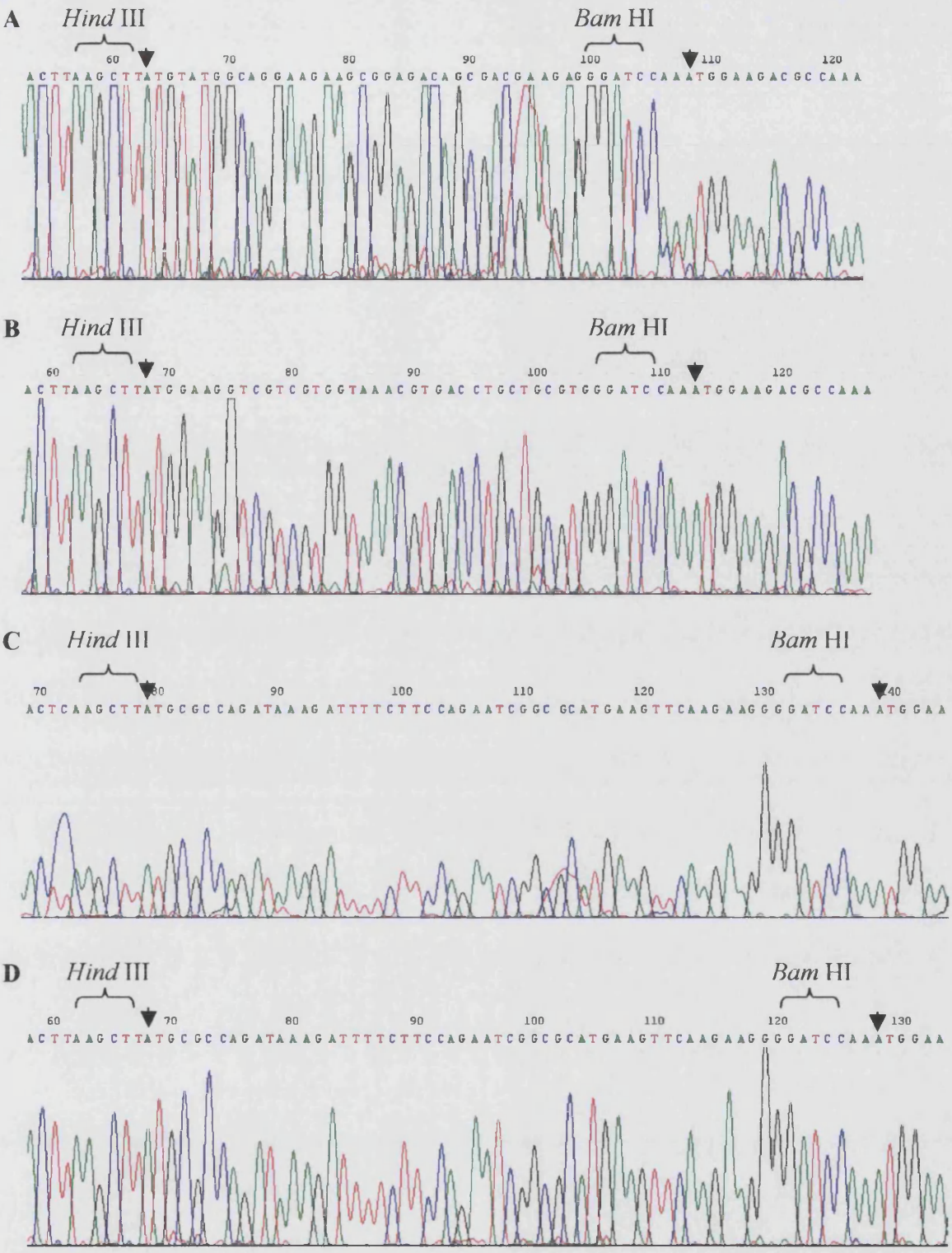

Figure 4.3. Insertion of short MTP coding sequences into pSAM1. Sequence traces showing the insertion of the oligonucleotides encoding HIV Tat (A), Drome (B), wild type penetratin (C) or mutant penetratin (D) into pSAM1 using the restriction sites *Hind* III and *Bam* HI. In-frame, N-terminal fusions of each sequence with luciferase were therefore generated (the start codon for each MTP is highlighted by an arrow, and the redundant start codon for luciferase, which is now a Met residue, is also highlighted in each case).

A AAGCTT**ATG**ACCTCTCGCCGCTCCGTGAAGTCGGGTCCGC
GGGAGGTTCCGCGCGATGAGTACGAGGATCTGTACTACAC
CCCGTCTTCAGGTATGGCGAGTCCCGATAGTCCGCCTGAC
ACCTCCCGCCGTGGCGCCCTACAGACACGCTCGCGCCAGA
GGGGCGAGGTCCGTTTCGTCCAGTACGACGAGTCGGATTA
TGCCCTCTACGGGGGCTCGTCATCCGAAGACGACGAACAC
CCGGAGGTCCCCCGGACGCGGCGTCCCGTTTCCGGGGCGG
TTTTGTCCGGCCCGGGCCTGCGCGGGCGCCTCCGCCACCC
GCTGGGTCCGGAGGGGCCGGACGCACACCCACCACCGCCC
CCCGGGCCCCCCGAACCCAGCGGGTGGCGTCTAAGGCCCC
CGCGGCCCCGGCGGCGGAGACCACCCGCGGCAGGAAATC
GGCCCAGCCAGAATCCGCCGCACTCCCAGACGCCCCCGCG
TCGACGGCGCCAACCCGATCCAAGACACCCGCCAGGGGCT
GGCCAGAAAGCTGCACTT

B CACTTTAGCACCGCCCCCCCAAACCCC
GACGCGCCATGGACCCCCCGGGTGGCCGGCTTTAACAAGC
GCGTCTTCTGCGCCGCGGTCGGGCGCCTGGCGGCCATGCA
TGCCCGGATGGCGGCGGTCCAGCTCTGGGACATGTCGCGT
CCGCGCACAGACGAAGACCTCAACGAACTCCTTGGCATCA
CCACCATCCGCGTGACGGTCTGCGAGGGCAAAAACCTGCT
TCAGCGCGCCAACGAGTTGGTGAATCCAGACGTGGTGCAG
GACGTCGACGCGGCCACGGCGACTCGAGGGCGTTCTGCGG
CGTCGCGCCCCACCGAGCGACCTCGAGCCCCAGCCCGCTC
CGCTTCTCGCCCCAGACGGCCCGTCGAGCGGATCCAAA**ATG**

Figure 4.4. Insertion of VP22 coding sequence into pSAM1. Sequence data demonstrating the insertion of VP22 cDNA into the MCS of pSAM1 using the restriction sites *Hind* III and *Bam* HI (restriction sites underlined). An in-frame, N-terminal fusion of VP22 with luciferase is therefore generated (the start codon for VP22 is highlighted in bold type, and the redundant start codon for luciferase, which is now a Met residue, is also highlighted). (A) Sequence obtained using the pSAM1 sequencing primer. (B) Reverse complementary sequence of the sequence obtained using the pSAM1 reverse sequencing primer. Sequence shared between the two traces is indicated by linked black boxes. The point mutation within the sequence, A397C, which results in a threonine to serine change at residue 135, is highlighted in red.

4.2.3 Characterisation of the pSAM1 Family of Expression Vectors

Having successfully inserted each of the MTPs sequences into pSAM1 to enable the expression of N-terminal fusions of the MTPs to luciferase it was necessary to confirm that the vectors produced active gene products. COS-7 cells were transfected with 1 μg vector DNA using GeneJuice and the activity of cytosolic cell extracts measured 24 and 48 hours post-transfection.

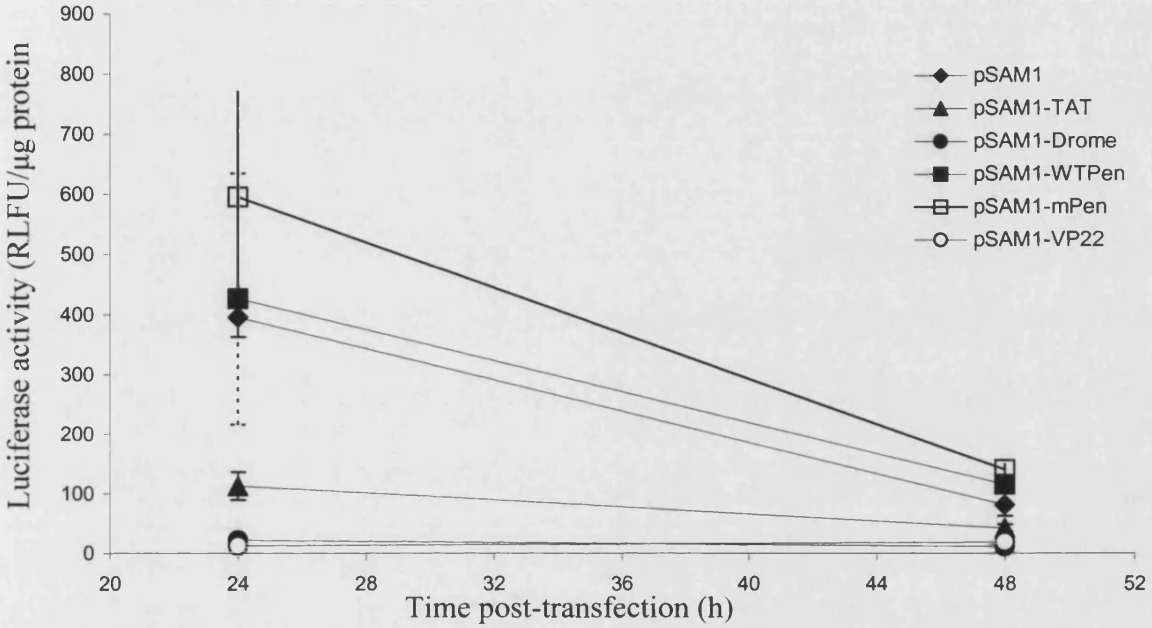

Figure 4.5. Time course of luciferase activity. COS-7 cells were transiently transfected with pSAM1 or each pSAM1-MTP fusion constructs. Luciferase activity of cytosolic extracts was measured 24 and 48 h post-transfection. Measurements were performed in triplicate, values are an average of two experiments ± S.D. (NB S.D. for pSAM1-mPen, no horizontal bar; S.D. for pSAM1-WTPen, broken line.) A pcDNA3.1(+) transfected control is not shown as background activity was $\geq 10^4$ fold lower than any of the other samples.

Each pSAM1-MTP construct generated an active luciferase fusion product, though the level of activity detected in transfected cells did vary considerably, depending on which vector was used in the transfections (Figure 4.5). With the exception of VP22 all the activity of all samples decreased from 24-48 h. To explore whether the differences in luciferase activity exhibited by the cells were

due to differences in expression levels, or changes in the intrinsic activity of luciferase as a result of being expressed as a fusion protein, Western blot analysis directed against luciferase was performed on cytosolic extracts (Figure 4.6). Analysis was performed 48 h post-transfection as the differences in activity were smaller at this time (a maximum difference of 12-fold between samples) than at 24 h post-transfection (a maximum difference of 50-fold).

	pSAM1	pSAM1-TAT	pSAM1-Drome	pSAM1-WTPen	pSAM1-mPen	pSAM1-VP22
Relative activity	1.00	0.39	0.087	0.89	1.18	0.057
Relative expression	1.00	0.18	—	0.36	0.40	—

Table 4.2. Comparison of luciferase activity and expression. The luciferase activity and expression levels of the transiently transfected samples in figure 4.6 are shown relative to that of pSAM1 transfected cells. Lines indicate data that were not quantifiable.

The activities of the samples harvested for immunoblotting were consistent with those observed in figure 4.5, though the pSAM1-mPen transfected cells exhibited a higher activity than the pSAM1 transfected cells (Figure 4.6 A). The relative activities of the samples can be seen in table 4.2. Western Blot analysis was undertaken with recombinant luciferase (Sigma) as a control. The control protein is visible at 66 kDa (Fig. 4.6 B). The samples expressing luciferase fusion proteins with the short MTP sequences (12 or 17 residues) would be expected to run only about 2 kDa heavier than luciferase when expressed alone. Bands were clearly visible for luciferase alone (luc) and the fusion proteins TAT-luc, WTPen-luc, and mPen-luc. No band was detected for Drome-luc. The fusion protein VP22-luc would have a molecular weight of about 104 kDa as the full length VP22 protein was used (38 kDa). However, no band was detected at this weight using Western blot analysis. The relative levels of expression, where determinable, are shown in table 4.2.

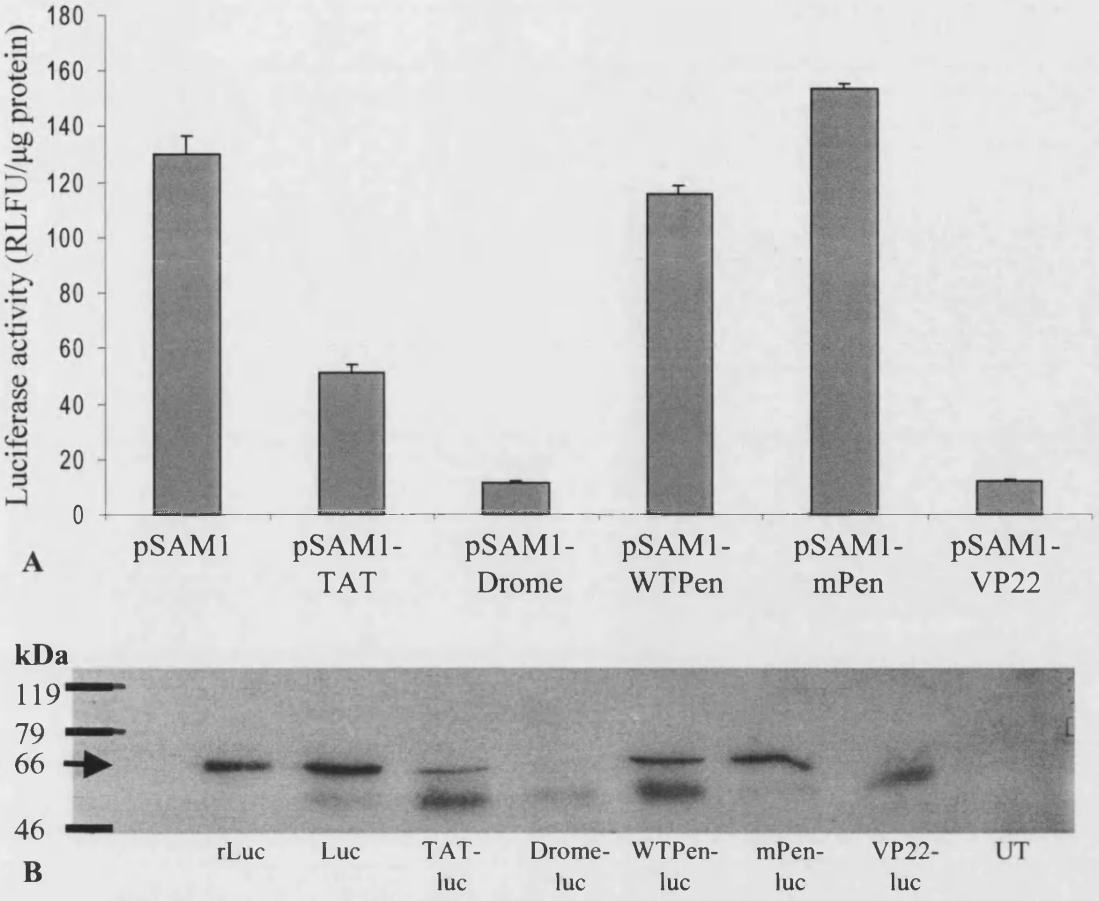

Figure 4.6. Activity and expression of pSAM1-MTP products. COS-7 cells were transiently transfected with 1 µg of either pSAM1 or a pSAM1-MTP fusion construct. (A) Forty eight hours post-transfections luciferase activity in cytosolic extracts was measured. Measurements were performed in triplicate and values show an average ± S.D. (B) To compare expression levels of the constructs Western blotting against luciferase was carried out on the same samples, using recombinant luciferase (rLuc) as a positive control. A sample of untransfected COS-7 cells is shown as a control (UT). The experiment was carried out three times and the samples presented here are representative of the data collected. The relative activity and expression levels for each sample is shown below in Table 4.2).

The levels of activity detected in the samples seem to correspond to changes in the levels of expression of active fusion proteins. Cells transfected with the vectors pSAM1-Drome and pSAM1-VP22 give measurable activities of less than 10 % that of samples transfected using pSAM1, and Western blot analysis cannot detect any fusion protein within these samples. The samples TAT-luc and WTPen-luc, which have activities about 60 % and 10 % lower, respectively, than luciferase alone, are detected by Western blotting with expression levels lower than that of luciferase. Both samples have a second, lower molecular weight band detected by the blot, possibly representing an incomplete expression product. If this is the case, the product may have a limited activity that could account for the discrepancies in the differences observed between the relative activity and expression levels measured for the fusion proteins.

4.2.4 Quantification of Protein Transduction Using Luciferase as a Reporter Protein

4.2.4.1 Detection of Protein Transduction

To harness the sensitivity potential of luciferase as a reporter protein it was necessary to develop a means by which cells expressing the luciferase fusion proteins could be distinguished and separated from non-transfected cells. Assessment of the latter sample of cells for luciferase activity would determine whether protein transduction had occurred. A comparison of the total activity of the cells with the activity exhibited by the non-expressing cells would allow quantification of the efficiency with which the transduction of the active protein had taken place.

Segregation of non-transfected cells from transfected ones was to be undertaken through cell sorting by FACS analysis. For this to take place a characteristic of the two cell samples must differ sufficiently to allow a population designation to be made. By creating one fluorescent population cells from this sample are easily distinguishable from non-fluorescent cells, and can be separated. This could be done by immunofluorescence directed against a cell-type specific epitope, as was undertaken in the transduction studies of GFP in co-cultures. However, unless the epitope is located on the outside of the cell some form of

fixation must take place which may be deleterious to the activity of luciferase, or may introduce translocation artefacts, as discussed in the introduction.

The use of GFP expression to distinguish the cell populations would allow FACS analysis of live cells to be undertaken, and was thus chosen. However, rather than transiently transfect cells with a GFP expression vector a COS-7 cell line would be generated to constitutively express GFP. Co-culture experiments could then be undertaken utilising pSAM1-transfected COS-7 cells and non-transfected GFP expressing cells. Cell sorting to isolate the fluorescent cells would eliminate non-GFP-positive, and therefore transfected cells from the harvested population, and so activity within this population would be attributable only to protein transported to these cells.

4.2.4.2 Generation of a Stable Cell Line Constitutively Expressing EGFP

The vector pEGFP-N1 allows selection for transfected cells using the antibiotic G418. COS-7 cells were initially analysed to determine their susceptibility to G418 by growth in medium supplemented with different concentration of the antibiotic. Cells were seeded in non-supplemented medium at a density of 5 x 10^4 cells per 35 mm dish. Growth medium was supplemented with different concentration of G418 24 h after seeding, and medium was changed every 48 h. Cell counts were performed 3 days after seeding, and then every 48 h. The growth of the COS-7 cells was monitored for two weeks in G418-supplemented medium to generate a 'kill curve' for the cells, which is shown in figure 4.7.

From the kill curve a concentration of 700 μg/ml was chosen to allow selection of pEGFP-N1 transfected cells over a time period of about 14 days. This concentration would ensure that non-transfected COS-7 cells were killed over the selection period, whilst the concentration was not too high to risk a toxic insult to transfected cells. Fourteen days would also allow formation of growth plaques of stable cells that could be harvested for critical assessment of their characteristics.

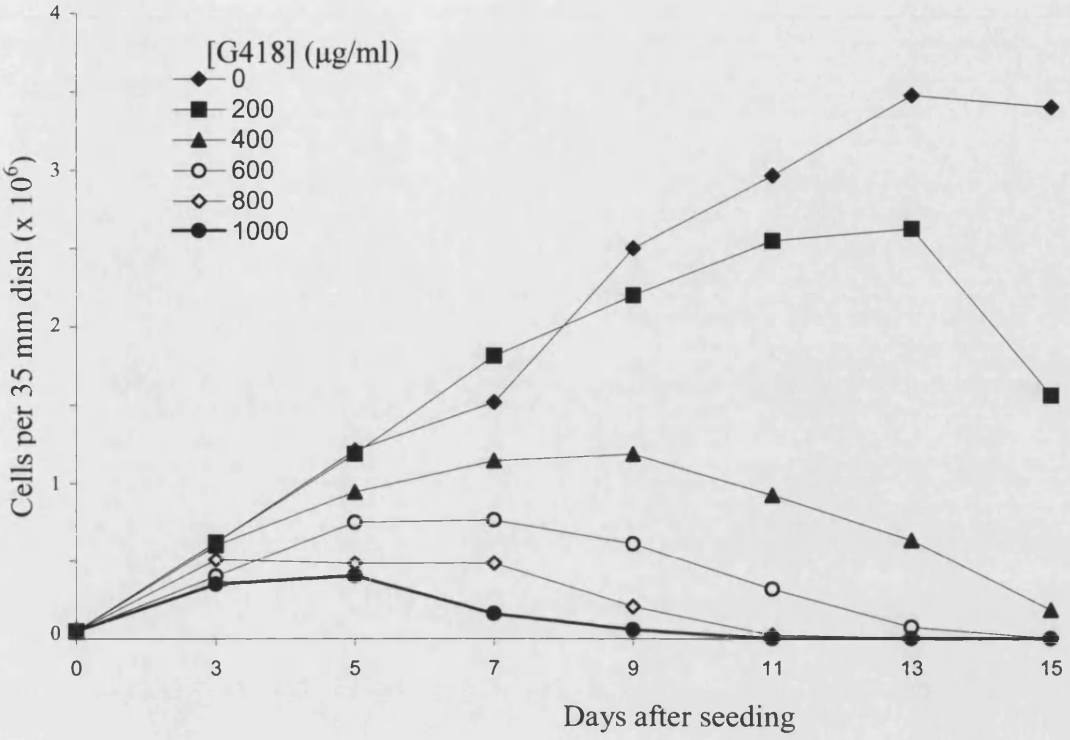

Figure 4.7. Kill curve of COS-7 cells with G418. COS-7 cells were grown in medium supplemented with the antibiotic G418, at the concentrations indicated, for two weeks. Cell counts were performed every 48 h.

COS-7 cells in 35 mm dishes were transfected with 2 µg pEGFP-N1 using PEI. Twenty-four hours post-transfection growth medium was supplemented with 700 µg/ml G418. Cells were washed and the supplemented medium changed every 48 h. Eighteen days post-transfection plaques of cells had formed that were not susceptible to G418. These plaques were individually harvested and cultivated in supplemented growth medium to increase the cell populations. The proliferation of the cells was monitored, and the expression levels of EGFP assessed by fluorescence microscopy. Potential stable cell lines for use in the co-culture experiments were then examined by FACS analysis to determine the number of cells exhibiting GFP expression. Of the cell populations examined, the cell line COS-EGFP6 was determined to have the most suitable characteristics for use in the co-culture experiments. Representative micrographs and FACS data can be seen in figure 4.8.

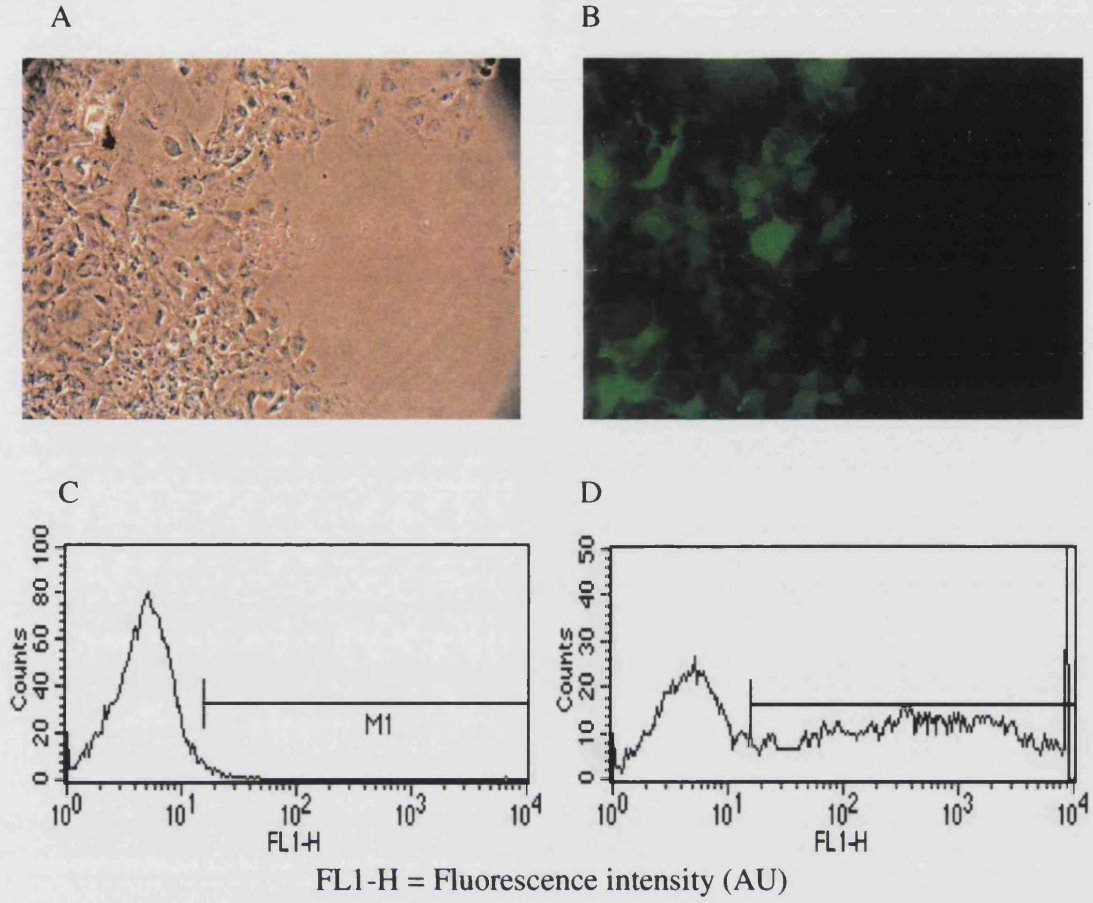

Figure 4.8. The stable cell line COS-EGFP6. COS-7 cells were transfected with the vector pEGFP-N1 and grown in growth medium supplemented with 750 µg/ml G418 for 14 days to select cells constitutively expressing EGFP. (A and B) The cell line COS-EGFP6 shown under transmitted light and GFP expression viewed by excitation at 488 nm, respectively. (D) FACS analysis of COS-EGFP6 shows the stable cell line to contain a significantly higher number of cells exhibiting GFP fluorescence compared with untransfected COS-7 cells (C) (percent events with fluorescence intensity 15-10,000 AU: COS-7 = 1.74, COS-EGFP6 = 64.00).

4.2.4.3 Cell Sorting by FACS

From the preliminary FACS data for the COS-EGFP6 cells the number of cell with a fluorescence intensity above background was found to be about 60 % (see figure 4.8 C vs. 4.8 D). Though this was not the 'gold standard' of 100 % of cells constitutively expressing EGFP it was determined that in a co-culture of COS-7 cells with COS-EGFP6 cells there would be sufficient cells to act as recipient cells for transduced luciferase fusion proteins. In a co-culture of transfected COS-7 cells with untransfected COS-EGFP6 cells, at a ratio of 1:1, about 30 % of the population would still act as recipient cells that exhibit a level of fluorescence sufficiently intense to allow sorting and collection of this population from the transfected cell population.

To determine the efficiency with which FACS analysis would allow separation and collection of cells trial sorting was undertaken using a population of COS-EGFP6 cells alone. The FACS machine was calibrated using a sample of non-fluorescent COS-7 cells. A region of fluorescence intensity was established whereby less than 1 % of the COS-7 cell population was detected within this gated region (figure 4.9 A and table 5), and settings applied that would allow collection of all cells occupying the region of high fluorescence intensity. A large sample of COS-EGFP6 cells (about 7 x 10^5) was then analysed by FACS, and cells detected in the high fluorescence region collected. Representative FACS data can be seen in figure 4.9 B and table 4.3. The harvested cells were concentrated by centrifugation prior to re-analysis. Figure 4.9 C shows representative FACS data of the collected sample of cells, and the percent events in both the low and high fluorescence intensity regions are presented in table 4.3.

Sample	% low fluorescence	% high fluorescence
COS-7	99.5	0.5
COS-EGFP6	47.6	52.4
Harvested COS-EGFP6	39.7	60.3

Table 4.3. FACS analysis and cell sorting of COS-EGFP6.

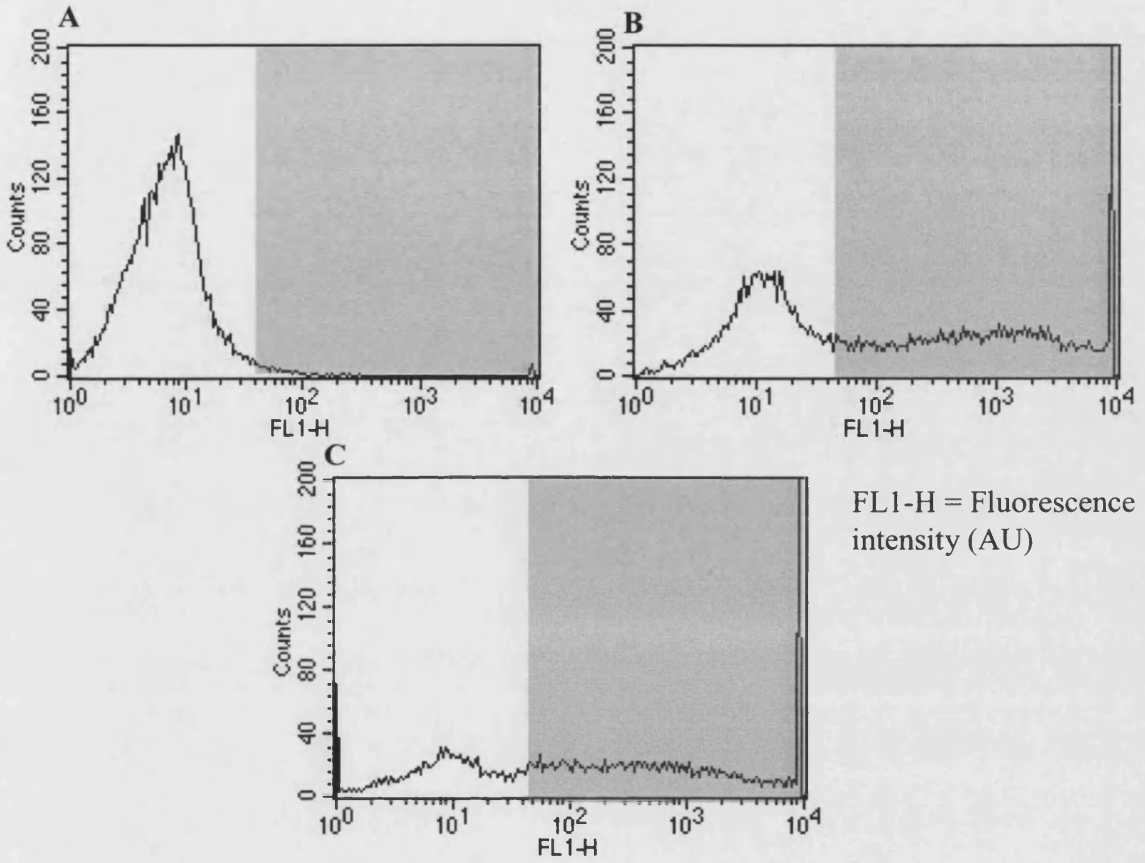

Figure 4.9. Cell sorting of COS-EGFP6 cells. (A) COS-7 cells were analysed for GFP fluorescence (FL1-H) and a gate set so ≤ 0.5% of the sample (10,000 events) was detected in this region of fluorescence intensity (shaded area). About 700,000 COS-EGFP6 cells were sorted, and cells in the gated, high-fluorescence region harvested. (B) A representative sample of COS-EGFP6 subjected to sorting. (C) Re-analysis of harvested COS-EGFP6 cells. Table 4.3 shows the percent of cells from the samples in the low and high-fluorescence regions.

Three separate populations of COS-EGFP6 cells were analysed in this way, and these results are representative of the data collected.

From the FACS data it can be seen that, though the proportion of cells exhibiting high fluorescent intensity was enriched following sorting of COS-EGFP6 cells, there was still a significant percentage of the population (about 40 %) displaying low levels of fluorescence intensity. For the planned luciferase transduction co-culture experiments this population of cells would include COS-7 cells transfected with the luciferase fusion constructs. The presence of luciferase expressing cells in the harvested population would result in detection of luciferase activity within the sample whether transduction had taken place or not.

In addition, the number of cells collected was very low relative to the total number of cells sampled. When the COS-EGFP6 cells were analysed as described above, only about 3 % of the total sample was collected for re-analysis. As around 50 % of the initial population consisted of cells demonstrating high fluorescence, the 6 % of this sample harvested represents a very low sorting efficiency.

The combination of these two factors makes this particular approach impossible using the equipment available. Contamination of the harvested sample with cells expressing a luciferase fusion product raises the background levels of luciferase activity within the sample, decreasing the sensitivity of the method for detecting transduction. The low number of cells harvested, and the time required for this process, makes the sorting of co-cultured samples a very inefficient and time-consuming process.

4.3 Discussion

Though there have been no reports published with luciferase acting as a direct reporter for protein transduction, Ye *et al.* recently undertook work using luciferase expression to quantify the intercellular delivery of chimeric proteins containing either the Tat PTD or VP22 (Ye et al., 2002). The chimeric proteins comprised of the yeast Gal4 DNA-binding domain and the VP16 transactivating domain with the MTP module. Purified bacterially-expressed fusion proteins were applied to "reporter" cells transfected with a luciferase gene that was regulated by upstream sites that bound the Gal4 DNA-binding domain. In this way, induction of luciferase expression would unambiguously confirm delivery of the proteins to the reporter cells. For the work reported here it was hoped that the use of luciferase as a reporter protein would provide a means by which quantitative comparisons of protein transduction could be accurately determined.

Luciferase was chosen because of the sensitivity that can be achieved by assaying cells expressing the protein. For GFP, even when using the mutant analogues with improved fluorescence intensities such as EGFP (Patterson et al., 1997), it is estimated that to double the fluorescence of a typical cell (with a volume of about 1-2 pL) above endogenous autofluorescence levels somewhere in the region of 10^5 copies of the protein are required in that cell (representing a concentration of about 0.1 μM EGFP) (Niswender et al., 1995; Tsien, 1998). For luciferase, where current methods using luminometers allow detection of as little as 10^{-20} moles (Wood, 1991), the same number of enzyme copies is required per sample, and not per cell. This sensitivity is a result of both the enzymic nature of the system, allowing each copy of protein to amplify the signal, and because there are no endogenous substrates for luciferase in mammalian cells minimises background.

Luciferase is usually employed as a reporter for transcriptional activity, with levels of expression monitored in response to changes to promoter and enhancer regions. Luciferase can also be used in imaging studies of cells using low-light visualisation technology (see Greer and Szalay, 2002, for review), but this equipment is not widely available and equipment analogous to FACS systems

does not exist for high-throughput quantitative analysis. The studies here were to be undertaken using luciferase fusion proteins to explore protein transduction, which can introduce additional problems due to an absence of research using such fusions. The addition of the MTP sequences could affect the expression or activity of luciferase.

The *luc* gene was successfully transferred from the pGEM-*luc* vector, which is not intended for expression of luciferase, into the pcDNA3.1(+) vector. This vector is used specifically for expression in mammalian cells, and has enhancer-promoter sequences from the immediate early gene of human cytomegalovirus (CMV) for high-level expression, together with polyadenylation signal and transcription termination sequences from the bovine growth hormone to enhance mRNA stability. Expression of active luciferase product from the pcDNA-*luc* vector was confirmed in COS-7 cells, and the remaining restriction sites within the MCS would then allow insertion of the MTP sequences to create C-terminal luciferase fusion proteins.

Insertion of the MTP sequences was next carried out, and sequencing confirmed that in-frame fusions of each sequence with luciferase had been accomplished. The VP22 sequence showed only a single point mutation leading to a change-of-residue mutation (T135S). However, previous demonstrations that 158 N-terminal residues can be removed with no discernable effect on the translocatory behaviour of VP22 (Kueltzo et al., 2000) prompted the decision to use this construct in the investigation. Cells transfected with each of the constructs demonstrated luciferase activity, which decreased between 24 h and 48 h post-transfection (except in the case of VP22 where a marginal increase in activity was observed). Western blotting gave an indication that a difference in the level of expression between vectors could account for the observed variation in the activity exhibited by the samples. The same result would, however, also be observed if incomplete protein not detected by the Western blot was being expressed with diminished activity, or if the addition of the MTP sequence partially masked both the Western epitope and the active site. However, as all of the fusion proteins demonstrated luciferase activity over 4 orders of magnitude greater than that measured in cells transfected with the control vector

pcDNA3.1(+), the system was determined to retain a sufficient level of sensitivity to continue with the luciferase reporter approach.

In order to distinguish cells expressing the luciferase fusion proteins from cells into which the reporter had been transported, an approach was adopted whereby FACS would be carried out to sort a co-culture of non-transfected, fluorescent cells with transfected, non-fluorescent cells. Detection of luciferase activity within the fluorescent sample of cells following their separation from the non-fluorescent cells would demonstrate translocation of the fusion proteins. So as not to introduce any fixation artefacts the analysis would be carried out on live cells, which negated the need for IF staining to differentiate two different cell lines in co-culture by use of cell line-specific antibodies, such as COS-7 cells from Rat-1 cells. Similarly, by using live cells the potential of fixative chemicals interfering with the activity of luciferase would be abrogated. Therefore, a cell line was to be generated to constitutively express EGFP, and direct measurements of this fluorescence exploited to sort the cells.

Having determined a suitable concentration of antibiotic to eliminate susceptible cells, COS-7 cells were transfected with pEGFP-N1 and the antibiotic G418 used to select for resistant cells. A number of lines were established with promising attributes, but the line COS-EGFP6 was chosen for the proliferation and fluorescence characteristics it possessed. However, when a trial sort was carried out on these cells it was found that, though the population of cells collected was enriched with EGFP positive cells, about 40 % of the cells collected from the high fluorescence region exhibited fluorescence levels comparable to non-fluorescent COS-7 cells. This was not satisfactory as it was the non-fluorescent cells that would be transfected with the pSAM1 luciferase expression vectors.

Luciferase was chosen because of the sensitivity the reporter offered. If, however, 'contamination' from expressing cells occurred at the level demonstrated by the test sort, detection of low-level transduction, implicated by the GFP transduction studies, would not be possible. The high levels of activity displayed by the transfected cells would instead reduce the sensitivity of the

system by increasing the background activity observed, and thus mask the signal attributable to the fluorescent cells. In addition to this the number of cells harvested by FACS was very low in proportion to the number of cells sampled. Of a sample of about 7 x 10^5 cells processed for sorting it was only ever possible to collect about 6 % of the theoretical maximum (around 50 % of those sampled were in the high fluorescent region), just 3 % of the cells analysed. This is a low sorting efficiency, and is reduced further still as only 60 % of the collected cells were from the desired population.

Summary

Constructs for the expression of C-terminal fusions of each MTP sequence with luciferase were successfully generated, and cells transfected with the constructs expressed active protein. A cell line constitutively expressing the reporter protein EGFP was established with about 60 % of the cells exhibiting fluorescent intensities above background. Examination of this cell line by FACS demonstrated that inefficient and inaccurate sorting would result in a low number of harvested cells contaminated with cells not expressing EGFP.

CHAPTER 5
PRO-LESS CASPASE-3 AS A REPORTER FOR PROTEIN TRANSDUCTION

5.1 Introduction

As neither GFP nor luciferase could be utilised to quantify protein transduction using the protocols developed a new reporter was required. A reporter was sought that would allow the amplification of a signal following intercellular transport from expressing cells to maintain a system with high sensitivity. If the effect of this amplification could be visualised through microscopy, in addition to being quantified by means of an assay, the system would have a combination of the attributes offered by the other two reporters.

5.1.1 Intracellular Signalling Pathways

Cells have a number of pathways to amplify signals, allowing weak or low level signals to be increased into a distinctive response by a cell. These pathways operate through signalling cascades whereby a single member is able to exert its effect on a number of molecules of a downstream mediator, whilst it remains active. As each of these components is in turn able to interact with its own substrate molecules the amplitude of the signal can be greatly increased. An example of this is the amplification in the light-induced catalytic cascade in vertebrate rods where the absorption of a single photon of light by a single rhodopsin molecule leads to the hydrolysis of more than 10^5 cyclic GMP molecules in a cascade lasting for about 1 second (Lagnado and Baylor, 1992). This is a very specific example of a signalling pathway that operates in only one cell type. However, there are other pathways familiar to many different cell types, and one that is ubiquitous to mammalian cells is that of apoptosis.

5.1.2 Programmed Cell Death

Multicellular animals have a requirement to eliminate cells that are in excess, in the way, or potentially dangerous. For this purpose there is dedicated molecular machinery that allows the removal of specific cells in a tightly regulated manner. Programmed cell death has been observed for two centuries (Vaux and

Korsmeyer, 1999), but it was in 1972 that Currie and colleagues coined the term apoptosis to describe cells undergoing cell death in a manner that was morphologically different from necrosis. The term was taken from the Greek word that describes the falling off of leaves from trees (Kerr et al., 1972).

Apoptosis is a form of cellular suicide that can be triggered by a variety of stimuli, including cytokines, hormones, viruses, and toxic insults. The initial definition of apoptosis from Kerr *et al.* was purely morphological, with apoptotic cells exhibiting characteristic membrane blebbing, cell shrinkage, chromatin condensation and formation of membrane-enclosed vesicles (apoptotic bodies). It took over 20 years for the break-through to be made in identifying the driving force behind the terminal morphological changes associated with apoptosis (Lazebnik et al., 1994). The biochemical alterations within apoptotic cells were found to be a result of the cleavage of a specific subset of cellular polypeptides by a family of cysteine-dependent aspartate-directed proteases that have consequently been termed caspases (Alnemri et al., 1996). Caspases act on polypeptides by cleaving them at specific sites on the carboxyl side of an aspartate residue. The specific cleavage sequence, determined by the three residues preceding the required aspartate residue, is particular for each caspase, and therefore determines the substrates for the enzyme (Talanian et al., 1997; Thornberry et al., 2000; Thornberry et al., 1997). There is a huge amount of interest in the area of apoptosis and caspases, and consequently there is a vast wealth of material available on the topic. A simple literature search will reveal over 135 reviews encompassing the term 'caspase' in the title alone (source: Web of Science, September 2003). Rather than an account detailing the mechanisms of apoptosis, outlined below is a synopsis of programmed cell death, with the role of some specific caspases within it, in order to consider candidates suitable for use as 'reporters' in the study of protein transduction. For a comprehensive description of apoptosis see Refs. Cohen, 1996; Earnshaw et al., 1999; Wyllie, 1997.

5.1.3 Caspases and the Initiation of Apoptosis

Caspases are constitutively and ubiquitously synthesised as precursor proteins, zymogens, with little or no activity. To date 14 known mammalian caspases

have been cloned. Caspase activation requires cleavage to produce a mature protein with full enzymic activity (Earnshaw et al., 1999). This cleavage usually occurs through the action of another, previously activated, caspase. It appears

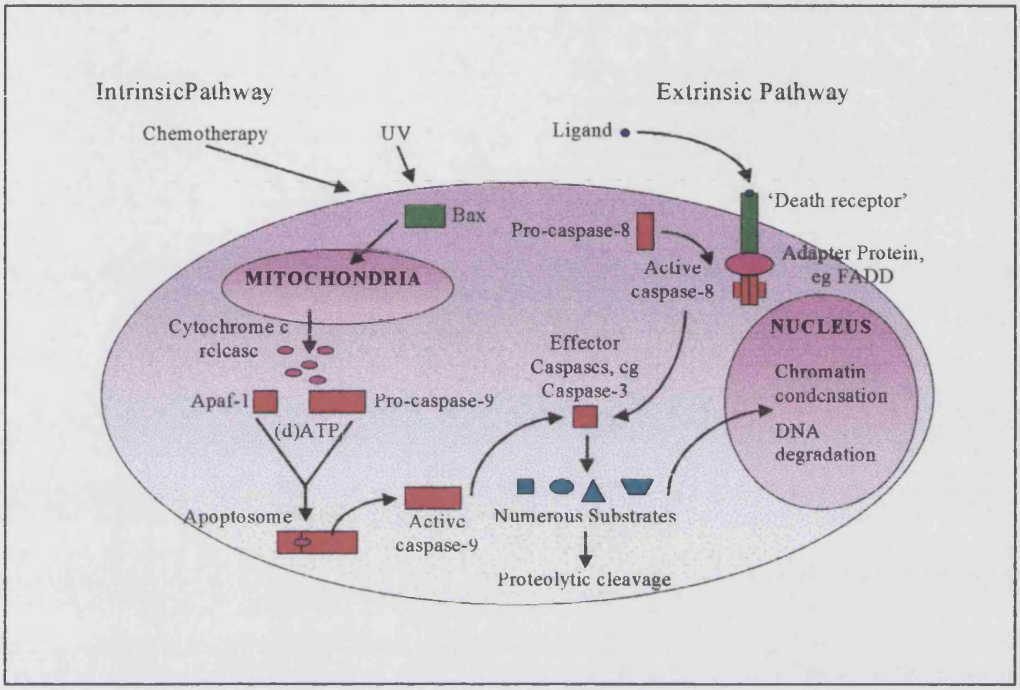

Figure 5.1. The intrinsic and extrinsic cell death pathways. In this simplified scheme, exogenous ligand, binding to a death receptor, initiates the extrinsic pathway by recruitment of an adaptor protein, e.g. FADD. Through the interaction death effector domain (DED) modules pro-caspase-8 is recruited, and, when a critical concentration is reached, active caspase-8 is generated through autocatalytic cleavage of internal sites. The intrinsic pathway, generally initiated as a result of an insult to the cell, involves the translocation to the mitochondria of pro-apoptotic Bcl-2 family members, such as Bax. In the presence of dATP or ATP, the resultant release of mitochondrial cytochrome c into the cytosol allows the generation of the apoptosome through oligomerisation with Apaf-1 and pro-caspase-9, leading to subsequent activation of caspase-9. Activation of these 'initiator' caspases activates downstream 'effector' caspases, exemplified by caspase-3, which carry proteolytic cleavage of numerous substrates leading to diverse results which culminates in the controlled execution of the cell.

that there are at least two mechanisms by which the most upstream caspases can be activated and the cascade initiated: induced proximity and association with a regulatory subunit. Simplistically, these methods of initiation correspond, respectively, to stimuli resulting in two distinct, but convergent, cascade pathways – extrinsic and intrinsic (summarised in figure 5.1).

The extrinsic pathway begins outside the cell with a ligand binding to its respective so-called death-receptor, resulting in activation of the receptor. This growing family of receptors all share a conserved cytoplasmic protein-protein interaction module termed the death domain (DD). Activation of the receptor results in recruitment of DD-containing adaptor proteins, forming the death-induced signalling complex (DISC). The adaptor proteins present allow the recruitment of upstream caspases (pro-caspase-8 and/or pro-caspase-10) via interaction of another module, the death effector domain (DED). These pro-caspases possess minimal, but discernable, proteolytic activity, and recruitment to the DISC increases the concentration in the local microenvironment to levels where autoactivation is possible (Muzio et al., 1998; Salvesen and Dixit, 1999). Once activated, these initiator or instigator caspases directly, or indirectly, activate downstream effector caspases responsible for execution of the cell.

The intrinsic pathway is responsible for integrating stress, such as DNA damaging agents, and some developmental apoptotic stimuli. Such an insult to the cell triggers translocation into the mitochondria of a pro-apoptotic Bcl-2 family member, such as Bax, and subsequent release of mitochondrialy compartmentalised cytochrome c. Once in the cytoplasm, cytochrome c can bind to the pro-apoptotic regulatory subunit Apaf-1, and in the presence of dATP or ATP an oligomeric assembly is formed (Liu et al., 1996; Zou et al., 1997). It is likely that the conformation of Apaf-1 is altered through this association making its amino-terminal caspase recruitment domain (CARD) more readily available, consequently allowing binding to pro-caspase-9 through a reciprocal CARD domain, generating the 'apoptosome' (Li et al., 1997). Once bound to pro-caspase-9, Apaf-1 triggers caspase-9's proteolytic self-activation (Srinivasula et al., 1998a) and subsequent activation of downstream effector caspases.

These convenient descriptions of intrinsic and extrinsic pathways are undoubtedly simplified, as is demonstrated by the involvement of the mitochondrial pathway in receptor initiated cell death through the intermediate Bid (Cheng et al., 2001a; Ruffolo et al., 2000). However, it is clear that both pathways converge at the point of the effector caspases. In particular, caspase-3 is activated from its zymogen by both caspase-8 (Muzio et al., 1998; Srinivasula et al., 1996; Stennicke et al., 1998) and caspase-9 (Deveraux et al., 1998; Li et al., 1997; Srinivasula et al., 1998a). Caspase-3 is often referred to as the 'point of no return' for cells following the onset of apoptosis. Once caspase-3 is activated cells are generally seen as terminally committed to suicidal destruction due to the nature and number of substrates on which the active enzyme acts. Exceptions to this rule have been observed, but only where other factors have altered the normal course of apoptosis progression (Racke et al., 2002; Wright et al., 1997). Targets for caspase-3 include pro-caspases (for reviews see Fraser and Evan, 1996, and Nicholson and Thornberry, 1997), which serve to act as an amplification loop for the apoptotic signal (Slee et al., 1999). With apoptosis resulting in a well-characterised change in morphological and biochemical features, it is an easily identifiable and measurable event; indeed there is a wide range of products available for its quantification. As caspase-3 acts at such an important juncture during this process, and with amplification of the apoptotic signal occurring through this point, the feasibility of using this enzyme as a reporter molecule for protein transduction was explored.

5.1.4 Caspase-3

As with the other caspases, caspase-3 (CPP32, apopain, Yama) is synthesised as a single-chain inactive zymogen with an N-terminal prodomain plus a large and small catalytic subunit (Cohen, 1997; Nicholson et al., 1995; Nicholson and Thornberry, 1997). Caspase-3 comes from a family of caspases known as the effector or executioner caspases which act downstream in the caspase pathway and that are activated, at least in part, by initiator caspases. In contrast to the initiator caspases, the executioner caspase zymogens contain short prodomains with neither DED nor CARD motifs (the prodomain of the executioner caspases 6 and 7 number only 23 amino acids (aa), whereas caspase-1, an activator

caspase, has a 119 aa prodomain, and caspase-10, another activator caspase, has the longest prodomain of the known caspases at 219 aa). Mature caspase-3 is generated from a 32-kDa zymogen by a sequential two-step mechanism. The initial cleavage occurs to produce the small p12 subunit and a p20 peptide. p20 is further processed, whereby the prodomain is removed, resulting in generation of the mature large p17 subunit (Han et al., 1997). The active enzyme is composed of two heterodimers of the p12 and p17 subunits generated (Rotonda et al., 1996), see figure 5.2.

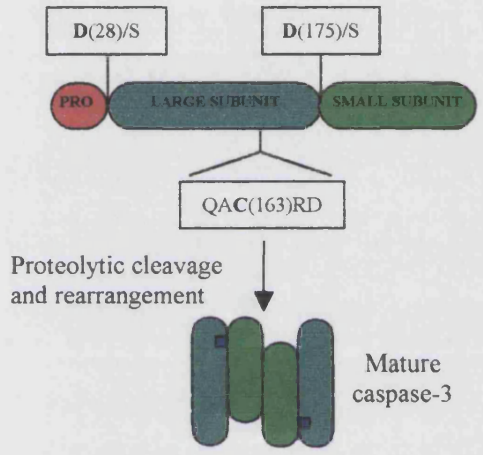

Figure 5.2. Maturation of caspase-3. The caspase-3 zymogen is composed of a short prodomain, a large subunit and a small subunit. Proteolytic cleavage at two internal sites by upstream caspases and subsequent rearrangement of subunits results in the formation of the mature heterotetramer caspase-3 enzyme. The residues present in the active site of caspase-3 are shown, and their location within the mature molecule indicated by blue squares.

Over-expression of the long prodomain initiator caspases in mammalian cells results in apoptosis-induced cell death as a result of their activation, probably through autocatalysis (Kumar et al., 1994). In contrast, overexpression of caspase-3 was not shown to result in activation of the enzyme, and apoptosis was not evident in the expressing cells (Colussi et al., 1998b). Because of the processing requirement of procaspase-3 its use as a reporter molecule would necessitate treatment of cells with pro-apoptotic stimuli in order to generate the mature, active enzyme capable of eliciting a measurable effect. However, this would also result in activation of the pool of the ubiquitously expressed zymogen. More desirable would be a caspase-3 analogue with intrinsic activity, by-passing the requirement of processing for activation. However, investigation into the factors influencing caspase-3 activation have resulted in the generation

of vectors capable of expressing constitutively active forms of the enzyme (Meergans et al., 2000; Srinivasula et al., 1998b), see figure 5.3. In the first of these reports the order of the proteins subunits was swapped so the coding sequence for the small subunit preceded that of the large subunit (Srinivasula et al., 1998b). The recombinant molecule was capable of autoprocessing and inducing apoptosis *in vivo* independent of the upstream caspases. In the second report the coding sequence for the 28 amino acids of the prodomain were omitted from the expression vector (Meergans et al., 2000). Again, autoprocessing was observed prior to activation in transiently expressing cells. The implication of these reports is that the short prodomain suppresses the spontaneous activation of the inactive zymogen, with this restraint removed when a pro-less variant is expressed, or masked when there is a rearrangement of the subunit order. Either of these variants fulfills the criterion of an active caspase-3 analogue, and so could potentially be used as a reporter. However, further complications remain: Can potential apoptosis of expressing cells, induced by active MTP fusion protein, be delayed or prevented in order to allow a pool of transducible protein to build up? Will generation of chimeric fusions of the enzymes impair activity?

Figure 5.3. Analogues of procaspase-3 exhibiting intrinsic activity. Representation of the two different strategies used to generate analogues of procaspase-3 (A) with intrinsic activity with no requirement for processing by upstream caspase. (B) Rearrangement of the p20 subunit, containing the pro-domain (red) and the p17 large subunit (dark green), with the small p12 small subunit (light green). (C) Removal of the 28 residues corresponding to the pro-domain.

The first of these questions is answered thanks to the work of Nicholson *et al.* (Nicholson et al., 1995). This research originally identified caspase-3 as the heteromeric apopain enzyme composed of a large and small subunit, derived from the proenzyme CPP-32. One of the potential substrates for this enzyme was poly (ADP-ribose) polymerase (PARP), which had a known internal site of cleavage corresponding to DEVD/G. Through the generation of a tetrapeptide

aldehyde based on this sequence (Ac-DEVD-CHO) it was possible to prevent both camptothecin-induced apoptotic cell death of osteosarcoma cells and to inhibit completely the activity of apopain by addition of this peptide to cultured cells or purified enzyme. Currently, there are a number of products available for the inhibition of caspase-3 with differing properties of specificity, permeability and reversibility (see Oncogene catalogue (CNBiosciences, UK) for a detailed list).

The effect of generating fusion proteins with either of the intrinsically active forms of caspase-3 would be unknown until the proteins were examined. Little work has been published on caspases expressed as fusion proteins. GFP fusions have been generated to study subcellular localisation of the both full-length caspases and of the long prodomains of the initiator caspases (Colussi et al., 1998a; Shikama et al., 2001). Where the activity of the enzymes was examined it was not perturbed by N- or C-terminal fusions. Caspase-3 fusion proteins have also been generated to study the influence of long prodomains on autoactivation of the enzyme (Colussi et al., 1998b; Racke et al., 2002). In these reports replacement of the short prodomain of caspase-3 with the prodomain of either caspase-2 or caspase-1 resulted in activation of the caspase, probably through the induced proximity model previously described. The only other examples of fusion proteins reported have been generated through the addition of targeting sequences to the full-length protein to determine the effect on intra- and inter-cellular localisation (Harada et al., 2002; Vocero-Akbani et al., 1999). The activity of these proteins was unaffected by the addition of short peptide sequences preceding the prodomain, most likely as their small size did not interfere with the processing of the native protein at the internal cleavage sites.

Selection of the intrinsically active caspase-3 used required consideration of the potential influence that the addition of a peptide sequence could have on the activity of the enzyme, directly or otherwise. Examination of the structure of the active caspase-3 heterodimer shows that rearrangement of the large and small subunits occurs in a manner whereby the active site is formed by residues situated near the C-terminus of the large subunit (Earnshaw et al., 1999). By using the Srinivasula *et al.* model for active caspase-3 (Srinivasula et al.,

1998b), addition of a sequence to the C-terminus of the protein would put the additional residues in a region close to the active site residues. Screening of the fusion products would have to be undertaken in order to assess the effect on activity the MTP sequences had. As there are not usually residues at the N-terminus of the small subunit following processing in the wild-type caspase-3 protein, the addition of residues here could interfere in someway with the formation of the heterodimer necessary for full enzyme activity. The addition of any sequence to the N-terminal of the Meergans *et al.* pro-less variant (Meergans et al., 2000) may prevent processing by acting in a manner analogous to the wild-type pro-domain. By generating C-terminal fusions this inhibitory potential would be removed. However, the possibility of the sequences interfering with the dimerisation or activity of caspase-3 would remain, and activity assays would have to be undertaken to examine this.

Due to potential processing problems associated with the N-terminal fusions (the additional sequences acting to interfere with oligomerisation or as a pro-domain for the rearrangement or pro-less models, respectively) neither strategy was explored. Instead, a strategy was proposed to generate C-terminus fusions with the pro-less caspase-3 model. This region is not in the immediate vicinity of the active site, unlike a C-terminal fusion with the rearrangement model, and so appeared the best model, and fusion option for generating an intrinsically active protein.

5.2 Results

5.2.1 Generation of an Expression System for Pro-Less Caspase-3

Work previously undertaken by Meergans *et al.* to characterise a pro-less caspase-3 variant (PLCasp3) used a Tet-Off tetracycline-regulated expression system and vectors that simultaneously co-express the luciferase reporter protein to monitor and normalise the expression levels between different transfections (Meergans et al., 2000). A regulated expression system was attractive to enable suppression of PLCasp3 fusion protein expression. In addition, co-expression of a reporter protein such as luciferase would allow normalisation of expression levels between transfections with fusion constructs. Co-expression of a reporter such as GFP would allow differentiation of transfected from non-transfected cells, and visualisation of the cellular morphologies exhibited by those cells expressing the PLCasp3 fusion proteins.

The strategy adopted was to use the expression vector pBI (Clontech). This is a bi-directional expression vector allowing the simultaneous expression of two genes under the control of a single tetracycline-response element. By using Tet-Off cells (Clontech) expression of both genes would be down regulated in response to treatment with tetracycline (Tc) or Tc derivatives, such as doxycycline (dox). The PLCasp3 sequence would be inserted into one MCS of pBI, and another reporter gene (luciferase or EGFP) would be inserted into the other MCS. The aim would be to then insert each of the MTP sequences in such a way as to form in-frame fusions with PLCasp3. As PLCasp3 exhibits intrinsic activity, with no pro-enzyme processing requirement, it is able to process caspase-3 target proteins, and detection of such activity in non-transfected cells would indicate transduction of the protein from transfected cells.

5.2.2 Regulation of Expression in Tet-Off Cells

To develop a protocol to quantify protein transduction using the PLCasp3 approach outlined above it was necessary to determine methods to control expression in Tet-Off cells.

5.2.2.1 Regulation of Expression of pBI-3K

In order to study regulation of expression in Tet-Off cells, the expression vector pBI-3K was used. This vector was a generous gift from Thomas Meergans, University of Konstanz, Germany, and was the construct described in his pro-less caspase-3 paper (Meergans et al., 2000). In this paper the vector was used for the regulated co-expression of PLCasp3 and luciferase in HeLa Tet-Off cells. However, examination of the expression of these proteins in the HeLa Tet-Off cells used in these studies yielded no caspase-3 activity above background. The same cells did, however, express active luciferase, and so luciferase activity was monitored during the regulation studies.

Figure 5.4 shows HeLa Tet-Off cells transfected with 1 μg pBI-3K, and grown in medium supplemented with different concentrations of Tc at the time of transfection. Twenty-four hours post-transfection the cytosolic extract of the transfected cells was assayed for luciferase activity. The activity of samples is shown relative to a sample of transfected cells grown in medium without Tc. The expression of luciferase in cells treated with 1μg/ml Tc is about 7-fold lower than in the untreated sample.

Regulation of luciferase expression was next examined using a Tc analogue doxycycline (dox). Dox is more stable than Tc and the protocol recommends supplementation of growth medium every 48 h, compared with every 24 h with Tc. This would make the use of dox preferential in expression studies, providing it was still able to control tightly expression of the target gene.

Figure 5.5 shows the luciferase activity in the cytosolic extracts of HeLa Tet-Off cells transfected with 1 μg pBI-3K, with growth medium supplemented with different concentrations of dox at the time of transfection. The extracts were harvested 24 h post-transfection. Down regulation of expression is observed with dox concentrations as low as 2 pg/ml, with full repression occurring at about 0.2 ng/ml. The concentrations necessary for down regulation are lower than those required when Tc is used, which is preferential as this will limit any potential deleterious side effects attributable to the antibiotic, or solvent used in

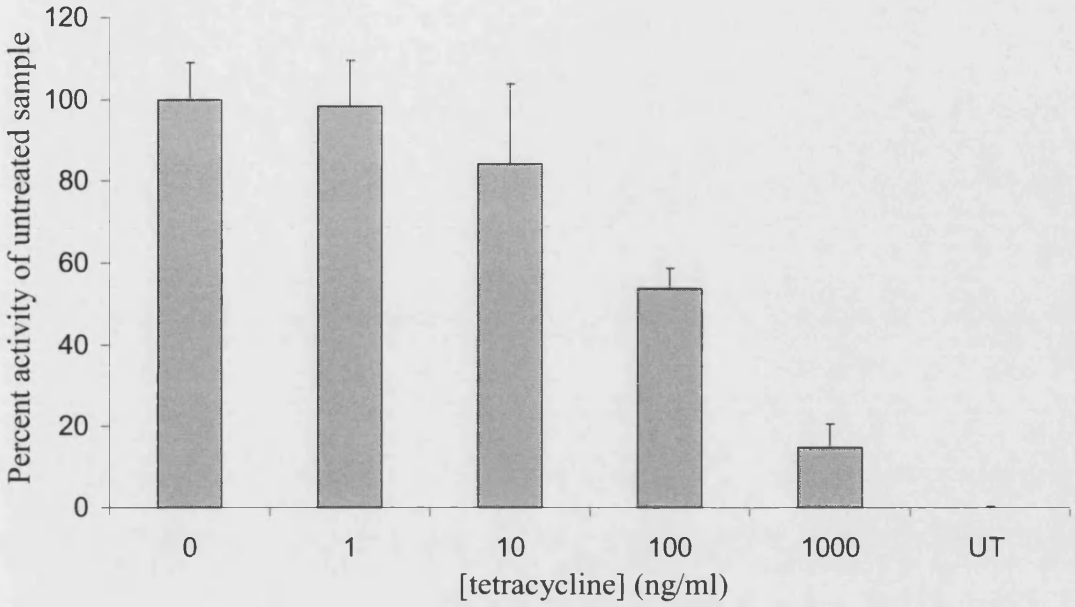

Figure 5.4. Regulation of expression by tetracycline. HeLa Tet-Off cells were transfected with pBI-3k. Tetracycline was added at the concentrations indicated at the time of transfection. Luciferase activity was measured in cytosolic extracts from transfected cells 24 h after transfection. Measurements were performed in triplicate, values are an average of two experiments ± S.D. Values are presented in terms of activity relative to a transfected sample not supplemented with tetracycline, with a sample of untransfected cells (UT) shown as a control.

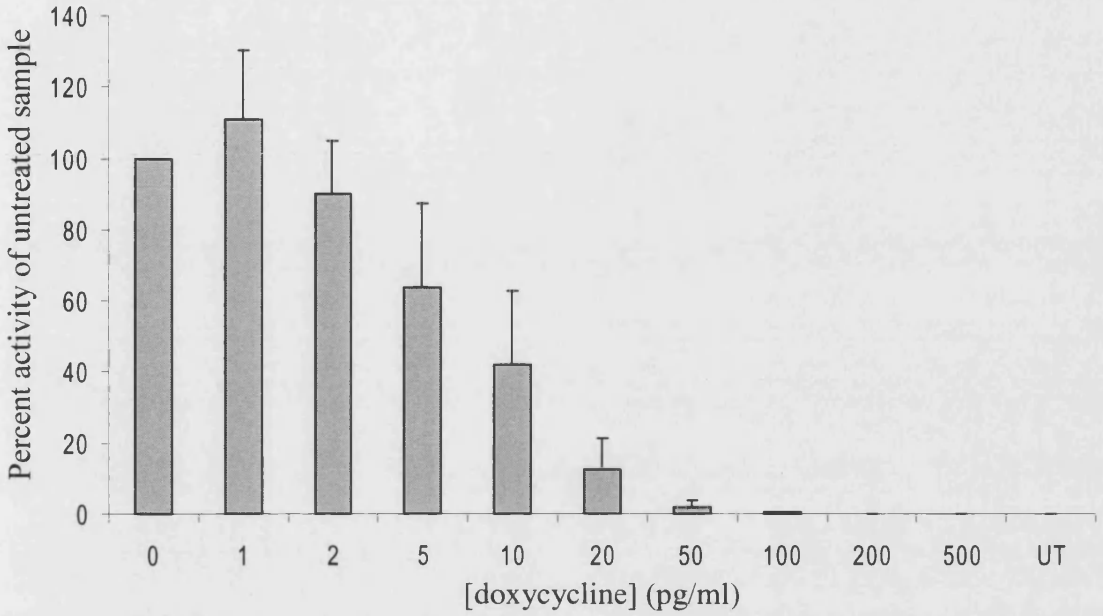

Figure 5.5. Regulation of expression by doxycycline. HeLa Tet-Off cells were transfected with pBI-3k. Doxycycline was added at the concentrations indicated at the time of transfection. Luciferase activity was measured in cytosolic extracts from transfected cells 24 h after transfection. Measurements were performed in triplicate, values are an average of three experiments, and error bars indicate S.E.M. Values are presented in terms of activity relative to a transfected sample not supplemented with doxycycline, with a sample of untransfected cells (UT) shown as a control.

its preparation. Therefore, where regulation of expression was required, dox was used.

5.2.2.2 Recovery of Expression in Doxycycline Down-Regulated HeLa Cells

With down regulation of expression achieved it was necessary to determine the period of time necessary for expression to be recovered following removal of the regulatory antibiotic. HeLa Tet-Off cells were transfected with pBI-3K and growth medium supplemented with 200 pg/ml dox. Twenty-four hours post-transfection cells were washed and fresh, supplemented growth medium applied. At various times over a 12 h time course cells were again washed and the growth medium replaced with non-supplemented medium. The luciferase activity in the cytosolic extracts of the cells was measured either 36 h or 48 h post-transfection, allowing luciferase activity to be determined up to 24 h following removal of dox from the growth medium.

As shown in figure 5.6 the recovery of luciferase expression is dependent on the time cells are exposed to dox-free medium. The data up to 12 h following removal of dox represent the activity of cells 36 h post-transfection (filled circles and solid line), whereas the data from 12-24 h represent activity measured 48 h post-transfection (circles and broken line). As was found previously (see figure 4.5) luciferase activity decreased when measured at 24 h and 48 h. This was observed here as the two samples measured 12 h following the removal of dox demonstrate.

Though the activity within the cells does not appear to have reached a maximum 12 h following the removal of dox, a longer incubation in dox-free medium may result in a lower measured activity due to the observed decrease in luciferase activity with time. This would not be detected, however, if all of the samples were harvested at the same time, as in the protocol undertaken here, since the activity of each sample would decrease to the same extent. For studies where the measurement of activity was necessary following removal of the regulatory antibiotic, activity would be measure at around 12 h following replacement of dox-supplemented medium.

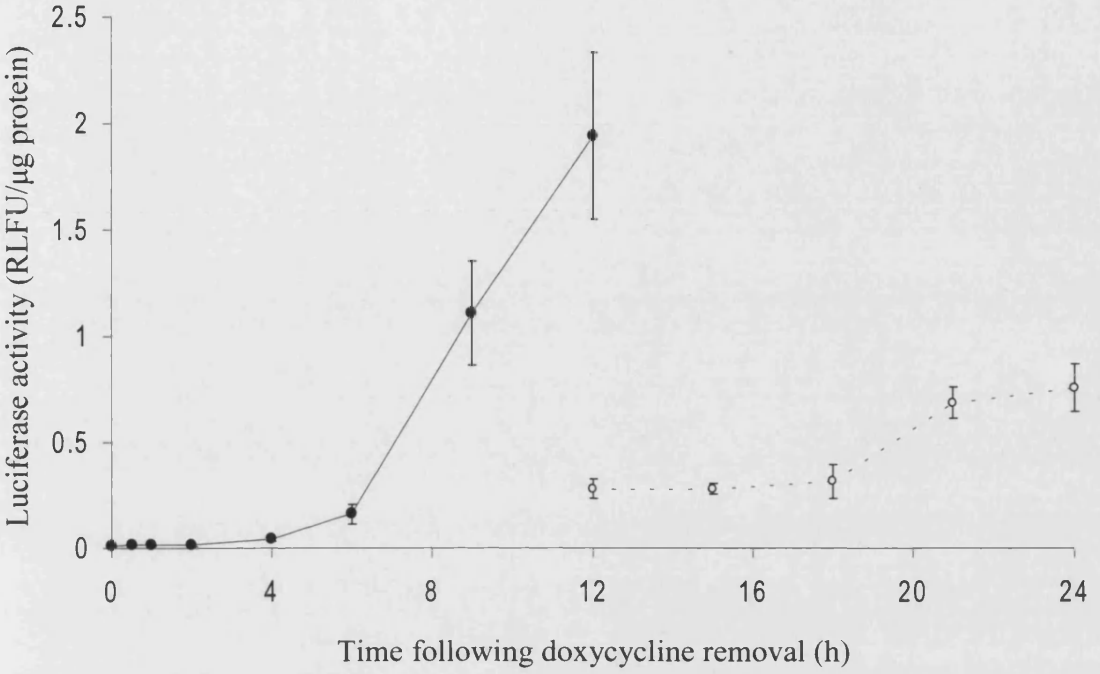

Figure 5.6. Recovery of luciferase expression following removal of doxycycline. HeLa Tet-Off cells were transfected with pBI-3K and cells supplemented with 200 pg/ml doxycycline (dox). Twenty four hours post-transfection cells were washed twice with PBS, and fresh dox-supplemented growth medium applied as before. At the time intervals 0, 3, 6, 8, 10, 11, 11.5 and 12 h (filled circles and solid line), or 0, 3, 6, 9 and 12 h (circles and dashed line) cells were washed as before and fresh, unsupplemented growth medium applied. Luciferase activity in the cytosolic extracts of cells was measured 36 h post-transfection (filled circles and solid line) or 48 h post-transfection (circles and broken line). Measurements were performed in triplicate, values are an average of three experiments, and error bars indicate S.E.M.

5.2.3 Regulation of Caspase-3 Activity

As discussed previously, PLCasp3 exhibits capase-3-like activity and is capable of cleaving caspase-3 substrates. Production of PLCasp3 or PLCasp3 fusion proteins could therefore result in apoptosis of expressing cells, preventing an accumulation of protein for transduction. To protect against this, caspase-3 activity would require inhibiting with a reversible inhibitor to enable recovery of reporter activity subsequent to inhibition.

As there was no discernable caspase-3 activity in pBI-3K transfected cells an alternative method was required to follow caspase-3 inhibition and activity recovery. Staurosporine (STS) is a well-known inducer of apoptosis, and treatment of cells with STS results in increased levels of caspase-3 activity. STS-induced apoptosis was, therefore, used as a mechanism to study caspase-3 inhibition.

5.2.3.1 Inhibition of Caspase-3 Activity

As it was necessary to inhibit caspase activity within the cultured cells, initial studies were undertaken using a cell-permeable inhibitor. The sequence Asp-Glu-Val-Asp represents the site of caspase-3 cleavage in poly (ADP-ribose) polymerase (PARP). This sequence is capable of binding to the active site of caspase-3, and inhibitors have been designed around the affinity of caspase-3 to the tetrapeptide. The inhibitor N-acetyl-AAVALLPAVLLALLAP-DEVD-CHO (cp-DEVD-CHO) consists of this sequence preceded by a peptide corresponding to the hydrophobic region of the Kaposi fibroblast growth factor added to increase the cell permeability of the inhibitory sequence (Lin et al., 1995), and the aldehyde nature of the peptidyl mimetic results in reversible rather than irreversible binding to caspase-3.

Confluent monolayers of HeLa Tet-Off cells were pre-incubated with different concentrations of cp-DEVD-CHO for 2 h. STS was added to the cells to a concentration of 1 μM and the cells were incubated for a further 3 h. Cytosolic extracts were harvested and caspase-3 activity was measured as the rate of change in absorbance at 405 nm by cleavage of the substrate N-acetyl-Asp-Glu-Val-Asp ρ-nitroanilide (Ac-DEVD-ρNA).

Figure 5.7 shows the caspase-3 activity measured in STS treated cell pre-treated with 0-50 μM cp-DEVD-CHO. A sample of cells not subjected to STS treatment shows the background level of Ac-DEVD-pNA cleavage, which is due to non-specific processing of the substrate by other proteases. Though some inhibition of caspase-3 activity is observed at 20-50 μM cp-DEVD-CHO, the activity was never reduced below 65 % the activity of a sample with no pre-incubation treatment with cp-DEVD-CHO.

A second inhibitor was examined to determine whether the inhibition demonstrated by cp-DEVD-CHO could be improved upon. The inhibitor N-acetyl-DEVD-CHO (Ac-DEVD-CHO) lacks the cell permeable sequence of the cp-DVD-CHO inhibitor, but has been shown to inhibit caspase-3 activity when added exogenously to cells subsequently treated with STS (Gurtu and Zhang, 1997).

HeLa Tet-Off cells were treated as before, but with just a one hour pre-incubation with Ac-DEVD-CHO. Figure 5.8 shows the caspase-3 activity measured in cells pre-treated with 0-100 μM Ac-DEVD-CHO. Pre-incubation with only 1 μM Ac-DEVD-CHO resulted in a 50 % reduction in measurable caspase-3 activity, and as the inhibitor concentration was increased the activity was decreased further. Total inhibition to background levels was experienced at 100 μM inhibitor, though very little observable Ac-DEVD-pNA cleavage was observed at 50 μM.

The studies have shown that the inhibitor Ac-DEVD-CHO was able to inhibit caspase-3 activity, induced by treatment with STS, when added exogenously to cells in culture to a greater extent than its cell-permeable analogue, cp-DEVD-CHO. To achieve a similar level of inhibition pre-incubation for 1 h with only 1 μM Ac-DEVD-CHO was necessary compared with pre-incubation for 2 h with 50 μM cp-DEVD-CHO. This made the inhibitor Ac-DEVD-CHO the lead candidate for the studies using PLCasp3. However, the degree to which the inhibition was reversible was an important consideration, and had to be assessed.

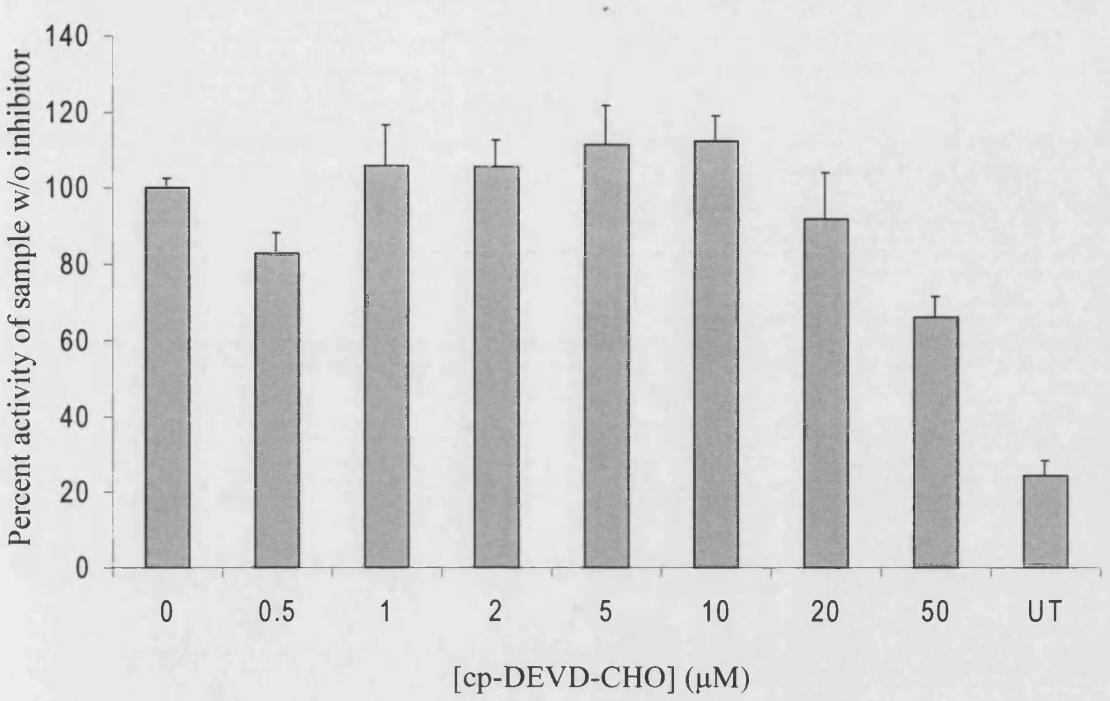

Figure 5.7. Effect of a cell permeable inhibitor on the caspase-3 activity in staurosporine treated cells. HeLa Tet-Off cells were pre-incubated with varying concentrations of the inhibitor cell permeable-DEVD-CHO (cp-DEVD-CHO) for 2 h. After this period cells were treated with staurosprorine (STS) to allow induction of apoptosis. Caspase-3 activity was then measured in cytosolic extracts of treated cells. Measurements were performed in triplicate, values are an average of two experiments ± S.D. Values are presented in terms of activity relative to a sample not supplemented with cp-DEVD-CHO, with a sample of cells not treated with STS (UT) shown as a control.

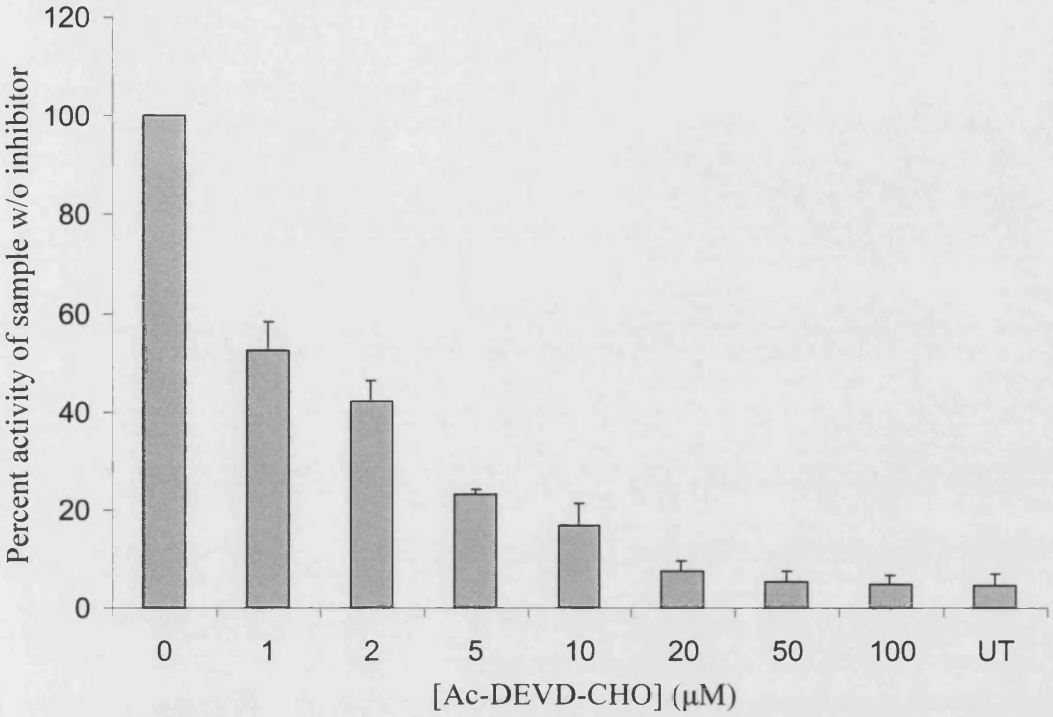

Figure 5.8. Effect of an inhibitor on the caspase-3 activity in staurosporine treated cells. HeLa Tet-Off cells were pre-incubated with the indicated concentrations of the inhibitor acetyl-DEVD-CHO (Ac-DEVD-CHO) for 1 hour. After this period cells were treated with staurosporine (STS) to allow induction of apoptosis. Caspase 3 activity was then measured in cytosolic extracts of treated cells. Measurements were performed in triplicate, values are an average of three experiments, and error bars indicate S.E.M. Values are presented in terms of activity relative to a sample not supplemented with Ac-DEVD-CHO, with a sample of cells not treated with STS (UT) shown as a control.

5.2.3.2 *Recovery of Caspase-3 Activity*

HeLa Tet-Off cells were pre-incubated for 1 h with 100 μM Ac-DEVD-CHO. The inhibitor was removed by thorough washing of the cells with PBS, and fresh growth medium added. At different times following the removal of the inhibitor growth medium was supplemented with STS to a concentration of 1 μM. Cytosolic extracts were harvested after 3h treatment with STS, and caspase-3 activity measured as before.

As figure 5.9 shows, full caspase-3 activity, as demonstrated by the sample with no inhibitor pre-incubation (w/o Ac-DEVD-CHO), was recovered 6 h following removal of Ac-DEVD-CHO from cells. This recovery was from total inhibition to background levels, represented by Ac-DEVD-ρNA cleavage evident in a sample of cell subjected to no treatment. As a result, it should be possible to use Ac-DEVD-CHO to inhibit the caspase-3 activity of PLCasp3, providing the inhibitor retained functionality against the enzyme, allowing expression to occur within transfected cells without compromising cell viability. This would allow time for the formation of a pool of PLCasp3-MTP fusion protein to accumulate, and for translocation of the protein to neighbouring, non-expressing cells to take place. Removal of the inhibitor by washing the cells would then enable the activity of PLCasp3 to return to normal over a 6 h period, and observations could be made for evidence of this activity in non-transfected cells.

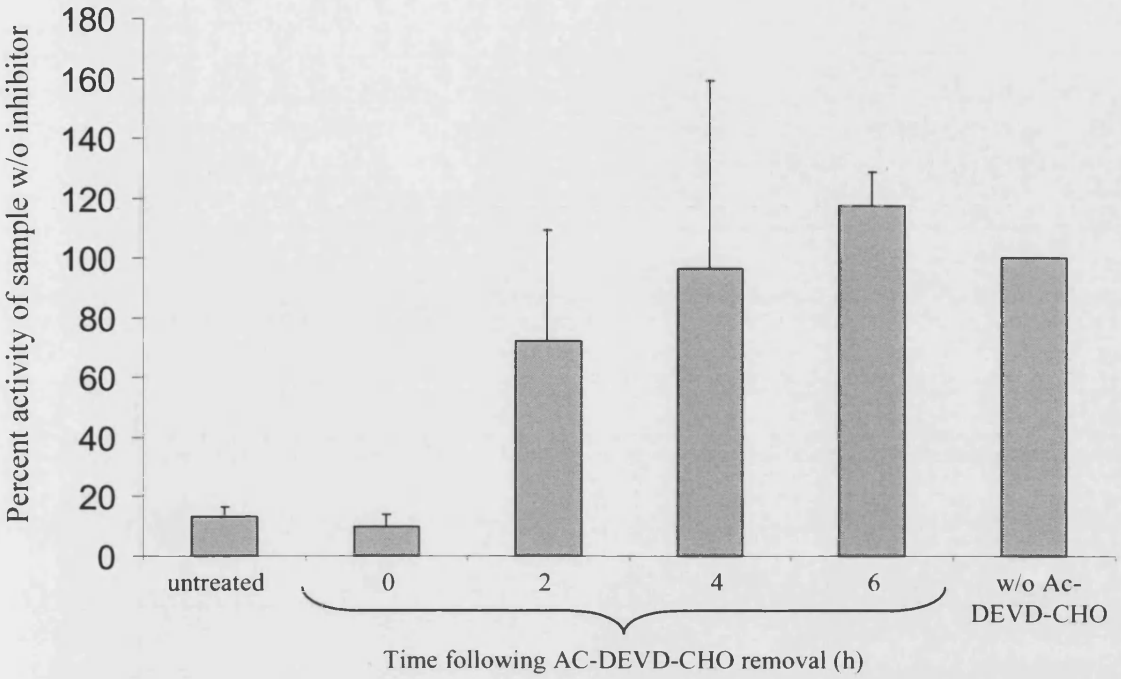

Figure 5.9. Recovery of caspase-3 activity in staurosporine treated cells following removal of the inhibitor Ac-DEVD-CHO. HeLa Tet-Off cells were treated with 100 μM Ac-DEVD-CHO for 1 h. Cells were washed to remove the inhibitor, and at the time intervals indicated growth media was supplemented with staurosporine (STS) to induce apoptosis, applied. After 3 hours, caspase-3 activity was measured in cytosolic extracts of treated cells. Measurements were performed in triplicate, values are an average of three experiments, and error bars indicate S.E.M. Values are presented in terms of activity relative to a sample not supplemented with Ac-DEVD-CHO (w/o Ac-DEVD-CHO), with a sample of cells not treated with STS shown as a control.

5.2.4 Strategy and Construction of Pro-Less Caspase-3 Expression Vectors

Once the reagents necessary to regulate expression in HeLa Tet-Off cells and to control caspase-3 activity in cells had been determined, it was necessary to generate a system for the expression of PLCasp3. As discussed previously, the vector chosen was pBI, and outlined below is the cloning strategy undertaken to generate vectors enabling the co-expression of luciferase or EGFP with PLCasp3 or PLCasp3-MTP fusion proteins. A schematic of the strategy is shown in figure 5.10

5.2.4.1 Generation of pBI-GFP and pBI-luc

Both the luciferase gene and the GFP gene were to be inserted into the MCS II site of pBI. Both sequences would be excised from vector already used during the course of this work, luciferase from pGEM-*luc* and EGFP from pEGFP-N1. Excision of the genes would take place through *Sal* 1/*Not* 1 and *Not* 1/*Pst* 1 double digests for luciferase and EGFP, respectively, with insertion taking place following digestion of pBI with the same two restriction enzymes. The pairs of enzymes have compatible restriction buffer requirements and all digests were undertaken simultaneously. Fragments were inserted through simple ligation with the linearised vector, and transformed *E. coli* screened for the presence of constructs containing the insert by restriction analysis of their DNA with the same pair of inserts. Figure 5.11 A shows the successful insertion of EGFP into pBI, and figure 5.11 B the successful insertion of luciferase. The vectors will be referred to as pBI-GFP and pBI-luc.

5.2.4.2 Generation of Vectors for the Co-Expression of PLCasp3

The sequence coding for PLCasp3 was to be inserted into MCS I of each of pBI-GFP and pBI-luc. This insertion was limited to only 2 restriction enzymes, *Mlu* 1 and *Nhe* 1. However, as MTP sequences were to be added to produce constructs able to express PLCasp3-MTP fusion proteins it would be necessary to introduce an additional restriction site for these insertions to take place. In order to do this, the reverse primer designed for the amplification of PLCasp3 would contain additional bases to include the restriction site for *Bcl* 1. Restriction sites were incorporated in the primers in addition to the complementary annealing bases. These would allow insertion of the PLCasp3

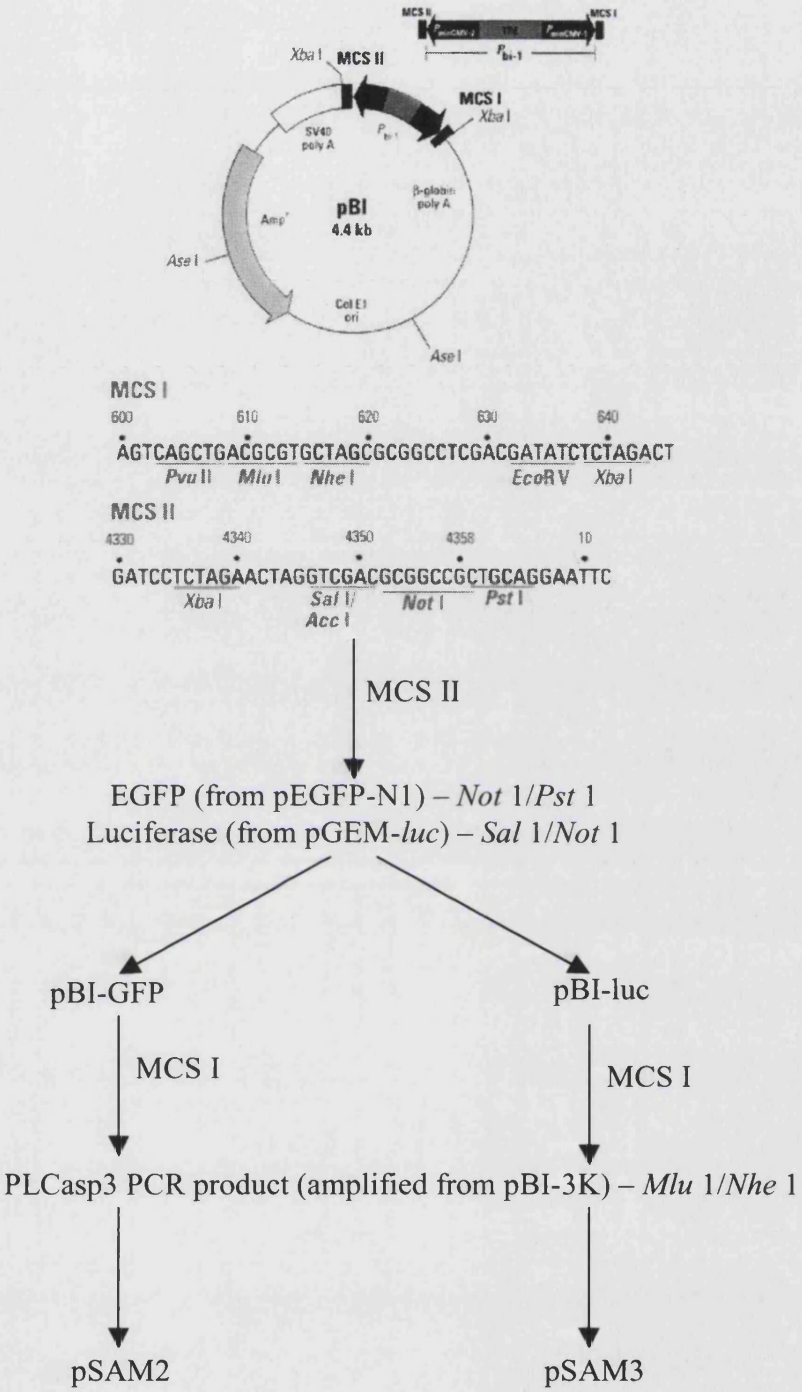

Figure 5.10. Schematic demonstrating the cloning strategy for the generation of PLCasp3 expressing vectors. Either the EGFP or the luciferase coding sequence would be inserted in to the second multiple cloning site of pBI (MCS II), generating pBI-GFP and pBI-luc, respectively. Pro-less caspase-3, amplified from pBI-3K by PCR, would then be inserted into MCS I to generate the bi-expression vectors pSAM2 and pSAM3.

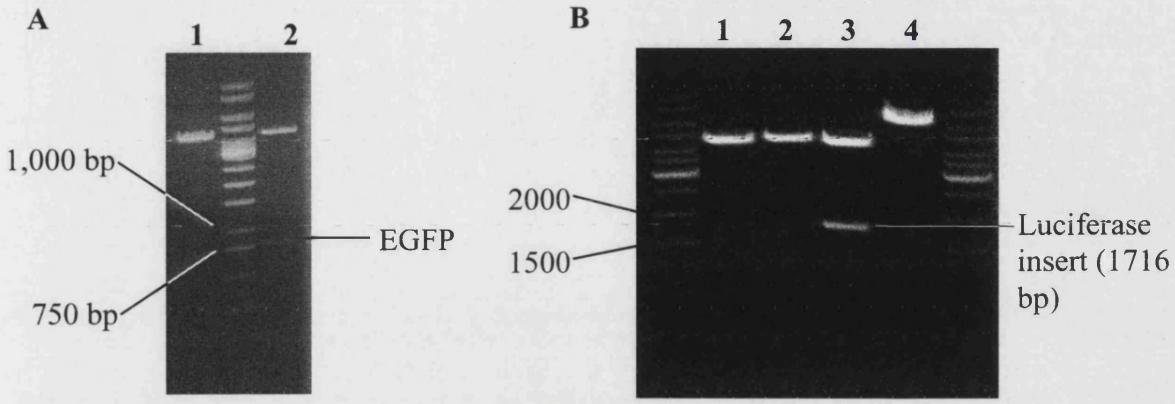

Figure 5.11. Restriction analysis of pBI-GFP and pBI-luc. (A) Restriction analysis of pBI-GFP. Lanes 1 and 2 show *Pst* I/*Not* I double digests of pBI and pBI-EGFP, respectively. Lane 2 shows insertion of the EGFP cassette into MCS II of pBI. (B) Restriction analysis of pBI-luc. Lane 1, *Sal* I/*Not* I double digest of pBI. Lane 2, *Pst* I/*Not* I double digest of pBI. Lane 3, *Sal* I/*Not* I double digest of pBI-luc showing insert of luciferase cassette into MCS II of pBI. Lane 4, *Pst* I/*Not* I double digest of pBI-luc.

sequence into pBI MCS I, and then permit subsequent insertion of MTPs to form C-terminal fusions with PLCasp3. The additional bases were as follows:

a) 5' *Mlu* 1 restriction site immediately preceding a start codon on the forward primer.
b) 5' *Nhe* 1 restriction site immediately preceding a stop codon on the reverse primer.
c) Codons for a tri-glycine repeat separating the stop codon from downstream *Bcl* 1 restriction site on the reverse primer.
d) Additional 5' bases preceding both the *Mlu* 1 and *Nhe* 1 restriction sites to allow successful digestion of the PCR fragment.

Insertion of PLCasp3 into pBI-GFP and pBI-luc would therefore take place on an *Mlu* 1/*Nhe* 1 double digest. The inserted sequence would be that of PLCasp3 with a C-terminal tri-glycine repeat. Insertion of each MTP sequence would then take place using a *Bcl* 1/*Nhe* 1 double-digest, forming C-terminal fusions

with PLCasp3. Primers for the amplification of PLCasp3 from the vector pBI-3K are shown in table 5.1.

Forward Primer	Reverse Primer
5' AATCTCACGCGTATGTCTGG AATATCCCTGGAC 3'	5' TCATAGCTAGCTTATCCTCCTCCT GATCAGTGATAAAAATAGAGTTCTT TTG 3'

Table 5.1. Primers for amplification of PLCasp3.

Amplification of PLCasp3 from pBI-3K was carried out using the following reaction conditions:

Reagent	Volume (µl)
Reaction mix	25
MgCl	6
Template* (PGE155)	1
Sense primer**	1
Anti-sense primer**	1
H_2O	16

* 100 ng ** 10 pmol

Temperature (°C)	Time (s)	
95	120	30 cycles
94	45	
60	60	
72	60	
72	600	
4	hold	

Following amplification, the PLCasp3 fragment was gel purified, digested by *Mlu* 1/*Nhe* 1 double digest, and the DNA ready for insertion into pSAM1 gel purified again. The vector pBI-GFP was prepared to accept the fragment by sequential digests with the same enzymes as simultaneous digestion was not possible due to the close proximity of the two restriction sites. Ligation of PLCasp3 and pBI-GFP was undertaken, and transformed *E. coli* screened to determine the presence of the inert in pBI-GFP by restriction analysis of their DNA using the same 2 restriction enzymes. Where an insert was detected DNA was sent for sequencing, using the pBI sequencing primer shown in appendix B12, to check for mutations within the PLCasp3 sequence.

The sequence data obtained for pBI-GFP-PLCasp3 is shown is figure 5.12. The *Mlu* 1 and *Nhe* 1 sites are underlined, and the start codon for PLCasp3 is highlighted in bold. The sequence for PLCasp3 was without mutation. However, the sequence for the *Bcl* 1 restriction site, highlighted in red, contained a single point mutation, underlined, which resulted in destruction of the restriction site.

ACGCGT**ATG**TCTGGAATATCCCTGGACAACAGTTATAAAA
TGGATTATCCTGAGATGGGTTTATGTATAATAATTAATAAT
AAGAATTTTCATAAAAGCACTGGAATGACATCTCGGTCTG
GTACAGATGTCGATGCAGCAAACCTCAGGGAAACATTCAG
AAACTTGAAATATGAAGTCAGGAATAAAAATGATCTTACA
CGTGAAGAAATTGTGGAATTGATGCGTGATGTTTCTAAAG
AAGATCACAGCAAAAGGAGCAGTTTTGTTTGTGTGCTTCT
GAGCCATGGTGAAGAAGGAATAATTTTTGGAACAAATGGA
CCTGTTGACCTGAAAAAAATAACAAACTTTTTCAGAGGGG
ATCGTTGTAGAAGTCTAACTGGAAAACCCAAACTTTTCATT
ATTCAGGCCTGCCGTGGTACAGAACTGGACTGTGGCATTG
AGACAGACAGTGGTGTTGATGATGACATGGCGTGTCATAA
AATACCAGTGGAGGCCGACTTCTTGTATGCATACTCCACA
GCACCTGGTTATTATTCTTGGCGAAATTCAAAGGATGGCTC
CTGGTTCATCCAGTCGCTTTGTGCCATGCTGAAACAGTATG
CCGACAAGCTTGAATTTATGCACATTCTTACCCGGGTTAAC
CGAAAGGTGGCAACAGAATTTGAGTCCTTTTCCTTTGACG
CTACTTTTCATGCAAAGAAACAGATTCCATGTATTGTTTCC
ATGCTCACAAAAGAACTCTATTTTTATCAC**TGATCC**GGAG
*GAGGATAA*GCTAGC

Figure 5.12. Insertion of pro-less caspase-3 into pBI-GFP. Sequence data showing insertion of pro-less caspase-3 cDNA into MCS1 of pBI-GFP using the restriction sites *Mlu* I and *Nhe* I (restriction sites underlined). The start codon for the coding sequence is highlighted in bold. Additional bases coding for a C-terminal tri-glycine repeat and a stop codon, in frame with pro-less caspase-3, are shown in italics. The mutated *Bcl* 1 site is highlighted in red, where an A to C point mutation (underlined) has destroyed the restriction site.

The mutation resulted in a vector that would co-express EGFP and PLCasp3, but that could not be used for subsequent subcloning to make PLCasp3-MTP fusion proteins. The vector pBI-GFP-PLCasp3 with the redundant *Bcl* 1 restriction site

will be referred to as mpSAM2 (pSAM2 would refer to a vector that subcloning could take place in).

Further attempts at generating an insert without mutation yielded no results, and so site-directed mutagenesis was used to correct the mutation in the restriction site, allowing insertion of the MTP sequences between that site and the downstream *Nhe* 1 site. However, to simplify future subcloning, rather than correct only the point mutation in mpSAM2, the *Bcl* 1 site would be replaced with a site for restriction with the enzyme *Age* 1. *Bcl* 1 cleavage of DNA is blocked by Dam methylation, requiring preparation of DNA from a bacterial strain devoid of Dam methylase, such as strain GM2163. As with the other restriction enzymes used in the cloning in these studies, *Age* 1 is unaffected by the methylation state of DNA, enabling the normal JM109 strain to be used for the preparation of DNA.

The primers in table 5.2 were used for the site directed mutagenesis, following the manufacturers protocol.

Forward Primer	Reverse Primer
5' GAACTCTATTTTTATCAC**ACCGG** TGGAGGAGGATAAGCTAGCTAGCG CGGCCTCGAC 3'	5' GTCGAGGCCGCGCTAGCTTATCCT CCTCC**ACCGGT**GTGATAAAAATAG AGTTC 3'

Table 5.2. Primers for site directed mutagenesis of mpSAM2. Forward and reverse primers to replace the mutated *Bcl* 1 site in mpSAM2 with an *Age* 1 restriction site (*Age* 1 recognition sequence highlighted in bold).

Screening of colonies from the site directed mutagenesis was undertaken by restriction analysis using *Age* 1. Figure 5.13 shows a mutagenesis product that has been successfully digested using *Age* 1, with mpSAM2 failing to digest.

Sequencing of the product using the pBI (MCS I) sequencing primer (see appendix B12) showed PLCasp3 with no mutations. The *Mlu* 1, *Nhe* 1, and *Age* 1 restriction

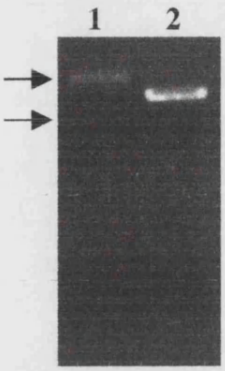

Figure 5.13. Restriction analysis of mpSAM2 site-directed mutagenesis product. Lanes 1 and 2 show *Age* I digests of mpSAM2 and of its mutagenesis product, respectively. The pair of bands in lane 1, highlighted by arrow, show undigested vector. The single band in lane 2 is a result of a single *Age* I restriction site within the mutagenesis product

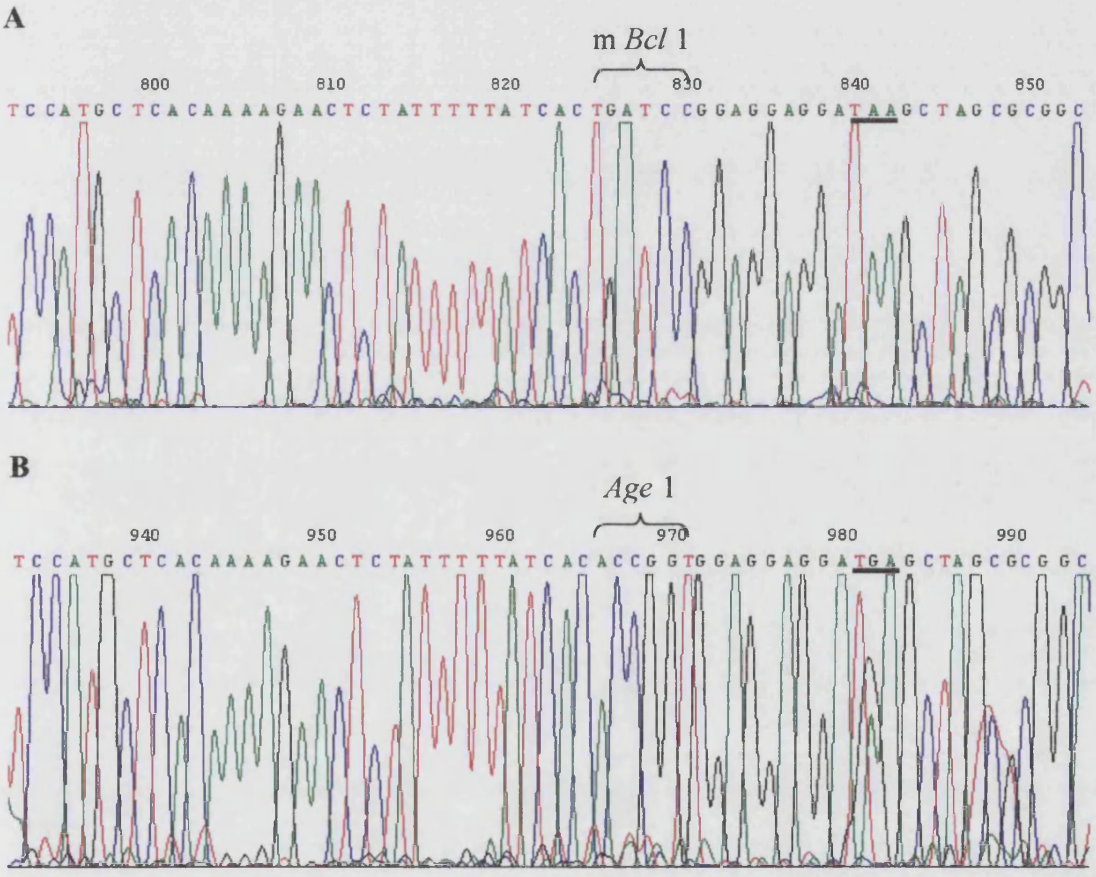

Figure 5.14. Sequence comparison of mpSAM2 and mutagenesis product. (A) Trace of C-terminal pro-less caspase-3 sequence from mpSAM2. Mutated *Bcl* I restriction site is highlighted. (B) Corresponding trace of product from site-directed mutagenesis of mpSAM2. As highlighted, mutagenesis was successful in changing the mutated *Bcl* I site to an *Age* I restriction site. Stop codons are underlined. A silent, change-of-base point mutation in the mutagenesis product is underlined.

sites were also present without mutation. Figure 5.14 is a comparison of the traces from the sequencing of mpSAM2 (A) and the product of the site directed mutagenesis performed using this vector as a template (B). The only mutation identified from the sequencing was a silent point mutation in the stop codon of PLCasp3 (underlined).

However, neither caspase-3 activity, nor EGFP expression was detected in cells transfected with the mutagenesis product (data not shown). The vector was subjected to RFLP analysis, and as figure 5.15 shows, digestion did not take place with the enzyme *Pst* 1.

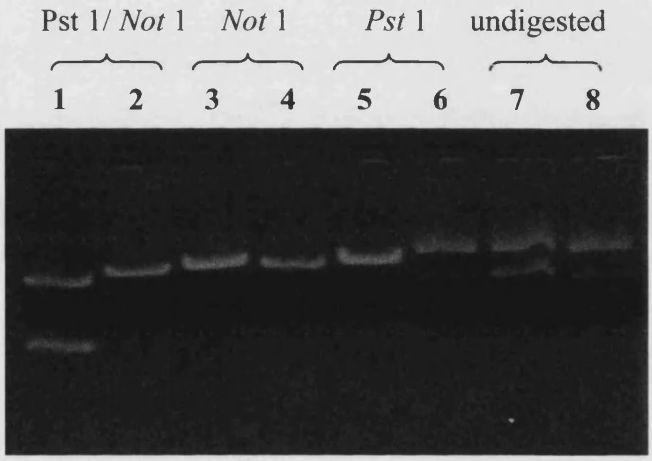

Figure 5.15. Restriction analysis of the mpSAM2 site-directed mutagenesis product. RFLP analysis of mpSAM2 (lanes 1, 3, 5, and 7) and its site-directed mutagenesis product (lanes 2, 4, 6, and 8) was undertaken. The restriction analysis showed the destruction of the *Pst* I site from the MCS II of pBI in the mutagenesis product.

The *Pst* 1 site is located in proximity to (about 10 bp distant from) the start of the CMV promoter site that drives expression of inserts in MCS II, and to the Tet responsive element for the vector. It is possible that a loss-of-function mutation, caused by a large deletion in either/both of the regions was unintentionally introduced during site-directed mutagenesis of mpSAM2.

5.2.5 Characterisation of PLCasp3 Expression Vectors

Though mpSAM2 could not be utilised for the generation of PLCasp3 fusion proteins it could be used to characterise the viability of the caspase-3 approach to study protein transduction. In addition to this vector, the PLCasp3 sequence, shown in figure 5.12, was excised and inserted into the vector pBI-luc on an *Mlu* I/*Nhe* I double digest, generating pBI-luc-PLCasp3, which will be referred to as mpSAM3.

5.2.5.1 Characterisation of mpSAM3

The vector mpSAM3 was studied to determine the conditions necessary to regulate expression of the vector, and to control the activity of the PLCasp3 protein expressed. From the previous studies on luciferase expression using pBI-3K, dox-regulated co-expression of PLCasp3 and luciferase was examined. Figure 5.16 shows that both proteins were expressed in HeLa Tet-Off cells transfected with mpSAM3. Both the luciferase and the caspase-3 activity exhibited by the cells decreased as the concentration of dox was increased. Both activities were reduced to background levels when the cells were subjected to 200 pg/ml dox.

It was necessary to determine whether the caspase-3 activity exhibited by the mpSAM3 transfected cells could be controlled in the same manner as the activity in staurosporine-treated cells. Cells transfected with mpSAM3 were treated with doxycycline and/or the inhibitor Ac-DEVD-CHO. Figure 5.17 shows that, as determined above, treatment with dox results in decreased caspase-3 and luciferase activities. Treatment with Ac-DEVD-CHO does not affect the luciferase activity exhibited in transfected cells, but does decrease the caspase-3 activity of the cells. This is, therefore, due to inhibition of the PLCasp3 protein rather than a decrease in the amount of protein expressed. The caspase-3 activity can be recovered, however, by removal of the inhibitor by washing, followed by a recovery period of 6 hours.

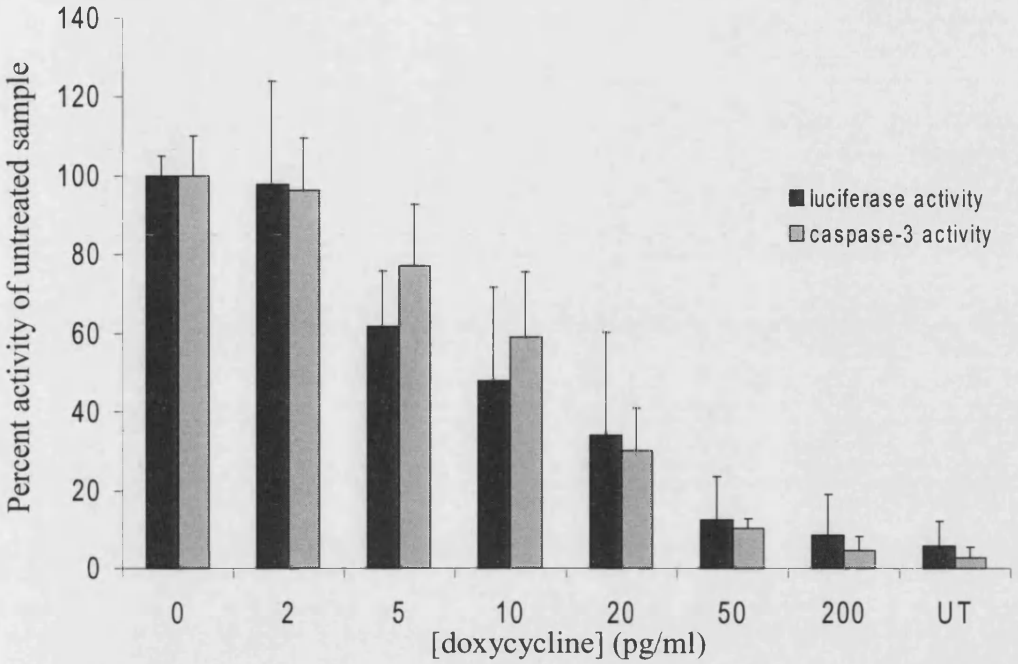

Figure 5.16. Regulation of expression in mpSAM3 transfected cell by doxycycline. HeLa Tet-Off cells were transfected with expression construct mpSAM3. Doxycycline (dox) was added at the time of transfection at the concentrations indicated. Luciferase and caspase-3 activity was measured in cytosolic extracts from transfected cells 24 h after transfection. Measurements were performed in triplicate, values are an average of two experiments ± S.D. Values are presented in terms of activity relative to a transfected sample not supplemented with dox, with a sample of untransfected cells (UT) shown as a control.

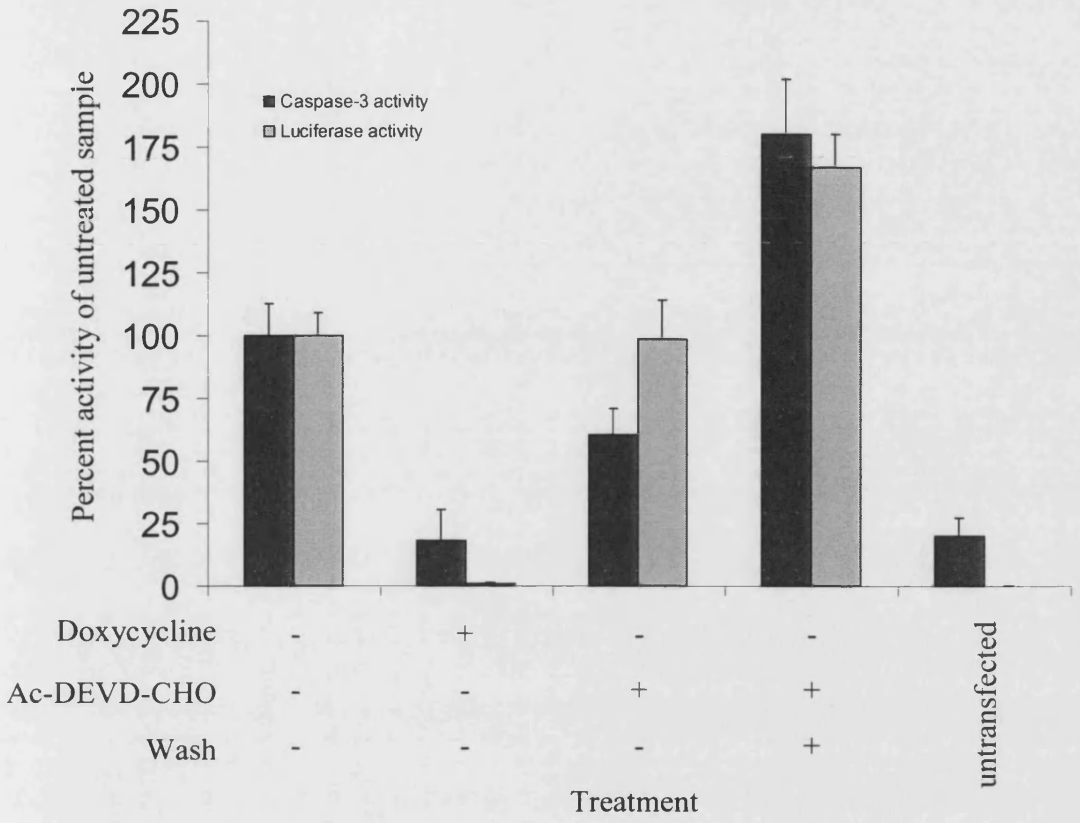

Figure 5.17. Regulation of activity exhibited by cells transiently transfected with mpSAM3. HeLa Tet-Off cells were transfected with mpSAM3, and growth media supplemented with 200 pg/ml doxycycline (dox) and/or 100 μM Ac-DEVD-CHO. Eighteen hours post-transfection cells were washed, where indicated, and fresh growth medium applied. Luciferase and caspase-3 activity was measured in cytosolic extracts of transfected cells 24 h post-transfection Measurements were performed in triplicate, and values are an average of two experiments ± S.D. Values are presented in terms of activity relative to a transfected sample with no medium supplementation, with a sample of untransfected cells shown as a control

5.2.5.2 Characterisation of mpSAM2

With regulation of mpSAM3 determined, mpSAM2 was assessed for PLCasp3 and EGFP expression. Figure 5.18 A shows that expression of PLCasp3 in mpSAM2 transfected cells is also regulated by dox. Examination of the transfected cells confirmed that the cells also expressed EGFP (figure 5.18 C and D). It was anticipated that apoptosis would occur in the cells expressing PLCasp3 as a result of the intrinsic activity exhibited by the pro-less caspase-3 variant. Figure 5.18 A shows the nuclear morphologies of cells treated with staurosporine. Apoptosis has been induced in the cells, and this is characterised in the micrographs by chromatin condensation. A representative sample of non-apoptotic cells is shown in figure 5.18 E for comparison. However, the mpSAM2 transfected cells, identified by EGFP expression, were visible exhibiting the morphologies of both apoptotic and non-apoptotic nuclei, represented by the images captured in figure 5.18 C and D, respectively. This is an indication that though the pro-less caspase-3 variant does exhibit caspase-3 activity, the activity alone may be insufficient to cause apoptosis in expressing cells.

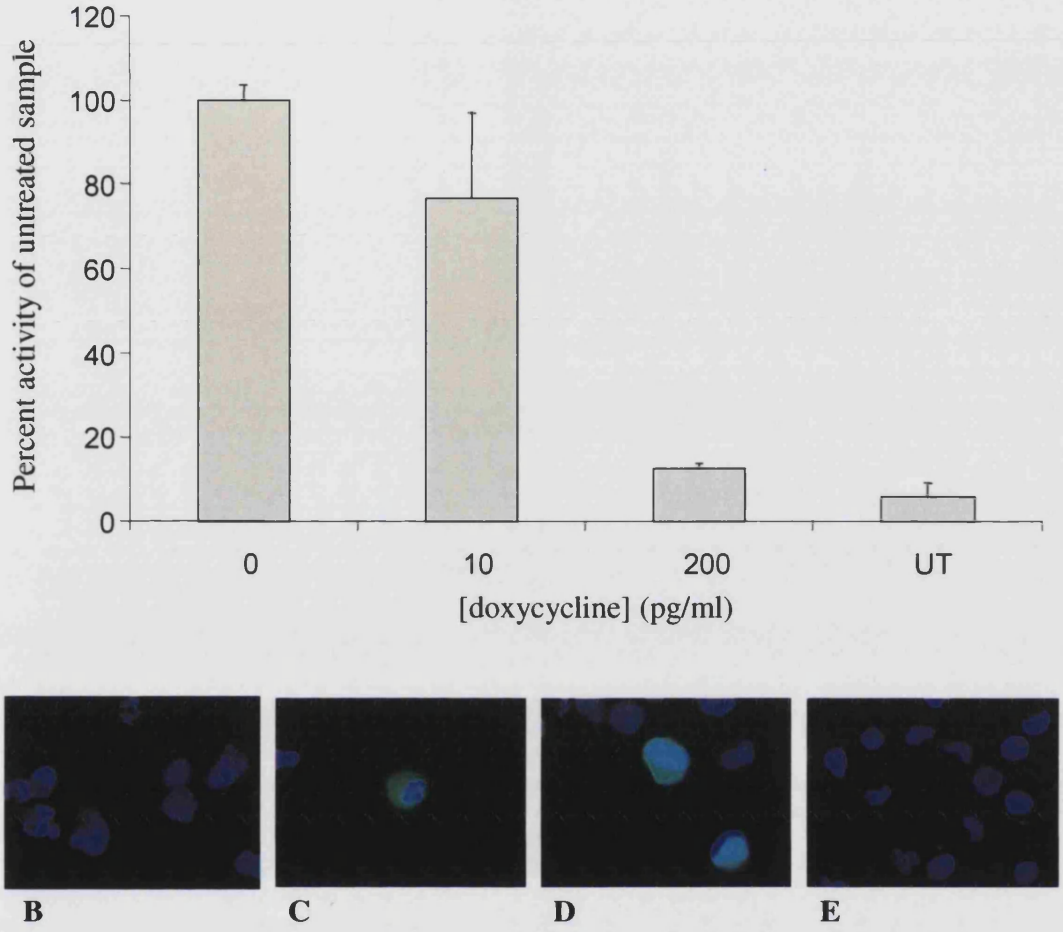

Figure 5.18. Regulation of activity exhibited by cells transiently transfected with mpSAM2. HeLa Tet-Off cells were transfected with mpSAM2. Doxycycline (dox) was added at the concentrations indicated at the time of transfection. (A) Caspase-3 activity was measured in cytosolic extracts from transfected cells 24 h after transfection. Measurements were performed in triplicate, values are an average of two experiments ± S.D. Values are presented in terms of activity relative to a transfected sample not supplemented with dox. A sample of untransfected cells (UT) is shown as a control. (B-E) Representative fluorescent microscope images of DAPI stained cells (blue) to study nuclear morphology. (B) HeLa Tet-Off cells treated for three hours with staurosporine (STS) prior to harvesting. (E) Untreated HeLa Tet-Off cells. (C and D) Images of mpSAM2 transfected HeLa Tet-Off cells, untreated with dox, harvested prior to lysis for caspase-3 activity determination, expressing EGFP (green). (C) Transfected cell exhibiting apoptotic nuclear morphology. (D) Transfected cells exhibiting normal nuclear morphology.

5.3 Discussion

A number of investigations have been undertaken exploring the potential of protein transduction for use in relation to apoptosis, both for protection against apoptosis (Denicourt and Dowdy, 2003; Dietz et al., 2002; Embury et al., 2001; Gustafsson et al., 2002; Ribeiro et al., 2003), and to eliminate cells either directly of indirectly through induction of apoptosis (Bandara et al., 1997; Chen et al., 1999; Cheng et al., 2001c; Giorello et al., 1998; Harada et al., 2002; Herbert et al., 2000; Holinger et al., 1999; Kanovsky et al., 2001; Kim et al., 1999; Li et al., 2002; Phelan et al., 1998; Schimmer et al., 2001; Tasciotti et al., 2003; Vocero-Akbani et al., 2000; Vocero-Akbani et al., 1999; Zender et al., 2002). However, only two studies have examined direct transport of a caspase in fusion with an MTP, and both focused on transport of caspase-3 analogues mediated by the Tat PTD (Harada et al., 2002; Vocero-Akbani et al., 1999). The proteins in question were modified to alter the conditions under which they were activated. Vocera-Akbani *et al.* modified the internal cleavage sites of capsase-3 to those recognised by the HIV protease, instigating processing and activation of the analogue in HIV infected cells only (Vocero-Akbani et al., 1999). Harada *et al.* included an oxygen-dependent degradation domain in the fusion protein studied, leading to degradation of the caspase in cells not subjected to hypoxic conditions whilst inducing increased levels of apoptosis in cells under oxygen-limited conditions (Harada et al., 2002). In contrast to these investigations the approach that was adopted for the work undertaken here was to generate an intrinsically active analogue of caspase-3 and utilise the activity of this protein to directly quantify protein transduction.

5.3.1 Regulation of Expression of pBI Vectors

Meergans *et al.* had previously developed a system for the regulated expression of an active caspase-3 analogue, using a coding sequence that omitted the pro-domain (Meergans et al., 2000). The Wendel group generously donated the vector characterised in this paper, pBI-3K, and a methodology exploiting the group's findings was adopted. Unfortunately, when the HeLa Tet-Off cells used for this study were transfected with pBI-3K they failed to exhibit caspase-3 activity. However, luciferase activity was detected, and this enabled characterisation of expression regulation in this cell line to be investigated.

The pBI expression vectors (Clontech), from which pBI-3K was derived, allow the simultaneous expression of two genes under the control of a single tetracycline-response element. Examination of luciferase expression in pBI-3K transfected cells demonstrated that doxycycline (dox) conferred a much tighter means of regulation than tetracycline (Tet) at 10^4 fold lower concentrations. Dox has the additional benefit of improved stability over Tet, allowing repeat applications every 48 h rather than 24 h. These findings made dox the analogue of choice for regulation of expression in these cells. Meergans *et al.* report Tet concentrations of 25 ng/ml for full repression of expression of activity from pBI-3K transfected HeLa Tet-Off cells (Meergans et al., 2000). Though this concentration is around 100 fold higher than the dox concentration required to limit expression in the HeLa Tet-Off cells used for the results reported here, it is substantially lower than the maximum Tet concentration used (1 μg/ml), where luciferase activity about 100 fold that of the negative control cells was still measured. The differences observed demonstrate the variation in samples of cells from the same cell line (all experiments were carried out in HeLa Tet-Off cells), and this natural variation may account for the absence of caspase-3 activity in the transfected pBI-3K cells. It may be that the HeLa Tet-Off cell line used by Meergans *et al.* had a slightly altered expression profile whereby the cells were less sensitive to the antibiotics regulating their expression, but that they expressed higher levels of the proteins when transfected with the pBI vector, enabling detection of caspase-3 activity from the pro-less caspase-3 analogue.

Having determined that expression could be controlled by dox it was necessary to determine whether expression and activity could be recovered in cells treated with dox. In cells harvested 36 h post-transfection a large increase in activity was measured 6-9 h following removal of dox from the cells, and a slightly smaller increase 9-12 h. However, cells harvested 48 h post-transfection demonstrated a markedly lower activity in samples incubated for 12 h in dox-free medium. An increase in activity was observed in these cells 12-24 h following dox removal, but the maximum levels exhibited were still lower than those in cells incubated for 9 h without dox and harvested 36 h post-transfection.

Theoretically, the two samples grown without dox for 12 h should exhibit the same levels of activity, yet the samples harvested 48 h post-transfection had an activity less than 20 % that measured for the samples harvested 36 h post-transfection. As the age of a culture of cells appears to influence the maximum level of expression recovery achievable, careful consideration would have to be given to the stage at which cells were harvested following repression of their expression with dox, with longer periods of incubation without the repressor not necessarily leading to higher levels of expression.

5.3.2 Inhibition of I*n Vivo* Caspase-3 Activity

Though it was now possible to regulate the expression of proteins in a pBI vector, the expression of the desired protein, an active caspase-3 analogue, may have the terminal effect of killing the cells expressing the protein. This was not desirable for quantification of protein transduction as accumulation of insufficient protein within the donor cells would be inhibited, thus analysing translocation of the fusion proteins would be difficult. Two caspase-3-specific, reversible inhibitors, cp-DEVD-CHO and Ac-DEVD-CHO, were examined to explore the extent to which the caspase-3 activity could be abrogated. In order to test the inhibitors cells were treated with staurosporine, which activates caspase-3 and results in apoptosis, as caspase-3 activity was not exhibited in cells transfected with the pBI-3K vector. The sole difference between the two inhibitors was that one, cp-DEVD-CHO, carried a 16 residue peptide corresponding to the hydrophobic region of the Kaposi fibroblast growth factor. Like the MTPs, this sequence is reported to enhance the cellular uptake of proteins to which it is attached (Lin et al., 1995). However, a greater degree of inhibition was observed in cells pre-treated with the inhibitor Ac-DEVD-CHO than with the cell permeable analogue cp-DEVD-CHO, and with a shorter pre-incubation time. Reversibility studies showed that full caspase-3 activity was recovered 6 h following removal of Ac-DEVD-CHO from cells pre-treated with the inhibitor. This inhibitor could therefore be used to inhibit the caspase-3 activity of the expressed fusion proteins, extending the period over which the protein could be synthesised without unnecessarily compromising the transfected cells' viability, optimising the amount of protein available for translocation. Reversal of inhibition following removal of Ac-DEVD-CHO

would allow PLCasp3 to act on its natural cellular substrates, and transduction could then be quantified.

5.3.3 Generation and Characterisation of PLCasp3-Expressing Vectors

Before this could be accomplished it was necessary to generate vectors to express PLCasp3 and the MTP fusion proteins. Two systems to co-express either EGFP or luciferase with PLCasp3, or the MTP fusion proteins, were chosen in order to increase the number of options available for measurement of transduction. It was hoped that the presence of PLCasp3 within cells would be sufficient to induce apoptosis. Determination of the number of cells in a transfected sample exhibiting apoptotic morphologies, but not expressing EGFP, would allow quantification of the transduction efficiency of a particular MTP. Similarly, measurements of the activity of downstream caspase-3 substrates could be normalised between samples by co-expression of luciferase, and thereby comparative quantification of the MTPs be undertaken. As a result of the feed-back loops existing in the caspase cascade it would even be possible to measure the caspase-3 activity of samples as one of the caspase-3 'downstream' substrates.

The two co-expression reporters were successfully inserted into the pBI vector, and amplification of PLCasp3 from pBI-3K undertaken, and due to the restrictive nature of pBI MCS I, with only 3 restriction sites, an additional restriction site, *Bcl* 1, had been inserted after the PLCasp3 coding sequence to allow the insertion of the MTPs. Sequencing of this vector showed that, though the correct coding sequence for PLCasp3 was present, a point mutation had destroyed the *Bcl* 1 site, rendering any further subcloning with the vector impossible. As the vector pBI-GFP-PLCasp3 was to be termed pSAM2, this vector was named mpSAM2.

Correction of the mutation was undertaken by site-directed mutagenesis to change the restriction site from a *Bcl* 1 site to an *Age* 1 site, which would simplify further subcloning. Though restriction analysis with *Age* 1 and sequencing of the mutagenesis product showed the mutation had been successfully undertaken, activity studies showed transfected cells demonstrated

neither PLCasp3 activity, nor did they exhibit EGFP fluorescence. Further restriction analysis was undertaken, and a *Pst* 1 RFLP was identified. This site is in close proximity to the CMV promoter site that drives expression of inserts in MCS II, and to the Tet responsive element for the vector. It appears that a deletion mutation in this region has destroyed the ability of the vector to express either of the proteins to any measurable degree.

Though the mpSAM2 vector was unsuitable for further subcloning, it was used to verify the viability of the pro-less caspase-3 approach for measuring protein transduction. To extensively investigate this potential the PLCasp3 sequence with the mutated *Bcl* 1 site was excised from mpSAM2 and inserted into pBI-luc to generate pBI-luc-PLCasp3, or mpSAM3. This vector was then used to confirm the regulation of expression by dox. Regulation of both luciferase and caspase-3 activity was substantiated, and the concentration of dox required for 'full' repression of expression was found to be the same as that used in the pBI-3K studies. PLCasp3 activity was also found to be inhibited by Ac-DEVD-CHO in a similar way to caspase-3 in staurosporine treated cells, whilst luciferase activity was unaffected by the inhibitor. As with the studies using staurosporine to activate caspase-3, removal of the inhibitor led to return of PLCasp3 activity in the transfected samples. In these samples the measured PLCasp3 activity was in excess of the levels exhibited by untreated transfected cells, as was the luciferase activity. This is probably a consequence of cells undergoing apoptosis where PLCasp3 is not inhibited by Ac-DEVD-CHO. As the cells expressing PLCasp3 are also expressing luciferase, death of these cells would reduce the luciferase activity measured. For samples incubated with Ac-DEVD-CHO PLCasp3 activity is repressed until the inhibitor is removed. Activity is subsequently recovered and peaks 6 hours following removal of the inhibitor. Inhibition of the PLCasp3 actvitity provides a period during which cells can produce the protein without being subjected to the protein's potentially lethal effects, enabling these samples to have an activity greater then samples where the intrinsically active enzyme is able to carry out its normal function. In terms of the MTP-PLCasp3 fusion proteins, this period would allow protein to be expressed and translocate to other cells without the integrity of the expressing cells being compromised.

Having demonstrated that the luciferase-PLCasp3 co-expression vector would respond to the regulatory agents previously tested the EGFP-PLCasp3 co-expression vector was examined for expression of the proteins. Cells transfected with mpSAM2 exhibited caspase-3 activity, which, like mpSAM3 transfected cells, was regulated by altering the concentration of dox. The cells expressed EGFP as examination by fluorescence microscopy demonstrated. Cell counts were not performed to determine if the number of cells exhibiting EGFP fluorescence was also regulated by the presence of dox, but as the coding gene had been inserted into the same MCS as luciferase this would be expected to be so. Examination of the nuclear morphology of EGFP expressing cells showed that they demonstrated diffuse chromatin associated with viable cells, but also condensation of chromatin associated with cells undergoing apoptosis (Kerr et al., 1972). Meergans *et al.* reported that, despite high caspase-3 activity, only about 15 % of cells transfected with a EGFP-pro-less caspase-3 co-expression vector showed typical signs of apoptosis-like membrane blebbing or chromatin condensation (Meergans et al., 2000). Determination of the number of apoptotic cells expressing EGFP in a sample of mpSAM2-transfected cells was not undertaken here, but it was apparent that cells expressing EGFP were undergoing apoptosis. Even if only a relatively low percentage of cells harbouring PLCasp3 undergo apoptosis it may be possible to use this to quantify transduction efficiencies for the MTPs.

Summary

Attempts to generate constructs for the expression of an intrinsically active form of caspase-3, pro-less caspase-3, in fusion with the MTP sequences proved unsuccessful. However, constructs were generated that allowed the expression of PLCasp3 with either luciferase or EGFP. These constructs allowed the viability of a PLCasp3 approach to quantify protein transduction to be assessed.

Repression of co-expressed luciferase or EGFP with PLCasp3 in HeLa Tet-Off cells was possible through the use of dox, and recovery of expression of was possible by removing the regulatory antibiotic. The expressed PLCasp3 exhibited caspase-3 activity, which could be inhibited by treatment of

expressing cells with the caspase-3 inhibitor Ac-DEVD-CHO. This inhibition was reversible, and full activity was observed 6 h following removal of the inhibitor. Measurement of luciferase and PLCasp3 activity 24 h post-transfection showed cells transfected with mpSAM3 demonstrated higher levels of luciferase and PLCasp3 activity where PLCasp3 activity was inhibited for 18 h post-transfection than in untreated samples. This was probably a result of PLCasp3-induced apoptosis in the untreated samples. Cells transfected with mpSAM2 exhibited both PLCasp3 activity and EGFP fluorescence, with transfected cells demonstrating both apoptotic and non-apoptotic nuclear morphologies.

CHAPTER 6

CONCLUDING REMARKS AND FUTURE WORK

Gene therapy approaches for the treatment of disease have inherent complications associated with the introduction of genetic material into target cells. Where a condition does not require prolonged or regulated expression of a gene for correction, a realistic approach may be to deliver the gene product itself, circumventing a number of the problems associated with gene therapy. However, the plasma membrane of the target cells remains a significant obstacle, as it is naturally impermeable to peptides and proteins that lack specialised membrane receptors or transport proteins. In recent years a number of proteins have been reported to possess the innate ability to freely enter cells, and further investigation has led to the discovery of short peptide regions from some of these proteins, which govern this process. Included in this family are two peptide sequences and one full-length protein that have been shown to be able to transport a biologically active cargo with them as they travel into cells. These are the HIV Tat protein transduction domain (PTD) (Schwarze et al., 1999), penetratin peptide (Theodore et al., 1995), and VP22 (Elliott and O'Hare, 1997). The identification of these protein transducing sequences has opened new possibilities not only for the study of intracellular functions, but more strikingly as a means for delivering *trans*-gene products to cells for the treatment of disease.

With these and other proteins identified as possible vectors for protein delivery it is important to have some way by which their transport ability can be quantified and directly compared. The work discussed in this thesis focused on an investigation to develop a means to quantify the process of protein transduction. The three MTPs mentioned above were used as model vectors, which would enable the utility of a developed quantitation system to be assessed, and also allow comparative studies of the different MTPs to be undertaken.

Although addition of exogenously expressed recombinant proteins would allow application of known doses of the MTPs and their cargo to cells, such approaches introduce time-consuming and technically demanding components to any system developed. As the aim of the study was to develop a means by which not only these, but potentially novel MTPs could be quantitatively assessed for protein transduction efficiency it was important to develop a system where new vectors could be tested with ease. The recombinant approach would require protein purification steps, which would require tailoring for each new MTP tested. Instead, it was decided that a system of *de novo* synthesis would be employed, whereby cells would be transfected with constructs coding for each MTP and a cargo, and spread of the cargo throughout the cells quantified. Such a system allows simple introduction of new MTP sequences into the test vector, and testing can immediately be undertaken. Further testing using an exogenous, recombinant protein approach could be continued once the best candidate MTPs had been determined by this approach, limiting the number of samples for which purification protocols would have to be determined. As protein therapy would perhaps be the ultimate application for protein transduction technology the cargo to be examined throughout the course of this investigation was to be full-length proteins. By exploring the ability of the MTPs to transport reporter proteins between cells, and for the reporter to retain measurable activity, it was hoped that the transport would be representative for other proteins including therapeutic ones. The three MTPs studied here have all been shown to transport numerous cargo molecules, and a recent review covers many of the transported cargoes (see Leifert and Whitton, 2003).

The first part of this investigation, discussed in chapter 3, focuses on the use of GFP as a reporter for transduction. Three different approaches were employed in order to account for factors that may have influenced detection of protein translocation, for example denaturation of the protein, dilution of signal through diffusion of protein, identification of cells harbouring translocated protein, and inefficient transduction. However, with the exception of some apparent limited translocation by the TAT-EGFP and Drome-EGFP fusion proteins (figures 3.10 and 3.11), the approaches failed to confirm the transduction effect observed by other groups. A number of studies have been undertaken using GFP as a

reporter to study protein translocation, most commonly utilising full-length VP22 as the transducing peptide (Aints et al., 1999; Brewis et al., 2000; Elliott and O'Hare, 1999a; Elliott and O'Hare, 1999b; Lai et al., 2000; Wybranietz et al., 1999). However, a number of reports have disputed these findings, with Fang *et al.* initially questioning the findings in 1998 (Fang et al., 1998), and recently concerns have been raised that the methods employed to visualise protein transduction, focusing on the use of GFP as a reporter in particular, may introduce artefactual translocatory effects (Leifert et al., 2002; Lundberg et al., 2003; Richard et al., 2003). Where fixation was used to analyse fluorescent samples a PFA/methanol fixation protocol was followed. Redistribution of MTP-EGFP fusion proteins has been identified using fixation with each of these agents alone, yet no apparent spread of the fusion proteins throughout the sample cells in this study was recognised. There was no need to explore the effect of different fixation conditions on the distribution of the fusion proteins as no definitive translocation was observed.

As GFP had proved to be an inadequate reporter of protein transduction it was necessary to explore other avenues in order to firstly identify the translocation process, and to then quantify it. Chapter 4 introduces a novel reporter for protein transduction, luciferase. By using this highly sensitive system it would be possible to recognise even very minor incidences of translocation, and the nature of the assay would allow direct quantification of the process. Constructs were successfully generated allowing expression of chimeras of each MTP with luciferase, providing the tools with which transduction could be analysed. The approach adopted employed a co-culture system, and relied upon having a means by which transfected, expressing donor cells could be identified and isolated from untransfected recipient cells. Cells constitutively expressing EGFP were chosen to act as recipient cells as they would provide a distinctive parameter by which transfected, non-fluorescent cells could be sorted and removed from the co-culture sample by means of flow cytometry. However, when the sorting efficacy of the FACS apparatus was examined it was found that, though the cell sample exhibiting high levels of fluorescence intensity was enriched following sorting and collection of the cells, there was a high level of contamination from cells demonstrating only autofluorescence. In addition the

sorting procedure was very time consuming, and a large initial sample would yield only a relatively low number of assayable cells.

The low number of recipient cells collected, and the potential contamination within this sample by donor cells would negate the sensitivity provided by luciferase as a reporter using this approach. If the degree of separation of donor and recipient cells could be improved, through the use of an alternative flow cytometer or alternatively by using a different factor to distinguish and segregate the two samples, luciferase provides an attractive system by which quantification of protein transduction may be achieved.

A third system for quantification of protein transduction was explored, and chapter 5 outlines an approach employing an endogenous protein, caspase-3, for this purpose. An intrinsically active pro-less caspase-3 analogue (PLCasp3) (Meergans et al., 2000) was used to obviate the requirement of processing usually associated with activation of caspase-3. Characterisation of the regulation of the vector chosen to express the reporter, and studies into inhibition of staurosporine-activated endogenous caspase-3 provided information on the most favourable compounds to use. These were tested on vectors generated to co-express PLCasp3 with either luciferase or EGFP, and both the expression regulator dox, and the caspase-3 inhibitor Ac-DEVD-CHO were found to act as expected, providing a means to control the amount and activity of expressed PLCasp3. Interestingly, during this work an inhibitor was examined that contained a peptide sequence to enhance cellular uptake of the molecule, the hydrophobic region of the Kaposi fibroblast growth factor (Lin et al., 1995), a type of MTP. This inhibitor was, however, shown to reduce the caspase-3 activity around 50 fold less successfully than the same peptide inhibitor lacking this sequence.

The PLCasp3 expression vectors characterised in order to assess the viability of using this protein as a reporter were not suitable for insertion of additional sequences to generate fusion proteins with the MTPs. Attempts to correct the mutated restriction site responsible for this were unsuccessful, and so no work was undertaken using proteins with any translocatory sequences. However,

from the constructs produced throughout the course of this part of the investigation it would be possible to generate a vector that would allow further subcloning to create plasmids for the co-expression of EGFP or luciferase and PLCasp3-MTP fusion proteins. The preliminary data obtained from this work demonstrate that PLCasp3 has the potential to act as a reporter for protein transduction as it possesses an intrinsic activity. Under normal culture conditions active caspase-3 is synonymous with apoptosis, and this well-defined process should provide a means to quantify the transduction ability of MTPs using PLCasp3 as a reporter. By generating constructs that allow the expression of the PLCasp3-MTP fusion proteins it would be possible to test this using the data presented here to control the activity of the protein.

Of the three approaches developed to assess protein transduction, successful investigation of the process was only possible using EGFP as a reporter. In contrast to many early reports on protein transduction (Aints et al., 1999; Brewis et al., 2000; Elliott and O'Hare, 1999a; Elliott and O'Hare, 1999b; Lai et al., 2000; Wybranietz et al., 1999), but in agreement with more recent ones (Leifert et al., 2002; Lundberg et al., 2003; Richard et al., 2003) no definitive evidence of protein translocation was identified for any of the MTPs tested. Using luciferase as an active reporter was a novel approach, and the biological tools now exist to study this. However, the equipment available at the time of the investigation hindered the approach. If more suitable apparatus becomes available than this system is a very real means by which protein transduction could be quantified. In contrast to this, the final approach was impeded by difficulties in generating the constructs to test. All of the components necessary for creation of the constructs now exist - through digestion of mpSam2 or mpSam3 it would be possible to remove the PLCasp3 element, and this could be replaced by the PLCasp3 element from the mpSAM2 mutagenesis product, which has an intact *Age* I site, and would therefore permit future insertion of MTP sequences. The activity exhibited by the mutated PLCasp3 expression vectors, and control with which PLCasp3 expression and activity can be moderated by dox and Ac-DEVD-CHO, demonstrate that there is potential for this system to be utilised in an attempt to study protein transduction efficiencies.

Whether protein transduction is a novel system by which protein can gain access to the intracellular environment or not, the evidence suggests that proteins can be successfully delivered to cells using the protein transduction sequences (see chapter 1.3 for pharmacological evidence). As such it is necessary to investigate lead sequences to understand and improve factors influencing the process. A method is required by which comparative quantification of protein transduction mediated by MTPs can be undertaken. The biological tools for a novel approach using luciferase now exist, and a second methodology using pro-less caspase-3 has been characterised. In the future this knowledge may provide a means by which these essential comparisons can be carried out.

ABSTRACTS AND PUBLICATIONS

2003; Annual American Pharmaceutical Scientists meeting (AAPS)

Abstract: Protein translocation domains: an investigation of the influence of VP22, Penetratin, and HIV Tat translocation peptide fusion constructs on translocation of enhanced green fluorescent protein (EGFP).

REFERENCES

Aints, A., M.S. Dilber, and C.I.E. Smith. 1999. Intercellular spread of GFP-VP22. *Journal of Gene Medicine.* 1:275-279.

Aints, A., H. Guven, G. Gahrton, C.I. Smith, and M.S. Dilber. 2001. Mapping of herpes simplex virus-1 VP22 functional domains for inter- and subcellular protein targeting. *Gene Therapy.* 8:1051-6.

Alnemri, E.S., D.J. Livingston, D.W. Nicholson, G. Salvesen, N.A. Thornberry, W.W. Wong, and J.Y. Yuan. 1996. Human ICE/CED-3 protease nomenclature. *Cell.* 87:171-171.

Anderson, D.C., E. Nichols, R. Manger, D. Woodle, M. Barry, and A.R. Fritzberg. 1993a. Tumor-cell retention of antibody Fab fragments is enhanced by an attached HIV Tat protein-derived peptide. *Biochemical and Biophysical Research Communications.* 194:876-884.

Anderson, P.M., and M.A. Sorenson. 1994. Effects of route and formulation on clinical pharmacokinetics of interleukin-2. *Clinical Pharmacokinetics.* 27:19-31.

Anderson, W.F. 1998. Human gene therapy. *Nature.* 392:25-30.

Anderson, W.F., G.J. McGarrity, and R.C. Moen. 1993b. Report to the NIH-Recombinant-DNA-Advisory-Committee on Murine Replication-Competent Retrovirus (Rcr) Assays (February 17, 1993). *Human Gene Therapy.* 4:311-321.

Antequera, F., D. Macleod, and A.P. Bird. 1989. Specific protection of methylated CpGs in mammalian nuclei. *Cell.* 58:509-517.

Arnt, C.R., M.V. Chiorean, M.V. Heldebrant, G.J. Gores, and S.H. Kaufmann. 2002. Synthetic Smac/DIABLO peptides enhance the effects of chemotherapeutic agents by binding XIAP and cIAP1 *in situ*. *Journal of Biological Chemistry*. 277:44236-44243.

Arora, N., and S.H. Leppla. 1994. Fusions of Anthrax Toxin Lethal Factor with Shiga Toxin and Diphtheria-Toxin Enzymatic Domains Are Toxic to Mammalian-Cells. *Infection and Immunity*. 62:4955-4961.

Arora, N., L.C. Williamson, S.H. Leppla, and J.L. Halpern. 1994. Cytotoxic Effects of a Chimeric Protein Consisting of Tetanus Toxin Light-Chain and Anthrax Toxin Lethal Factor in Nonneuronal Cells. *Journal of Biological Chemistry*. 269:26165-26171.

Arya, S.K., C. Guo, S.F. Josephs, and F. Wong-Staal. 1985. Trans-activator gene of human T-lymphotropic virus type III (HTLV-III). *Science*. 229:69-73.

Ball, K.L., S. Lain, R. Fahraeus, C. Smythe, and D.P. Lane. 1997. Cell-cycle arrest and inhibition of Cdk4 activity by small peptides based on the carboxy-terminal domain of p21(WAF1). *Current Biology*. 7:71-80.

Bandara, L.R., R. Girling, and N.B. LaThangue. 1997. Apoptosis induced in mammalian cells by small peptides that functionally antagonize the Rb-regulated E2F transcription factor. *Nature Biotechnology*. 15:896-901.

Becker-Hapak, M., S.S. McAllister, and S.F. Dowdy. 2001. TAT-mediated protein transduction into mammalian cells. *Methods*. 24:247-56.

Bennett, R.P., B. Dalby, and P.M. Guy. 2002. Protein delivery using VP22. *Nature Biotechnology*. 20:20.

Berlose, J.P., O. Convert, D. Derossi, A. Brunissen, and G. Chassaing. 1996. Conformational and associative behaviours of the third helix of antennapedia homeodomain in membrane-mimetic environments. *European Journal of Biochemistry*. 242:372-86.

Bestor, T.H., and B. Tycko. 1996. Creation of genomic methylation patterns. *Nature Genetics*. 12:363-367.

Biggin, M.D., and R. Tjian. 1989. Transcription factors and the control of *Drosophila* development. *Trends in Genetics*. 5:377-83.

Blaese, R.M., K.W. Culver, A.D. Miller, C.S. Carter, T. Fleisher, M. Clerici, G. Shearer, L. Chang, Y.W. Chiang, P. Tolstoshev, J.J. Greenblatt, S.A. Rosenberg, H. Klein, M. Berger, C.A. Mullen, W.J. Ramsey, L. Muul, R.A. Morgan, and W.F. Anderson. 1995. T-Lymphocyte-Directed Gene-Therapy for Ada(-) Scid - Initial Trial Results after 4 Years. *Science*. 270:475-480.

Blaho, J.A., C. Mitchell, and B. Roizman. 1994. An Amino-Acid-Sequence Shared by the Herpes-Simplex Virus-1- Alpha Regulatory Protein-0, Protein-4, Protein-22, and Protein- 27 Predicts the Nucleotidylation of the U(L)21, U(L)31, U(L)47, and U(L)49 Gene-Products. *Journal of Biological Chemistry*. 269:17401-17410.

Bloch-Gallego, E., I. Le Roux, A.H. Joliot, M. Volovitch, C.E. Henderson, and A. Prochiantz. 1993. Antennapedia homeobox peptide enhances growth and branching of embryonic chicken motoneurons in vitro. *Journal of Cell Biology*. 120:485-92.

Bonfanti, M., S. Taverna, M. Salmona, M. Dincalci, and M. Broggini. 1997. p21(WAF1)-derived peptides linked to an internalization peptide inhibit human cancer cell growth. *Cancer Research.* 57:1442-1446.

Bosch, F.X., M.M. Manos, N. Munoz, M. Sherman, A.M. Jansen, J. Peto, M.H. Schiffman, V. Moreno, R. Kurman, K.V. Shah, E. Alihonou, S. Bayo, H.C. Mokhtar, S. Chicareon, A. Daudt, E. Delosrios, P. Ghadirian, J.N. Kitinya, M. Koulibaly, C. Ngelangel, L.M.P. Tintore, J.L. Riosdalenz, Sarjadi, A. Schneider, L. Tafur, A.R. Teyssie, P.A. Rolon, M. Torroella, A.V. Tapia, H.R. Wabinga, W. Zatonski, B. Sylla, P. Vizcaino, D. Magnin, J. Kaldor, C. Greer, and C. Wheeler. 1995. Prevalence of Human Papillomavirus in Cervical-Cancer - a Worldwide Perspective. *Journal of the National Cancer Institute.* 87:796-802.

Brewis, N., A. Phelan, J. Webb, J. Drew, G. Elliott, and P. O'Hare. 2000. Evaluation of VP22 spread in tissue culture. *Journal of Virology.* 74:1051-6.

Brugidou, J., C. Legrand, J. Mery, and A. Rabie. 1995. The Retro-Inverso Form of a Homeobox-Derived Short Peptide Is Rapidly Internalized by Cultured Neurons - a New Basis for an Efficient Intracellular Delivery System. *Biochemical and Biophysical Research Communications.* 214:685-693.

Chalfie, M., Y. Tu, G. Euskirchen, W.W. Ward, and D.C. Prasher. 1994. Green fluorescent protein as a marker for gene expression. *Science.* 263:802-5.

Chatelin, L., M. Volovitch, A.H. Joliot, F. Perez, and A. Prochiantz. 1996. Transcription factor hoxa-5 is taken up by cells in culture and conveyed to their nuclei. *Mechanisms of Development.* 55:111-7.

Chellaiah, M.A., N. Soga, S. Swanson, S. McAllister, U. Alvarez, D. Wang, S.F. Dowdy, and K.A. Hruska. 2000. Rho-A is critical for osteoclast podosome organization, motility, and bone resorption. *Journal of Biological Chemistry.* 275:11993-2002.

Chen, Y.N., S.K. Sharma, T.M. Ramsey, L. Jiang, M.S. Martin, K. Baker, P.D. Adams, K.W. Bair, and W.G. Kaelin, Jr. 1999. Selective killing of transformed cells by cyclin/cyclin-dependent kinase 2 antagonists. *Proceeding of the National Academy of Sciences of the United States of America.* 96:4325-9.

Cheng, E., M.C. Wei, S. Weiler, R.A. Flavell, T.W. Mak, T. Lindsten, and S.J. Korsmeyer. 2001a. BCL-2, BCL-X-L sequester BH3 domain-only molecules preventing BAX- and BAK-mediated mitochondrial apoptosis. *Molecular Cell.* 8:705-711.

Cheng, W.F., C.F. Hung, C.Y. Chai, K.F. Hsu, L. He, M. Ling, and T.C. Wu. 2001b. Enhancement of Sindbis virus self-replicating RNA vaccine potency by linkage of herpes simplex virus type 1 VP22 protein to antigen. *Journal of Virology.* 75:2368-2376.

Cheng, W.F., C.F. Hung, C.Y. Chai, K.F. Hsu, L. He, C.M. Rice, M. Ling, and T.C. Wu. 2001c. Enhancement of Sindbis virus self-replicating RNA vaccine potency by linkage of *Mycobacterium tuberculosis* heat shock protein 70 gene to an antigen gene. *Journal of Immunology.* 166:6218-26.

Chonn, A., and P.R. Cullis. 1995. Recent Advances in Liposomal Drug-Delivery Systems. *Current Opinion in Biotechnology*. 6:698-708.

Cleland, J.L., M.F. Powell, and S.J. Shire. 1993. The Development of Stable Protein Formulations - a Close Look at Protein Aggregation, Deamidation, and Oxidation. *Critical Reviews in Therapeutic Drug Carrier Systems*. 10:307-377.

Cohen, G.M. 1997. Caspases: the executioners of apoptosis. *Biochemical Journal*. 326:1-16.

Cohen, J.J. 1996. Apoptosis and its regulation. *Advances in Experimental Medicine and Biology*. 406:11-20.

Colussi, P.A., N.L. Harvey, and S. Kumar. 1998a. Prodomain-dependent Nuclear Localization of the Caspase-2 (Nedd2) Precursor. A NOVEL FUNCTION FOR A CASPASE PRODOMAIN. *Journal of Biological Chemistry*. 273:24535-24542.

Colussi, P.A., N.L. Harvey, L.M. Shearwin-Whyatt, and S. Kumar. 1998b. Conversion of procaspase-3 to an autoactivating caspase by fusion to the caspase-2 prodomain. *Journal of Biological Chemistry*. 273:26566-26570.

Condra, J.H., W.A. Schleif, O.M. Blahy, L.J. Gabryelski, D.J. Graham, J.C. Quintero, A. Rhodes, H.L. Robbins, E. Roth, M. Shivaprakash, D. Titus, T. Yang, H. Teppler, K.E. Squires, P.J. Deutsch, and E.A. Emini. 1995. *In-Vivo* Emergence of HIV-1 Variants Resistant to Multiple Protease Inhibitors. *Nature*. 374:569-571.

Cussac, D., M. Vidal, C. Leprince, W.Q. Liu, G. Tiraboschi, B.P. Roques, and C. Garbay. 1999. A Sos-derived peptidimer blocks the Ras signaling pathway by binding both Grb2 SH3 domains and displays antiproliferative activity. *FASEB Journal.* 13:31-39.

Dang, C.V., and W.M. Lee. 1989. Nuclear and nucleolar targeting sequences of c-erb-A, c-myb, N-myc, p53, HSP70, and HIV tat proteins. *Journal of Biological Chemistry.* 264:18019-23.

Debs, R.J., L.P. Freedman, S. Edmunds, K.L. Gaensler, N. Duzgunes, and K.R. Yamamoto. 1990. Regulation of Gene-Expression *In Vivo* by Liposome-Mediated Delivery of a Purified Transcription Factor. *Journal of Biological Chemistry.* 265:10189-10192.

Del Gaizo, V., and R.M. Payne. 2003. A novel TAT-mitochondrial signal sequence fusion protein is processed, stays in mitochondria, and crosses the placenta. *Molecular Therapy.* 7:720-730.

Denicourt, C., and S.F. Dowdy. 2003. Protein transduction technology offers novel therapeutic approach for brain ischemia. *Trends in Pharmacological Sciences.* 24:216-218.

Derer, W., H.P. Easwaran, H. Leonhardt, and M.C. Cardoso. 2001. A novel approach to induce cell cycle re-entry in terminally differentiated muscle cells. *FASEB Journal.* 15:U83-U94.

Derossi, D., S. Calvet, A. Trembleau, A. Brunissen, G. Chassaing, and A. Prochiantz. 1996. Cell internalization of the third helix of the Antennapedia homeodomain is receptor-independent. *Journal of Biological Chemistry.* 271:18188-93.

Derossi, D., G. Chassaing, and A. Prochiantz. 1998. Trojan peptides: the penetratin system for intracellular delivery. *Trends in Cell Biology*. 8:84-7.

Derossi, D., A.H. Joliot, G. Chassaing, and A. Prochiantz. 1994. The third helix of the Antennapedia homeodomain translocates through biological membranes. *Journal of Biological Chemistry*. 269:10444-50.

Deveraux, Q.L., N. Roy, H.R. Stennicke, T. Van Arsdale, Q. Zhou, S.M. Srinivasula, E.S. Alnemri, G.S. Salvesen, and J.C. Reed. 1998. IAPs block apoptotic events induced by caspase-8 and cytochrome c by direct inhibition of distinct caspases. *EMBO Journal*. 17:2215-2223.

Dewet, J.R., K.V. Wood, M. Deluca, D.R. Helinski, and S. Subramani. 1987. Firefly Luciferase Gene - Structure and Expression in Mammalian-Cells. *Molecular and Cellular Biology*. 7:725-737.

Dietz, G.P.H., E. Kilic, and M. Bahr. 2002. Inhibition of neuronal apoptosis *in vitro* and *in vivo* using TAT-Mediated protein transduction. *Molecular and Cellular Neuroscience*. 21:29-37.

Dilber, M.S., A. Phelan, A. Aints, A.J. Mohamed, G. Elliott, C.E. Smith, and P. O'Hare. 1999. Intercellular delivery of thymidine kinase prodrug activating enzyme by the herpes simplex virus protein, VP22. *Gene Therapy*. 6:12-21.

Doeberitz, M.V., T. Oltersdorf, E. Schwarz, and L. Gissmann. 1988. Correlation of Modified Human Papilloma-Virus Early Gene- Expression with Altered Growth-Properties in C4-1 Cervical- Carcinoma Cells. *Cancer Research*. 48:3780-3786.

Drin, G., M. Mazel, P. Clair, D. Mathieu, M. Kaczorek, and J. Temsamani. 2001. Physico-chemical requirements for cellular uptake of pAntp peptide. Role of lipid-binding affinity. *European Journal of Biochemistry.* 268:1304-14.

Earnshaw, W.C., L.M. Martins, and S.H. Kaufmann. 1999. Mammalian caspases: structure, activation, substrates, and functions during apoptosis. *Annual Review of Biochemistry.* 68:383-424.

Elliott, G., G. Mouzakitis, and P. O'Hare. 1995. VP16 Interacts Via Its Activation Domain with VP22, a Tegument Protein of Herpes-Simplex Virus, and Is Relocated to a Novel Macromolecular Assembly in Coexpressing Cells. *Journal of Virology.* 69:7932-7941.

Elliott, G., and P. O'Hare. 1997. Intercellular trafficking and protein delivery by a herpesvirus structural protein. *Cell.* 88:223-33.

Elliott, G., and P. O'Hare. 1998. Herpes simplex virus type 1 tegument protein VP22 induces the stabilization and hyperacetylation of microtubules. *Journal of Virology.* 72:6448-55.

Elliott, G., and P. O'Hare. 1999a. Intercellular trafficking of VP22-GFP fusion proteins. *Gene Therapy.* 6:149-51.

Elliott, G., and P. O'Hare. 1999b. Live-cell analysis of a green fluorescent protein-tagged herpes simplex virus infection. *Journal of Virology.* 73:4110-9.

Elliott, G., D. O'Reilly, and P. O'Hare. 1996. Phosphorylation of the herpes simplex virus type 1 tegument protein VP22. *Virology.* 226:140-5.

Elliott, G.D., and D.M. Meredith. 1992. The herpes simplex virus type 1 tegument protein VP22 is encoded by gene UL49. *Journal of General Virology*. 73:723-6.

Embury, J., D. Klein, A. Pileggi, M. Ribeiro, S. Jayaraman, R.D. Molano, C. Fraker, N. Kenyon, C. Ricordi, L. Inverardi, and R.L. Pastori. 2001. Proteins linked to a protein transduction domain efficiently transduce pancreatic islets. *Diabetes*. 50:1706-1713.

Engelmann, C., Y. Panis, J. Bolard, B. Diquet, M. Fabre, H. Nagy, O. Soubrane, D. Houssin, and D. Klatzmann. 1999. Liposomal encapsulation of ganciclovir enhances the efficacy of herpes simplex virus type 1 thymidine kinase suicide gene therapy against hepatic tumors in rats. *Human Gene Therapy*. 10:1545-1551.

Eum, W.S., I.S. Choung, A.Y. Kim, Y.J. Lee, J.H. Kang, J. Park, K.S. Lee, H.Y. Kwon, and S.Y. Choi. 2002. Transduction efficacy of Tat-Cu Zn-superoxide dismutase is enhanced by copper ion recovery of the fusion protein. *Molecules and Cells*. 13:334-340.

Ezhevsky, S.A., H. Nagahara, A.M. Vocero-Akbani, D.R. Gius, M.C. Wei, and S.F. Dowdy. 1997. Hypo-phosphorylation of the retinoblastoma protein (pRb) by cyclin D:Cdk4/6 complexes results in active pRb. *Proceedings of the National Academy of Science of the United States of America*. 94:10699-704.

Fahraeus, R., S. Lain, K.L. Ball, and D.P. Lane. 1998. Characterization of the cyclin-dependent kinase inhibitory domain of the INK4 family as a model for a synthetic tumour suppressor molecule. *Oncogene*. 16:587-596.

Fahraeus, R., and D.P. Lane. 1999. The p16(INK4a) tumour suppressor protein inhibits alpha(v)beta(3) integrin-mediated cell spreading on vitronectin by blocking PKC-dependent localization of alpha(v)beta(3) to focal contacts. *EMBO Journal.* 18:2106-2118.

Fahraeus, R., J.M. Paramio, K.L. Ball, S. Lain, and D.P. Lane. 1996. Inhibition of pRb phosphorylation and cell-cycle progression by a 20-residue peptide derived from p16CDKN2/INK4A. *Current Biology.* 6:84-91.

Falnes, P.O., S. Ariansen, K. Sandvig, and S. Olsnes. 2000. Requirement for prolonged action in the cytosol for optimal protein synthesis inhibition by diphtheria toxin. *Journal of Biological Chemistry.* 275:4363-4368.

Falnes, P.O., J. Wesche, and S. Olsnes. 2001. Ability of the Tat basic domain and VP22 to mediate cell binding, but not membrane translocation of the diphtheria toxin A-fragment. *Biochemistry.* 40:4349-4358.

Fang, B., B. Xu, P. Koch, and J.A. Roth. 1998. Intercellular trafficking of VP22-GFP fusion proteins is not observed in cultured mammalian cells. *Gene Therapy.* 5:1420-4.

Fawell, S., J. Seery, Y. Daikh, C. Moore, L.L. Chen, B. Pepinsky, and J. Barsoum. 1994. Tat-mediated delivery of heterologous proteins into cells. *Proceedings of the National Academy of Sciences of the United States of America.* 91:664-8.

Fisher, A.G., M.B. Feinberg, S.F. Josephs, M.E. Harper, L.M. Marselle, G. Reyes, M.A. Gonda, A. Aldovini, C. Debouk, R.C. Gallo, and et al. 1986. The trans-activator gene of HTLV-III is essential for virus replication. *Nature.* 320:367-71.

Francis, S.E., D.J. Sullivan, and D.E. Goldberg. 1997. Hemoglobin metabolism in the malaria parasite *Plasmodium falciparum*. *Annual Review of Microbiology*. 51:97-123.

Frankel, A.D., and C.O. Pabo. 1988. Cellular uptake of the tat protein from human immunodeficiency virus. *Cell*. 55:1189-93.

Fraser, A., and G. Evan. 1996. A license to kill. *Cell*. 85:781-784.

Fuki, I.V., M.E. Meyer, and K.J. Williams. 2000. Transmembrane and cytoplasmic domains of syndecan mediate a multi-step endocytic pathway involving detergent-insoluble membrane rafts. *Biochemical Journal*. 351:607-612.

Futaki, S., W. Ohashi, T. Suzuki, M. Niwa, S. Tanaka, K. Ueda, H. Harashima, and Y. Sugiura. 2001. Stearylated arginine-rich peptides: A new class of transfection systems. *Bioconjugate Chemistry*. 12:1005-1011.

Gehring, W.J. 1987. Homeo boxes in the study of development. *Science*. 236:1245-52.

Giorello, L., L. Clerico, M.P. Pescarolo, F. Vikhanskaya, M. Salmona, G. Colella, S. Bruno, T. Mancuso, L. Bagnasco, P. Russo, and S. Parodi. 1998. Inhibition of cancer cell growth and c-Myc transcriptional activity by a c-Myc helix l-type peptide fused to an internalization sequence. *Cancer Research*. 58:3654-3659.

Gius, D.R., S.A. Ezhevsky, M. Becker-Hapak, H. Nagahara, M.C. Wei, and S.F. Dowdy. 1999. Transduced p16INK4a peptides inhibit hypophosphorylation of the retinoblastoma protein and cell cycle progression prior to activation of Cdk2 complexes in late G1. *Cancer Research*. 59:2577-80.

Green, I., R. Christison, C.J. Voyce, K.R. Bundell, and M.A. Lindsay. 2003. Protein transduction domains: are they delivering? *Trends in Pharmacological Sciences*. 24:213-215.

Green, M., and P.M. Loewenstein. 1988. Autonomous functional domains of chemically synthesized human immunodeficiency virus tat trans-activator protein. *Cell*. 55:1179-88.

Greer, L.F., and A.A. Szalay. 2002. Imaging of light emission from the expression of luciferases in living cells and organisms: a review. *Luminescence*. 17:43-74.

Gregoriadis, G. 1995. Engineering liposomes for drug delivery: Progress and problems. *Trends in Biotechnology*. 13:527-537.

Guillaume, C., P. Delepine, B. Mercier, E. Gobin, J.P. Leroy, V. Morin, and C. Ferec. 2000. Phosphonocationic lipids in protein delivery to mice lungs. *Journal of Pharmaceutical Sciences*. 89:639-645.

Gurtu, G., and E. Zhang. 1997. Inhibition of CPP32 protease activity prevents staurosporine-induced apoptosis in CHO-K1 cells. *CLONTECHniques*. April.

Gustafsson, A.B., M.R. Sayen, S.D. Williams, M.T. Crow, and R.A. Gottlieb. 2002. TAT protein transduction into isolated perfused hearts - TAT-apoptosis repressor with caspase recruitment domain is cardioprotective. *Circulation*. 106:735-739.

Hall, H., E.J. Williams, S.E. Moore, F.S. Walsh, A. Prochiantz, and P. Doherty. 1996. Inhibition of FGF-stimulated phosphatidylinositol hydrolysis and neurite outgrowth by a cell-membrane permeable phosphopeptide. *Current Biology*. 6:580-587.

Hall, L.M., K.G. Draper, R.J. Frink, R.H. Costa, and E.K. Wagner. 1982. Herpes-Simplex Virus Messenger-RNA Species Mapping in EcoRI Fragment-I. *Journal of Virology*. 43:594-607.

Han, K., M.J. Jeon, K.A. Kim, J. Park, and S.Y. Choi. 2000. Efficient intracellular delivery of GFP by homeodomains of *Drosophila* Fushi-tarazu and engrailed proteins. *Molecules and Cells*. 10:728-732.

Han, Z.Y., E.A. Hendrickson, T.A. Bremner, and J.H. Wyche. 1997. A sequential two-step mechanism for the production of the mature p17:p12 form of caspase-3 in vitro. *Journal of Biological Chemistry*. 272:13432-13436.

Harada, H., M. Hiraoka, and S. Kizaka-Kondoh. 2002. Antitumor effect of TAT-oxygen-dependent degradation-caspase-3 fusion protein specifically stabilized and activated in hypoxic tumor cells. *Cancer Research*. 62:2013-2018.

Harms, J.S., X. Ren, S.C. Oliveira, and G.A. Splitter. 2000. Distinctions between bovine herpesvirus 1 and herpes simplex virus type 1 VP22 tegument protein subcellular associations. *Journal of Virology*. 74:3301-12.

Hawiger, J. 1999. Noninvasive intracellular delivery of functional peptides and proteins. *Current Opinion in Chemical Biology*. 3:89-94.

Hendrich, B., and A. Bird. 1998. Identification and characterization of a family of mammalian methyl-CpG binding proteins. *Molecular and Cellular Biology*. 18:6538-6547.

Herbert, T.P., R. Fahraeus, A. Prescott, D.P. Lane, and C.G. Proud. 2000. Rapid induction of apoptosis mediated by peptides that bind initiation factor eIF4E. *Current Biology*. 10:793-796.

Hildt, E., and S. Oess. 1999. Identification of Grb2 as a novel binding partner of tumor necrosis factor (TNF) receptor I. *Journal of Experimental Medicine*. 189:1707-1714.

Ho, A., S.R. Schwarze, S.J. Mermelstein, G. Waksman, and S.F. Dowdy. 2001. Synthetic protein transduction domains: enhanced transduction potential *in vitro* and *in vivo*. *Cancer Research*. 61:474-7.

Holinger, E.P., T. Chittenden, and R.J. Lutz. 1999. Bak BH3 peptides antagonize Bcl-x(L) function and induce apoptosis through cytochrome c-independent activation of caspases. *Journal of Biological Chemistry*. 274:13298-13304.

Hosotani, R., Y. Miyamoto, K. Fujimoto, R. Doi, A. Otaka, N. Fujii, and M. Imamura. 2002. Trojan p16 peptide suppresses pancreatic cancer growth and prolongs survival in mice. *Clinical Cancer Research*. 8:1271-1276.

Hung, C.F., W.F. Cheng, C.Y. Chai, K.F. Hsu, L.M. He, M. Ling, and T.C. Wu. 2001. Improving vaccine potency through intercellular spreading and enhanced MHC class I presentation of antigen. *Journal of Immunology*. 166:5733-5740.

Joliot, A., C. Pernelle, H. Deagostini-Bazin, and A. Prochiantz. 1991a. Antennapedia homeobox peptide regulates neural morphogenesis. *Proceedings of the National Academy of Sciences of the United States of America*. 88:1864-8.

Joliot, A.H., A. Triller, M. Volovitch, C. Pernelle, and A. Prochiantz. 1991b. Alpha-2,8-Polysialic Acid Is the Neuronal Surface-Receptor of Antennapedia Homeobox Peptide. *New Biologist.* 3:1121-1134.

Kafri, T., U. Blomer, D.A. Peterson, F.H. Gage, and I.M. Verma. 1997. Sustained expression of genes delivered directly into liver and muscle by lentiviral vectors. *Nature Genetics.* 17:314-317.

Kahn, T.W., R.N. Beachy, and M.M. Falk. 1997. Cell-free expression of a GFP fusion protein allows quantitation in vitro and in vivo. *Current Biology.* 7:R207-R208.

Kanovsky, M., A. Raffo, L. Drew, R. Rosal, T. Do, F.K. Friedman, P. Rubinstein, J. Visser, R. Robinson, P.W. Brandt-Rauf, J. Michl, R.L. Fine, and M.R. Pincus. 2001. Peptides from the amino terminal mdm-2-binding domain of p53, designed from conformational analysis, are selectively cytotoxic to transformed cells. *Proceeding of the National Academy of Sciences of the United States of America.* 98:12438-43.

Kardinal, C., B. Konkol, A. Schulz, G. Posern, H. Lin, K. Adermann, M. Eulitz, Z. Estrov, M. Talpaz, R.B. Arlinghaus, and S.M. Feller. 2000. Cell-penetrating SH3 domain blocker peptides inhibit proliferation of primary blast cells from CML patients. *FASEB Journal.* 14:1529-1538.

Kato, D., K. Miyazawa, M. Ruas, M. Starborg, I. Wada, T. Oka, T. Sakai, G. Peters, and E. Hara. 1998. Features of replicative senescence induced by direct addition of antennapedia-p16(INK4A) fusion protein to human diploid fibroblasts. *FEBS Letters.* 427:203-208.

Keller, J., I. Heisler, R. Tauber, and H. Fuchs. 2001. Development of a novel molecular adapter for the optimization of immunotoxins. *Journal of Controlled Release.* 74:259-61.

Kerr, J.F., A.H. Wyllie, and A.R. Currie. 1972. Apoptosis: A basic biological phenomenon with wide-ranging implications in tissue kinetics. *British Journal of Cancer.* 26:239-57.

Kim, A.L., A.J. Raffo, P.W. Brandt-Rauf, M.R. Pincus, R. Monaco, P. Abarzua, and R.L. Fine. 1999. Conformational and molecular basis for induction of apoptosis by a p53 C-terminal peptide in human cancer cells. *Journal of Biological Chemistry.* 274:34924-34931.

Kim, D.T., D.J. Mitchell, D.G. Brockstedt, L. Fong, G.P. Nolan, C.G. Fathman, E.G. Engleman, and J.B. Rothbard. 1997. Introduction of soluble proteins into the MHC class I pathway by conjugation to an HIV tat peptide. *Journal of Immunology.* 159:1666-8.

Kohl, N.E., E.A. Emini, W.A. Schleif, L.J. Davis, J.C. Heimbach, R.A.F. Dixon, E.M. Scolnick, and I.S. Sigal. 1988. Active Human Immunodeficiency Virus Protease Is Required for Viral Infectivity. *Proceedings of the National Academy of Sciences of the United States of America.* 85:4686-4690.

Koppelhus, U., S.K. Awasthi, V. Zachar, H.U. Holst, P. Ebbesen, and P.E. Nielsen. 2002. Cell-dependent differential cellular uptake of PNA, peptides, and PNA-peptide conjugates. *Antisense & Nucleic Acid Drug Development.* 12:51-63.

Koshizuka, T., H. Takakuwa, F. Goshima, T. Murata, and Y. Nishiyama. 2001. The US11 gene product of herpes simplex virus has intercellular trafficking activity. *Biochemical and Biophysical Research Communications*. 288:597-602.

Kuchler, K. 1993. Unusual routes of protein secretion: the easy way out. *Trends in Cell Biology*. 3:421-426.

Kueltzo, L.A., N. Normand, P. O'Hare, and C.R. Middaugh. 2000. Conformational lability of herpesvirus protein VP22. *Journal of Biological Chemistry*. 275:33213-21.

Kumar, S., M. Kinoshita, M. Noda, N.G. Copeland, and N.A. Jenkins. 1994. Induction of Apoptosis by the Mouse Nedd2 Gene, Which Encodes a Protein Similar to the Product of the *Caenorhabditis elegans* Cell-Death Gene Ced-3 and the Mammalian Il-1-Beta-Converting Enzyme. *Genes & Development*. 8:1613-1626.

Lagnado, L., and D. Baylor. 1992. Signal Flow in Visual Transduction. *Neuron*. 8:995-1002.

Lai, Z., I. Han, G. Zirzow, R.O. Brady, and J. Reiser. 2000. Intercellular delivery of a herpes simplex virus VP22 fusion protein from cells infected with lentiviral vectors. *Proceedings of the National Academy of Sciences of the United States of America*. 97:11297-302.

Lasic, D.D. 1998. Novel applications of liposomes. *Trends in Biotechnology*. 16:307-321.

Lazebnik, Y.A., S.H. Kaufmann, S. Desnoyers, G.G. Poirier, and W.C. Earnshaw. 1994. Cleavage of Poly(Adp-Ribose) Polymerase by a Proteinase with Properties Like ICE. *Nature*. 371:346-347.

Le Roux, I., A.H. Joliot, E. Bloch-Gallego, A. Prochiantz, and M. Volovitch. 1993. Neurotrophic activity of the Antennapedia homeodomain depends on its specific DNA-binding properties. *Proceedings of the National Academy of Sciences of the United States of America*. 90:9120-4.

Lee, H.J., and W.M. Pardridge. 2001. Pharmacokinetics and delivery of tat and tat-protein conjugates to tissues *in vivo*. *Bioconjugate Chemistry*. 12:995-999.

Leifert, J.A., S. Harkins, and J.L. Whitton. 2002. Full-length proteins attached to the HIV tat protein transduction domain are neither transduced between cells, nor exhibit enhanced immunogenicity. *Gene Therapy*. 9:1422-1428.

Leifert, J.A., and J.L. Whitton. 2003. 'Translocatory proteins' and 'Protein transduction domains': A critical analysis of their biological effects and the underlying mechanisms. *Molecular Therapy*. 8:13-20.

LeMay, D.R., M. Kittaka, E.M. Gordon, B. Gray, M.F. Stins, J.G. McComb, S. Jovanovic, P. Tabrizi, M.H. Weiss, R. Bartus, W.F. Anderson, and B.V. Zlokovic. 1998. Intravenous RMP-7 increases delivery of ganciclovir into rat brain tumors and enhances the effects of herpes simplex virus thymidine kinase gene therapy. *Human Gene Therapy*. 9:989-995.

Lercher, M.J., A.O. Urrutia, and L.D. Hurst. 2002. Clustering of housekeeping genes provides a unified model of gene order in the human genome. *Nature Genetics*. 31:180-183.

Levine, A.J. 1997. p53, the cellular gatekeeper for growth and division. *Cell.* 88:323-331.

Li, P., D. Nijhawan, I. Budihardjo, S.M. Srinivasula, M. Ahmad, E.S. Alnemri, and X.D. Wang. 1997. Cytochrome c and dATP-dependent formation of Apaf-1/caspase-9 complex initiates an apoptotic protease cascade. *Cell.* 91:479-489.

Li, Y., R.V. Rosal, P.W. Brandt-Rauf, and R.L. Fine. 2002. Correlation between hydrophobic properties and efficiency of carrier-mediated membrane transduction and apoptosis of a p53 C-terminal peptide. *Biochemical and Biophysical Research Communications.* 298:439-449.

Lidgate, D.M., P.L. Felgner, J.S. Fleitman, J. Whatley, and R.C.C. Fu. 1988. *In vitro* and *In vivo* Studies Evaluating a Liposome System for Drug Solubilization. *Pharmaceutical Research.* 5:759-764.

Lin, X.Y., P. Nelson, and I.H. Gelman. 2000. SSeCKS, a major protein kinase C substrate with tumor suppressor activity, regulates G(1)-> S progression by controlling the expression and cellular compartmentalization of cyclin D. *Molecular and Cellular Biology.* 20:7259-7272.

Lin, Y.Z., S.Y. Yao, R.A. Veach, T.R. Torgerson, and J. Hawiger. 1995. Inhibition of Nuclear Translocation of Transcription Factor Nf- Kappa-B by a Synthetic Peptide-Containing a Cell Membrane- Permeable Motif and Nuclear-Localization Sequence. *Journal of Biological Chemistry.* 270:14255-14258.

Lindberg, M., and A. Graslund. 2001. The position of the cell penetrating peptide penetratin in SDS micelles determined by NMR. *FEBS Letters.* 497:39-44.

Lindgren, M., M. Hallbrink, A. Prochiantz, and U. Langel. 2000. Cell-penetrating peptides. *Trends in Pharmacological Sciences*. 21:99-103.

Liu, C.S., B. Kong, H.H. Xia, K.A. Ellem, and M.Q. Wei. 2001. VP22 enhanced intercellular trafficking of HSV thymidine kinase reduced the level of ganciclovir needed to cause suicide cell death. *Journal of Gene Medicine*. 3:145-52.

Liu, G.S., M.V. Cohen, D. Mochly-Rosen, and J.M. Downey. 1999. Protein kinase c-e is responsible for the protection of preconditioning in rabbit cardiomyocytes. *Journal of Molecular and Cellular Cardiology*. 31:1937-1948.

Liu, X.S., C.N. Kim, J. Yang, R. Jemmerson, and X.D. Wang. 1996. Induction of apoptotic program in cell-free extracts: Requirement for dATP and cytochrome c. *Cell*. 86:147-157.

Loret, E.P., E. Vives, P.S. Ho, H. Rochat, J. Van Rietschoten, and W.C. Johnson, Jr. 1991. Activating region of HIV-1 Tat protein: vacuum UV circular dichroism and energy minimization. *Biochemistry*. 30:6013-23.

Lundberg, M., and M. Johansson. 2001. Is VP22 nuclear homing an artifact? *Nature Biotechnology*. 19:713-4.

Lundberg, M., and M. Johansson. 2002. Positively charged DNA-binding proteins cause apparent cell membrane translocation. *Biochemical and Biophysical Research Communications*. 291:367-71.

Lundberg, M., S. Wikstrom, and M. Johansson. 2003. Cell surface adherence and endocytosis of protein transduction domains. *Molecular Therapy*. 8:143-150.

Magzoub, M., L.E. Eriksson, and A. Graslund. 2002. Conformational states of the cell-penetrating peptide penetratin when interacting with phospholipid vesicles: effects of surface charge and peptide concentration. *Biochimica et Biophysica Acta.* 1563:53-63.

Magzoub, M., K. Kilk, L.E. Eriksson, U. Langel, and A. Graslund. 2001. Interaction and structure induction of cell-penetrating peptides in the presence of phospholipid vesicles. *Biochimica et Biophysica Acta.* 1512:77-89.

Mann, D.A., and A.D. Frankel. 1991. Endocytosis and targeting of exogenous HIV-1 Tat protein. *EMBO Journal.* 10:1733-9.

Manning, M.C., K. Patel, and R.T. Borchardt. 1989. Stability of Protein Pharmaceuticals. *Pharmaceutical Research.* 6:903-918.

Martin, A., P. O'Hare, J. McLauchlan, and G. Elliott. 2002. Herpes simplex virus tegument protein VP22 contains overlapping domains for cytoplasmic localization, microtubule interaction, and chromatin binding. *Journal of Virology.* 76:4961-70.

May, M.J., F. D'Acquisto, L.A. Madge, J. Glockner, J.S. Pober, and S. Ghosh. 2000. Selective inhibition of NF-kappa B activation by a peptide that blocks the interaction of NEMO with the I kappa B kinase complex. *Science.* 289:1550-1554.

Meergans, T., A.K. Hildebrandt, D. Horak, C. Haenisch, and A. Wendel. 2000. The short prodomain influences caspase-3 activation in HeLa cells. *Biochemical Journal.* 349:135-40.

Michel, N., W. Osen, L. Gissmann, T.N.M. Schumacher, H. Zentgraf, and M. Muller. 2002. Enhanced immunogenicity of HPV 16 E7 fusion proteins in DNA vaccination. *Virology*. 294:47-59.

Miller, N., and J. Whelan. 1997. Progress in transcriptionally targeted and regulatable vectors for genetic therapy. *Human Gene Therapy*. 8:803-815.

Miller, W., and R. Miller. 1980. Phosphorylation of acyclovir (acycloguanosine) monophosphate by GMP kinase. *Journal of Biological Chemistry*. 255:7204-7207.

Mutoh, M., F.D. Lung, Y.Q. Long, P.P. Roller, R.S. Sikorski, and P.M. O'Connor. 1999. A p21(Waf1/Cip1) carboxyl-terminal peptide exhibited cyclin- dependent kinase-inhibitory activity and cytotoxicity when introduced into human cells. *Cancer Research*. 59:3480-3488.

Muzio, M., B.R. Stockwell, H.R. Stennicke, G.S. Salvesen, and V.M. Dixit. 1998. An induced proximity model for caspase-8 activation. *Journal of Biological Chemistry*. 273:2926-2930.

Nagahara, H., A.M. Vocero-Akbani, E.L. Snyder, A. Ho, D.G. Latham, N.A. Lissy, M. Becker-Hapak, S.A. Ezhevsky, and S.F. Dowdy. 1998. Transduction of full-length TAT fusion proteins into mammalian cells: TAT-p27Kip1 induces cell migration. *Nature Medicine*. 4:1449-52.

Nicholson, D.W., A. Ali, N.A. Thornberry, J.P. Vaillancourt, C.K. Ding, M. Gallant, Y. Gareau, P.R. Griffin, M. Labelle, Y.A. Lazebnik, and et al. 1995. Identification and inhibition of the ICE/CED-3 protease necessary for mammalian apoptosis. *Nature*. 376:37-43.

Nicholson, D.W., and N.A. Thornberry. 1997. Caspases: killer proteases. *Trends in Biochemical Sciences*. 22:299-306.

Niswender, K.D., S.M. Blackman, L. Rohde, M.A. Magnuson, and D.W. Piston. 1995. Quantitative Imaging of Green Fluorescent Protein in Cultured- Cells - Comparison of Microscopic Techniques, Use in Fusion Proteins and Detection Limits. *Journal of Microscopy-Oxford.* 180:109-116.

Nori, A., K.D. Jensen, M. Tijerina, P. Kopeckova, and J. Kopecek. 2003. Tat-conjugated synthetic macromolecules facilitate cytoplasmic drug delivery to human ovarian carcinoma cells. *Bioconjugate Chemistry.* 14:44-50.

Patterson, G.H., S.M. Knobel, W.D. Sharif, S.R. Kain, and D.W. Piston. 1997. Use of the green fluorescent protein and its mutants in quantitative fluorescence microscopy. *Biophysical Journal.* 73:2782-2790.

Peck, D., and C.M. Isacke. 1998. Hyaluronan-dependent cell migration can be blocked by a CD44 cytoplasmic domain peptide containing a phosphoserine at position 325. *Journal of Cell Science.* 111:1595-1601.

Perez, F., A. Joliot, E. Bloch-Gallego, A. Zahraoui, A. Triller, and A. Prochiantz. 1992. Antennapedia homeobox as a signal for the cellular internalization and nuclear addressing of a small exogenous peptide. *Journal of Cell Science.* 102:717-22.

Phelan, A., G. Elliott, and P. O'Hare. 1998. Intercellular delivery of functional p53 by the herpesvirus protein VP22. *Nature Biotechnology.* 16:440-3.

Pietersz, G.A., W. Li, and V. Apostolopoulos. 2001. A 16-mer peptide (RQIKIWFQNRRMKWKK) from antennapedia preferentially targets the Class I pathway. *Vaccine.* 19:1397-405.

Pomeranz, L.E., and J.A. Blaho. 1999. Modified VP22 localizes to the cell nucleus during synchronized herpes simplex virus type 1 infection. *Journal of Virology*. 73:6769-81.

Qian, Y.Q., M. Billeter, G. Otting, M. Muller, W.J. Gehring, and K. Wuthrich. 1989. The structure of the Antennapedia homeodomain determined by NMR spectroscopy in solution: comparison with prokaryotic repressors. *Cell*. 59:573-80.

Racke, M.M., M. Mosior, S. Kovacevic, C.H.S. Chang, A.L. Glasebrook, N.W. Roehm, and S.Q. Na. 2002. Activation of caspase-3 alone is insufficient for apoptotic morphological changes in human neuroblastoma cells. *Journal of Neurochemistry*. 80:1039-1048.

Rainov, N.G. 2000. A phase III clinical evaluation of herpes simplex virus type 1 thymidine kinase and ganciclovir gene therapy as an adjuvant to surgical resection and radiation in adults with previously untreated glioblastoma multiforme. *Human Gene Therapy*. 11:2389-2401.

Ramjeesingh, M., L.J. Huan, M. Wilschanski, P. Durie, C.H. Li, K. Gyomorey, Y.C. Wang, G. Kent, K.A. Tanswell, E. Cutz, C. Ackerley, and C.E. Bear. 1998. Assessment of the efficacy of *in vivo* CFTR protein replacement therapy in CF mice. *Human Gene Therapy*. 9:521-528.

Ratner, L., W. Haseltine, R. Patarca, K.J. Livak, B. Starcich, S.F. Josephs, E.R. Doran, J.A. Rafalski, E.A. Whitehorn, K. Baumeister, L. Ivanoff, S.R. Petteway, M.L. Pearson, J.A. Lautenberger, T.S. Papas, J. Ghrayeb, N.T. Chang, R.C. Gallo, and F. Wongstaal. 1985. Complete Nucleotide-Sequence of the Aids Virus, HTLV-III. *Nature*. 313:277-284.

Ribeiro, M.M., D. Klein, A. Pileggi, R.D. Molano, C. Fraker, C. Ricordi, L. Inverardi, and R.L. Pastori. 2003. Heme oxygenase-1 fused to a TAT peptide transduces and protects pancreatic beta-cells. *Biochemical and Biophysical Research Communications*. 305:876-881.

Richard, J.P., K. Melikov, E. Vives, C. Ramos, B. Verbeure, M.J. Gait, L.V. Chernomordik, and B. Lebleu. 2003. Cell-penetrating peptides - A reevaluation of the mechanism of cellular uptake. *Journal of Biological Chemistry*. 278:585-590.

Riedel, H., N. Yousaf, Y.Y. Zhao, H.P. Dai, Y.P. Deng, and J. Wang. 2000. PSM, a mediator of PDGF-BB-, IGF-I-, and insulin-stimulated mitogenesis. *Oncogene*. 19:39-50.

Rotonda, J., D.W. Nicholson, K.M. Fazil, M. Gallant, Y. Gareau, M. Labelle, E.P. Peterson, D.M. Rasper, R. Ruel, J.P. Vaillancourt, N.A. Thornberry, and J.W. Becker. 1996. The three-dimensional structure of apopain/CPP32, a key mediator of apoptosis. *Nature Structural Biology*. 3:619-625.

Rousselle, C., P. Clair, J.M. Lefauconnier, M. Kaczorek, J.M. Scherrmann, and J. Temsamani. 2000. New advances in the transport of doxorubicin through the blood-brain barrier by a peptide vector-mediated strategy. *Molecular Pharmacology*. 57:679-86.

Ruffolo, S.C., D.G. Breckenridge, M. Nguyen, I.S. Goping, A. Gross, S.J. Korsmeyer, H. Li, J. Yuan, and G.C. Shore. 2000. BID-dependent and BID-independent pathways for BAX insertion into mitochondria. *Cell Death and Differentiation*. 7:1101-1108.

Ryser, H.J.P., I. Drummond, and W.C. Shen. 1982. The Cellular Uptake of Horseradish-Peroxidase and Its Poly(Lysine) Conjugate by Cultured Fibroblasts Is Qualitatively Similar Despite a 900-Fold Difference in Rate. *Journal of Cellular Physiology*. 113:167-178.

Salvesen, G.S., and V.M. Dixit. 1999. Caspase activation: The induced-proximity model. *Proceedings of the National Academy of Sciences of the United States of America*. 96:10964-10967.

Salvesen, G.S., and C.S. Duckett. 2002. IAP proteins: blocking the road to death's door. *Nature Reviews Molecular Cell Biology*. 3:401-10.

Sambrook, J., E.F. Fritsch, and T. Maniatis. 1989. Molecular cloning: a laboratory manual. Cold Spring Harbour Laboratory Press, New York.

Sandgren, S., F. Cheng, and M. Belting. 2002. Nuclear targeting of macromolecular polyanions by an HIV-Tat derived peptide - Role for cell-surface proteoglycans. *Journal of Biological Chemistry*. 277:38877-38883.

Schimmer, A.D., D.W. Hedley, S. Chow, N.A. Pham, A. Chakrabartty, D. Bouchard, T.W. Mak, M.R. Trus, and M.D. Minden. 2001. The BH3 domain of BAD fused to the Antennapedia peptide induces apoptosis via its alpha helical structure and independent of Bcl-2. *Cell Death and Differentiation*. 8:725-733.

Schutze-Redelmeier, M.P., H. Gournier, F. Garcia-Pons, M. Moussa, A.H. Joliot, M. Volovitch, A. Prochiantz, and F.A. Lemonnier. 1996. Introduction of exogenous antigens into the MHC class I processing and presentation pathway by *Drosophila* antennapedia homeodomain primes cytotoxic T cells *in vivo*. *Journal of Immunology*. 157:650-5.

Schwarz, E., U.K. Freese, L. Gissmann, W. Mayer, B. Roggenbuck, A. Stremlau, and H.Z. Hausen. 1985. Structure and Transcription of Human Papillomavirus Sequences in Cervical-Carcinoma Cells. *Nature*. 314:111-114.

Schwarze, S.R., A. Ho, A. Vocero-Akbani, and S.F. Dowdy. 1999. *In vivo* protein transduction: delivery of a biologically active protein into the mouse. *Science*. 285:1569-72.

Schwarze, S.R., K.A. Hruska, and S.F. Dowdy. 2000. Protein transduction: unrestricted delivery into all cells? *Trends in Cell Biology*. 10:290-5.

Sciortino, M.T., B. Taddeo, A.P. Poon, A. Mastino, and B. Roizman. 2002. Of the three tegument proteins that package mRNA in herpes simplex virions, one (VP22) transports the mRNA to uninfected cells for expression prior to viral infection. *Proceedings of the National Academy of Sciences of the United States of America*. 99:8318-23.

Sells, M.A., J. Li, and J. Chernoff. 1995. Delivery of Protein into Cells Using Polycationic Liposomes. *Biotechniques*. 19:72-&.

Shand, N., F. Weber, L. Mariani, M. Bernstein, A. Gianella-Borradori, Z. Long, A.G. Sorensen, and N. Barbier. 1999. A phase 1-2 clinical trial of gene therapy for recurrent glioblastoma multiforme by tumor transduction with the herpes simplex thymidine kinase gene followed by ganciclovir. *Human Gene Therapy*. 10:2325-2335.

Shapiro, A.M.J., J.R.T. Lakey, E.A. Ryan, G.S. Korbutt, E. Toth, G.L. Warnock, N.M. Kneteman, and R.V. Rajotte. 2000. Islet Transplantation in Seven Patients with Type 1 Diabetes Mellitus Using a Glucocorticoid-

Free Immunosuppressive Regimen. *National English Journal of Medicine.* 343:230-238.

Shen, W.C., and R. H.J. 1978. Conjugation of poly-L-lysine to albumin and horseradish peroxidase: A novel method of enhancing the cellular uptake of proteins. *Proceedings of the National Academy of Sciences of the United States of America.* 75:1872-1876.

Shibagaki, N., and M.C. Udey. 2003. Dendritic cells transduced with TAT protein transduction domain-containing tyrosinase-related protein 2 vaccinate against murine melanoma. *European Journal of Immunology.* 33:850-860.

Shikama, Y., M. U, T. Miyashita, and M. Yamada. 2001. Comprehensive Studies on Subcellular Localizations and Cell Death-Inducing Activities of Eight GFP-Tagged Apoptosis-Related Caspases. *Experimental Cell Research.* 264:315-325.

Sinha, V.R., and A. Trehan. 2003. Biodegradable microspheres for protein delivery. *Journal of Controlled Release.* 90:261-280.

Slee, E.A., M.T. Harte, R.M. Kluck, B.B. Wolf, C.A. Casiano, D.D. Newmeyer, H.G. Wang, J.C. Reed, D.W. Nicholson, E.S. Alnemri, D.R. Green, and S.J. Martin. 1999. Ordering the cytochrome c-initiated caspase cascade: Hierarchical activation of caspases-2, -3, -6, -7, -8, and -10 in a caspase-9-dependent manner. *Journal of Cell Biology.* 144:281-292.

Sodroski, J., R. Patarca, C. Rosen, F. Wong-Staal, and W. Haseltine. 1985a. Location of the trans-activating region on the genome of human T-cell lymphotropic virus type III. *Science.* 229:74-7.

Sodroski, J., C. Rosen, F. Wong-Staal, S.Z. Salahuddin, M. Popovic, S. Arya, R.C. Gallo, and W.A. Haseltine. 1985b. Trans-acting transcriptional regulation of human T-cell leukemia virus type III long terminal repeat. *Science.* 227:171-3.

Srinivasula, S.M., M. Ahmad, T. Fernandes-Alnemri, and E.S. Alnemri. 1998a. Autoactivation of procaspase-9 by Apaf-1-mediated oligomerization. *Molecular Cell.* 1:949-957.

Srinivasula, S.M., M. Ahmad, T. FernandesAlnemri, G. Litwack, and E.S. Alnemri. 1996. Molecular ordering of the Fas-apoptotic pathway: The Fas/APO-1 protease Mch5 is a CrmA-inhibitable protease that activates multiple Ced-3/ICE-like cysteine proteases. *Proceedings of the National Academy of Sciences of the United States of America.* 93:14486-14491.

Srinivasula, S.M., M. Ahmad, M. MacFarlane, Z.W. Luo, Z.W. Huang, T. Fernandes-Alnemri, and E.S. Alnemri. 1998b. Generation of constitutively active recombinant caspases-3 and -6 by rearrangement of their subunits. *Journal of Biological Chemistry.* 273:10107-10111.

Stennicke, H.R., J.M. Jurgensmeier, H. Shin, Q. Deveraux, B.B. Wolf, X.H. Yang, Q. Zhou, H.M. Ellerby, L.M. Ellerby, D. Bredesen, D.R. Green, J.C. Reed, C.J. Froelich, and G.S. Salvesen. 1998. Pro-caspase-3 is a major physiologic target of caspase-8. *Journal of Biological Chemistry.* 273:27084-27090.

Talanian, R.V., C. Quinlan, S. Trautz, M.C. Hackett, J.A. Mankovich, D. Banach, T. Ghayur, K.D. Brady, and W.W. Wong. 1997. Substrate specificities of caspase family proteases. *Journal of Biological Chemistry.* 272:9677-9682.

Tasciotti, E., M. Zoppe, and M. Giacca. 2003. Transcellular transfer of active HSV-1 thymidine kinase mediated by an 11-amino-acid peptide from HIV-1 Tat. *Cancer Gene Therapy*. 10:64-74.

Theodore, L., D. Derossi, G. Chassaing, B. Llirbat, M. Kubes, P. Jordan, H. Chneiweiss, P. Godement, and A. Prochiantz. 1995. Intraneuronal Delivery of Protein-Kinase-C Pseudosubstrate Leads to Growth Cone Collapse. *Journal of Neuroscience*. 15:7158-7167.

Thoren, P.E., D. Persson, M. Karlsson, and B. Norden. 2000. The antennapedia peptide penetratin translocates across lipid bilayers - the first direct observation. *FEBS Letters*. 482:265-8.

Thornberry, N.A., K.T. Chapman, and D.W. Nicholson. 2000. Determination of caspase specificities using a peptide combinatorial library. In: Apoptosis. Vol. 322. 100-110.

Thornberry, N.A., T.A. Ranon, E.P. Pieterson, D.M. Rasper, T. Timkey, M. GarciaCalvo, V.M. Houtzager, P.A. Nordstrom, S. Roy, J.P. Vaillancourt, K.T. Chapman, and D.W. Nicholson. 1997. A combinatorial approach defines specificities of members of the caspase family and granzyme B - Functional, relationships established for key mediators of apoptosis. *Journal of Biological Chemistry*. 272:17907-17911.

Troy, C.M., L. Stefanis, A. Prochiantz, L.A. Greene, and M.L. Shelanski. 1996. The contrasting roles of ICE family proteases and interleukin-1 beta in apoptosis induced by trophic factor withdrawal and by copper/zinc superoxide dismutase down-regulation. *Proceedings of the National Academy of Sciences of the United States of America*. 93:5635-5640.

Tsien, R.Y. 1998. The green fluorescent protein. *Annual Review of Biochemistry*. 67:509-44.

Tyagi, M., M. Rusnati, M. Presta, and M. Giacca. 2001. Internalization of HIV-1 tat requires cell surface heparan sulfate proteoglycans. *Journal of Biological Chemistry*. 276:3254-61.

Vaux, D.L., and S.J. Korsmeyer. 1999. Cell death in development. *Cell*. 96:245-254.

Vives, E., P. Brodin, and B. Lebleu. 1997a. A truncated HIV-1 Tat protein basic domain rapidly translocates through the plasma membrane and accumulates in the cell nucleus. *Journal of Biological Chemistry*. 272:16010-7.

Vives, E., C. Granier, P. Prevot, and B. Lebleu. 1997b. Structure-activity relationship study of the plasma membrane translocating potential of a short peptide from HIV-1 Tat protein. *Letters in Peptide Science*. 4:429-436.

Vocero-Akbani, A., N.A. Lissy, and S.F. Dowdy. 2000. Transduction of full-length Tat fusion proteins directly into mammalian cells: analysis of T cell receptor activation-induced cell death. *Methods in Enzymology*. 322:508-21.

Vocero-Akbani, A.M., N.V. Heyden, N.A. Lissy, L. Ratner, and S.F. Dowdy. 1999. Killing HIV-infected cells by transduction with an HIV protease-activated caspase-3 protein. *Nature Medicine*. 5:29-33.

Wang, J., H.P. Dai, N. Yousaf, M. Moussaif, Y.P. Deng, A. Boufelliga, O.R. Swamy, M.E. Leone, and H. Riedel. 1999. Grb10, a positive, stimulatory signaling adapter in platelet- derived growth factor BB-, insulin-like growth factor I-, and insulin-mediated mitogenesis. *Molecular and Cellular Biology*. 19:6217-6228.

Watson, K., and R.J. Edwards. 1999. HIV-1-trans-activating (Tat) protein: both a target and a tool in therapeutic approaches. *Biochemical Pharmacology*. 58:1521-8.

Watts, C. 1997. Capture and processing of exogenous antigens for presentation on MHC molecules. *Annual Review of Immunology*. 15:821-850.

Wender, P.A., D.J. Mitchell, K. Pattabiraman, E.T. Pelkey, L. Steinman, and J.B. Rothbard. 2000. The design, synthesis, and evaluation of molecules that enable or enhance cellular uptake: peptoid molecular transporters. *Proceedings of the National Academy of Sciences of the United States of America*. 97:13003-8.

Woo, M., R. Hakem, M.S. Soengas, G.S. Duncan, A. Shahinian, D. Kagi, A. Hakem, M. McCurrach, W. Khoo, S.A. Kaufman, G. Senaldi, T. Howard, S.W. Lowe, and T.W. Mak. 1998. Essential contribution of caspase 3 CPP32 to apoptosis and its associated nuclear changes. *Genes & Development*. 12:806-819.

Wood, K.V. 1991. Bioluminescence & Chemiluminescence: Current Status. John Wiley & Sons, Ltd.

Wright, S.C., U. Schellenberger, H. Wang, D.H. Kinder, J.W. Talhouk, and J.W. Larrick. 1997. Activation of CPP32-like proteases is not sufficient to trigger apoptosis: inhibition of apoptosis by agents that suppress activation of AP24, but not CPP32-like activity. *Journal of Experimental Medicine.* 186:1107-17.

Wybranietz, W.A., F. Prinz, M. Spiegel, A. Schenk, M. Bitzer, M. Gregor, and U.M. Lauer. 1999. Quantification of VP22-GFP spread by direct fluorescence in 15 commonly used cell lines. *Journal of Gene Medicine.* 1:265-74.

Wyllie, A.H. 1997. Apoptosis: an overview. *British Medical Bulletin.* 53:451-465.

Xia, H., Q. Mao, and B.L. Davidson. 2001. The HIV Tat protein transduction domain improves the biodistribution of beta-glucuronidase expressed from recombinant viral vectors. *Nature Biotechnology.* 19:640-4.

Yang, R., A.F. Gombart, M. Serrano, and H.P. Koeffler. 1995. Mutational Effects on the P16(Ink4a) Tumor-Suppressor Protein. *Cancer Research.* 55:2503-2506.

Ye, D.J., D. Xu, A.U. Singer, and R.L. Juliano. 2002. Evaluation of strategies for the intracellular delivery of proteins. *Pharmaceutical Research.* 19:1302-1309.

Zender, L., F. Kuhnel, R. Kock, M. Manns, and S. Kubicka. 2002. VP22-mediated intercellular transport of p53 in hepatoma cells *in vitro* and *in vivo*. *Cancer Gene Therapy.* 9:489-496.

Zou, H., W.J. Henzel, X.S. Liu, A. Lutschg, and X.D. Wang. 1997. Apaf-1, a human protein homologous to C-elegans CED-4, participates in cytochrome c-dependent activation of caspase-3. *Cell.* 90:405-413.

Zufferey, R., D. Nagy, R.J. Mandel, L. Naldini, and D. Trono. 1997. Multiply attenuated lentiviral vector achieves efficient gene delivery in vivo. *Nature Biotechnology.* 15:871-875.

Appendix A

Calibration Curve for Soluable Protein Content of Cell Extract

Calibration curve for protein concentration by Bradford assay using bovine serum albumin (BSA) as a standard. A one to ten dilution of a 10 mg/ml stock solution of BSA (New England Biolabs) was prepared and 100 µl samples were prepared in Milli-rho water containing 0, 4, 8, 12, 16 and 20 µg of protein. The following is representative of the linear regression analyses obtained:

Slope = 3.3×10^{-2} $(\mu g/ml)^{-1}$ Intercept = 5.9×10^{-3} r = 0.999

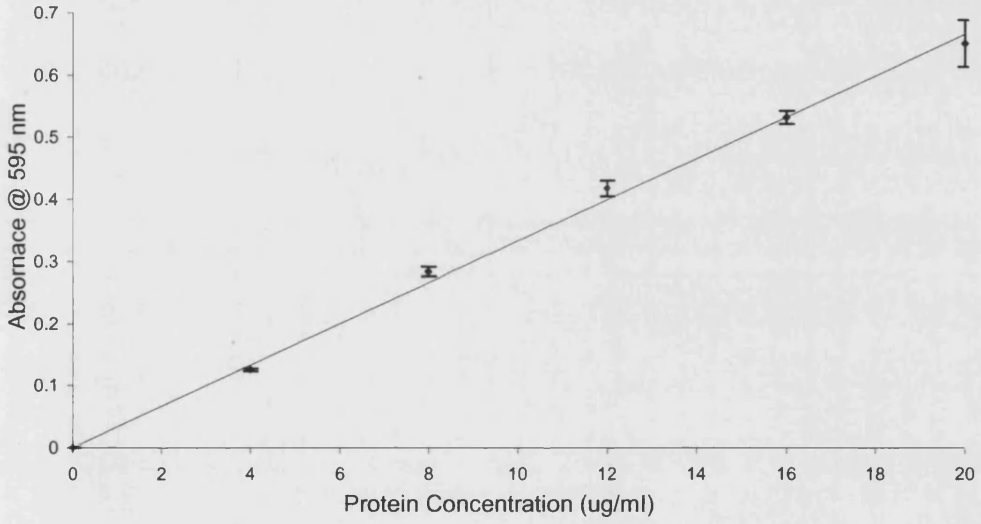

Appendix B

1 Phosphorylation and Annealing of Insert DNA

DNA inserts were constructed from complementary single stranded oligonucleotides purchased from Sigma Genosys, UK, on a 3 OD scale. The oligonucleotides were annealed prior to annealing using the following reaction mix:

DNA oligonucleotide (100 pmol/µl)	1 µl
ATP, 100 mM (Boehringer)	1 µl
Kinase 10x buffer	4 µl
T4 Polynucleotide Kinase (10U/µl)	1 µl
Nuclease free water up to	40 µl

The mix was incubated at 37 °C for 2 hours. Following incubation the two complementary strands were combined in a single tube and the tubes placed in a 500 ml beaker containing water. The water bath was heated to boiling and held at this temperature for 2 minutes. The water bath was then placed on ice and allowed to cool to 30 °C. The insert DNA was then ready for insertion into the desired vector.

2 Polymerase Chain Reaction

Polymerase chain reactions (PCRs) for the amplification of VP22 and PLCasp3 were undertaken using ReadyMix Taq PCR reaction mix (Sigma Aldrich, UK), according to the manufacturers instructions. The primers and specific conditions for the amplification reactions are detailed in the respective chapters.

3 Site-Directed Mutagenesis

Site-directed mutagenesis of the mpSAM2 vector was undertaken using the QuikChange Site-Directed Mutagenesis kit (Stratagene, UK) according to the manufacturers instructions. The primers used for the reaction are detailed in chapter 5.

4 Restriction of DNA using Restriction Endonucleases

Plasmid DNA restrictions were performed using New England Biolab (NEB) restriction enzymes. One of the two following reaction mixes was used for digests. The first mix was used if the restriction enzyme had been shown to exhibit 'star' activity. The second reaction mix was used if there was no 'star' activity associated with the enzyme of choice.

Reaction Mix 1

pDNA	1 µg
Buffer (10x)	3 µl
Milli-Q water up to	30 µl
Restriction enzyme 1 in 3 dilution (normally 10 U/µl)	1 µl

Reaction Mix 2

pDNA	1 µg
Buffer (10x)	3 µl
Milli-Q water up to	30 µl
Restriction enzyme (normally 10U/µl)	2 µl

The restriction enzyme was always added last to the reaction. The reaction tube was then mixed by 'flicking' and the contents collected at the bottom of the tube by a quick spin-down in a microcentrifuge. The reactions were carried out at 37 °C for three hours. Rather than use temperature or EDTA to stop the reaction in most cases the digested DNA was simply ethanol precipitated. Double digests were never used; instead the DNA was sequentially digested with an ethanol precipitation stage between the two digests. Restriction was confirmed by adding 2 µl loading buffer to 3 µl of digest and making up to 15 µl with water. This was then loaded on a 1 % agarose gel alongside undigested vector and a ladder. The gel was run at 90 V for 90 minutes. Where larger quantities of DNA were required the above reactions were either scaled up or altered to include more DNA in the reaction. However, a high ratio of restriction enzyme

to DNA was always maintained to ensure that the presence of undigested vector following the digestion reaction was minimalised.

5 Purification of DNA by Ethanol Precipitation

One tenth of the reaction volume of 3 M Sodium Acetate, pH 7.0, and two reaction volumes of ice cold 100 % ethanol were added to the reaction solution and mixed by vortexing briefly. The solution was incubated for one hour at –20 °C and centrifuged for 15 minutes at 4 °C. The supernatant was removed by pipetting, and 200 µl of 70 % ethanol was added. The sample was centrifuged for 5 minutes at 4 °C and the supernatant was removed. Washing was repeated and the DNA pellet air dried for 15-20 minutes. The purified DNA was dissolved in the desired volume of Milli-Q water.

6 Ligation

The concentration of the vector DNA was estimated by running an aliquot (the volume was dependant on the final volume in which the DNA was eluted using the purification kit) of the gel-purified DNA on a 1 % agarose gel alongside a known standard. A volume between 3 and 7 µl was used in each ligation reaction. The ligation reaction mixture was as follows:

Vector DNA	3-7 µl
Insert DNA/annealed oligonucleotides	25 pmol
Ligase 10x buffer	3 µl
Milli-Q water up to	30 µl
T4 DNA ligase (Boehringer 1 U/µl)	1 µl

Two controls were included in every ligation:

1. Plasmid, no insert DNA, no enzyme, buffer, Milli-Q water
2. Plasmid, no insert DNA, plus enzyme, buffer, Milli-Q water

The reaction mixes were incubated under one of the following conditions:

1. 4 °C overnight (16 hours)
2. 37 °C for 4 hours

3. Room temperature for 2 hours, followed by 37 °C for 2 hours

No single condition worked for every ligation, and a number of conditions were generally tried for each before successful ligation. The ligated DNA was transformed into JM109 cells using the protocol below and the entire ligation mix. In addition to the tubes of competent cells for each of the ligations two additional controls were added. The first, a negative control, involved transformation with no DNA, just water, and the second, a positive control, involved transformation using the original unrestricted vector.

7 Preparation of Competent *E. coli* JM109 Cells

TfbI Buffer

30 mM KCl	3 ml of 1 M stock
100 mM RbCl	1.209 g
10 mM $CaCl_2$	12.5 ml of 80 mM stock
50 mM $MnCl_2$	5 ml of 1 M stock
15 % (v/v) Glycerol	15 ml
Water to	100 ml

Adjust to pH 5.8 with 0.2 M Acetic acid. And filter sterilise.

TfbII Buffer

10 mM MOPS	0.209 g
75 mM $CaCl_2$	1.100 g
10 mM RbCl	0.121 g
15 % (v/v) Glycerol	15 ml
Water to	100 ml

Adjust to pH 6.0 with 1 M KOH and filter sterilise.

A single colony of *E. coli* JM109 was picked from a fresh agar plate and inoculated into 10 ml of LB medium and incubated at 37 °C overnight in a shaking incubator. The following morning, 1 ml of the culture was used to inoculate 100 ml of LB medium and this culture was grown under standard conditions until the optical density (OD_{550nm}) of the solution reached 0.48 (about

2–3 hours). The cell suspension was then chilled on ice for 5 minutes and centrifuged in sterile Greiner tubes for 5 minutes, 6000 rpm (Beckman J2-MC) at 4 °C. The supernatant was discarded and each of the two pellets re-suspended in 20 ml TfbI buffer and chilled on ice for 5 minutes. The cells were centrifuged as before and the supernatant discarded. The cells were subsequently re-suspended in 2 ml TfbII buffer and chilled on ice for 15 minutes. The suspensions were then mixed by vortexing and 300 µl aliquots distributed into 1.8 ml cryotubes. The cells were snap frozen in a dry-ice/ethanol bath and stored at –80 °C until required.

8 Transformation of Competent *E. coli* JM109 Cells

Competent cell suspensions were thawed on ice, and 100 µl added to each ligation mixture, 2 µl unrestricted plasmid (positive control) or to 2 µl water (negative control). Cells were mixed by gentle pipetting using a Gilson pipette tip followed by incubation on ice for at least 30 minutes. The cells were shocked by incubating at 43 °C for 45 seconds and then returned to ice for 2 minutes. The cell suspension was transferred to 1 ml LB medium and incubated at 37 °C for 90 minutes. After this time 200 µl was plated out on a LB-plate containing ampicillin at a concentration of 125 µg/ml. Plates were incubated at 37 °C overnight.

9 Colony Picking and Small Scale Plasmid Purification

After checking the controls, a sterile Gilson pipette tip was used to transfer single colony forming units from the LB plates into 3 to 5 ml LB medium containing the appropriate antibiotic. The cultures were incubated at 37 °C overnight in a shaking incubator. The next morning the 1.5 ml of this culture was transferred to a sterile microcentrifuge tube and centrifuged at 13,000 rpm for 5 minute in a MicroCentaur (MSE, UK). The supernatant was decanted from the tube, so as not to disturb the cell pellet. The plasmid DNA was isolated from the pellet using the Wizard Plus SV Minipreps DNA Purification System and Vac-Man vacuum manifold (Promega, UK) according to the manufacturers instructions. The miniprep DNA samples were then screened

using restriction digest followed by gel electrophoresis. If required, samples were stored at –20 °C.

10 Horizontal Agarose Gel Electrophoresis

Routinely, 1 % agarose gels were produced by dissolving 1 g electrophoresis grade agarose (Gibco BRL, UK) in 100 ml 1x TAE buffer (0.04 mM Tris-acetate, 0.01 M EDTA) at a high temperature in a microwave oven. The solution was cooled to about 60 °C, 4 µl ethidium bromide added and the gel poured into a casting tray and allowed to set at room temperature for about 30 minutes. The gel tray was then mounted in an electrophoresis tank (BioRad, UK) and submersed in 1x TAE. Electrophoresis was carried out at 90 V for sufficient time to produce separation of bands (normally 90 minutes). All gels were run with suitable ladders. The DNA bands were visualized using a UV transilluminator. Photographs were taken using a Polaroid MP4 camera and Polaroid 637 film.

11 DNA Preparation from Agarose Gel

DNA bands on an agarose gel were visualised on an UV transilluminator. The desired band(s) was (were) excised from the gel using a stainless steel razor blade. Each sample was weighed and the DNA isolated using the Qiaex II DNA Extraction Kit (Qiagen, UK) following the manufacturer's instructions. DNA was eluted with either TE buffer, pH 8.0, or Milli-Q water, pH 8.0, and stored at –20 °C.

12 DNA Sequencing

DNA sequencing was carried out at the automated DNA sequencing facility in the Department of Biology and Biochemistry, University of Bath using d-Rhodamine terminator dye chemistry (labelled dNTPs) and FS Taq polymerase (PE Applied Biosystems). The ABI377 DNA sequencer and cycle sequencer used were both from PE Applied Biosystems. The DNA samples for sequencing were supplied in 200 µl PCR tubes and contained 3 µl of miniprep DNA (200-500 ng) template, 10 pmol of primer and were made up to 6 µl with Milli-Q water.

The sequencing primers used for sequencing of oligonucletides and the VP22 PCR product inserted into pSAM1, and for confirming insertion of PLCasp3 into pBI-GFP (and checking the mpSAM2 mutagenesis product) are shown in the table below:

Primer name	Primer sequence
pSAM1 sequencing primer	5'-CCCACTgCTTACTggC-3'
pSAM1 reverse sequencing primer	5'-gCAgTTCTCTCCAgCgg-3'
PBI (MCS I) sequencing primer	5'-AATCAAgggTCCCCAAACTC-3'

Appendix C

Oligonucleotide Ladder

The 1 kb GeneRuler ladder (Fermentas, UK) was run for about 90 minutes on a 1 % agarose gel at 90 V to produce the following defined bands.

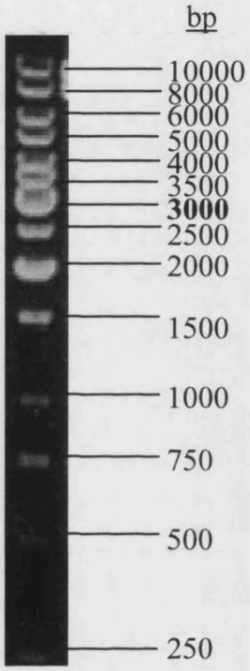

Appendix D

1 pEGFP-N1

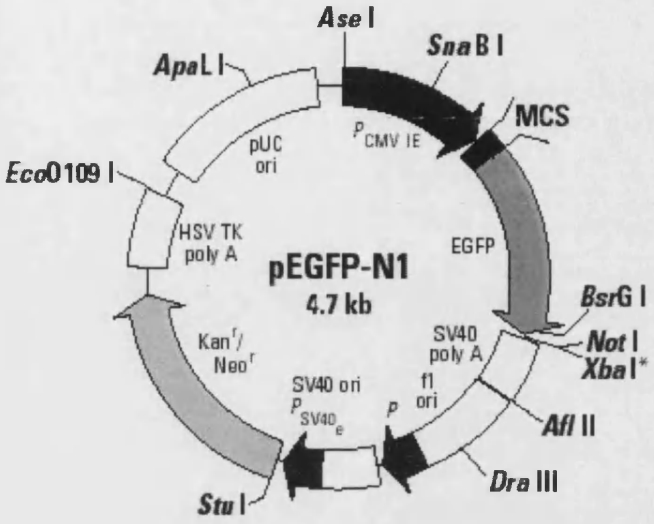

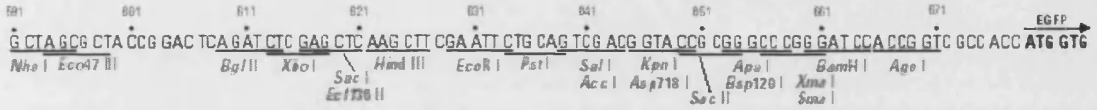

2 pGEM-*luc*

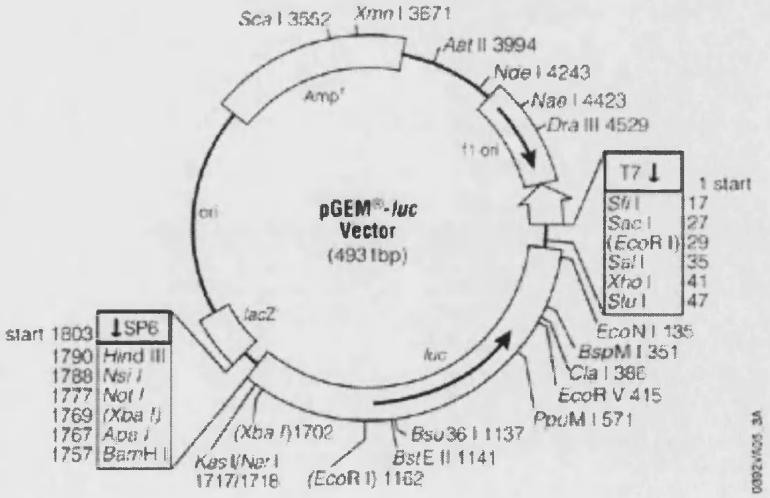

3 pcDNA3.1(+)

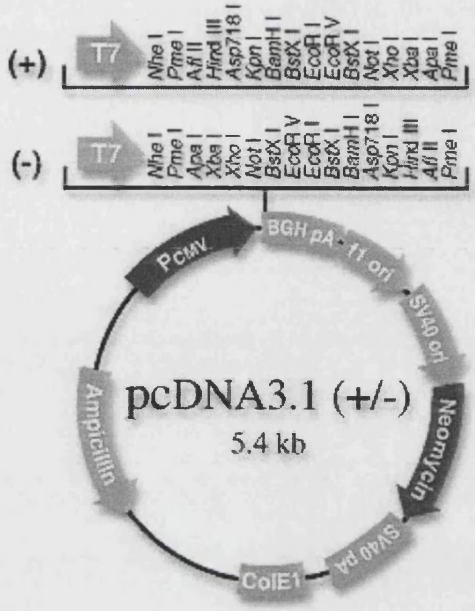

4 pBI

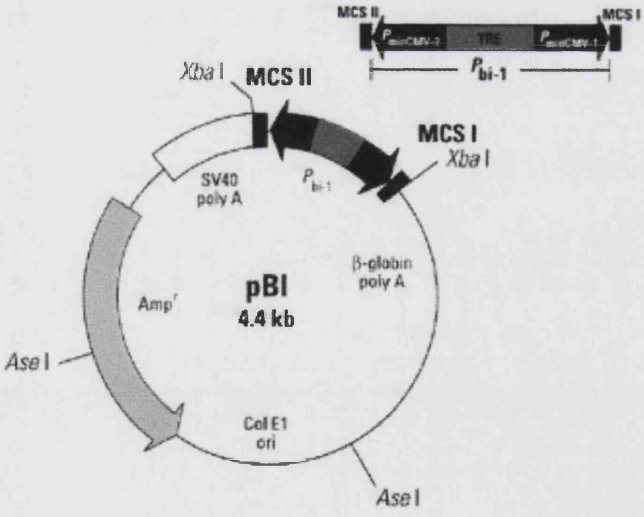

MCS I

600 610 620 630 640

AGTCAGCTGACGCGTGCTAGCGCGGCCTCGACGATATCTCTAGACT

Pvu II *Mlu* I *Nhe* I *EcoR* V *Xba* I

MCS II

4330 4340 4350 4358 10

GATCCTCTAGAACTAGGTCGACGCGGCCGCTGCAGGAATTC

Xba I *Sal* I/ *Acc* I *Not* I *Pst* I